Targeting Thyroid Stimulating Hormone Receptors in Radioiodine Resistant De-differentiated Thyroid Cancer

A thesis submitted to the University of London for the degree of Doctor of Philosophy

by

Ana Sousa Marcelino Boshoff

Centre for Molecular Oncology
Barts and The London School of Medicine and Dentistry
Queen Mary
University of London

DECLARATION

This report is a result of the independent work of Ana Marcelino. I certify that this report does not incorporate without the acknowledgement, any material previously submitted for a degree or diploma in any university, and that to the best of my knowledge and belief it does not contain any material previously published or written by another person where due reference is not made clear.

I actively and independently undertook the following experimental procedures:

- Size exclusion High Performance Liquid Chromatography (SE-HPLC), SDS-PAGE electrophoresis, cell lines maintenance, Fluorescence activated cell sorting (FACS), Real Time-Polymerase chain reaction (RT-PCR), Western blot, radioiodination of antibodies with Iodogen, Instant Thin Layer Chromatography (ITLC), saturation binding assays, immunoreactive fraction assays, TSHR coated tube assays, Conjugation with DOTA and labeling with ^{111}In, Blood plasma stability studies, Reverse-Phase HPLC, radiolabelling using the lactoperoxidase enzymatic substitution method and internalisation and externalisation assays.

I undertook the following experiments with the help and support of colleagues (as acknowledged in the acknowledgments section):

- Immunohistochemistry experiments
- SPECT/CT and biodistribution *in vivo* studies

ABSTRACT

The most common type of thyroid cancer, differentiated thyroid cancer (DTC), is diagnosed by radioactive iodine whole body scanning (WBS) and treated with radiotherapy using iodine-131 (^{131}I). The success of this diagnosis/treatment approach relies on the relatively selective localisation of the sodium/iodide symporter (NIS) in cells of the thyroid gland. However, in some de-differentiated thyroid cancers, NIS expression is lost. This results in the inability of WBS to stage the disease and it also decreases the effectiveness of treatment with ^{131}I. A number of reports have shown that de-differentiated thyroid carcinomas, however, continue to express thyroid stimulating hormone receptor (TSHR). TSHR is, therefore, a potential target for the diagnosis and treatment of radioiodine resistant de-differentiated thyroid carcinoma. In this study an anti-TSHR monoclonal antibody (mAb9) and human recombinant TSH (rhTSH) were radiolabelled and evaluated for their potential use in the diagnosis and treatment of radioiodine resistant thyroid cancer. A number of radiolabelling methods and quality control experiments were initially carried out to ensure high purity radiolabelled mAb9 and rhTSH were produced. *In vitro* studies were conducted to assess the binding affinity of ^{125}I-mAb9, ^{111}In-mAb9 and ^{125}I-rhTSH to the TSHR in thyroid cancer cell lines, TPC-1, FTC-133, and FRTL5, and in a TSHR transfected cell line, GPI. SPECT/CT animal studies were performed in mice to investigate whether ^{125}I-mAb9, ^{111}In-mAb9 and ^{125}I-rhTSH bound to TSHR in the thyroid of mice *in vivo*.

^{125}I-mAb9, ^{111}In-mAb9 and ^{125}I-rhTSH bound to GPI cells but did not bind specifically to the TSHR in FTC-133, TPC-1 and FRTL5 cells as well as to the thyroid of normal mice *in vivo*. Radiolabelled mAb9 and radiolabelled rhTSH are therefore unlikely to be of use in the diagnosis and treatment of radioiodine resistant de-differentiated thyroid cancer.

ACKNOWLEDGEMENTS

I would like to thank my supervisor Stephen Mather for all his help and support throughout my PhD.

I would also like to thank my second supervisor Paul Banga for giving me the opportunity to work with the mAb9 antibody and for all his help and guidance when needed and thank you as well to all his staff and students at King's College London.

I am grateful to Ciara Finucane, Julie Foster and Jerome Burnet for all their help with the SPECT/CT imaging and biodistributions studies.

Thank you to all the Centre for Molecular Oncology staff for all their help and support, including Torkjel Matzow and David Ellison.

A very special thank you to Jane Sosabowski, Roxana Kashani, Chantelle Hudson, Ciara Finucane and Julie Foster for being amazing colleagues and friends.

I appreciate Eugene Boshoff's (King's College London) help with the immunohistochemistry experiments.

Thank you to my sponsor CRUK for giving me the opportunity to perform this project.

Also, a special thank you to my husband Eugene for all his patience, encouragement, love, support and belief in me.

And last, but not least, I am eternally grateful to my parents for their love, support and providing me with great opportunities in life. They will always have a special place in my heart.

CONTENTS

CHAPTER 1. INTRODUCTION 14

1.1 THE THYROID GLAND AND THYROID CELLS 14
1.2 SYNTHESIS OF THYROID HORMONES 15
1.3 THYROID HYPOTHALAMIC-PITUITARY-THYROID AXIS. 18
1.4 TSH STRUCTURE 19
1.5 TSHR 21
1.6 LOCALISATION OF TSHR 24
1.7 TSHR INTERNALISATION 24
1.8 THE SODIUM IODIDE SYMPORTER (NIS) 25
1.9 NIS LOCALISATION 26
1.10 THYROID CANCER 27
1.10.1 Diagnosis and treatment of thyroid cancer 28
1.10.1 Recurrent thyroid cancer 29
1.11 USE OF RHTSH 31
1.12 NIS IN THYROID TUMOURS 33
1.13 TSHR IN THYROID TUMOURS 34
1.14 USE OF MONOCLONAL ANTIBODIES FOR THE DIAGNOSIS AND TREATMENT OF CANCER. 36
1.15 TSHR AS A POTENTIAL NEW TARGET FOR THE DIAGNOSIS AND TREATMENT AND OF RADIOIODINE RESISTANT THYROID CANCER 40
1.16 MAB9 MONOCLONAL ANTIBODY 41
1.17 4C1 MONOCLONAL ANTIBODY 42
1.18 OVERVIEW OF THYROID CANCER AND TSHR EXPRESSING CELL LINES USED 43
1.18.1 FTC-133 43
1.18.2 TPC-1 44
1.18.3 FRTL5 45
1.18.4 GPI 46
1.19 RADIOPHARMACEUTICALS AND CANCER 46
1.19.1 Radiopharmaceuticals for therapy 47
1.19.2 Diagnosis 48
1.20 SPECT AND SPECT/CT IN THYROID CANCER 51
1.21 SPECT/CT IN SMALL ANIMAL RESEARCH 51
1.22 RADIOIODINATION OF MONOCLONAL ANTIBODIES AND PEPTIDES 53
1.22.1 Radioiodination using Chloramine T 54
1.22.2 Iodogen 55
1.22.3 Lactoperoxidase 56
1.23 RADIOLABELLING BY CONJUGATION 57
1.24 SCOPE OF PROJECT 59

CHAPTER 2. MATERIALS AND METHODS 61

2.1 MATERIALS 61
2.2 METHODOLOGY 1 (THIS METHODOLOGY RELATES TO THE MAB9 RESULTS SECTION) 63
2.2.1 Size Exclusion High Performance Liquid Chromatography (HPLC) 63
to confirm the purity of mAb9 antibody 63
2.2.2 SDS-PAGE electrophoresis of unlabelled mAb9 63
2.2.3 Maintenance of CHO, GPI, MKN45, TPC-1, FTC-133 and FRTL5 cell lines ... 64

2.2.4 Fluorescence activated cell sorting (FACS) analyses to determine levels of TSHR in TPC-1, FTC-133 and GPI cells. ... *65*
2.2.5 Immunohistochemistry of FTC-133, TPC-1, GPI and CHO cells ... *67*
2.2.6 RT-PCR ... *69*
2.2.7 Western blot analysis with FTC-133, TPC-1 and GPI cells ... *73*
2.2.8 Radioiodination of mAB9 antibody with Sodium [^{125}I]-Iodide using Iodogen ... *74*
2.2.9 Determination of purity and labelling efficiency of mAb9 ... *75*
2.2.10 TSHR Binding assays ... *77*
2.2.11 Cell binding assays ... *78*
2.2.12 Assessing the in vivo binding of ^{125}I radiolabelled mAb9 to TSHRs in the mouse thyroid using SPECT/CT imaging and biodistribution ... *81*
2.2.13 Radiolabelling of mAb9 with ^{111}In ... *83*
2.2.14 ^{111}In binding to BzScnDOTA mAb9 ... *84*
2.3 METHODOLOGY 2 (THIS METHODOLOGY RELATES TO THE RESULTS SECTION IN CHAPTER 4) ... 87
2.3.1 Radioiodination of rhTSH using enzymatic substitution ... *87*
2.3.2 Effect of glucose oxidase and lactoperoxidase on ^{125}I-rhTSH labeling efficiency. ... *88*
2.3.3 SE-HPLC with rhTSH and ^{125}I-rhTSH ... *88*
2.3.4 Reverse phasse HPLC ... *89*
2.3.5 Ion pairing RP-HPLC ... *89*
2.3.6 ^{125}I-rhTSH binding assays ... *91*
2.3.7 ^{125}I-rhTSH internalisation and externalisation assays ... *92*
2.3.8 ^{125}I-rhTSH in vivo studies ... *94*

CHAPTER 3. MAB9 STUDY ... 98

3.1 MAB9 STUDY RESULTS ... 99
3.1.1 Confirmation of the integrity and purity of unlabelled mAb9 ... *99*
3.1.2 Binding of mAb9 to the TSHR in pre-coated tubes and cells ... *102*
3.1.3 Characterising TSHR in cell lines ... *113*
3.1.4 Radiolabelling of mAb9 with ^{125}I ... *115*
3.1.5 ^{125}I-mAb9 binding Assays ... *118*
3.1.6 Imaging ... *127*
3.1.7 Radiolabelling of mAb9 with ^{111}In ... *133*
3.1.8 ^{111}In-mAb9 binding assays ... *138*
3.1.9 SPECT/CT imaging of ^{111}In-mAb9 in mice ... *140*
3.2 DISCUSSION OF MAB9 STUDIES ... 146
3.2.1 Confirming the purity and immunological integrity of mAb9 ... *147*
3.2.2 Binding of unlabelled mAb9 to TSHR pre-coated in tubes ... *148*
3.2.3 Binding of unlabelled mAb9 to cells. ... *149*
3.2.4 FACS with unlabelled mAb9 ... *149*
3.2.5 Immunohistochemistry to characterise TSHR in cells ... *151*
3.2.6 Characterising TSHR in cell lines ... *152*
3.2.7 Radiolabelling of mAb9 with ^{125}I-iodide ... *154*
3.2.8 ^{125}I-mAb9-TSHR binding assays ... *154*
3.2.9 SPECT/CT imaging experiments ... *158*
3.2.10 ^{111}In-labelled mAb9 ... *160*
3.2.11 SPECT/CT imaging of ^{111}I-mAb9 in mice ... *162*
3.2.12 Conclusion for mAb9 studies ... *163*

CHAPTER 4. RHTSH STUDY 164

4.1 RHTSH STUDY RESULTS 165

4.1.1 Radioiodination of rhTSH using enzymatic substitution 165

4.1.2 HPLC Studies with rhTSH and ^{125}I-rhTSH 166

4.1.3 ^{125}I-rhTSH binding assays 174

4.1.4 ^{125}I-rhTSH internalisation and externalisation assays 177

4.1.5 In vivo binding 180

4.2 DISCUSSION OF RHTSH STUDIES 186

4.2.1 Radioiodination of rhTSH with ^{125}I 187

4.2.2 HPLC studies with rhTSH 188

4.2.3 Binding of radiolabelled rhTSH to the TSHR in vitro 193

4.2.4 Internalisation and externalisation assays 195

4.2.5 In vivo binding 197

4.2.6 Conclusion of rhTSH studies 200

CHAPTER 5. GENERAL SUMMARY AND CONCLUSIONS 201

6. REFERENCES 206

List of Figures

Chapter 1

Figure 1.1: Anatomy of the human thyroid and thyroid cells…… 14
Figure 1.2: Chemical structures of T_3 and T_4. …….. 17
Figure 1.3: Thyroid hormone synthesis steps…… 18
Figure 1.4: Thyroid hormone negative feedback loop.…….. 19
Figure 1.5: Structure of α and β TSH subunit genes…….. 20
Figure 1.6: Typical N-linked oligosaccharides of human TSH……..… 21
Figure 1.7: Thyroid stimulating hormone receptor structure…….……. 23
Figure 1.8: Receptor internalisation of GPCRs…… 25
Figure 1.9: Structure of IgG antibodies…….. 37
Figure 1.10: SPECT/CT in thyroid cancer…….……. 51
Figure 1.11: NanoSPECT/CT imaging……..… 53
Figure 1.12: Iodination by Chloramine T……..…. 55
Figure 1.13: Iodination by Iodogen……...…. 56
Figure 1.14: Iodination using Lactoperoxidase…….. 57
Figure 1.15: Schematic representation of ^{111}In labelling of ScnBzDota-antibody…… 59

Chapter 3

Figure 3.1: UV chromatogram (280nm) of mAb9 size exclusion HPLC……..... 99
Figure 3.2: UV chromatogram of Biorad gel filtration standards (280nm). …….……100
Figure 3.3: Biorad gel filtration molecular weight standards……100
Figure 3.4: Linear regression of retention time obtained in SE-HPLC against Log standard molecular weight……... 101
Figure 3.5: SDS page electrophoresis analysis of mAb9……. 101
Figure 3.6 Competition assay of ^{125}I-TSH with unlabelled mAb9 in TSHR pre coated tubes…… 102
Figure 3.7: FACS analysis of TSHR expression in GPI and CHO cells…….…….…103
Figure 3.8: FACS analysis of TSHR expressed in TPC-1 and MKN45 cells…….…… 104
Figure 3.9: FACS analysis of TSHR expressed in FTC-133 and MKN45 cells…….……. 105
Figure 3.10: FACS analysis of TSHR expressed in FRTL5 and CHO cells…….….. 106
Figure 3.11: Comparison of mean fluorescent units (MFUs) of performed FACS with both 4C1 and mAb9 at 1 µg /ml and 10 µg /ml……..……..……..… 107
Figure 3.12: Immunohistochemistry performed on CHO cells to investigate TSHR expression…..….... 109
Figure 3.13Immunohistochemistry performed on FTC-133 cells to investigate TSHR expression...…110
Figure 3.14: Immunohistochemistry performed on TPC-1 cells to investigate TSHR expression…….. 111
Figure 3.15: Immunohistochemistry performed on GPI cells to investigate TSHR expression. ……... 112
Figure 3.16: Quantitative RT-PCR to determine TSHR expression over CHO (calibrator) in all thyroid cell lines……..… 114
Figure 3.17 Western blot analysis of cell lysates with 4C1 and mAb9 antibodies in GPI cells…….….. 115
Figure 3.18: Analysis of the radiolabelled product using ITLC-SG strips run on 85% methanol……. . 116
Figure 3.19: Representative examples of results of ITLC quality control of ^{125}I-mAb9 radiolabelling efficiency……..……. 116
Figure 3.20: Radio-HPLC analysis of ^{125}I radiolabelled mAb9……...…….....…117

Figure 3.21: SDS page gel autoradiography of binding of ^{125}I-mAb9 to the TSHR in pre coated tubes…….…..…. 118
Figure 3.22: Competition assay of ^{125}I-mAb9 with unlabelled mAb9 to the TSHR in pre coated tubes …119
Figure 3.23: Competition assay of ^{125}I-mAb9 with 'oxidised mAb9' and 'cold labeled mAb9' in TSHR pre coated tubes …… 120
Figure 3.24: FACS analysis on GPI cells using different mAb9 preparations……..…..…120
Figure 3.25: FACS analysis of 4C1 preparations…….…….....121
Figure 3.26: Effect of temperature and time in the binding of ^{125}I-mAb9 to GPI cells…….. 122
Figure 3.27: TCA precipitation assay of ^{125}I-mAb9over a period of 6 hours……..… 123
Figure 3.28: Graph showing binding of ^{125}I-mAb9 to GPI cells in different buffers…….. 124
Fig 3.29: Immunoreactive fraction assay with ^{125}I-mAb9 in GPI cells……... 125
Figure 3.30: Equilibrium saturation binding of ^{125}I-mAb9 to GPI cells……..… 125
Figure 3.31: Equilibrium saturation binding of ^{125}I-4C1 to GPI cells……..… 126
Figure 3.32: Equilibrium saturation binding of ^{125}I-mAb9 to FRTL5 cells…….……126
Figure 3.33: % of injected dose of radioactivity in the thyroid gland and salivary gland…….…. 132
Figure 3.34: Size-exclusion HPLC with ScnBzDOTA-mAb9……. .. 120
Figure 3.35: FACS analysis with Bz-DOTA-mAb9……... 135
Figure 3.36: Competition assay of ^{125}I-TSH with Bz-DOTA-mAb9 to the TSHR in pre coated tubes 136
Figure 3.37: Radio size-exclusion HPLC with ^{111}In-mAb9…… 137
Figure 3.38: Analysis of the radiolabelled product using ITLC-SG strips run in 0.1M ammonium acetate/EDTA pH 5.5……..…. …. 137
Figure 3.39: Competition assay of ^{111}In-mAb9 with unlabelled mAb9 in TSHR pre coated tubes ……138
Figure 3.40: Equilibrium saturation binding of ^{111}In-mAb9 to GPI cells…… 139
Figure 3.41: Equilibrium saturation binding of ^{111}In-mAb9 to FRTL-5 cells……. 140
Figure 3.43: Biodistribution of ^{111}In-mAb9…… 144
Figure 3.44: Phosphorimager image of non reduced SDS-page electrophoresis of ^{111}In-mAb9 incubated in the blood of mice…….…..… 145

Chapter 4

Figure 4.1: Phosphorimager images of ITLC and SDS PAGE electrophoresis analysis of ^{125}I-rhTSH……... 165
Figure 4.2: Relationship between glucose oxidase and lactoperoxidase in the ^{125}I-rhTSH radioiodination reaction against the labelling efficiency……...… 166
Figure 4.3: UV size exclusion HPLC chromatogram (280 nm) of rhTSH……..……..… 166
Figure 4.4: UV size exclusion chromatogram (280 nm) of BioSep molecular weight standards…..…... 167
Figure 4.5: UV size exclusion HPLC chromatogram of carbonic anydrase and lysosyme……..…..… 167
Figure 4.6: Size exclusion radio-HPLC analysis of ^{125}I radiolabelled rhTSH…….…. 168
Figure 4.7: Gradient elution pattern of rhTSH in RP-HPLC…….…... 169
Figure 4.8: UV chromatogram of the elution of rhTSH from RP-HPLC using a C18 column and mobile phase 0.1%TFA/water and ACN/TFA (pH 2.5)…….…... 172
Figure 4.9: Organic solvent gradient used to elute rhTSH in RP-HPLC……. 170
4.10: UV chromatogram and radiochromatogram of the elution of unlabelled rhTSH from a RP-HPLC using a C18 column and 0.1%TFA/water and ACN/TFA (pH 2.5) mobile phase……..…..… 170

Figure 4.11: Radiochromatogram of the elution of ^{125}I-rhTSH from a RP-HPLC using a C18 column and mobile phase 0.1%TFA/water and ACN/TFA (pH 2.5)…….…..… 170
Figure 4.12: SDS gel electrophoresis of ^{125}I-rhTSH, treated with pH 2.5 and pH 7……...… 171
Figure 4.13: RP-HPLC of rhTSH with 0.01M TEAA/water pH 5.5 and 0.01MTEAA/water pH 7…… 172
Figure 4.14: Radio RP-HPLC chromatograms of ^{125}I-rhTSH with 0.01M TEAA/water, pH 5.5 and 0.1M TEAA/water pH 7…….…… 173
Figure 4.15: 'Oxidised rhTSH' analysis in RP-HPLC with 0.1M TEAA/water pH7……..…. 174
Figure 4.16: 'cold labelled' rhTSH analysis in RP-HPLC with 0.1M TEAA/water pH7……..…. 174
Figure 4.17: Effect of buffers used on binding to cells in cell binding assays……. 175
Figure 4.18: Competition assay of ^{125}I-rhTSH with unlabelled rhTSH to the TSHR in pre coated tubes 175
Figure 4.19: Equilibrium saturation binding of ^{125}I-rhTSH to GPI cells……..…… 176
Figure 4.20: competition assay of ^{125}I-rhTSH with unalabelled rhTSH in GPI cells……...…… 177
Figure 4.21: Internalisation assay to determine the amount of conjugate that is internalised over a period of 120 minutes……...…..…. 177
Figure 4.22: TCA precipitation assay to determine the amount of protein bound radioactivity over a period of 120 minutes…….…...…. 178
Figure 4.23: Time dependant externalisation of pre-internalised ^{125}I-rhTSH in GPI cells, in the presence and absence of competitor……..……. 179
Figure 4.24: TCA precipitation assay to determine the amount of protein bound radioactivity over a period of 120 minutes ……..…...…. 180
Figure 4.25: SPECT/CT imaging of mice at 2.5 hour time point after ^{125}I injection……..…….…… 181
Figure 4.26: Invivoscope ROI quantification analysis of ^{125}I-rhTSH and blocking control. ……..…..…. 182
Figure 4.27: Biodistribution of ^{125}I-rhTSH in mice…….…...….183
Figure 4.28: TCA precipitation assay on blood removed from mice 2 hour post injection of ^{125}I-rhTSH and ^{125}I-TI…….…….....… .183
Figure 4.29: Phosphorimager image of reduced and non reduced SDS-page electrophoresis of ^{125}I-rhTSH incubated in the blood of mice……..……. 184
Figure 4.30: Biodistribution of ^{125}I-rhTSH, ^{125}I-CA and blocking control in mice……..…..185

List of tables

Chapter 2

Table 2.1: Table of cell lines grown…….……. 64
Table 2.2: RNA/primer mixture ……..……..…….……71
Table 2.3: cDNA synthesis mixture.……..……...……. 71
Table 2.4: PCR master mix ……..……72
Table 2.5 RT-PCR Instrument Settings……72.
Table 2.6: concentrations used for the lactoperoxidase radioiodination method.……...… 87
Table 2.7: Preparation of 'oxidised rhTSH' and 'cold labelled rhTSH' reaction mixtures…….. 90

Chapter 3

Table 3.1 Biorad gel filtration molecular weight standards ……..…. 100
Table 3.2: Representative examples of results of ITLC quality control of ^{125}I-mAb9 radiolabelling efficiency. 116
Table 3.3: % of injected dose of radioactivity in the thyroid gland and salivary gland.…….. 132

ABBREVIATIONS

^{111}In: Indium 111

^{125}I: Iodide-125

^{125}I-TSH: Iodide-125 radiolabelled thyroid stimulating hormone

^{131}I: Iodide-131

^{18}F: Fluorine-18

^{99m}Tc: Technetium-99m

ADCC: Antibody dependent cellular cytotoxicity

AP2: Adapter protein 2

ATC: Anaplastic thyroid carcinoma

ATP: Adenosine tri-phosphate

Barr: B-arrestins

Bmax: number of receptors

bTSH: bovine TSH

BSA: Bovine serum albumin

Bz-DOTA-mAb9: Benzyl- Tetraazacyclododecanetetraacetic acid-mAb9

C: Constant region of antibody

CA: Carbonic anydrase

cAMP: Cyclic adenosine monophosphate

cDNA: complementary DNA

CDC: Complement-dependent cytotoxicity

Chloramine T: N-chloro-p-toluene sulphonamide

CHO: Chinese hamster ovary cells

CPM: Counts per minute

CT: Computed tomography

Ct: Threshold cycle

Da: Dalton

DAB: Diaminobenzidine

DMEM: Dulbecco's Modified Eagle Medium

DTC: Differentiated thyroid cancer

DTPA: Diethylenetriamine-penta-acetic acid

DOTA: Tetraazacyclododecanetetraacetic acid

DIT: Diiodotyrosine

ECD: Ectodomain

EDTA: Ethylenediaminetetraacetic acid

EtOH: Ethanol

Fab: Fragment antigen binding

FACS: Fluorescence activated cell sorting

FBS: Foetal bovine serum

Fc: Antibody fragment crystallisable region

FDA: Food and drug administration

FDG: Fluorodeoxyglucose

FITC: Fluorescein isothiocyanate

FSC-H: Forward scatter

FSH: Follicle-stimulating hormone

FTC: Follicular thyroid carcinomas

GADPDH: Glyceraldehyde 3-phosphate dehydrogenase

GPCR: G protein coupled receptor

GPKs: G protein coupled receptor kinases

HBSS: Hank's Balanced Salt Solution

HCL: Hydrochloric acid

HEPES: 4-(2-hydroxyethyl)-1-piperazineethanesulfonic acid

HPLC: High pressure liquid chromatography

HRP: Horseradish peroxidase

hTSHR: Human thyroid stimulating hormone receptor

IC_{50}: Inhibitory concentration at 50%

IgG: Immunoglobulin G

IHC: Immunohistochemistry

IMS: Industrial methylated spirits

IP: Intraperitoneal

ITLC: Instant thin layer chromatography

IVS: In vivo scope

IV: Intravenous

IRF: Immune reactive fraction

KI: Potassium [^{127}I] iodide

Kd: Dissociation constant

kDa: Kilodaltons

keV: Kiloelectron volt

LH: Luteinising hormone

LET: Linear energy transfer

MAb: Monoclonal antibody

MEM: Non-Essential Amino Acids Solution Monoiodotyrosine

MFU: Mean fluorescence units

MIT: Monoiodotyrosine

Mwt: Molecular weight

mRNA: Messenger ribonucleic acid

NIS: Sodium iodide symporter

NTC: No template control

PBS: Phosphate buffer saline

PCR: Polymerase chain reaction

PET: Positron emission tomography

PFA: Paraformaldehyde

RAI: Radioactive iodine

rhTSH: Human recombinant thyroid stimulating hormone or Thyrogen®

ROI: Region of interest

RP-HPLC: Reverse phase HPLC

RT: Retention time

RT-PCR: Real time PCR

SE-HPLC: Size exclusion HPLC

scFv: single variable fragment chain

SCID: Severe combined immunodeficiency

SDS: Sodium dodecyl sulfate

STD: Standard tandom repeat

SPECT: Single photon emission computed tomography

SPECT/CT: Single photon emission computed tomography with computed tomography

SSC-H: Side scatter

T_1: Monoiodotyrosine

T_2: Diiodotyrosine

T_3: Triiodothyronine

T_4: Thyroxine

TCA: trichloacetic acid

TEAA: Triethylammonium acetate

TEMED: Tetramethylethylenediamine

TFA: Trifluoroacetic acid

Tg: Thyroglobulin

THOX: Thyroid oxidase

TI: Trypsin inhibitor

TPO: Thyroid peroxidise

TRH: Thyrotropin releasing hormone

TSH: Thyroid stimulating hormone

TSHR: Thyroid stimulating hormone receptor

TTF-1: Thyroid transcription factor 1

UV: Ultra violet

V: Antibody variable region

WBS: Whole body scan

CHAPTER 1. INTRODUCTION

1.1 The Thyroid Gland and Thyroid Cells

The thyroid gland is a butterfly-shaped organ located in the neck inferior to the larynx (voice box). This gland is composed of right and left lateral lobes, which lie on either side of the trachea. Connecting the lobes is a mass of tissue called the isthmus that lies anterior to the trachea (**figure 1.1**) [1, 2]. The thyroid gland is made mostly by thyroid follicles, which are microscopic spherical sacs. The wall of each follicle consists primarily of cells called follicular cells, most of which extend to the lumen (internal space) of the follicle [1]. When the follicular cells are inactive, their shape is low cuboidal to squamous, but under the influence of TSH they become cuboidal or low columnar and actively secretory. Parafollicular or C cells, which produce the hormone calcitonin and comprise around 1% of human thyroid cells, can also be found adjacent to the thyroid follicles and reside in the connective tissue. Calcitonin regulates calcium homeostasis [1, 2].

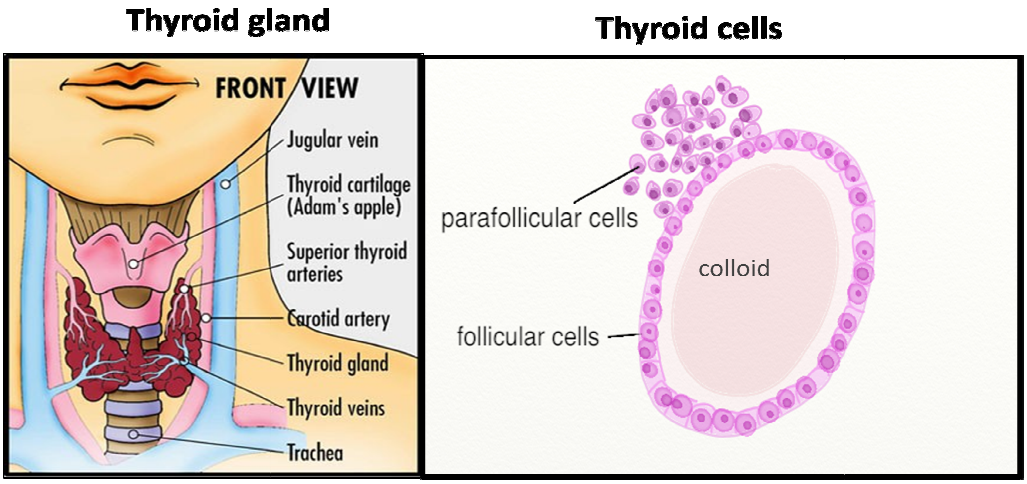

Figure 1.1: Anatomy of the human thyroid and thyroid cells. Adapted from [3].

The thyroid is essential for normal development, differentiation, and metabolic balance. Most, if not all of the actions of thyroid hormones occur as thyroid hormones bind and activate their nuclear receptors. The thyroid hormone receptors are chromatin bound and

alter the transcription of specific genes. Thyroid hormones increase basal metabolic rate (BMR) by stimulating the use of cellular oxygen to produce ATP [1, 2]. Plasma membrane Na^+/K^+ ATPase pumps act to maintain the Na^+/K^+ gradients in all cells of the body and use a large portion of the ATP produced by most cells. A major effect of the thyroid hormones is to stimulate synthesis of Na^+/K^+ ATPase. As cells use more oxygen to produce ATP, more heat is given off, and body temperature rises. This phenomenon is called the calorigenic effect of the thyroid hormones and in this way the thyroid hormones play an important role in the maintenance of normal body temperature [1, 2]. In the regulation of metabolism, the thyroid hormones stimulate protein synthesis and increase the use of glucose for ATP production. They also increase lipolysis and enhance cholesterol excretion in bile, thus reducing blood cholesterol levels [1, 2]. Furthermore, the thyroid hormones also enhance some actions of the catecholamines (norepinephrine and epinephrine) because they up-regulate β adrenal receptors. Together with human growth hormone and insulin, thyroid hormones accelerate body growth and are, thus, essential for normal human development. The important role of the thyroid in development is illustrated by the fact that regions of iodine deficiency have a high occurrence of cretinism. Cretinism is characterised by mental retardation, short stature, delay in motor development, coarse hair and a protuberant abdomen [1, 2].

1.2 Synthesis of Thyroid hormones

The thyroid gland produces two principal hormones: tetraiodothyronine (T_4 or thyroxine) and triiodothyronine (T_3), which contain four and three atoms of iodine respectively [1, 2].

The major steps in the synthesis, storage and release of thyroid hormones include: the uptake of iodide ion by the thyroid, the oxidation of iodide into iodine and the iodination of tyrosyl groups on thyroglobulin, coupling of iodotyroside residues to

generate iodotyrosines, the conversion of T_4 to T_3 in the thyroid and the release of T_3 and T_4 into the blood, and each of these steps are described below [1, 2].

In the first step, iodide ingested in the diet is actively transported by thyroid follicular cells from the blood into the cytosol of the thyroid follicular cells via a specific, membrane-bound protein, the sodium iodide symporter (NIS) [4-6], and this process is called iodine trapping. The sodium ATP-ase pump localised in the basolateral region of follicular cells generates a sodium electrochemical gradient by actively transporting sodium into the follicular cells. NIS utilises this sodium gradient to transport iodide into the cell [4-6]. For every two sodium ions that are transported along the sodium gradient out of the cells, one iodide is transported into the follicular cells. As a result, the I^- concentration inside follicular cells is 20-40 times that of blood plasma [4-6]. The iodide transport system is stimulated by the thyroid stimulating hormone (TSH) and is also controlled by a negative feedback loop control mechanism, in which decreased levels of iodine in the thyroid lead to an increase in iodide uptake and the administration of iodide can reverse this situation. NIS has been identified in many other tissues, including the salivary gland, gastric mucosa, midportion of the small intestine, choroid plexus, skin and mammary glands, all of which maintain a concentration of iodide greater than that of the blood [7]. It is not clear what the purpose of the NIS is in these other sites; however it is evident that NIS is not unique to the thyroid gland. At the same time that the follicular cells trap I^-, they also synthesise thyroglobulin, a high molecular weight glycoprotein (approximately 660 kDa) that contains around 5500 amino acid residues. More than 100 of these amino acids are tyrosines, a few of which become iodinated. Negatively charged iodide ions ($2I^-$) cannot bind to tyrosine until they undergo oxidation to form iodine (I_2). The enzyme that catalyses this reaction is thyroid peroxidase in the presence of hydrogen peroxide (H_2O_2). In thyroid follicular cells thyroid peroxidise is mostly concentrated close to or in the membrane adjacent to the

colloid. H_2O_2, that is needed as a substrate for this reaction, is produced by a generator system of H_2O, in which thyroid oxidases 1 and 2 (THOX 1 and 2) are essential [2]. This organification process is completely inhibited by tiocine, perchlorate and other anions [8, 9]. As the iodide ions are being oxidised, they pass through the apical membrane into the colloid where they react with tyrosine amino acids that are part of thyroglobulin (Tg) molecules in the colloid. Binding of a single iodine atom to a tyrosine yields monoiodotyrosine (T_1), while binding of two iodines yields diiodotyrosine (T_2) [2].

During the last step in the synthesis of the thyroid hormones, two T_2 molecules join to form T_4, or one T_1 and one T_2 join to form T_3 (**figure 1.2**). Each Tg ultimately contains about six T_1, five T_2, and one T_4. There is a single T_3 in one of every four thyroglobulins. Thus, thyroid hormones are stored as part of Tg molecules within the colloid [2]. Vesicles of colloid containing Tg are taken up into follicular cells by pinocytosis and once inside the follicular cell they merge with lysosomes. Digestive enzymes then break down Tg, cleaving off molecules of T_3 and T_4. T_1 and T_2 are also released, but they undergo deiodination and the liberated iodine is reused to synthesise more T_3 and T_4. Because T_3 and T_4 are lipid-soluble, they diffuse through the plasma membrane to enter the blood and more than 99% of both the T_3 and the T_4 combine with transport proteins in the blood, mainly thyroxine-binding globulin [2]. An illustration of thyroid hormone synthesis can be found in **figure 1.3.**

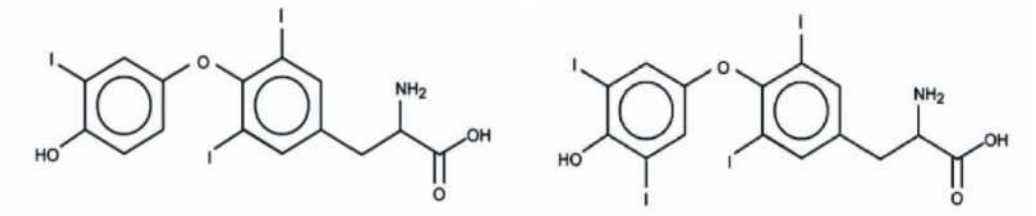

Figure 1.2: Chemical structures of T_3 and T_4. T_3 is on the left side and T_4 on the right side. Adapted from [10]

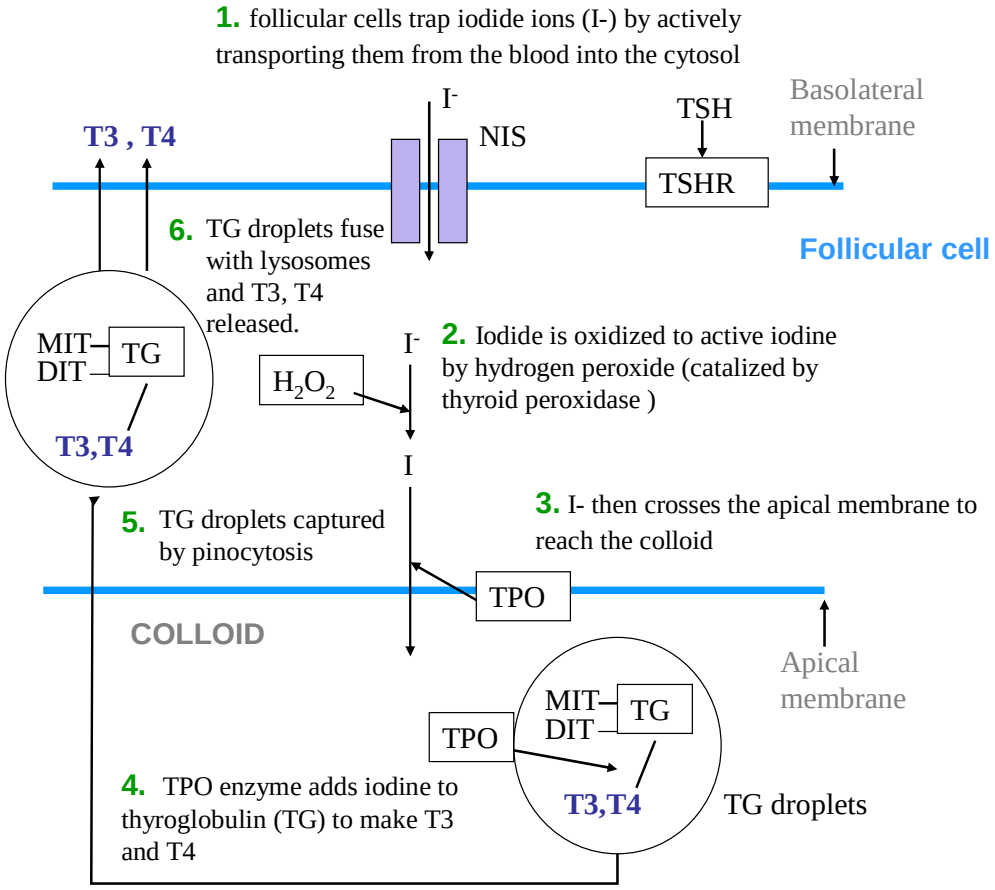

Figure 1.3: Thyroid hormone synthesis steps. Adapted from [1, 2] Including the uptake of iodide ion by the thyroid, the oxidation of iodine and the iodination of tyrosyl groups of thyroglobulin, coupling of iodotyroside residues to generate iodotyrosine and the release of T_3 and T_4 into the blood. Abbreviations: NIS- Sodium Iodide symporter; TSH- Thyroid stimulating hormone; TSHR- thyroid stimulating hormone receptor; TPO- thyroid peroxidase; TG- thyroglobulin; MIT- monoiodotyrosine; DIT – diiodotyrosine; T_3- triiodothyronine; T_4- thyroxine

1.3 Thyroid hypothalamic-pituitary-thyroid axis.

Thyroid stimulating hormone (TSH) is secreted by the pituitary gland and it acts to regulate thyroid function. The binding of TSH to the thyroid stimulating hormone receptors (TSHRs) on the thyroid follicular cells ultimately mediates thyroid hormone synthesis and secretion [11]. The thyroid stimulating hormone receptor (TSHR) on the thyroid follicular cells is a member of the family of G protein coupled receptors (GPCRs). TSHR activates adenylyl cyclase via Gαs which leads to an increase in intracellular cyclic adenosine monophosphate (cAMP). cAMP is the main second messenger of TSH action in the human thyroid. Intracellular concentrations of cAMP control the maintenance of the differentiated phenotype of thyrocytes, the level of

functional activity of the gland (trapping of iodide, secretion of thyroid hormones) and growth [12, 13]. TSH production in turn is controlled by thyrotropin releasing hormone, (TRH), which is produced in the hypothalamus and transported to the anterior pituitary gland (**figure 1.4**). TRH binds and activates the TRH receptor on the cell membranes of the thyrotrophs, and this stimulates an increase in both the synthesis and release of TSH [2]. The level of thyroid hormones (T_3 and T_4) in the blood has an effect on the pituitary release of TSH; when the levels of T_3 and T_4 are low, the production of TSH is increased, and, on the converse, when levels of T_3 and T_4 are high, TSH production is decreased. This effect creates a regulatory negative feedback loop.

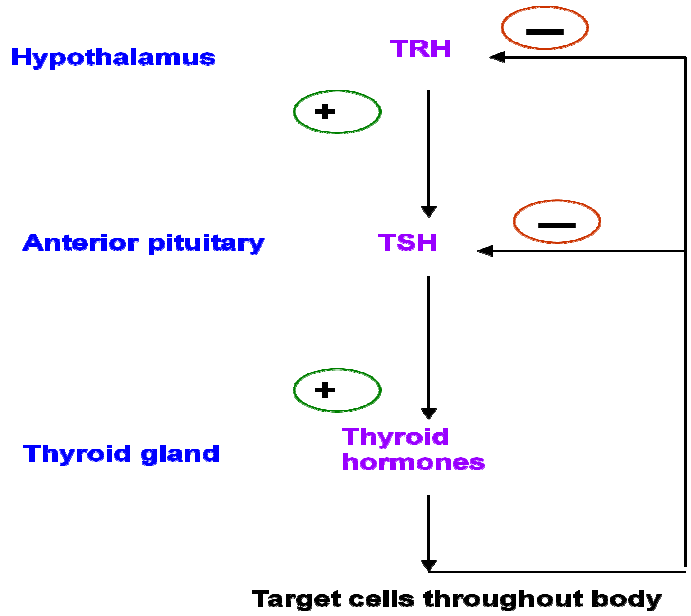

Figure 1.4: Thyroid hormone negative feedback loop. Abbreviations: TRH- thyroid releasing hormone; TSH- thyroid stimulating hormone. Adapted from [1, 2]

1.4 TSH structure

TSH, also known as thyrotropin, is a glycoprotein with approximate molecular weight of 28-30 kDa, consisting of two distinct subunits, an α subunit and a β subunit, joined by non-covalent bonds. Each subunit forms a cysteine knot structure with three disulfide bridges [14]. The mature human TSH β subunit shares between 88-92% amino acid

identity with canine, rat, equine, mouse, bovine, porcine, and feline TSH β [14]. The mature human α subunit shares 69%-73% amino acid identity with canine, rabbit, rat, mouse, bovine, porcine, feline and equine α subunit [14]. The synthesis of the α and β subunit of TSH occurs in the thyrotrophs, which comprise around 5% of anterior pituitary gland. The gene that encodes the α subunit is located on chromosome 5, while the β subunit gene is located on chromosome 2 [14]. The TSH α subunit contains 92 amino acids with five disulfide bridges contributing to its tertiary structure and the β subunit contains 118 amino acids with six disulfide bridges (**figure 1.5**) [14]. The glycoprotein hormones TSH, FSH, and LH all share a common α subunit, however the β subunit is specific to TSH. In order for TSH to exert biological activity the two subunits must be joined [14].

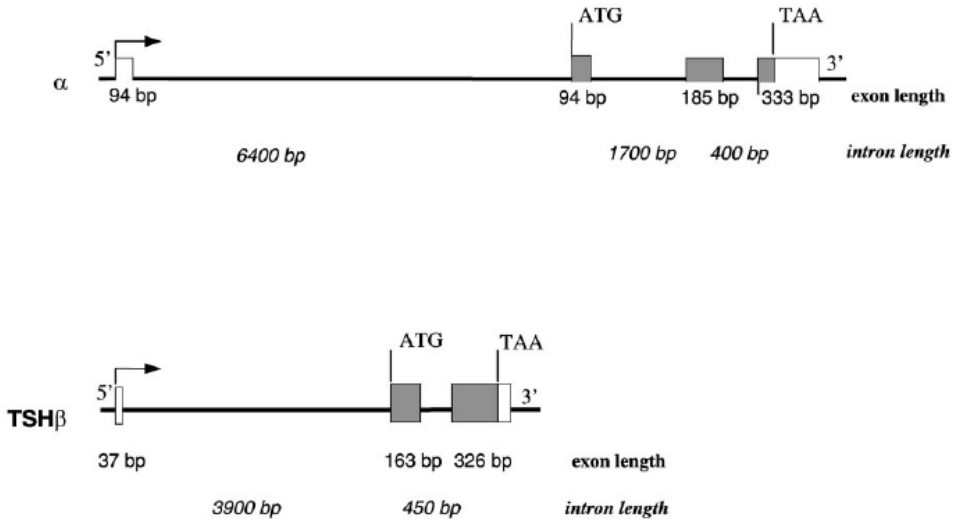

Figure 1.5: Structure of α and β TSH subunit genes. Exons are denoted by the boxes, and introns or flanking DNA sequences are denoted by lines. The length of exons and introns are shown in base pairs. Coding regions of exons are shaded; noncoding regions are white. Transcription start site is shown by a bent arrow. Adapted from SZKUDLINSKI *et al*.[14].

TSH is glycosylated, which protects it from intracellular degradation, and it also enables it to fold properly by allowing the formation of disulfide bonds. The carbohydrate chains in the human TSH constitute 15-25% of its molecular weight [14-16].

The human TSH α subunit has two carbohydrate chains linked to Asn-52 and Asn-78, respectively, and the human TSH β subunit has one carbohydrate chain attached at Asn-23 (**figure 1.6**). The carbohydrate chains of the α subunit are particularly important for TSH stimulated post-receptor transduction [17] while glycosylation of the β subunit is essential for its stability and secretion [18]. The two carbohydrate chains in the α subunit have different functions: the glycosylation site at Asn-78 has a role in the integrity of the hormone as the carbohydrates joined to Asn-78 take part in the 'folding' of the β subunit, while the carbohydrates joined to glycosylation site Asn-52 increase the stability of the heterodimer, making it therefore important for the association of the two subunits in the intact heterodimer of TSH

. The structure and charge of the three N-linked carbohydrate chains influence TSH activity; the most complex forms have lower activity but a longer half life [14,19].

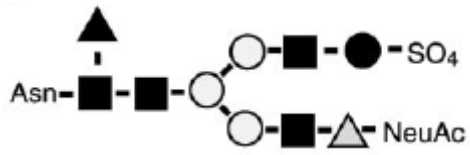

Figure 1.6: Typical N-linked oligosaccharides of human TSH. Carbohydrate residues are marked as follows: mannose (O), N-acetylglucosamine (_), N-acetylgalactosamine (●), fucose(▲), galactose (△),and sialic acid (NeuAc) (■) [14].

1.5 TSHR

TSHR is a G protein coupled receptor (GPCR) located on the basal surface of thyroid follicular cells. The TSHR structure is highly homologous between species when bovine [20], canine [21], human [22], murine [23], porcine and rat [24] receptor sequences are compared. A high sequence identity at both the nucleic acid and the amino acid level exists, with the overall DNA sequence identity varying from 75 to 90% between the different TSHR cDNAs. The human TSHR gene is located on chromosome 14q31 and is composed of 10 exons [25, 26]. The TSHR is a 764 amino acid protein with predicted

molecular weight of 84.5 kDa. TSHR, like most GCPRs, contains a large extracellular N-terminal domain or ectodomain (ECD), a 7 transmembrane domain and a short c-terminal cytoplasmic tail [25-27]. The 7 TMDs are joined intracellularly by connecting loops that interact with G proteins when the receptor is activated [28] whereas the extracellular loops, outside the cell, have secondary roles in receptor structure and activation (**figure 1.7**) [29]. The transmembrane domain and the intracellular domain are coded for by 9 exons (exon 2-8). The ECD domain is composed of a highly glycosylated structure of 394 amino acids coded by the tenth and largest exon. [25-27].

The TSHR structure includes 2 non homologous segments within the TSHR ECD (residues 38–45 and 316–366) not found in otherwise closely related glycoprotein hormone receptors such as luteinising hormone (LH) and follicle-stimulating hormone (FSH) [25-27]. TSHR, unlike the other glycoprotein hormone receptors, is first synthesised as a single chain molecule (precursor) and then cleaved into two disulphide-linked subunits [25-27]. The A or α subunit, wich comprises the large extracellular ectodomain is encoded by exons 1-8 and it binds TSH. The B or β subunit, which comprises a short transmembrane and intracellular domain, is encoded by exons 9-10 and interacts with G proteins to initiate signalling [25, 26]. The hydrophilic A subunit has a molecular weight of about 50 kDa and the hydrophobic B subunit has a molecular weight of about 35 kDa [25-27]. The ligand-binding glycoprotein A subunit is linked to the membrane-spanning B subunit by disulfide bonds [25-27]. The extracellular domain is approximately 414-418 amino acids long and contain six potential N-linked glycosylation sites in the human TSHR [25, 26].

Studies demonstrated that TSH does not bind with high affinity to recombinant TSHR ECD, expressed in isolation [30, 31]. However, when the TSHR ECD is anchored to the plasma membrane through a short lipid tail, the TSH is able to bind with high affinity

[32, 33]. Therefore, the TSHR ECD, consisting mainly of 9 leucine-rich repeats (LRRs) and an N-terminal tail, forms the binding domain for TSH.

Shepherd *et al.* used monoclonal antibodies that recognise a number of different sequences on the human native TSHR ECD [34]. This study concluded that region 337-342 is not involved in binding TSH, region 355-358 is near to an interaction site and region 381-384 is part of a TSH interaction site because all the antibodies which reacted with this site inhibited radiolabelled TSH binding. The findings from this study agrees with results from the Kosugi *et al.* study [32], in which a mutation of Tyr385 affected TSH binding and De Roux *et al.* [35] in which a mutation in Cys390 inhibited the binding of radiolabelled TSH. Overall these studies together conclude that region 381-384 of the TSHR is the ligand binding site of TSH. Recent studies have documented the tendency of G protein–coupled receptors to form homo- and heterodimeric forms, and these forms may have functional roles in protein trafficking [36], internalisation [37], receptor stability [38], and signalling [39]. While unstimulated TSHRs were found in multimeric forms [40], this multimeric state was reversed by TSH [41].

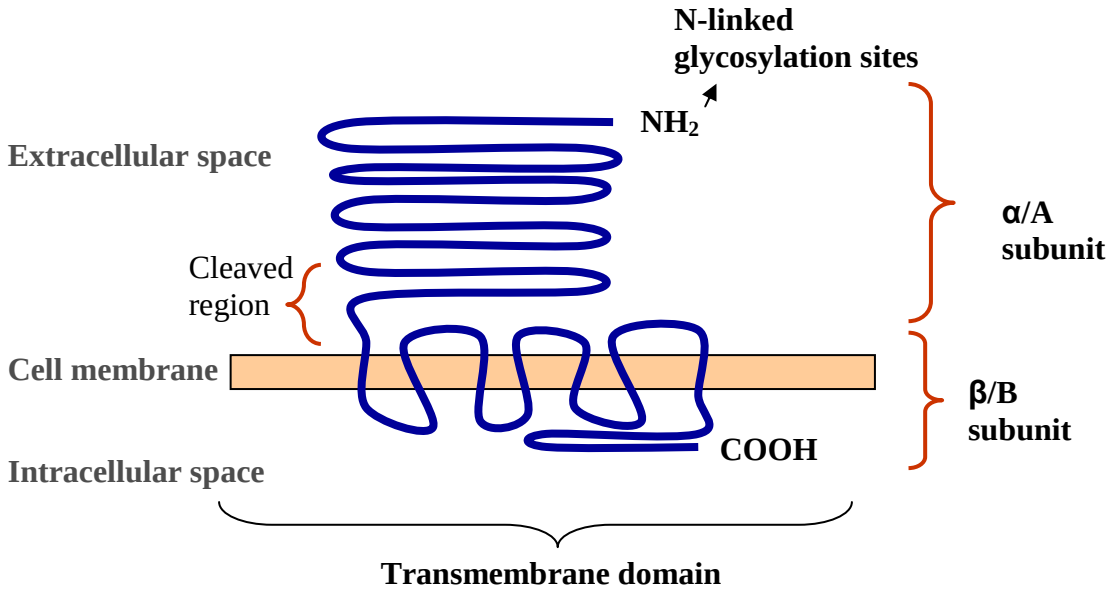

Figure 1.7: Thyroid stimulating hormone receptor structure. Adapted from [26].

1.6 Localisation of TSHR

TSHR has been shown to be expressed at low levels on the surface of thyrocytes [42] and the number of receptors expressed per cell vary from about 2 x 10^4 to 2 x 10^6 sites in different studies [43-45]. The expression of TSHR has been reported not only in the thyroid [11, 46-50] but also in several other sites including adipose [51], adrenal [52], brain[53, 54], eye [55], heart [56], kidney [52], skin [57], and thymus [52].

The physiological significance of the extra-thyroidal TSHR expression is still poorly understood. However, there have been several studies indicating that TSH may regulate the functions of many organs. For example it has been shown that it regulates the functions of intraepithelial lymphocytes as well as enterocytes via a TSHR-mediated mechanism [58]. In support of this concept, mice with TSHR mutations were reported to display signs of impaired gastrointestinal immunity [23, 58]. Additionally, further studies on TSHR knock out mice suggested that TSH may serve as a negative regulator of osteoblast and osteoclast formation [59,60].

1.7 TSHR internalisation

As with other GPCRs, prolonged stimulation of the TSHR by TSH leads to their internalisation into endosomes [61-64].

Internalisation not only serves as a major mechanism of signal desensitisation but also has been shown to function in receptor resensitisation [64-66]. Also, some GPCRs have been shown to translocate to the nucleus where they might activate gene transcription [67]. Upon agonist binding to the TSHR, the GPCR goes through a conformational change and G protein coupled receptor kinases (GPKs) then phosphorylate the agonist activated GPCR on intracellular domains. This initiates arrestin recruitment. Arrestin binding to the receptor inhibits G protein coupling and terminates signalling, a process called desensitization. Receptor/arrestin complexes are

then targeted to chlatrin-coated pits, where arrestin forms a multicomponent complex with clathrin, adapter protein 2 (AP2) and phosphoinositides, resulting in receptor internalisation into endosomes. The endocytosed receptors can either be dissociated from the ligand and the receptors recycled back to the cell surface or directed into the lysosomes where they are degraded (**figure 1.8**) [68, 69].

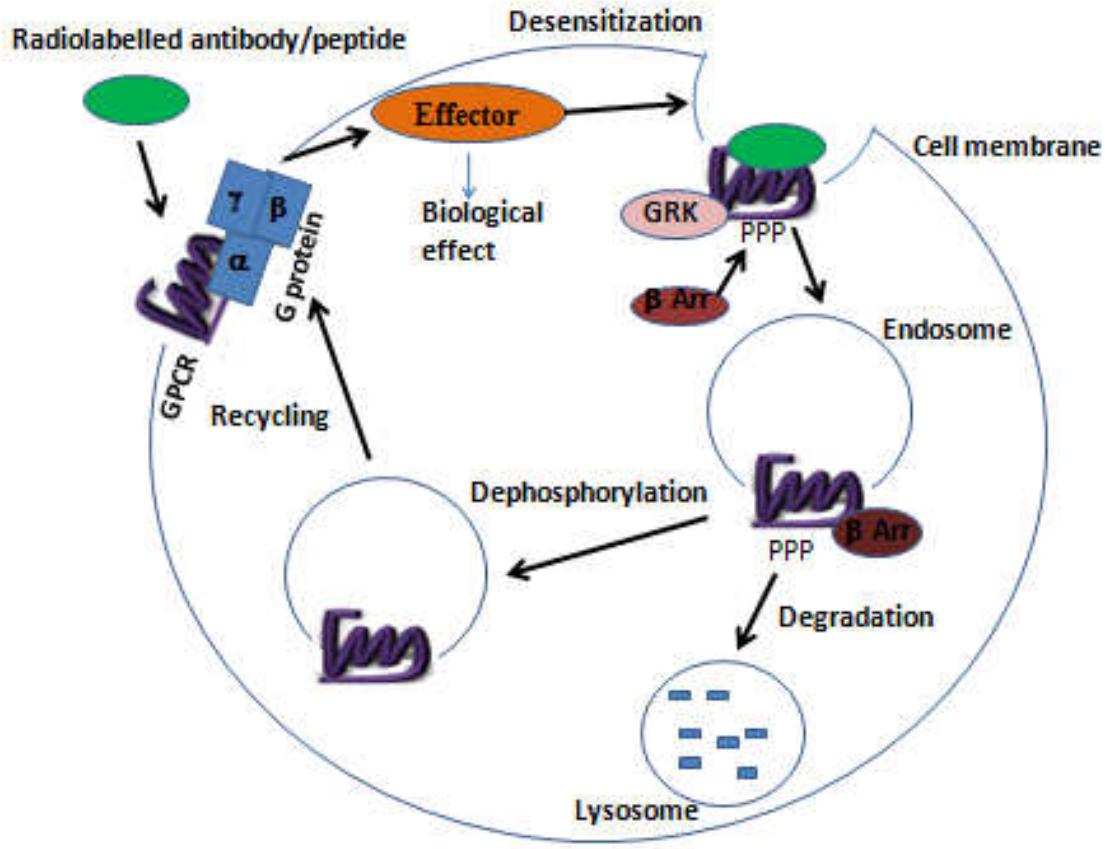

Figure 1.8: Receptor internalisation of GPCRs. Binding of radiolabelled antibody/peptide to the TSHR (GPCR) leads to the activation of heteromeric G protein, which in turn stimulate or inhibit effector proteins. Persistant stimulation of GCPRs leads to their phosphorylation by GRKs and GRKs recruitment of B-arrestins (Barr), events responsible for signal desensitisation. Subsequently, GCPRs are often internalised into endosomes. Internalised GPCRs are either targeted to lysosomes for degradation or dephosphorylated and recycled back to the membrane. Adapted from [68, 69].

1.8 The sodium iodide symporter (NIS)

NIS is a glycoprotein of 643 amino acids and molecular weight of 70-90 kDa. It has 84% amino acid identity with rat NIS. The NIS secondary structure was described by Levy *et a.l.* [70] and is composed of 13 transmembrane segments, one extracellular N-

terminal domain and one intracellular C-terminal domain. The transmembrane segments are composed of 20 to 28 amino acids, apart from the V segment that has 18 amino acids. The NIS protein contains 7 hydrophilic segments, 5 of which are extracellular [71]. The carboxy terminal is a large hydrophilic region composed of 94 amino acids and one potential site for cAMP dependent phosphorylation. NIS has 3 potential glycosylation sites: aspargine position 225, 485 and 497, that can be glycosylated in the endoplasmatic reticulum. Glycosylation is not essential for the function of the protein since non glycosylated NIS can be localised in the plasma membrane and transport iodide, with a similar value to the glycosylated NIS [70]. Levy *et al.* [70] conducted an *in vivo* study with high affinity anti-NIS antibodies in FRTL5 cells, and showed that NIS protein is initially synthesised as a precursor, with molecular weight of 56 kDa, and after glycosylation, it evolves into a mature form. In order for the iodine transport to occur it is necessary for the NIS protein to be expressed, migrated and localised in the plasma membrane.

1.9 NIS localisation

With the cloning of NIS in 1996 [5], molecular studies were performed to detect NIS expression in tissues. NIS mRNA expression was detected not only in the thyroid but also in non-thyroid tissues which have been shown to be able to concentrate radioiodine including salivary glands, stomach, thymus and breast [72, 73]. Lower levels of expression were detected in prostate, ovary, adrenal gland, lung and heart [72, 73].

Under physiological conditions, the salivary glands and stomach accumulate iodide via NIS, however in other glands, the functional expression occurs only in the final stages of pregnancy and lactation. The cDNA of the NIS cloned from these three organs is identical to the thyroid [72]. NIS mRNA was detected in various other tissues, however only salivary glands and gastric mucosa exhibit sodium dependent accumulation of

iodine and are sensitive to perchlorate [74] suggesting that the detection of mRNA is not sufficient for the functional expression of NIS.

1.10 Thyroid cancer

Thyroid cancer is one of the most common endocrine malignancies but overall constitutes less than 1% of all human cancers in the world [75-81]. Furthermore, there is evidence that thyroid cancer incidence is rapidly increasing in the western world [82]. Despite this relatively low figure, the prevalence of thyroid cancer in the western world is high (approximately 1 in 1000) due to the long survival of most patients [82].

The most common thyroid carcinomas are differentiated thyroid carcinomas (DTC) which account for 94% of thyroid cancers reported per year in the United States [75-81]. DTCs derive from thyroid follicular cells and cause either papillary or follicular thyroid cancer. Another 5% derive from the parafollicular cells of the thyroid and cause medullary thyroid carcinomas. DTC survival rates are generally high, ranging from 92 to 98% in the western world [75-81].

1 to 2% of thyroid cancers can de-differentiate into very aggressive thyroid cancers, which have an extremely low survival rate of 13% in the Western World [77, 80, 81, 83] and these de-differentiated thyroid cancers also account for more than half of the 1200 deaths per year attributed to thyroid cancer in the United States [80, 81, 83]. Long term survival of de-differentiated thyroid carcinoma is rare, with >75% of patients presenting cervical nodal disease, >50% of patients presenting with metastases and another 25% developing metastasis during the course of the illness [79, 82, 84, 85]. The most common sites of metastasis are the lungs (80%), bone (6-15%) and the brain (5-13%) [86]. Most de-differentiated thyroid cancers derive from a pre existing thyroid nodular goitre or DTC and are usually associated with p53 gene mutations [78, 80, 81, 86] . The peak incidence of the disease is from 60 to 70 and is most common in women

[78, 80, 81, 86]. De-differentiated thyroid carcinoma is usually characterised by being radioiodine resistant [78, 80, 81, 86]. This is due to the loss of the sodium iodide symporter (NIS), which is responsible for the uptake of iodine into the thyroid [87-89].

1.10.1 Diagnosis and treatment of thyroid cancer

The cancerous growth of thyroid tissue usually gives rise to abnormally high levels of TSH, T_4 and T_3 and the development of radioimmunoassay and, more recently, chemiluminescent and enzyme-linked immunoassays for T_4, T_3 and TSH have greatly improved the laboratory diagnosis of thyroid disorders [90]. However measurement of the total hormone concentration in plasma may not give an accurate picture of the activity of the thyroid gland as it does not distinguish between bound and free T_4/T_3. Most of the thyroid hormone circulating in the blood is bound to transport proteins. Only a very small fraction of the circulating hormone is free (unbound) and biologically active, hence measuring concentrations of free thyroid hormones is of great diagnostic value. When thyroid hormone is bound, it is not active, so the amount of free T_3/T_4 is what is important. For this reason, measuring total thyroxine in the blood can be misleading. When thyroid cancer is suspected, a thyroid nodule physical examination is normally conducted to detect a suspected abnormal growth [76, 77, 80]. However, this nodule examination cannot distinguish a benign from a malignant nodule. Fine needle aspiration cytology should therefore be carried out to determine if the nodule is malignant or benign [76, 77, 80]. If a malignant tumour is identified, surgery should be conducted to remove all cancerous tissue of the thyroid. Total thyroidectomy, where all (or virtually all) of the thyroid is removed is the most common chosen method as it results in a lower recurrence rate. Thyroidectomy is usually followed by radioactive ablative therapy with ^{131}I [76, 77, 80]. Ablative therapy with ^{131}I is carried out in order to kill most of the remaining thyroid cells to try and prevent the recurrence of the cancer

[76, 77, 80, 91]. Differentiated thyroid cancer cells are characterised by presenting a number of features that are found in the normal thyroid cells. For example, most differentiated thyroid cancer cells express proteins that are normally expressed in follicular thyroid cells, such as thyroglobulin and NIS [76, 77, 80, 91]. It is due to these features that patients with differentiated thyroid cancer can be given therapeutic doses of ^{131}I after total thyroidectomy [76, 77, 80, 91]. However, in some cases not all thyroid cancer cells are destroyed and this results in the recurrence of thyroid cancer. Approximately 10% to 30% of patients thought to be disease-free after initial treatment will develop recurrence and/or metastases [92]. In the majority of these cases, thyroid cancer recurs in the differentiated form. These patients again undergo radioiodine therapy which cures most cases. However, in a small proportion of patients the therapy fails and the cancer transforms into de-differentiated thyroid cancer which is associated with normal thyroglobulin levels but lack of radioiodine uptake [76, 77, 80]

1.10.1 Recurrent thyroid cancer

To diagnose differentiated recurrent disease, serum thyroglobulin testing (Tg) is used, followed by radioactive iodine (RAI) whole body scanning (WBS) [76, 77, 80]. Thyroglobulin is a glycoprotein that is produced only by normal or cancerous thyroid follicular cells. Therefore if a patient (after total thyroidectomy) has thyroglobulin in the blood, it indicates the presence of recurrent disease [76, 77, 80].

Although thyroglobulin testing already confirms the presence of thyroid cancer, it is essential to carry out a WBS, so that the cancer can be staged and metastasis detected. Staging thyroid cancer with WBS will also help to plan and prepare further treatment options [76, 77, 80].

Diagnosing de-differentiated thyroid cancer with WBS causes a major problem as de-differentiated tumours lose the ability to express NIS, which is responsible for the

uptake of iodide into the thyroid [91]. This results in the inability of WBS to stage de-differentiated thyroid cancer [78, 80, 81, 86].

De-differentiated metastatic cancer is usually untreatable and palliative approaches are used in order to increase the quality of life of the patient. Surgery is considered to relieve airway obstruction, however it does not usually alter the course of the disease. External beam radiation with ^{131}I has some benefits, though most of these cancers are resistant to radiotherapy and treatment is usually unsuccessful [76, 77, 80].

New treatment approaches have been evaluated for their ability to improve the outcome of de-differentiated thyroid carcinoma.

Studies in rat thyroid cancer cells (FRTL-Tc) without iodide transport activity showed that transfection with rat NIS cDNA using electroporation restored radioiodine accumulation *in vitro* and *in vivo*. However, the effective half life of ^{131}I in NIS-transfected FRTL-Tc xenografts in rats was only 6 hours and did not allow a therapeutic effect of ^{131}I (1 mCi) [93]. Mitchell *et al.* [94] reported that 10 of 17 patients who received high dose radiotherapy had a partial or complete response, however the toxicity was intolerable [94]. De-differentiated thyroid cancer treated with radiotherapy in combination with doxorubicin (used as a radiosensitizing agent) was also studied, but results were again poor [95]. Hyperfractionated local radiotherapy studies have also been carried out, but again, initial results were disappointing, particularly due to the high sensitivity of patients to adverse effects caused by radioiodine radiotherapy [95].

Overall, none of these approaches so far proved successful in the treatment of de-differentiated thyroid cancer. It is therefore essential to carry out more research in this area.

1.11 Use of rhTSH

Post-thyroidectomy radioiodine ablative therapy of thyroid remnant tumour is recommended for many patients with differentiated thyroid carcinoma (DTC). Even in those patients in which recurrence rates and mortality are not directly modified by this treatment, the follow-up with serum thyroglobulin (Tg) and iodine-131 scanning facilitates the ablation of thyroid remnants [76, 77, 80] . After the initial treatment of DTC, the recurrence rate can reach 35% in a period of 40 years, with most cases in the first decade.

Therefore, the long-term follow-up, especially in the first year after treatment, is fully justified. Whereas the early detection of relapse may influence the outcome of therapy , sensitive tests should be used to follow these patients.

The measurement of Tg and TSH in serum is currently the most sensitive test for the diagnosis of persistent or tumor recurrence [76, 77, 80]. The radioactive whole body scan is traditionally, the most frequently used test to be used to identify the location of metastases, however, some metastasis still cannot be detected with this diagnostic scan and for these a new tracer, the ^{18}F fluorodeoxyglucose (FDG) has proved promising. ^{18}F-FDG is a radiolabelled sugar (glucose) molecule. Imaging with ^{18}F-FDG PET is used to determine sites of abnormal glucose metabolism and can be used to characterise and localise many types of tumours.

In order for the radioactive iodine whole body scan and the FDG positron emission tomography to be successful, high levels of TSH are required [76, 77, 80]. High TSH levels lowers thyroid hormone levels and causes the pituitary gland to release more TSH, which in turn stimulates thyroid cancer cells to take up the radioactive iodine. Until recently this was only possible through the withdrawal of thyroid hormone, therapy, resulting in a poorer quality of life, due to symptoms of hypothyroidism (i.e

tiredness, depression, weight gain, sleepiness, constipation, muscle aches, and reduced concentration), aggravation of the disease and the possibility of tumour growth due to prolonged exposure to elevated TSH. Another way to raise TSH levels before a scan is to administer an injectable form of TSH (rhTSH or Thyrogen®) to the patient, which can make it unnecessary to withhold thyroid hormone therapy for a long period of time and thus avoids the side effects caused by thyroid hormone withdrawal [96]. Since its approval for clinical use in 2001 in Europe (1998 in the USA), rhTSH has greatly enhanced the surveillance of thyroid cancer patients [96].

Currently, rhTSH is only approved for diagnostic monitoring of differentiated thyroid cancer patients. However, rhTSH can potentially also be used to assist treatment of patients with thyroid cancer and nodular goiter.

rhTSH was successfully produced *in vitro* by transfecting both the TSH β subunit and common α subunit into Chinese hamster ovary cells (CHO) [96-98]. The recombinant TSH produced in CHO cells is not glycosylated as the endogenous TSH produced by the human thyroid, as CHO cells do not have the ability to fully glycosylate the TSH. rhTSH produced in CHO cells is therefore mostly made of TSH in which the three carbohydrate chains terminate in sialic acid residues without the penultimate N-acetylgalactosamine and terminal sulphate moieties [96-98].

Still, studies performed with rhTSH demonstrated that rhTSH mimicked endogenous human TSH as rhTSH stimulated cAMP, cell proliferation and Tg production *in vitro* [99].

The effect of rhTSH has also been comprehensively studied in mice [100] , which makes the mouse a good species candidate to study the effects of TSH *in vivo*. In mice, rhTSH induces an increase in T_3 levels [100], while in humans, rhTSH has been shown to increase the levels of T_3 and T_4 [101] and also to increase radioactive iodine uptake [102].

Although rhTSH has only been approved for the diagnostic imaging of thyroid cancer, some studies demonstrated that it can also be used successfully to prepare patients for thyroid remnant ablation with ^{131}I [103, 104]. This is because high levels of TSH in the blood would lead to an increase in NIS expression and consequently result in a more successful radioactive iodine therapy. rhTSH was also found to be successful in the ^{131}I treatment of recurrent metastatic differentiated thyroid cancer, where patients were stimulated with rhTSH prior to ^{131}I treatment [105].

1.12 NIS in thyroid tumours

The ability of the thyroid to concentrate iodine has great importance in the evaluation, diagnosis and treatment of various thyroid maladies including cancer. The understanding of the complex mechanisms that regulate the uptake of iodine via NIS, could potentially lead to better therapy options in tumours that cannot uptake iodine. One of the first hypothesis proposed for the reduced function of NIS was the mutation of the NIS gene, however Russo *et al.* [106] did not find any mutation in the samples of papillary cancers studied. By using RT-PCR, Rturi *et al.* [107] found the loss of expression of NIS in some papillary, follicular and anaplastic tumours. In 1997, Smamik *et al.* [74] detected lower levels of NIS mRNA in thyroid cancer samples compared with normal thyroid tissues, using Northern blotting. Other authors that quantified NIS mRNA with RT-PCR also found lower levels in tumour nodules [108], [109].

From these studies it can be observed that varying levels of NIS mRNA expression are found in thyroid cancers. However, these variation found in levels of mRNA may not reflect the expression of NIS protein, nor its cellular localization, since NIS goes through a complex transcriptional, post-transcriptional and post-transductional process.

So the mere fact that mRNA is present is not sufficient to indicate the quantity of NIS protein, localisation or function [110]. Neumann *et al.* [108] showed that NIS mRNA quantity did not reflect the quantity of NIS protein expression in cold nodules of thyroid, suggesting that post-transcriptional factors play an important role. For this reason it is important to also study the expression of the NIS protein which can be done via immunohistochemistry. One advantage of this technique is that it also gives indication about the cellular localisation of NIS protein. Immunohistochemistry studies of NIS protein in thyroid tumours showed a decrease in the basolateral localisation of the protein, when compared with normal tissues. Cailou *et al.* [111] studied follicular, papillary and anaplastic cancers and showed decreasing immunoereactivity for the NIS protein in follicular and papillary cancers and lack in anaplastic cancer which suggested that the higher the de-differentiation, the lower the immuno-positivity of the protein. Jhiang *et al.* [112] did not detect NIS protein in a small sample of thyroid cancers and Castro *et al.* [113, 114] confirmed the lack of immunopositivity of NIS protein in anaplastic and Hurthle cells.

It is apparent from these studies that there are discrepancies in the NIS expression profile. These reported differences could be due to a number of reasons such as: methodologies employed, non-pairing of tumour samples, size of analysed samples, lack of information about TSH value in patients and possible use of levothyroxine, histological types analysed and finally the complexity of transcritptional and post-transcriptional processes in the synthesis of NIS.

1.13 TSHR in thyroid tumours

It is thought that reduced TSHR expression in thyroid cancers may occur as a consequence of de-differentiation and it has been shown that loss of TSHR expression is usually associated with loss of a number of thyroid differentiation markers.

A study by Gerard *et al.* [115] used immunohistochemistry in order to detect thyroid specific markers such as thyroglobulin, T_4-thyroglobulin, NIS, penderin, TPO, THOXs and TSHR. In this study normal human thyroid tissues were used together with thyroid cancer tissue samples. This study concluded that TSHR was expressed not only in normal thyroid tissue but also in lower levels in follicular and papillary thyroid cancer tissues. It concluded therefore that TSHR was expressed in virtually all cases of thyroid tissues.

Another study used RT-PCR and RNase protective assays to measure the expression of NIS, Tg and TSHR mRNA in primary and metastatic thyroid carcninoma tissues [116]. The expression of NIS, Tg and TSHR mRNA was studied in 23 cases of papillary carcinoma and the expression of NIS mRNA was studied in 7 pairs of primary and lymph node metastastic tissues. The expression of TSHR was detected in all papillary carcinoma samples however at lower levels than normal thyroid tissue [116]. Matsumoto *et al.* [117] investigated 15 papillary thyroid cancer tissues, 8 poorly differentiated thyroid cancers (which are defined between differentiated papillary thyroid cancer and de-differentiated cancer) and de-differentiated (or undifferentiated) thyroid cancer using immunohistochemistry. All papillary thyroid cancer tissues and poorly differentiated thyroid cancer tissues expressed TSHR. However the undifferentiated (de-differentiated) thyroid cancer tissue did not express the receptor. Another group [118] assessed the expression levels of TSHR, Tg and TPO mRNA in normal and neoplastic human thyroid tissues, 6 adenomas and 7 carcinomas, were investigated by Northern-blot and slot-blot analysis. The authors found that TSHR mRNA expression together with Tg mRNA levels were significantly lower in cancer tissues than in normal thyroid tissues. These results suggest that TSHR mRNA is expressed in relation to their degree of differentiation. Elisei *et al.* [119] used Northern blot analysis to study the mRNA expression of the TSHR, Tg, TPO, and calcitonin (CT)

genes in a total of 53 tissues from 30 patients with thyroid carcinoma and from 9 patients with benign thyroid diseases. With various degrees of expression, all differentiated thyroid carcinomas (20 papillary and 2 follicular) expressed TSH-R, Tg, and TPO, but not calcitonin mRNAs. On the contrary, samples from 2 patients with anaplastic carcinoma did not express TSHR, Tg, or TPO mRNA, but 1 of them expressed calcitonin mRNA. This study concludes that TSHR is expressed in all follicular and papillary thyroid cancers and in some medullary thyroid cancers. The expression of TSHR in anaplastic thyroid cancer was however lost.

From the majority of these studies it is clear that TSHR is expressed in most cases of thyroid cancer, however there is a trend to its expression decreasing in relation to the levels of ongoing de-differentiation of the tumours. It is also noted from looking at these different studies that there appears to be discrepancies in the reported levels of expression of the TSHR in the different samples of thyroid carcinoma. This could be due to the sensitivity of the methodologies employed, differences in the tumour samples used in different studies, and differences in the sizes of the tissue samples.

1.14 Use of Monoclonal antibodies for the diagnosis and treatment of cancer.

Antibodies have a molecular weight of approximately 150 kDa and are composed of two polypeptide chains, a heavy chain (50 kDa) and a light chain (25kDa) [120]. The two chains are bound together by disulphide bounds. These molecules can be proteolytically cleaved to yield two Fab fragments (the antigen-binding part of the molecules) and an Fc fragment (the part of the molecule responsible for secondary biological functions of the antibody, e.g. the complement activation). Both the heavy and light chains are divided into V (variable) and C (constant) regions [120]. The V regions contain the antigen-binding site and the C region determines the fate of the bound antigen (**figure 1.9**).

.

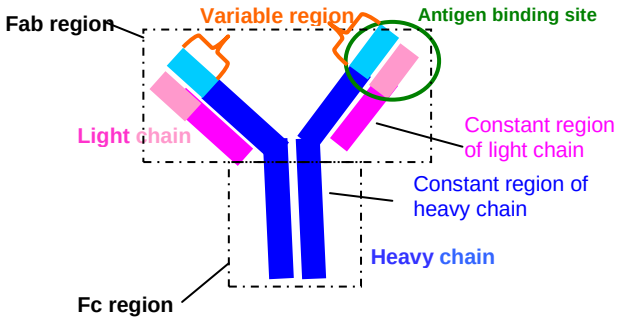

Figure 1.9: Structure of IgG antibodies. Adapted from [120].

Antibodies have two main functions in the body. Firstly they recognise and bind with high specificity and affinity to a specific target (antigen) usually located in a bacterium, virus, or other pathogen but it can also be located on our own tissues. After binding to an antigen, they also stimulate a secondary immune response to the antigens (e.g. complement activation and phagocytosis) [120].

The invention of a manufacturing process using hybridomas allowed monospecific antibodies to be generated [121]. This procedure has been standardised and applied on a massive scale to the preparation of monoclonal antibodies useful for research and clinical applications [120]. The basic technology involves fusion of an immortal cell with a specific predetermined antibody-producing B cell from immunised animals (usually mice). The resulting hybridoma cell is immortal and synthesises homogenous specific mAb which can be made in large quantities [121].

Cancer targeting with monoclonal antibodies have proved advantageous, particularly due to the antibody specificity as well as effective manufacturing processes. [122, 123].

Usually conventional cancer treatment using chemotherapy has produced a number of side effects (such as hair loss, fatigue, nausea,vomiting, and depression of the immune system) as they also damaged non cancerous healthy cells. Antibody therapy has the potential to reduce these side effects by only targeting specific proteins/molecular

pathways that are primarily found in cancer cells [122, 123]. These target proteins/molecular pathways in cancer cells should be ideally present in high levels [122, 123]. The recent manufacturing process using hybridoma technology followed by purification also ensures that mAbs for radiolabelling are homogenous and free of contaminants that could compromise their safety and efficacy.

Attaching radioactive compounds to monoclonal antibodies offer the potential of increasing the effectiveness and decreasing the side effects of radiotherapy [124-129]. The monoclonal antibodies used in radioimmunotherapy act as vehicles that transport the therapeutic radioiosotope to the tumour and these antibodies have cytotoxic effects mediated by apoptosis, complement-dependent cytotoxicity (CDC) and antibody-dependent cellular cytotoxicity (ADCC). Furthermore the characteristics of the antigen against which a particular antibody is directed determines, in most cases, the efficiency of both the antibody and the directed radiation. In this way, the choice of antibody, target antigen and radioisotopes are critical for the success of radioimmunotherapy [124, 125].

The ideal radiopharmaceutical should after *i.v* injection, travel to target cells and interact exclusively with the desired protein, then quickly be excreted from the body [123, 126, 127]. A successful radioimmunopharmaceutical should be retained in the site of the tumour in enough quantities and for long enough in order to destroy the tumour. The success of a radioimmunopharmaceutical depends on five main parameters: physical characteristics of the radionuclide, access to the tumour, specificity of the antibody, affinity of the antibody, and *in vivo* stability of the radionuclide in the site of tumour. The specificity of radiolabelled monoclonal antibodies is determined mainly by the antigens that they are directed against, which should be specific to the tumour with minimal or no expression in non cancerous tissues. However, in practice, the majority of antibodies are not solely specific to the tumour. This means that epitopes to

which the antibody binds are also expressed on the surface of non tumour cells, organs and tissues (depending on the antigen), although usually in smaller percentages or reduced numbers [124].

The first radiolabelled monoclonal antibody to be approved by the FDA for the diagnostic imaging of cancer was an ^{111}In labelled monoclonal antibody, CYT-103 (OncoScint OV/CR). CYT-103 is a murine monoclonal antibody (mAb) that binds to TAG-72, a cell surface antigen expressed at high levels on the majority of colorectal and ovarian adenocarcinomas. ^{111}In CYT-103-mAb imaging in patients with suspected recurrent colorectal carcinomas prevents many patients from undergoing unnecessary surgery.

So far, two radiolabelled antibodies have been approved by FDA for the treatment of non-Hodgkins lymphoma, ^{131}I-tositumomab (Bexxar) from Corixa Corporation and ^{90}Y-tiuxetan-ibritumomab (Zevalin) from Schering corporation [128, 129]. Both are murine mAb and target the CD20 antigen expressed on the surface of normal and malignant B lymphocytes [128-131]. These radiolabelled antibodies have proved very successful in comparison with chemotherapy and unlabelled mAbs [128-131].

Antibodies can also be conjugated to drugs or toxins to make them more effective.

For example, a recombinant anti-CD33 monoclonal antibody attached to the cytotoxic anti-tumour antibiotic calicheamicin (Mylotarg, Wyeth pharmaceuticals) has recently been approved by the FDA for the treatment of Acute Myeloid Leukemia. After binding to the cancer cells, the anti-CD33 antibody- calicheamicin conjugate is internalised and the toxin binds to the minorgroove of DNA, causing double strand DNA breaks and resulting in inhibition of DNA synthesis, which leads to cell death [132-135].

Although antibody-based therapy has proved successful, some problems have been encountered [122, 136]. One problem was the murine origin of most mAbs, which

caused the immune systems of patients to recognise them as foreign proteins and therefore inactivate them by stimulating host anti murine immune response. This anti murine immune responses may induce severe side effects such as nausea, chills, diarrhoea, vomiting, headache, seizures and coma. This problem was solved by the production of chimeric antibodies, in which mouse framework regions are replaced with human sequences [122, 136-138].

Another problem was the large size of mAbs which prevented them from being effectively distributed to certain tumours. It also resulted in them being cleared out at a slow rate from the body [122, 136, 137]. This was solved by creating smaller sized antibodies containing only the binding site region, Fab. The enzyme papain can be used to cleave a whole antibody into Fab fragments [122, 136, 137].

Also, variable regions of the heavy and light chains can be fused together by recombinant techniques to form a single variable fragment chain (scFv), which is only half the size of the Fab fragment but still retains the specificity of the antibody [122, 136, 137].

1.15 TSHR as a potential new target for the diagnosis and treatment and of radioiodine resistant thyroid cancer

TSHR ligands can potentially be used as imaging agents for thyroid cancer or to deliver drugs to cancer cells expressing TSHRs. TSHR ligands can also be used as probes to define the molecular mechanism of TSHR activation, that is, the conformational changes that mediate conversion of inactive to active states of TSHR. A number of different potential TSHR ligands have been developed, including TSH analogs, antibodies and small-molecule compounds.

While most de-differentiated thyroid carcinoma lose expression of NIS, some do continue to express thyroid hormone stimulating receptor (TSHR) [46, 47]. TSHR is

therefore a potential target for the diagnosis and treatment of metastatic recurrent de-differentiated thyroid carcinoma.

1.16 mab9 monoclonal antibody

mAb9 anti-TSHR antibody was developed by Gilbert *et al.* from an experimental murine model of hyperthyroid Graves' disease that exhibit potent thyroid-stimulating activity [139]. Graves' disease is an organ-specific autoimmune disorder characterised by a variety of circulating antibodies, including common autoimmune antibodies, as well as anti−thyroid peroxidase (anti-TPO) and antithyroglobulin (anti-TG) antibodies. The most important autoantibody in Graves disease is thyroid-stimulating immunoglobulin (TSI). These autoimmune stimulatory IgG antibodies bind and activate the TSHR [140, 141], reproducing the same actions of TSH on the thyroid. These thyroid-stimulating stimulatory antibodies cause release of thyroid hormone and thyroglobulin that is mediated by cyclic AMP, and they also stimulate iodine uptake, protein synthesis, and thyroid gland growth. As a result, iodide trapping by the thyroid increases, the synthesis and secretion of both T_3 and T_4 increase, and the thyroid grows in size producing a goiter. If untreated, the affected individual becomes hyperthyroid.

mAb9 monoclonal antibody was developed by injecting Balb/c mice with a recombinant adenovirus expressing the TSHR A-subunit and then selecting antibodies with the highest thyroid stimulating activity levels for hybridoma production [139].

mAb9 (KSAb1) and another antibody KSAb2 were selected due to their ability to inhibit TSH binding. The H and L chain subtypes for mAb9 and KSAb2 were shown to be IgG2b and IgG2a, respectively [139]. Both these antibodies were then tested to determine their thyroid stimulating activity, their ability to block of TSH-mediated stimulation (TSBab) activity, their ability to compete with ^{125}I-TSH for the binding of TSHR, as well as their ability to stimulate cAMP [139]. *In vivo* studies were also carried

out to assess the ability of both antibodies to induce hyperthyroidism [139]. The thyroid stimulating activity was measured with cAMP assays which determined the ability of both antibodies to stimulate cAMP production in CHO cells stably transfected with human TSHR (JP09 cells) [139]. Both antibodies showed full agonist activity by achieving near maximal cAMP stimulatory responses. The ability of mAb9 and KSAb2 IgG to block TSH-mediated stimulation of cAMP in TSHR expressed JP09 cells was measured [139]. mAb9 showed negligible thyroid stimulating blocking antibody (TSBAb) activity. Competition assays using TRAK II DYNO test human kits (tubes pre-coated with the TSHR) showed that 100 ng/ml of both antibodies was sufficient to inhibit 95% of ^{125}I-TSH binding [139]. Saturation assays performed in the coated tubes with ^{125}I radiolabelled mAb9 and KSAb2 were also performed and showed that both bound TSHR with high affinities of 4.5×10^{10} litre/mol and 6.25×10^{10} litre/mol [139]. Passive transfer studies on mAb9 and KSAb2 IgG were also performed in which 10 or 100 µg of both antibodies were injected *i.v* into mice, and the induced hyperthyroxinemia was measured [139]. This study concluded that these antibodies induced rapid hypersecretion of thyroxine, leading to hyperthyroidism with considerable morphological changes but with minimal mononuclear cell infiltrate in the thyroid glands [139]. Due to these characteristics, and particularly the ability of mAb9 to bind with high affinity to TSHR, mAb9 was used in this study as a potential candidate to target the TSHR.

1.17 4C1 monoclonal antibody

4C1 is a commercially available IgG2b mouse monoclonal anti-TSHR antibody. 4C1 cross reacts with human TSHR and it is predicted to also react with rat, pig, sheep, mouse, dog and cat TSHR. 4C1 binds to the native TSHR protein and studies showed

binding to residues 378-384 of the human TSHR. 4C1 antibody has been successfully used in immunohistochemistry and FACS studies to detect human TSHR [34].

4C1 was generated with recombinant ECD produced in *e.coli* [34]. 4C1 antibody inhibited the binding of ^{125}I-TSH by an order of 70-80% at 1 µg/ml however it did not stimulate cAMP production in human TSHR expressing cell lines. FACS studies also determined that 4C1 antibody bound to hTSHR [34]. This antibody was used as a positive control anti-TSHR antibody in this study.

1.18 Overview of thyroid cancer and TSHR expressing cell lines used

Cell lines are important tools to study mechanisms involved in cancer as well as to serve as pre-clinical models to assess the efficacy of novel therapies. Cell lines have the advantage of growing in cultures for long periods of time and hence being able to generate high volumes of research material. They can also be used in genetic manipulation studies, and for both *in vitro* and *in vivo* (xenografts) studies. Over the years, a number of thyroid tumour cell lines derived from different pathologic origins have been developed, including differentiated follicular carcinomas (FTC), papillary thyroid carcinomas (PTC) and de-differentiated highly aggressive anaplastic carcinomas (ATC). However a disadvantage that is associated with cell lines is that they lose their original phenotype. An additional problem is that some cell lines develop different phenotypes from cells in the *in vivo* tumours and current estimates indicate that 18 to 36% of cell lines are cross-contaminated or misidentified, including cell lines within the original supposedly reliable source [142-145].

1.18.1 FTC-133

The FTC-133 cell line was obtained originally from a lymph node metastasis of a differentiated follicular thyroid carcinoma from a 42-year-old male [146]. Their

morphology differs from flat polygonal to spindle shaped cells. These cells could be propagated in serum free medium, contained thyroglobulin and EGF receptors, lacked any fibroblast contamination, and responded to TSH and local active growth factors such as EGF and IGF with a stimulated (^{3}H)thymidine incorporation [146]. They were shown to retain differentiated thyrocyte function and responsiveness to TSH.

TSH was also shown to have the same stimulatory effects on metabolism, DNA synthesis and cell growth in FTC-133 cells as is observed in human endogenous thyrocytes. FTC-133 cells proved therefore to be of particular value in assessing the thyrotrophic effects that TSH stimulates in thyroid cells. Schweppe *et al.* used standard tandom repeat (STR) genetic analysis to compare their obtained profile for a number of selected thyroid cancer cell lines to those in cell lines databases (e.g. ECACC) [147]. This study found that FTC-133 profile was consistent with that of ECACC database. It also concluded that the FTC-133 cell line is unique and expressed high levels of Pax-8 and TTF-1 transcription factor mRNA, which confirmed the human thyroid origin. Paired box gene 8 (Pax-8) and thyroid transcription factor-1 (TTF-1) are specifically involved in thyroid development and are also involved in the regulation of the expression of thyroid-specific genes. Pax-8 and TTF-1 are used as markers of thyroid cancer cell lines because they are mainly found in thyroid cancer cells.

1.18.2 TPC-1

The TPC-1 cell line was obtained originally from a differentiated papillary thyroid carcinoma. This cell line was initially shown to retain differentiated thyrocyte function and thyrocyte responsiveness to TSH. Schweppe *et al.* found TPC-1 cell lines to harbour Pax-8 mRNA however unlike FTC-133 cells, TTF-1 mRNA was not detected. These results supported that TPC-1 cell lines were of thyroid origin. In another study [148], as was observed with the Schweppe study [147], Pax-8 thyroid transcription

factor was also detected in TPC-1 cells lines, however, in contrast with the Schweppe study, a small amount of TTF-1 expression was also detected. The cells were also found to contain a large number of chromosomal abnormalities, which suggests that this cell line although being of thyroid origin has most likely acquired characteristics of fully de-differentiated thyroid cancer cells.

1.18.3 FRTL5

The Fischer Rat derived thyroid cell line, FRTL-5, represents one of the best available *in vitro* models for studying thyroid specific proteins in a native thyroid cell line. The FRTL-5 cell line is a widely used model for normal thyroid function as these cells show responsiveness to TSH over a long period of time and also TSH stimulated iodide uptake, thyroglobulin (Tg) iodination and thyroid hormone secretion [149]. FRTL-5 cells exhibit a TSH-responsive adenylate cyclase, ion flux and phospholipid metabolic shift as well as an absolute growth requirement for TSH. These cells can lose their diploid characteristics while retaining functional characteristics, for a period of at least 1 year. However, after variable time periods, these non-diploid cells can lose responsiveness to TSHR autoantibody stimulators. Therefore, the uniformity of the FRTL-5 cells needs to be confirmed by monitoring of the thyroid markers. FRTL-5 cells are useful in three main assays. Firstly, they are employed to detect thyroid stimulating autoantibodies and immugobulin Gs present in the patients with Graves' disease by measuring the increase in cAMP levels [150, 151]. Secondly, they have been described to effectively measure the uptake of iodine, and thereby they have been used to measure the growth stimulatory or inhibitory activity of IgG preparations from patients with autoimmune thyroid disease by determining labeled thymidine uptake [150, 151].

1.18.4 GPI

In these cells, TSHR extracellular domain (ECD) is expressed in isolation on the cell surface of CHO cells with the use of a glycosylphosphatidylinositol (GPI) anchor sequence [152]. The GPI anchored ECD was recognised by experimental and pathological antibodies. Flow cytometry studies showed that the ECD was expressed at 10-fold higher levels than the highest expressing full length receptor clone [152]. Additionally, radioligand studies showed that the anchored ECD bound TSH with a high affinity similar to the full length TSHR [152]. This cell line proved to be useful in studying structure function relationships of TSHR as well as interactions of TSH, and anti-TSHR antibodies and autoantibodies with the TSHR [14, 153, 154].

1.19 Radiopharmaceuticals and cancer

Radiopharmaceuticals include any radiolabelled molecules that are used in the diagnosis and treatment of diseases. These radiolabelled molecules are designed to deliver diagnostic and therapeutic doses of ionising radiation to target sites within the body. Radiopharmaceuticals have the ability to kill cells through radiation and to emit radiation with sufficient energy and quantity to be detected externally. For this reason, radiopharmaceuticals can be useful in the diagnosis and treatment of cancer [155, 156].

The radionuclides of major interest in nuclear medicine are the ones with short half-lives. Several radionuclides are used to diagnose and treat diseases and conventional nuclear medicine began with applying ^{131}I (half life of 193 hours), exclusively to study the thyroid gland and it was later used in the radiolabelling of a number of radiopharmaceuticals. Another commonly used marker is ^{111}In (half life of 67 hours). ^{111}In allows for sequential imaging to be obtained over a period of a few days as well as it plays an important role in the evaluation of inflammatory diseases (such as leucocytes with ^{111}In) as well as in imaging with antibodies and peptides. ^{67}Ga (half life of 78

hours) is now widely used to trace tumours and infection sites, while ^{201}Tl (half life of 73 hours), is an agent used in myocardial scintigraphy. The most used radioisotope in nuclear medicine is ^{99m}Tc (half life of 6 hours) due to its favourable decay characteristics, it easy production in generators and its ability to radiolabel various molecules [155, 156].

1.19.1 Radiopharmaceuticals for therapy

Radiopharmaceuticals used for therapeutic purposes should be able to selectively destroy the tissue of interest. The design and selection criteria for therapeutic radiopharmaceuticals include; half-life, the types of emission (α, β, γ, auger or conversion electrons), specific activity, chemistry, internal dosimetry, intra-tumour distribution, pharmacokinetics of the radiopharmaceutical and size of the tumour [156]. In addition to their biological, physical and chemical properties, radiation safety, energy, cost of production and availability should also be taken into account when selecting suitable radiopharmaceuticals for therapeutic use [156]. The half life of the radionuclide should be in a range of hours to days for clinical applications. If the half-life is too short, there is not enough time to prepare the radiopharmaceutical for administration to the patient, as most of the decay will have occurred before the compound reaches the target tissue. On the other hand, if the half-life is too long the radiopharmaceutical can be metabolised/excreted, and also the number of disintegrations occurring at the target would be too low, which would result in an insufficient radiation dose being delivered to the tumour [156].

The specific activity of the radionuclide determines the mass of compound needed to achieve the desirable activity to perform the study. The molecular weight should be ideally be low and the specific activity high. If the specific activity is low only a small proportion of the administered molecules will be radioactive [156]. The nature of the

particle emission is also important to consider to ensure maximum therapeutic effectiveness. β-particles, α-particles and auger electrons all have different effective ranges and linear energy transfer (LET) properties. LET describes the rate at which energy is transferred from ionising radiations to soft tissue. The unit that quantifies LET is kiloelectron volts of energy transferred to soft tissue per micrometer of length traveled (keV/μm).

A β-particle is an electron emitted from the nucleus of a radioactive atom. β-particles are most widely used in targeted radiotherapy and have the advantage of relatively low homogeneous radiation doses but produce lower ionisation density and high LET [156]. The chemical properties of a radionuclide are also very important, because they determine if the radionuclide would easily label the molecules.

Radiation damage can result from direct ionisation of the DNA molecule, or some other cellular component critical to the survival of the cell. Such an interaction may affect the ability of the cell to reproduce and, thus, survive. If enough atoms are affected such that the chromosomes do not replicate properly, or there is a significant alteration in the information carried by the DNA molecule, then the cell may be destroyed. However, in clinical therapy, damage is most commonly caused by indirect ionisation via free-radical intermediaries formed from the radiolysis of cellular water. Radiation can also affect the processes of the cell cycle necessary for cell growth, cell senescence, and apoptosis [156].

1.19.2 Diagnosis

Radiopharmaceuticals used in diagnosis should be either gamma emitters or positron (B^+) emitters, because their decay generates electromagnetic radiation that can penetrate the tissues and this radiation can be detected and used to image [156]. The energy of the photons should be between 50 and 600 KeV.

Photons with very low energy (lower than 50 keV) have a greater chance of interacting with the body, and not being detected externally [156]. The radiopharmaceuticals used for diagnostic proposes may be classified into perfusion radiopharmaceuticals and target-specific radiopharmaceuticals. Perfusion radiopharmaceuticals are transported in the blood and reach the target tissue in proportion to blood flow. They do not have specific sites of binding and are thought to be distributed according to size and charge. Target-specific radiopharmaceutical are directed by biologically active molecules, such as antibodies and peptides that bind to cell receptors or are transported into cells [156].

1.19.2.1 Positron emission tomography (PET)

PET is a diagnostic technology which produces 3-D and CT images of the distributrion of positron emitters in the body. A tumour-targeting radiotracer is intravenously injected, and upon targeting the cancer, it emits positrons. A positron is a particle equivalent to an electron, however with positive charge. The collision of a positron with an electron causes the release of two gamma photons at 180° to each other. This coincidence of events can be detected, reconstructed and analysed to determine the location and concentration of radiation within the body. The subtracts targeted by the radioiosotopes in PET include cellular metabolic substracts, drugs, antibodies, neurotransmitters and other biologically active molecules [157, 158]. The images obtained provide information on blood flow, glucose metabolism, amino acid transport, neuroreceptors, oxygen consumption, amongst others.

The most common radiotracer in use is fluorine-18 bound to fluorodeoxyglucose [^{18}F]-(FDG). This tracer is a glucose analogue that is taken up by glucose-using cells (elevated in rapidly growing malignant tumours). As a result, FDG-PET can be used for diagnosis, staging, and monitoring treatment of cancers, particularly in Hodgkin's lymphoma, non-Hodgkin lymphoma, and lung cancer [159].

1.19.2.2 SPECT/CT

Single photon emission computed tomography (SPECT) has enabled the evaluation of disease processes based on functional and metabolic information of organs and cells. In SPECT, a single gamma-ray is emitted per nuclear disintegration. SPECT images are produced from multiple 2D projections by rotating one or more gamma cameras around the body to achieve complete 360° angular sampling of photons from the body. Reconstruction using methods similar to those used in X-ray CT provides 3D data sets allowing the tracer biodistribution to be displayed in orthogonal planes [160].

Because SPECT acquisition is very similar to planar gamma camera imaging, the same radiopharmaceuticals may be used. Integration of X-ray computed tomography (CT) into SPECT has recently emerged as a useful diagnostic tool in medical imaging, where anatomical details may complement functional and metabolic information [160].

SPECT/CT can be used in a range of malignancies such as prostate, lung, brain and neuroendocrine tumours as well as bone lesions and infections. In cardiology, SPECT is used to assess the viability of the heart muscle to help differentiate between ischaemia and infarction. In the brain SPECT is used to measure cerebral blood flow and brain patency in patients with stroke and tumour. Liver disease can be imaged using SPECT to determine the existence of sarcoma, hepatic tumour, haemangioma, metastases, cysts, glycogen storage disease, and Menetrier's disease. In the lung, radioisotope imaging is carried out most commonly to measure the ventilation and perfusion status of the lung.

PET cameras have the advantage over SPECT cameras of being more sensitive and possessing higher resolution. There is also higher flexibility to incorporate positron emitters into biomolecules, while PET's main disadvantage is its higher cost as well as the need for a nearby cyclotron. The SPECT system offers significant advantages relating to price, smaller size, ease of installation and the application of a large variety of procedures performed in nuclear medicine [160].

1.20 SPECT and SPECT/CT in thyroid cancer

Planar ^{131}I scintigraphy is routinely used to detect radioiodine avid metastases of differentiated thyroid carcinoma (DTC). However, the modality has limitations, such as low sensitivity and lack of anatomic landmarks. The use of radioiodine-131 (^{131}I) single SPECT/CT after thyroidectomy for thyroid cancer offers improvement over planar scans in detecting metastases, and can potentially be used to guide disease management. SPECT/CT can also avoid additional imaging tests for thyroid cancer evaluation and prompt changes in risk classification and treatment management among intermediate- and high-risk patients, according to a study [161, 162]. SPECT/CT has also been found to be useful in detecting thyroid cancer lymph node metastasis early [163]. Researchers were also able to accurately distinguish between cancerous cells in regional lymph nodes and normal residual thyroid tissue directly after surgery with SPECT/CT (**figure 1.10**) [164].

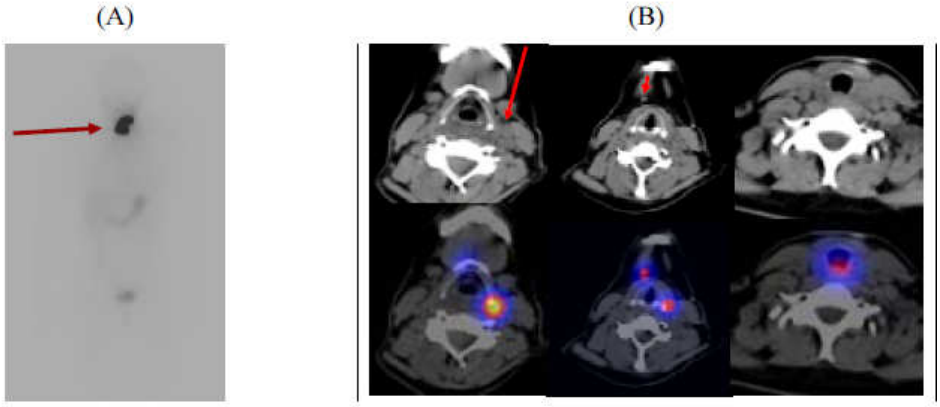

Figure 1.10: (A) SPECT/CT in thyroid cancer. The planar scan post-radioiodine ablation of thyroid remnants shows radioiodine-avid tissue in the neck of a patient after total thyroidectomy, without the possibility of discriminating ^{131}I uptake in remnant normal thyroid parenchyma from possible lymph node metastasis. (B) SPECT/CT demonstrates two cervical lymph nodes in this patient (arrows) that cannot be differentiated from benign remnant tissue in the planar scan [164].

1.21 SPECT/CT in small animal research

Non invasive imaging of molecular events and interactions in living small animal models using small animal SPECT/CT has gained increasing importance in researching

novel drugs and radiopharmaceuticals. The main advantages of this technology are quantitative accuracy independent of location in the subject body, and direct translation to human clinical setting. Also, imaging with small animal SEPCT/CT can substantially reduce the number of animals needed in order to obtain statistically significant data as well as the study in detail the biodistribution/kinetics of radiopharmaceuticals/radiotracers in tumour-bearing animal models [165].

The NanoSPECT system (Bioscan) uses a patented multiplexed, multipinhole SPECT technology that allows the system to operate in the sub-millimeter resolution range required to image small animals such as mice [166]. Instead of acquiring images through a single pinhole, NanoSPECT acquires images through thirty six or smaller pinholes. The use of small pinholes ensures high resolution (<1mm) while the projection of images through multiple pinholes simultaneously ensures high detection sensitivities [166]. Due to this approach, NanoSPECT manages to produce high resolution and high sensitivity images. To help locate tumours in the animal body, SPECT can be combined with CT. Numerous animal studies have been performed with a wide range of applications using nanoSPECT/CT technologies [165]. Animal studies are carried out by injecting an animal (usually mice) with the radiopharmaceutical (usually 37 MBq or less), placing it in the SPECT bed then collecting projections (typically 16 to 64) with an aim of 2 million total counts. Mice are imaged with a radius of rotation near 30 mm. The data acquired can be transferred to images or video formats, allowing for visualisation of the behaviour of the ligand *in vivo* over prolonged time points (**figure 1.11**). NanoSPEC/CT can be routinely used to image and to quantify NIS activity in mouse thyroids. Previous studies used ^{99m}Tc and ^{123}I to quantify the uptake of iodine via NIS into the thyroid of mice [167].

In this study SPECT/CT was used for *in vivo* imaging studies with both radiolabelled mAb9 and radiolabelled rhTSH.

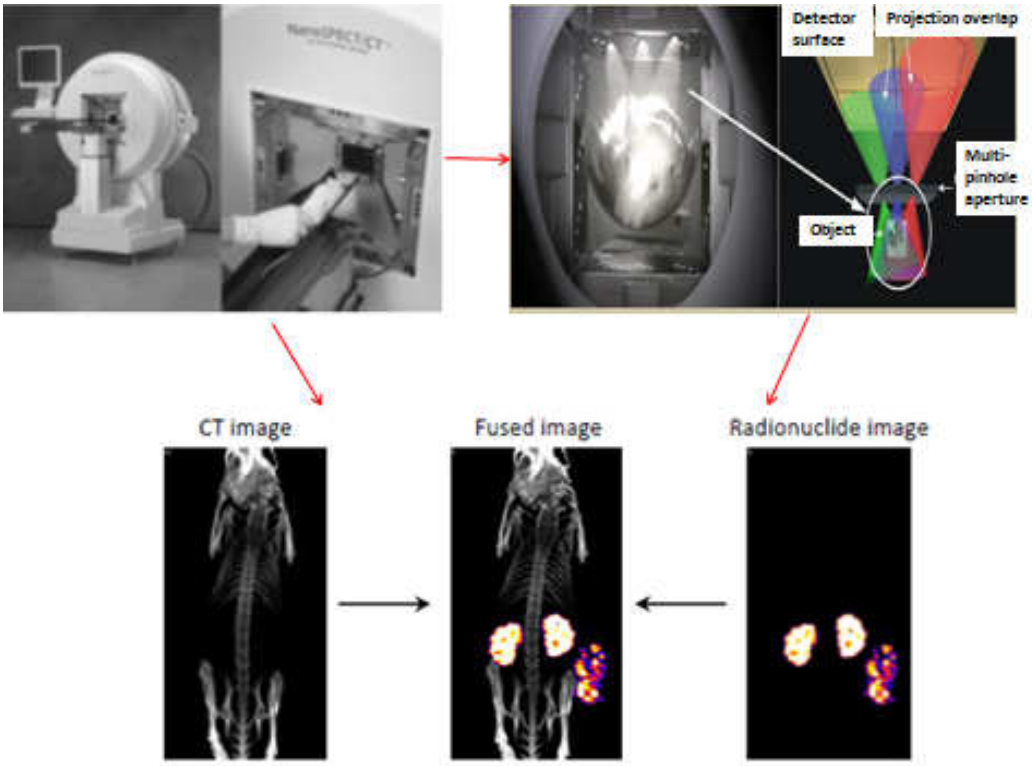

Figure 1.11: NanoSPECT/CT imaging. After administering a radiopharmaceutical or tracer the single photon emissions are projected through multi-pinholes on four detectors surrounding the mouse. Adapted from [168].

1.22 Radioiodination of monoclonal antibodies and peptides

A number of methods can be employed in the radioiodination of proteins, antibodies, antibody fragments and peptides.

Compounds can be directly radiolabelled through electrophilic oxidative substitution reactions that are catalysed by either oxidising agents, such as Iodogen or chloroamine T, or by enzymes, such as lactoperoxidase [169]. An overview of these reactions are given below.

Almost all proteins can be radiolabelled with ^{125}I, the radioactive isotope of iodine which has a half life of 60 days and which emits gamma radiation of 35 KeV [169].

The iodination is achieved by substituting a hydrogen atom on the phenyl ring of the tyrosine by one atom of oxidised iodine, via the activation of the ortho position of the aromatic ring of the tyrosine [169]. Additionally, ^{125}I can also be incorporated chemically and enzymatically into lysine, histidine amino acids in proteins or antibodies [169].

^{125}I is a gamma emitter, and for that reason it can be counted directly in a gamma counter without the need for sample preparation in contrast with beta emitting radionuclides such as ^{3}H and ^{14}C. For most purposes, it is essential to have the labeled species as pure as possible. However most radioiodinated compounds after the radioiodination procedure will contain some proportion of components such as unlabeled protein, free radioiodine, mineral salts and enzyme (in the case of lactoperoxidase). It is therefore important to apply purification methods to the radioiodinated compound before using it [169].

1.22.1 Radioiodination using Chloramine T

Radioiodination with chloramine T (N-chloro-p-toluene sulphonamide) is rapid and efficient. Chloramine T oxidises iodide into iodine, which reacts in turn with tyrosine and histidine residues of proteins (**figure 1.12**) [170]. With chloramine T, the iodination reaction is usually stopped by adding free tyrosine and sodium metabisulfite to the reaction mixture, which reduces the volatile iodine to iodide. The disadvantage of chloramine T is that some proteins may be oxidised in this process.

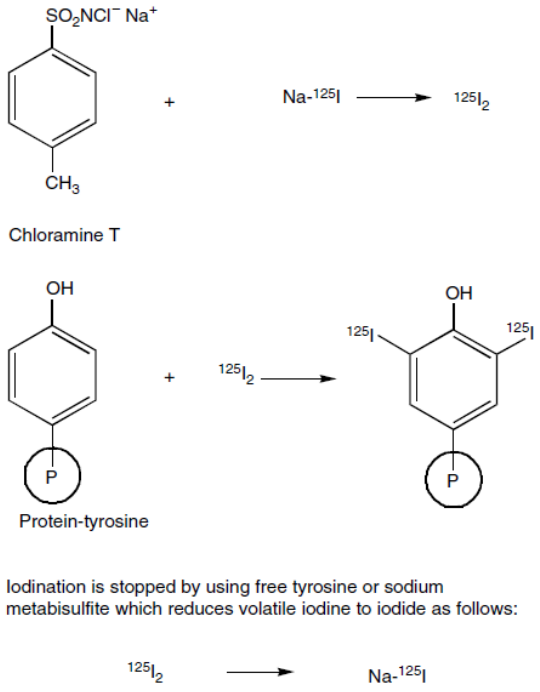

Figure 1.12: Iodination by Chloramine T. Iodide is oxidised to iodine (I_2),which reacts with tyrosyl and histidyl side chains of proteins. Adapted from [170].

1.22.2 Iodogen

Iodogen allows efficient incorporation of iodide and can be used with a great variety of proteins producing a stable labelling agent that remains stable for at least 3 months [171].

In this procedure, the oxidant iodogen (1,3,4,6-tetrachloro-3alpha,6alpha-diphenylglucoluril) is coated into a reaction vessel. A solution containing iodide and the target protein is then added to the vessel. Once added to the vessel, iodogen oxidises the iodide in the solution to free iodine (I_2) , which in turn reacts with tyrosine and histidine residues on the protein in the solution (**Figure 1.13**) [171].

In some sensitive proteins this oxidation can decrease the biological activities of the protein. However, antibodies are not generally affected by this oxidation, and therefore this method is often useful for antibody labelling.

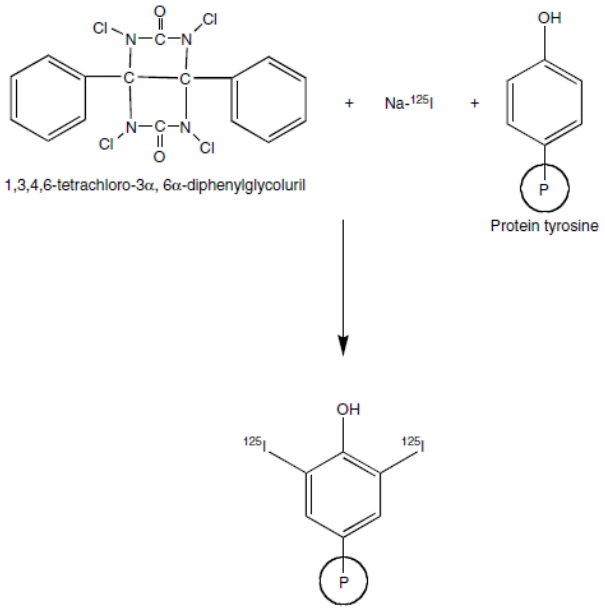

Figure 1.13: Iodination by Iodogen. Iodogen oxidises iodide to iodine, which then reacts with tyrosine and histidine residues of the protein. Adapted from [171].

1.22.3 Lactoperoxidase

This method, introduced by Marchalonis [172], employs lactoperoxidase in the presence of a trace of hydrogen peroxide to oxidise radioactive iodide to produce the reactive species I_2 or I^+. These reactive species substitute mainly into tyrosine residues of the protein, although substitution into other amino acid residues can occur under certain conditions (**figure 1.14**). Hydrogen peroxide can be obtained from a chemical stock or can be produced enzymatically, usually by using glucose oxidase. The oxidation can be stopped by simple dilution. This technique usually results in less denaturation of susceptible proteins than the chloramine T method, however it is sometimes technically demanding.

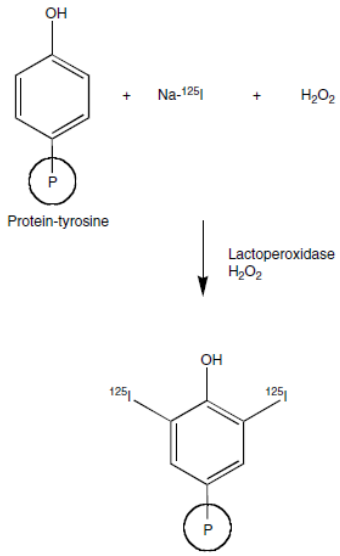

Figure 1.14: Iodination using Lactoperoxidase. Lactoperoxidase catalyses the oxidation of iodide to iodine in the presence of the oxidant hydrogen peroxide (H_2O_2). Adapted from [172].

1.23 Radiolabelling by conjugation

Metallic radioisotopes such as ^{111}In, ^{90}Y, ^{67}Ga do not form strong covalent bonds with protein structures and therefore they cannot be used to directly label the protein.

Techniques can however be used to indirectly complex these radioisotopes to proteins with the use of bifunctional agents [173]. In these techniques, proteins are first tagged by conjugating a suitable chelating agent to the protein that has a high affinity for one of the aforementioned radioisotopes.

A number of chelating agents have been developed and their chelating properties depend on the structure and lipophilicity that the chelating agents take up after being complexed to a protein. Ideally the chelator must form stable complexes with the radioisotope of interest, strong enough so that the complex does not dissociate in biological setting in which it will be used. It must also be possible to react the chelator with the protein without adversely affecting its chelating properties.

The first bifunctional chelating agents to be used were introduced by Sundberg and Meares [174]. These agents are EDTA (Ethylenediaminetetraacetic acid) and DTPA

(diethylene triamine pentaacetic acid). These compounds have been used extensively and form stable complexes with ^{111}In, ^{67}Ga and ^{90}Y. However, administration of some DPTA conjugated ^{90}Y radiolabelled monoclonal antibodies to humans has been shown to lead to hematopoietic toxicity due to detachment of ^{90}Y from the antibody and subsequent absorption of free ^{90}Y into the skeleton [175]. In the late 1990s other chelating agents became available, the macrocyclic compounds known as 1,4,7-triazacyclononane-N,N',N''-triacetic acid (NOTA), tetraazacyclododecanetetraacetic acid (DOTA), diethylene triamine pentaacetic acid (modified DTPA) and 1,4,8,11-tetraazacyclotetradecane (TETA) [176, 177].

DOTA is a bifunctional chelating agent that is commonly used as to conjugate a number of different radioisotopes to proteins including radioisotopes that emit photons such as ^{111}In and ^{67}Ga, radioisotopes emitting positrons such as ^{68}Ga, ^{86}Y, ^{64}C and beta emitting ^{90}Y. DOTA has previously successfully been used to conjugate a number of peptides [178] including octreotide (DOTA-d-Phe(1)-Tyr(3)-octreotide) , lanreotide (DOTA-lanreotide), and vapreotide (DOTA- vapreotide). DOTA complexes are more thermodynamically and kinetically stable than the DTPA (diethylenetriaminepentaacetic acid) complexes. However, DOTA has the disadvantage of requiring a degree of heating to aid their formation, whereas the less stable DTPA complexes can be formed at room temperature. In this project, Scn-Bz-DOTA was conjugated to mAb9 and then radiolabelled with ^{111}In (**figure 1.15**).

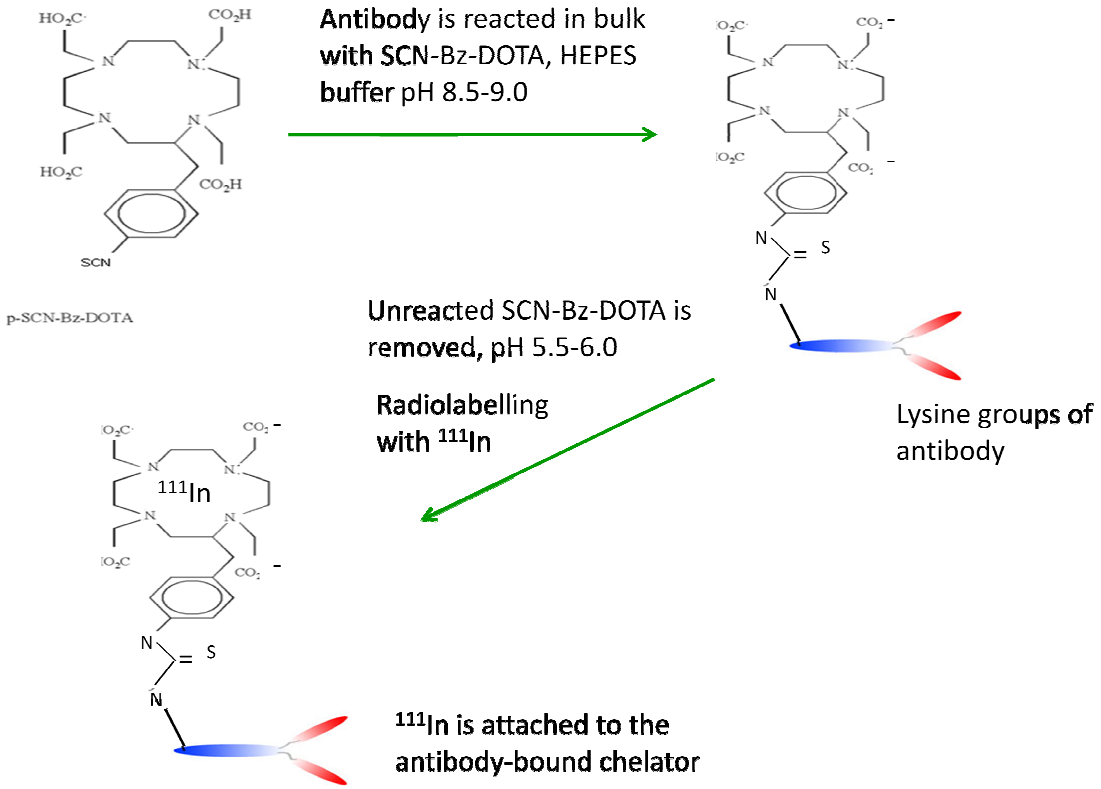

Figure 1.15: Schematic representation of ^{111}In labelling of ScnBzDota-antibody. Adapted from [173].

1.24 Scope of project

Radioiodine resistant de-differentiated thyroid cancer remains difficult to diagnose and treat. Survival rates are poor due to the lack of uptake of radioactive iodine, making it impossible to stage and treat the disease with conventional radioactive iodine therapy.

The rationale behind this project was to produce a radiopharmaceutical that would bind specifically to the TSHR, which has been shown by some papers to still be expressed in a number of de-differentiated thyroid cancers that have lost the ability to take up radioiodine into the tumour via NIS.

Ideally this radiolabelled compound would show robust binding to the TSHR, both *in vivo* and *in vitro*, and after an *i.v* injection, bind specifically to TSHR expressed in the thyroid or grafted thyroid tumours, clear the circulation rapidly and allow effective targeting of the cancer for diagnostic and therapeutic proposes.

The main aims of this project were three fold. The first aim of the project was to determine the level of expression of the TSHR in a number of different thyroid cancer cell lines *in vitro*. The second aim was to radiolabel mAb9 monoclonal antibody and subsequently rhTSH. The final aim of the project was to determine the binding affinity of radiolabelled mAb9 and rhTSH to TSHR expressing cells initially *in vitro* and then to the thyroid of mice, and to thyroid tumours grafted into mice.

1.25 Hypothesis

The hypothesis behind this project is that de-differentiated thyroid cancer cells continue to express TSHR, and therefore that the TSHR can be used to target radioiodine resistant thyroid cancer.

The hypothesis behind the mAb9 antibody chapter is that this high affinity radiolabelled anti-TSHR monoclonal antibody will bind to the TSHR *in vitro* in a number of differentiated human thyroid cancer tumours and *in vivo* in TSHR positive xenografted tumours and the thyroid of mice and thus can be of suitable use for the diagnosis and treatment of radioiodine resistant de-differentiated thyroid cancer.

The hypothesis behind the rhTSH chapter is that this well established peptide will bind to TSHR both in vitro and in vivo and thus can be potentially used in the diagnosis and treatment of radioiodine resistant de-differentiated thyroid cancer.

CHAPTER 2. MATERIALS AND METHODS

2.1 MATERIALS

Reagent	Supplier
0.25% (w/v) Trypsin – 0.53 mM EDTA solution	Cambrex
10x Tris/Glycine/SDS buffer electrophoresis grade	National Diagnostics
2x TY media	Cancer Research UK
3,3',5,5'-tetramethylbenzidine (TMB)	Sigma-Aldrich
4C1 anti-TSHR monoclonal antibody	Abcam, UK
A	
Acetone	VWR
Acetonitrile – HPLC grade	Aldrich Chemicals Co.
Agarose	Sigma-Aldrich
Albumin, bovine	Sigma-Aldrich
Ammonium persulfate	Sigma-Aldrich
B	
Beta-mercaptoethanol	VWR
Brilliant blue R staining	Sigma-Aldrich
Bovine serum albumin (BSA)	Sigma-Aldrich
SuperScript® III first-strand synthesis system	Invitrogen
C	
CHO (Chinese hamster ovary cells)	Clare Hall, Cancer Research
F	
Foetal bovine serum	Invitrogen
First strand cDNA synthesis Kit	Invitrogen
FTC-133 cells	Paul Banga, King's College
G	
D-(+)-Glucose (>99.5%)	Sigma-Aldrich
Glycerol	VWR
Glycine (>99%)	Sigma-Aldrich
Goat anti-mouse alexa488 IgG	Invitrogen
GPI cells	Paul Banga, King's College
H	
HEPES buffer	Sigma-Aldrich
Hydrogen peroxide (30%)	VWR
I [125I]	Perkin Elmer
ITLC-silica gel	Pall
L	

L-glutamine	Sigma-Aldrich
M	
mAB9 anti-TSHR monoclonal antibody	Kindly provided by Dr. Paul Banga
Marvel milk powder	Premier International Food Ltd
Methanol (HPLC grade >99%)	BDH Laboratory
MKN45 (human gastric adenocarcinoma cells)	Clare Hall, Cancer Research
Monoclonal anti-mouse IgG (whole molecule peroxidase)	Sigma-Aldrich
Mouse monoclonal anti-human GAPDH control	Abcam, Cambridge
Nitrocellulose membrane	BDH Laboratory
P	
Para-formaldehyde	Sigma-Aldrich
Phosphate-buffered saline (PBS)	Cancer Research
Pierce iodination tubes	Pierce
Polyacrylamide	National Diagnostics Ltd
PR1A3 monoclonal antibody	Nuclear medicine Barts hospital, London
Precision plus protein standard	BioRad
Protease inhibitors cocktail set I	Calbiochem
Protein assay kit	BioRad
R	
rhTSH	Genzyme, UK
S	Pierce
Slide-A-lyzer dialysis cassettes	Perkin Elmer
Sodium [125I]-iodide	
T	
Tetramethylethylenediamine (TEMED)	GE Healthcare
TPC-1 (thyroid papillary carcinoma cells)	Paul Banga, King's College London
Taq polymerase	Invitrogen
Triethylamine (>99.5%)	VWR
Trifluoroacetic acid (TFA) (>(99.5)	Thermo Scientific
Tween 20	Sigma-Aldrich
V	
Versene	Cancer Research UK
E3MM Blot paper	Whatman International Ltd

2.2 Methodology 1 (this methodology relates to the mAb9 results section)

2.2.1 Size Exclusion High Performance Liquid Chromatography (HPLC) to confirm the purity of mAb9 antibody

10 µl of mAb9 (1 mg/ml) (kindly provided by Dr. Paul Banga, King's College London). was injected into an high performance liquid chromatography (HPLC) system with a size exclusion Phenomenex BioSep-sec-s-2000 column (300 × 7.00 mm, 5 micron, Phenomenex) and a Beckman 166 UV detector (Beckman). mAb9 was analysed in Size exclusion HPLC (SE-HPLC) using 0.1M phosphate buffer pH 7.2, 10% EtOH and 100 mM EDTA (as a mobile phase for 30 minutes at a flow rate of 0.5 ml/min using UV detection at 168-280 nm.

10 µl of Bio-Rad's gel filtration standards (Biorad) were also analysed in SE-HPLC using the same settings in order to calibrate the size exclusion column and to determine the approximate molecular weight of mAb9. Bio-Rad's gel filtration standard is a lyophilised mixture of molecular weight markers ranging from 1,350 to 670,000 daltons. The mixture contains thyroglobulin, γ-globulin, ovalbumin, myoglobin, and vitamin B12.

2.2.2 SDS-PAGE electrophoresis of unlabelled mAb9

10 µg of mAb9 was analysed by SDS-PAGE using 10% homogeneous gels prepared from acrylamide in 0.375 M Tris-HCl, pH 8.8, containing 0.1% (w/v) SDS, 0.1% (w/v) ammonium persulfate and 0.1% (v/v) tetramethylethylenediamine (TEMED) for resolving gels, and in 0.125 M Tris-HCl, pH 6.8, containing 0.1% (w/v) SDS, 0.1% (w/v) ammonium persulfate and 0.1% (v/v) TEMED for stacking gels. Samples were heated in loading buffer at 95°C for 3 min to linearise proteins, and were run

concurrently with a protein standard in 1 x Tris-glycine-SDS buffer, pH 8.3, at 150 V and 40 mA per gel for 1.5 h. Gels were stained with Brilliant Blue R (0.5%, w/v) in ethanol:acetic acid:water (9:2:9, by vol) for 2 h to visualise bands for determination of molecular weights.

2.2.3 Maintenance of CHO, GPI, MKN45, TPC-1, FTC-133 and FRTL5 cell lines

Cell line	Description	Species
CHO	Chinese hamster ovary cells	chinese hamster
GPI	CHO cells stably transfected with TSHR	chinese hamster-transfected
FTC-133	follicular thyroid carcinoma	human
TPC-1	papillary thyroid carcinoma	human
FRTL-5	fisher rat thyroid glands	rat
MKN45	gastric adenocarcinoma cells	human

Table 2.1: Table of cell lines grown.

A short description of all cell lines used is given in **table 2.1.** The human cell lines TPC-1, FTC-133 and MKN45 were grown in Dulbecco's Modified Eagle Medium, DMEM (Invitrogen) that contained 10% of foetal bovine serum. CHO and GPI cells were grown in HAMS-F12 media (Invitrogen) with 10% FBS. FRTL5 cells were gown in HAMS-F12 media (Invitrogen) with L-glutamine supplemented with 10% charcoal stripped FBS and a mixture of insulin (10 µg/ml), hydrocortisone (3.6 ng/ml), transferrin (5 µg/ml), Glycyl-l-lysine acetate (10 ng/ml), somatostatin (0.01 µg/ml), bovine TSH (1mU/ml), MEM non essential amino acids (1x), and penicillin-streptomycin (100 µg/ml).

The cells were grown at 37°C in a 5% CO^2 incubator and were passaged when they reached 70-80% confluency. The cells were passaged by removing the media from the flask and washing them with 10 ml of autoclaved phosphate buffer saline (PBS). After washing, 3 ml of Trypsin/EDTA solution was added in order to detach cells from the flask. The majority of the trypsin was quickly aspirated and cells were incubated in a film of trypsin solution for 5 minutes before being diluted in a fresh aliquot of complete

growth media. The cells were then split into new filter-lidded T75 (75 cm) flasks at a 1 in 10 dilution. In the case of GPI cells, the antibiotic Geneticin was added every other passage. Geneticin antiboiotic is used for the selection of transfected mammalian cells.

2.2.4 Fluorescence activated cell sorting (FACS) analyses to determine levels of TSHR in TPC-1, FTC-133 and GPI cells.

FACS experiments were performed using FTC-133, TPC-1, FRTL-5 and GPI cells and with 4C1 (Abcam, Cambridge, UK) and mAb9 antibodies. FACS assays were also performed with the following preparations:

mAb9 incubated alone in an Iodogen tube- '***oxidised mAb9'***: in this preparation 10 µg of mAb9 was added to an Iodogen tube and incubated for 10 minutes.

mAb9 co-incubated with cold iodine (potassium [^{127}I] iodide-KI) in an Iodogen tube – *'cold labelled' mAb9:* In this preparation 10 µg of mAb9 was mixed with 0.11 µg of potassium iodide (quantity calculated to give 2 x mol of mAb9 antibody) and then added to an Iodogen tube and incubated for 10 minutes.

mAb9 mixed with potassium iodide (KI) – *'mixed mAb9'*: In this preparation 10 µg of mAb9 was mixed with 0.11 µg of Potassium iodide.

Cells were grown in 2 x T75 culture flasks and then detached from plates using versine when the cells reached around 80% confluency. The cells were then collected from the flasks into culture medium and centrifuged for 3 minutes at 1200 rpm. Next, the cells were resuspended in 10 ml 0.1% PBS/BSA solution. The cells were centrifuged again and the pellet resuspended at a concentration of 4 x 10^6 cells per ml. 50 µl of cells were added to 50 ml falcon tubes and placed on ice. Thereafter, 1, 5, 10 and 20 µg/ml concentrations of 4C1 antibody (abcam) and mAb9 were prepared in 0.1%PBS/BSA and kept on ice. A negative control isotype antibody was also made to 1, 5, 10 and 20 µg/ml concentrations in 0.1%PBS/BSA. 50 µl of the primary antibody was added to the test tubes and 50 µl of the control isotype was added to the control tubes.

The tubes were then incubated for 45-60 minutes on ice. After the incubation, the tubes were washed twice with 0.1%PBS/BSA solution by adding 2 ml to each tube and centrifuging for 3 minutes at 1200 rpm. After the second wash, the supernatant was poured off in order to leave about 50 µl of cell suspension in the tube. 50 µl of diluted Goat anti-mouse Alexa Fluor 488 secondary antibody at 8 µg/ml was added to each Flacon tube. The tubes were then left on ice in the dark for 30 minutes. Finally, the tubes were washed twice in 0.1%PBS/BSA, and the final pellet was resuspended in 400 µl of 0.1%PBS/BSA solution and kept on ice.

The samples were read in a flow cytometer LSR 1 (Becton Dickinson, New Jersey, USA) equipped with 3 lasers: an argon ion laser emitting at light 488 nm, a HeNe laser emitting light at 635 nm and a HeCd UV laser emitting light at 325 nm. 50 µl of propidium iodide (5 mg/ml) (Invitrogen, Paisley, UK) a nucleic acid stainer that detects cell death was added to the cells prior to the FACS reading. Both propidum iodide and Goat anti-mouse Alexa Fluor 488 secondary antibody are excited by the 488 nm laser. However, as they emit at different wavelengths, the Alexa Fluor 488 was detected by the FL1 detector and the propidium iodide was detected by the FL3 detector. A gate was set on a 2 parameter dot plot of forward scatter versus side scatter to exclude debris and another was set on a histogram of PI fluorescence intensity to include live cells (PI negative). A third gate was created to combine these two gates and events falling within this were analysed for expression of the TSHR. Data was analysed using CELLQuest software.

2.2.5 Immunohistochemistry of FTC-133, TPC-1, GPI and CHO cells

2.2.5.1 Coating of Glass Coverslips with Poly-D-lysine for Use in Cell Culture Experiments

13 mm glass coverslips were coated with poly-D-lysine (Sigma-adrich). Batches of ~300 coverslips were immersed and agitated in an 80% ethanol solution for 2 h at RT to sterilise the coverslips. The coverslips were then rinsed 3 x with sterile dH_20 to remove all traces of ethanol. Thereafter, the coverslips were immersed and agitated in a 0.1 mg/ml poly-D-lysine solution (made up in dH_2O) for 3h at RT. The coverslips were then again washed 3 x in dH_2O, this time to remove any unbound poly-D-lysine. The poly-D-lysine coated coverslips were then stored in dH_2O in a sealed sterile container kept in the fridge.

2.2.5.2 Visualisation of Staining using the HRP/DAB ABC Method

FTC-133, TPC-1, CHO and GPI cells were paraformaldehyde (PFA) fixed. After growing the cells as described in section 2.3.2, media was removed from the cultures, after which the cultures were washed with PBS, and then fixed by incubating the cultures in ice cold 4% PFA (dissolved in D-PBS, pH7.6) for 10 minutes at RT. The PFA-fixed cell cultures were washed with TBS (10 x TBS stock: 12.1g Tris (base), 40.0g NaCl, water adjusted to 500 ml, pH 7.6) and the cultures then incubated for 10 minutes in a 3% hydrogen peroxide solution (dissolved in H_2O) to inactivate any endogenous peroxidise activity. Thereafter, cultures were washed with PBS, and incubated for 10 minutes with blocking buffer (1% BSA and 10% NaAz dissolved in 0.5 M TBS, pH 7.6) to block non-specific binding sites. To detect TSHR, cells were then incubated with either mAb9 or 4C1 primary antibodies overnight at RT. In all cases, cultures were then incubated with a goat anti-human biotinylated secondary antibody (for 1 h at RT).

An avidin-biotin-HRP complex was freshly prepared using a Vectorlabs ABC kit solution (Vectorlabs). This was done by mixing/diluting solution A (Avidin-OH) with solution B (biotinylated HRP) in an appropriate ratio in TBS (10 µl of solution A and B was added to every 1 ml of 0.5 M pH 7.6 TBS solution. Sections were washed for 10 minutes in TBS to remove any excess unbound secondary antibody, and then incubated for 1 hour in the freshly prepared avidin-biotin-HRP complex to allow the complex to conjugate to the biotinylated secondary antibody bound in the sections. Sections were washed in TBS to remove any excess unbound avidin-biotin-HRP complexes. Finally, antigen localisation was visualised by incubating the sections in a 0.05% diaminobenzidine (DAB)/0.03%H_2O_2 solution dissolved in TBS (0.1 M TBS, pH 7.6) for 10 minutes. This results in a brown coloured stain developing in the close vicinity of the antibody-localised antigen, as the HRP enzyme converts DAB into a brown coloured water insoluble precipitate in the presence of hydrogen peroxide. Following this, sections were removed from the DAB solution and thoroughly washed in dH_2O to remove any remaining DAB solution from the slides. Sections were subsequently counterstained with haematoxylin to visualise cell nuclei. The sections were immersed in a Mayer's haematoxylin solution (0.1% haematoxylin, 5% alum, 0.02% sodium iodate, 2% acetic acid, dissolved in dH_2O) for ~ 90 seconds, and thereafter, the sections were thoroughly washed with dH_2O, and staining differentiated by immersing in a differentiation solution (0.5% HCl dissolved in 70% industrial methylated spirits (IMS) for ~60 sec. Thereafter, sections were firstly dehydrated by immersing them in 100% IMS for 4x 2 minute time-periods, and then subsequently cleared by immersing them in 100% xylene for 2 x 5 minute time-periods, with solution changes separating each immersion period. Glass coverslips were then finally mounted on top of the immunohistochemically stained sections using the hydrophobic mountant, dibutyl phthalate in xylene (DPX). Images of the HRP/DAB stained sections were acquired

using a standard Zeiss bright field microscope fitted with an Axiocam colour camera and using Axiovision image analysis software.

2.2.6 RT-PCR

There are two types of RT-PCR; absolute quantification and relative quantification. In the experiments carried out in this study, relative quantification was used. Relative quantification determines the change in expression of a nucleic acid sequence (target) in a test sample relative to the same sequence in a calibrator sample, which was a non-TSHR-expressing cell line, CHO. In addition an endogenous control housekeeping gene, Glyceraldehyde 3-phosphate dehydrogenase (GAPDH), was also run in parallel. GAPDH is expressed in all the samples at consistent levels and due to this its frequently used as a reference gene in RT-PCR reactions. The GAPDH endogenous control is used to normalise the quantification of the cDNA target for differences in the amount of cDNA added to each reaction. A two-step reaction was performed, in which total RNA was first transcribed into cDNA, and then amplified by PCR.

2.1.6.1 RNA Isolation

Cells were detached from flasks using Versene instead of 0.25% (w/v) Trypsin / 0.53 mM EDTA solution, to eliminate any possibility of the expressed receptor being cleaved. Detached cells were washed twice in PBS and the pellet was taken forward for RNA isolation using the RNeasy Mini Kit (Qiagen) as per manufacturer's instructions. A negative TSHR cell-line, CHO, served as the control. The kit comprises a spin column which allows up to 100 μg of total RNA of minimum length at 200 bases (mainly mRNA) to bind to a silica-gel membrane, with the aid of a specialised high-salt buffer. The addition of ethanol ensures the binding of total RNA to the column membrane, and contaminants are efficiently washed away.

The pellet, comprising approximately $5x10^6$ cells, (counted using a haemocytometer) was homogenised in 350 µl of lysis buffer containing guanidine thiocyanate, and β-mercaptoethanol (10% of final volume) to inactivate RNase. Thorough mixture of cells and buffer was achieved by pipetting followed by vortexing for 1 minute. To the homogenised lysate, 350 µl of 70% (v/v) ethanol was added and mixed well, before transferring all the lysate, including any precipitate that formed, to an RNeasy mini-column equipped with a 2 ml collection tube, and centrifuging for 15 s at 8000 g. The flow-through was discarded, and the column was washed. DNase I was applied to the column membrane and incubated at room temperature for 15 minutes, followed by wash buffer (350 µl). The column was re-centrifuged, again discarding the flow-through, then washed again twice with the appropriate buffer before being transferred to a new collection tube. RNase free-water (50 µl) was applied directly onto the membrane and the column was centrifuged for 1 min at 8000 g to recover the eluted RNA. RNA yield and purity was determined spectrophotometrically using a NanoDrop spectrophotometer (Thermo scientific) at 260 and 280 nm. Recovered total RNA gave A260/A280 >1.9. Samples were stored at -80°C until needed or used for cDNA synthesis.

2.2.6.2 cDNA Synthesis

cDNA synthesis was performed using a cDNA synthesis kit (SuperScript® III first-strand synthesis system, Invitrogen) as per manufacturer's instructions. Defrosted RNA samples were placed on ice with other kit components. The concentration of RNA was measured again to ensure that the freeze-thawing process had not damaged it. In a 0.5 ml tube, the following components (**table 2.2**) were mixed together to generate the RNA/primer mixture:

Components	Volume (µL)
5 µg total RNA	1-7
random hexamers	1
10 mM dNTP mix	1
RNase free water	To a total of 10

Table 2.2: RNA/primer mixture.

Random hexamers are a mixture of oligonucleotides representing all possible sequences for a hexamer.

After mixture, samples were incubated at 65 °C for 5 minutes, then placed on ice for a minimum of 1 minute. A cDNA synthesis mixture was prepared, adding each component in the order shown in **table 2.3**.

Components	Volumes (µL)
10x RT buffer	2
25 mM $MgCl_2$	4
0.1 M DTT	2
RNaseOUT™	1
SuperScript™ III	1

Table 2.3: cDNA synthesis mixture.

RT Buffer comprised of 200 mM Tris-HCl, pH 8.4 / 500 mM KCl. RNaseOUT protects against degradation of target RNA due to ribonuclease contamination and SuperScript III RT is used to synthesise first-strand cDNA. cDNA synthesis mixture (10 µl) was mixed gently with the RNA/primer mixture, then incubated on the thermo-cycler (BioRad) at 25°C for 10 minutes, followed by 50°C for 50 minutes, and finally 85°C for 5 minutes, after which samples were chilled on ice. In parallel, a reverse-transcriptase control without RNA was also prepared. Brief centrifugation ensured collection of each sample without any air bubbles before the addition of 1 µl of RNase H solution to each tube and incubation at 37°C for 20 minutes. Samples were used for PCR immediately or stored at -20°C in aliquots to minimise repeat freeze-thaw cycles.

2.2.6.3 Real-Time PCR – Experimental Protocol

RT-PCR was performed by setting up a PCR master mix for a 20 µl reaction, for both the tested gene and the endogenous (GAPDH) control (**table 2.4**)

Master Mix		
Components	Tested Gene (µL per reaction tube)	Endogenous Control (µL per reaction tube)
TaqMan	10.0	10.0
TaqMan Gene	1.25	-
GAPDH Gene	-	1.25
Water	4.75	4.75

Table 2.4: PCR master mix.

The PCR master mixture was distributed in 16 µl aliquots into the wells of a RT-PCR plate at room temperature. To this, 4 µl of cDNA template was added and mixed by pipetting. The plate was briefly centrifuged to collect the contents at the bottoms of the wells, then stored on ice until used.

The plate was placed in the RT-PCR instrument (7900HT Fast real-time PCR system, Applied Biosystems) and incubated, using the following settings (**table 2.5**).

RT-PCR Settings			
	Repetitions	Temperature (°C)	Time
Reverse Transcription	1	50	2 min
Enzyme Activation	1	95	10 min
PCR Cycle (melt)	40	95	15 s
PCR Cycle (anneal & Extend)	40	60	1 min

Table 2.5: RT-PCR Instrument Settings

An amplification plot for each sample was obtained and further analysis was performed on the threshold cycle (Ct) values acquired.

The Ct values obtained were quantified and compared with those derived from a calibrator, here the non-TSHR expressing cell line, CHO. Results were expressed in terms of the ratio of the level of expression of the base sequence in a given cell line to that found in the calibrator.

The comparative Ct method is also known as the 2–ΔΔCt method, where:

$$\Delta\Delta C_t = \Delta C_{t\ sample} - \Delta C_{t\ reference}$$

ΔCtsample is the Ct value for the tested cell line normalised to the endogenous housekeeping gene and ΔCt, reference is the Ct value for the calibrator also normalised to the endogenous housekeeping gene.

For the ΔΔCt calculation to be valid, the amplification efficiencies of the target and the endogenous reference must be approximately equal. This was established by observing how ΔCt varied with template dilution

2.2.7 Western blot analysis with FTC-133, TPC-1 and GPI cells

FTC-133, TPC-1, CHO and GPI cells grown in T75 flasks were lysed with 0.5 ml ice-cold NP40 lysis buffer containing 10% protease cocktail inhibitor (Sigma aldrich). Lysed FTC-133, TPC-1, CHO and GPI cells protein concentrations were determined by the Bradford assay (Biorad). 50 μg of Protein lysates containing ¼ volume of 5 x SDS loading buffer (20 ml: 7.5 ml water, 2.5 ml 1 M Tris HCl. pH 6.8, 6 ml glycerol, 0.04 g 0.5% (w/v) Bromephenol blue, 4 ml SDS (10% w/v)) and rainbow molecular weight markers (GE Healthcare) were then run on a denaturing SDS-PAGE gel (10% polyacrilamide) at 150 V for approximately one and a half hour. The gel, together with two fibre pads and two pieces of Whatman 3MM paper, was then blotted onto a PVDF membrane (Millipore, Watford, United Kingdom) for 1 hour at 190 mA. This blotting was assembled in 1 X WB transfer buffer (100 ml methanol, 400 ml 1 x TRIS-glycine,

SDS buffer). Once blotted, the membrane was blocked with 5% non fat milk in TBST (100 ml 10 X TBS stock, 900 ml water, 1 ml Tween-20) for 2 hours and rinsed with TBST 4 times for 5 minutes. The membrane was then incubated at 4ºC overnight with either 4C1 primary antibody (1:2000 dilution) or mAb9 antibody (1:2000 dilution) together with mouse monoclonal anti human GAPDH control antibody (1:10,000 dilution). After the overnight incubation, the membrane was rinsed with TBST and washed 4 times for 5 minutes. Thereafter, Goat anti mouse secondary antibody conjugated to HRP (1:2000 dilution) was added to the membrane and left to incubate for 30 minutes. The membrane was then rinsed with TBST and washed 4 times for 5 minutes. Proteins were visualised by ECL™ Western Blotting Detection Reagent (GE healthcare) as per manufacturer's instructions.

2.2.8 Radioiodination of mAB9 antibody with Sodium [^{125}I]-Iodide using Iodogen

All radiolabelling procedures were performed according to good radiation safety practice. Radioiodinations were performed in a well-ventilated fume hood and all containers were shielded by keeping them in small lead pots. Iodine-125 (^{125}I) is used to radiolabel antibody fragments, reacting with tyrosine and some histidine residues in proteins or peptides by electrophilic substitution [171]. Na ^{125}I was purchased from IMS30 Amersham at a concentration of 3.7 GBq/ml. This procedure is adapted from Fraker PJ and Speck JC Jr. [179].

2.2.8.1 Radiolabelling of mAb9 for *in vitro* experiments

For efficient labelling of mAb9 antibody, iodinations were conducted in glass tubes (12 x 75 mm) coated at the bottom with the oxidant Iodogen (1,3,4,6-tetrachloro-3α, 6α-diphenylglycoluril) (Perbio, UK. Part of Thermo Fisher Scientific) for the activation of ^{125}I. 5 μg, 10 μg or 100 μg of mAb9 antibody were added to the Iodogen tube together

with 4 MBq of Na ^{125}I. This was then mixed gently and incubated for 10 minutes. Next, PBS was added to make up the volume to 100 µl and the sample was transferred to a clean 1.5 ml eppendorf tube and kept at 4°C until used.

2.2.8.2 Radioiodination of mAB9 for imaging experiment

To radiolabelling of mAb9 for imaging experiments the same method was used as for the *in vitro* experiments (2.2.8.1). However, instead of 4 MBq of ^{125}I, 40 MBq was used. Also, an additional purification step was performed by running the samples through a Nap5 column (GE healthcare). This additional purification step was performed to ensure that radioiodinated mAb9 injected into mice was of a maximum purity. Thereafter 5 ml tubes were labelled 1 to 10 and the radiolabelled antibody was inserted into the Nap5 column, 550 µl of 0.1% PBS/BSA was added to the column and the solution allowed to elute into tube 1. Fractions of 250 µl 0.1% PBS/BSA were eluted into tubes 2-6 and fractions of 1 ml 0.1% PBS/BSA were eluted into tubes 7,8,9 and 10. The radioactivity in tubes 1 to 10 was then measured. The radiolabelled samples in the tube with the greatest activity were then used in imaging experiments.

Confirmation of successful labelling was achieved by Instant Thin Layer Chromatography (ITLC) and radio-HPLC of the samples, as explained in 2.2.9.

2.2.9 Determination of purity and labelling efficiency of mAb9

2.2.9.1 Instant thin layer chromatography (ITLC)

Samples on ITLC-Silica Gel (ITLC-SG) strips (1 x 8 cm) were developed in duplicate, in 85% methanol. A 1 µl fraction of labelled mAb9 was spotted onto strips, which were developed to within 1 cm of the top. Strips were removed from the solvent tank, dried, and the labelled antibody fragments were visualised using a phosphor imager.

2.2.9.2 Radio-High Performance Liquid Chromatography (radio-HPLC)

A Beckman System Gold running 24 Karat proprietary software was used for radio HPLC analysis with a size exclusion Phenomenex BioSep-sec-s-2000 column, 300 × 7.00mm 5 micron (Phenomenex), and a Beckman 166 UV detector in series with a GABI sodium iodide radioactivity monitor (Raytest). HPLC was run using 0.1M phosphate pH 7.2, 10% EtOH 100 mM EDTA as a mobile phase for 30 minutes at a flow rate of 0.5 ml/min and UV detection at 168-280nm.

2.2.9.3 SDS-PAGE gel electrophoresis and phosphor imaging system to determine molecular weight and purity of ^{125}I-mAb9

Electrophoresis of ^{125}I-mAb9 was performed on a PHAST system® (GE healthcare, Bucks, United Kingdom) using 15% gradient SDS-PAGE. The PHAST system® automatically separates and stains proteins under controlled energy and temperature conditions. The PHAST system® assures reproducibility with quality-tested precast gels, buffer strips, and staining kits. A 7.5% SDS Phast gel (GE healthcare, Bucks, United Kingdom) was used. The Phast gel was inserted into the gel bed in the machine and next the transfer buffer strips (GE healthcare, United Kingdom) were inserted into the Phastgel. 10 µl of Tris buffer was added to the ^{125}I-mAb9 sample. Molecular weight standards (supplied by GE healthcare, Bucks, United Kingdom) already contained Tris buffer. The samples were then heated to 95°C for 5-10 minutes. 6 µl of samples were then aligned in a piece of parafilm and then the samples were aspirated with a plastic capillary applicator and then inserted into the PHAST system machine. The machine was set on a programme appropriate to the 7.5% Phast gel.

When the run was finished, the gel was placed in a container filled with fixing and staining solution and left to incubate overnight. The next day the gel was destained with destaining solution and allowed to dry overnight. The gel was then analysed by digital

autoradiography using a Packard Cyclone phosphor imaging system using OptiQuant version 3.00 (Perkin-Elmer, Ohio, USA).

2.2.10 TSHR Binding assays

2.2.10.1 Coated tube assay for the measurement of TSHR binding to mAb9

This assay was obtained from B-R-A-H-M-S Aktiengesellschaft (Hennigsdorf, Germany).

200 µl of buffer B (supplied with the kit) was added to the coated tubes. Next, 100 µl of unlabelled mAb9 radiolabelled with a lower (10 µg mAb9 with 5 MBq ^{125}I) and higher (5 µg mAb9 with 10 MBq ^{125}I) specific activity, and PR1A3 (murine monoclonal antibody against the carcinoembryonic antigen, Nuclear Medicine Barts Hospital, London, UK) were added at 5 different concentrations: 3000 ng/ml, 1000 ng/ml, 300 ng/ml, 100 ng/ml, 30 ng/ml. Thereafter the tubes were incubated for 2 hours at room temperature while shaking at 300 rpm. The coated tubes were washed twice with 2 ml of washing solution (provided by the kit) and then allowed to dry in a blotting paper for 10 minutes. Next, either 200 µl ^{125}I radiolabelled TSH (supplied by the kit) or 200 µl ^{125}I-mAb9 (50 ng/ml) was pipetted into the tubes. The tubes were then incubated for 1 hour at room temperature while shaking (300 rpm). Following the 1 hour incubation time, the coated tubes were washed twice with 2 ml of washing solution and dried on a blotting paper for 30 minutes before being read in a gamma counter.

The oxidation and labelling effect of iodine was also tested in the coated tube assay in which ‘oxidised mAb9’ ‘cold labelled’ mAb9 (prepared as in section 2.2.4) were used in the coated tubes as explained above.

2.2.11 Cell binding assays

2.2.11.1 Effect of temperature and time on TSHR binding

20 nM of ^{125}I-mAb9 was added to FTC-133, TPC-1 and GPI cells previously plated in 6 well plates and incubated for 2 hours at 4ºC, room temperature and 37ºC. The medium was then aspirated carefully to avoid disrupting the cells, which were washed twice with PBS. The cells were then lysed with NaOH for a period of 10 minutes and the radioactivity read in the gamma counter. The bound percentage was calculated.

A TCA precipitation assay was performed over a 6 hour period to find out if the antibody remained bound to ^{125}I and did not dissociate. The supernatants were collected and 20% trichloroacetic acid (TCA) was added to each sample fraction to form a final solution of 10% TCA as to precipitate the protein in solution. After centrifuging the protein into a pellet, the supernatant was removed and both fractions were counted using the gamma counter. Both the supernatant and the pellet were analysed

2.2.11.2 Effect of media in binding assay:

^{125}I-mAb9 was made up in different buffers –DMEM, HBSS, Krebs and PBS/0.1BSA (all with 10% FBS and 0.04% sodium azide and pH 7). They were added to GPI cells plated in 6 well plates and incubated for 2 hours at RT. The cells were then lysed with 1M NaOH and read in the gamma counter and the % of antibody bound to the cells calculated.

2.2.11.3 Assessment of the binding of ^{125}I-mAb9 to TSHR in cells using the immunoreactive fraction assay.

The immunoreactive fraction assay has been adapted from a method published by Lindmo [180]. 15 x 10^6 FTC-133 cells, TPC-1 cells and GPI cells were harvested. Cells were detached from the tissue culture flasks using versine/EDTA and the cell

concentrations counted using a haemocytometer. The final concentration was diluted to $4x10^6$ cells/ml in cold 0.1% BSA/PBS. 0.5 ml of cell suspension was pipetted into two eppendorf tubes and a series of 5 one in two dilutions were made. Next, 200 μg of unlabelled antibody was added to two additional tubes containing 0.5 ml of cell suspension. 50 to 100 ng of ^{125}I-mAb9 was then added to all the tubes including the empty tubes. Thereafter the tubes were incubated for 2 hours at room temperature in a mechanical shaker. The tubes were left in ice for 10 minutes to cool and then centrifuged at high speed (>1000rpm) for 2 minutes. The supernatant was carefully removed and discarded and another 0.5 ml of cold 0.1%BSA/PBS was added. The tubes were again centrifuged, their supernatant discarded after which they were ready to be read in the gamma counter. The data obtained from the gamma counter was analysed by dividing the counts in the tubes containing cells and ^{125}I-mAb9 (bound counts) by an average of the counts in tubes containing just ^{125}I-mAb9 (total counts). This allowed for the fraction of counts bound to the cells to be calculated for each cell concentration.

2.2.11.4 Saturation binding assays

Saturation binding assays were carried out using GPI, FTC-133, TPC-1 and FRTL5 cells. Forty-eight hours prior to the experiment, adherent cells ($1x10^6$ per well), in 2 ml of cell growth medium (HAMSF12 or DMEM 10% FBS) per well, were seeded in a 6-well plate. One plate was prepared for each of the following concentrations of radioligand: 25, 10, 7.5, 5, 2.5, 1 and 0.1 nM.

Prior to experimentation, cells in the plates were checked to ensure they had fully adhered to the wells and were not over-confluent. The medium was aspirated carefully to avoid disturbing the cells, which were washed twice in PBS to remove any that were not adhering. Fresh medium (1.2 ml/well) containing 1% (w/v) FBS and 0.1% (w/v)

sodium azide was added and plates were returned to the incubator until needed. The remaining medium was kept at 4°C.

mAb9 and 4C1 were radiolabelled to produce ^{125}I-mAb9 and ^{125}I-4C1 and the radiochemical purity determined (section 2.2.8 and 2.2.9). The radiolabelled antibodies were prepared at 10 x the concentration ultimately required. Assays were performed in triplicate, and for each concentration of radiolabelled peptide, a duplicate well containing unlabelled competitor was set up. Competitor wells received, in 1% PBS-BSA, 150 µl of unlabelled mAb9 and 4C1 at a final concentration of 1 mM. The corresponding non-competitor wells received 150 µl 1% PBS-BSA to bring the protein concentration and volume to the same values. All wells received 150 µl of the appropriate concentration of labelled mAb9 and 4C1, added dropwise to the contents of each well, avoiding contact with the walls to prevent non-specific binding to the plastic. Plates were gently swirled to ensure even dispersion of the radioligand, then incubated at 37°C under 5% (v/v) CO_2/air for 90 minutes.

After incubation, the medium was aspirated and the cells washed twice in 1% FBS, then in medium containing 0.1% (w/v) sodium azide, and finally in ice cold PBS, taking care not to disturb the cells. To each well, 1 ml of 1 M NaOH was added to lyse the cells and left until lysis became apparent (10 min). Thereafter, three 5 µl aliquots per well were transferred to a 96-well plate for determination of protein concentration. Protein was assayed using the Bio-Rad Protein Assay Kit (Bio-Rad), as per manufacturer's instructions, and the plate was measured in the plate reader at 595 nm. The remaining supernatant samples were transferred into scintillation tubes, together with the washings from two 1 ml fractions of PBS for each well, and the tubes were then counted on the gamma counter. This experiment was performed three separate times for each cell line.

2.2.12 Assessing the *in vivo* binding of ^{125}I radiolabelled mAb9 to TSHRs in the mouse thyroid using SPECT/CT imaging and biodistribution

All animal procedures were undertaken in accordance with the UK Animals (Scientific Procedures) Act 1986.

Four groups of C57 mice (n=2) (Charles River Research Animal Diagnostic Services, London) were used in imaging experiments. Because ^{125}I is also taken up by the thyroid gland, all mice were given potassium iodide for 3 days prior to imaging. The 4 groups received the following treatments:

Group A (mouse 1 and 2): ^{125}I radiolabelled mAb9 (2 MBq *i.v*)
Group B (mouse 3 and 4): Sodium perchlorate (5 mg *i.p*) followed 30 minutes later by ^{125}I radiolabelled mAb9 (*i.v*).
Group C (mouse 5 and 6): ^{125}I-iodide (2 MBq *i.v*)
Group D (mouse 7 and 8): Sodium perchlorate (5 mg *i.p*) followed 30 minutes later by ^{125}I-iodide (*i.v*).

A SPECT/CT scanner (Bioscan, UK) was used to image the area around the neck (CT was used to focus the scan) at time points of 4 hours and 24 hours post *i.v* injection of ^{125}I-iodide (^{125}I) and ^{125}I-mAb9. The injections were staggered by 30 minutes since the total imaging (SPECT scan = 20 minutes, CT= 3 minutes) and set up times were approximately 30 minutes. Approximately 2 MBq of ^{125}I-mAb9 and ^{125}I were injected into each mouse. A 4-head small animal NanoSPECT/CT (Bioscan Inc., Washington DC) imaging camera with 1.4mm pinhole apertures was used to image the thyroid of the mice. The mice were anaesthetised using isoflurane (Induction – 4% Isoflurane, 0.5-1L/min O2; Maintenance – 2% Isoflurane, 0.5-1L/min O2) and placed on a heated animal bed. A topogram was acquired to focus the scan on the neck area.

A CT scan was acquired with the following parameters:

No of projections = 180 projections

Frame resolution = Standard

Exposure time = 1000ms

Tube Voltage = 45kVp

Duration = 3 minutes.

Scan range = approx 20mm.

SPECT scans were acquired with following parameters:

No of projections = 16 projections

Time per projection = ranged from 300-400ms

Duration of 20mins/scan (4hours) and 26mins/scan (24hours)

Scan range = same as CT.

Images were reconstructed in a 256 x 256 matrix using HiSPECT (Scivis GmbH), a reconstruction software package, and images were fused using Bioscan InVivoScope (IVS) software.

For biodistribution studies, the mice used for imaging were removed from the SPECT/CT camera after the 24 hour time point scan and were immediately culled by CO_2 anaesthesia and the thyroids were dissected and counted.

Empty scintillation tubes were weighed with their lids prior to the experiment, and reweighed after filling to obtain the weights of the excised thyroid tissue. The thyroid, (within the scintillation tubes) was then counted in the gamma counter. As a control to standardise the experiment, a 100-μL dose (assuming an injected dose of that volume) was dispensed into a polypropylene 15-mL falcon tube containing 9.9 mL of 1% PBS-BSA. Three 1-mL fractions from the 10-mL control sample, neat and after dilution (1:10 and 1:100) were also read in the gamma counter. The counts obtained from the counted tissues were compared with counts obtained from the control standards which were corrected for dilution to obtain CPM per mL and the percentage of injected dose per gram of tissue was calculated.

2.2.13 Radiolabelling of mAb9 with ^{111}In

^{111}In does not form strong interactions directly with antibodies but can form highly stable complexes with a number of bifunctional chelating agents which have a chemically active group that can bind covalently to the antibody.

2.2.13.1 Conjugation of mAb9 with Bz-Scn-DOTA

Conjugation was achieved by using mini dialysis cassettes (Slide-A-lyzer mini dialysis cassettes, Pierce). mAb9 antibody was added to the dialysis cassette and placed in Hepes buffer pH 8 overnight at 4°C. The antibody was then removed from the dialysis cassette and its concentration was calculated by measuring the absorbance of the sample at 280 nm in a UV spectrophotometer (protein concentration = absorbance/1.4=mg/ml). 8 times molar excess of ScnBzDOTA was calculated and added to mAb9. ScnBzDOTA mAB9 was then placed in the cassette and in Hepes buffer pH 6 for two days. After two days, the final concentration of ScnBzDOTA-mAb9 was calculated as well as the pH checked. After conjugation it was necessary to go through a purification step to remove the free chelate before the radioisotope is added. For the purification step, ScnBzDOTA-mAb9 was added to a new dialysis cassette with a syringe and placed in a metal free plastic container with 1 litre of newly made 0.1M ammonium acetate pH 5.5-6.0 in metal free water. The 0.1M ammonium acetate pH 5.5-6.0 buffer was exchanged for 6 x 3 hour periods and for a 1 x 12 hour period. Thereafter, the contents of the dialysis cassette were transferred to a metal-free plastic test tube with a syringe. The final protein concentration was measured in a UV spectrophotometer at 280nm.

2.2.13.2 Assessing the purity and integrity of ScnBzDOTA-mAB9 complex with SE-HPLC.

SE-HPLC was used to assess the purity of the ScnBzDOTAmAB9. 10 µg of ScnBzDOTAmAB9 was injected into a SE-HPLC column using the same methodology and equipment as explained in detail in section 2.2.1.

2.2.13.3 FACS analysis to assess the binding of SCNBzDota-mAb9 to the TSHR in cells

1 and 10 µg of SCNBzDota-mAb9 were used in GPI cells for the FACS experiment using the same methodology, equipement and materials as detailed in section 2.2.4.

2.2.13.4 Coated tube assay to assess the binding of SCNBzDota-mAb9 to the TSHR in cells

A TSHR coated tube assay was carried out with increasing concentrations of cold SCNBzDota-mAb9 and ^{125}I-TSH supplied by the kit using the same methodology detailed in section 2.2.10.1.

2.2.14 ^{111}In binding to BzScnDOTA mAb9

For the labeling reaction, 5 MBq of ^{111}In (Covidien-Petten, Netherlands) was added to 50 µg SCNBzDOTA-mAb9. 1 M ammonium acetate buffer, pH 6, was also added to the reaction to maintain the pH in this range (pH 6). The reaction was then incubated for 1 h at 37 °C and thereafter quenched by 10% (vol/vol) 0.1 M ammonium acetate buffer, pH 6, containing 50 mM EDTA. Thereafter the reaction was mixed well and left for 5 min at room temperature.

2.2.14.1 Assessing labelling efficiency of ^{111}In-mAb9

ScnBzDOTA-mAb9^{111}In (^{111}In-mAb9) labelling efficacy was confirmed by Size exclusion HPLC (SE-HPLC) and ITLC using the same methodology as explained in section 2.2.1

2.2.14.1.1 TSHR Pre-coated tube assay with ^{111}In-mAb9

^{111}In-mAb9 was used with increasing concentrations of cold mAb9 in the TSHR coated tube assay and the assay was performed as previously described in section 2.2.10.1.

2.2.14.1.2 ^{111}In-mAb9 saturation cell binding assays

This saturation assay was carried out exactly as described in section 2.2.11.4 but instead using ^{111}In-mAb9 with GPI, FRTL5, TPC-1 and FTC-133 cells.

2.2.14.2 SPECT/CT imaging of ^{111}In mAb9 in mice

Thus, this experiment was performed in order to assess the binding of ^{111}In-mAb9 to the TSHR expressed in the normal thyroid of mice. Because it was set up as a preliminary experiment, only two mice were used initially.

Two C57 (Charles River Research Animal Diagnostic Services, London) mice were injected *i.v.* with 200 µl (5.5 MBq) of the radiolabelled antibody and imaged in the NanoSPECT at 4 hours, 24 hours and 48 hours time point so that the levels of thyroid uptake could be determined. In one mouse the whole body was imaged while in the other mouse the neck region was imaged. The two imaging mice were also biodistributed at 48 hours. Imaging uptake was quantified using In-vivoscope software.

A SPECT/CT scanner (Bioscan, UK) was used to image the area around the neck of one mouse (CT was used to focus the scan) and the whole body of another mouse at 4 hour, 24 hour and 48 hour time points post *i.v.* injection of ^{111}In-mAb9. The injections were

staggered by 30 minutes since the total imaging (SPECT scan = 20 minutes, CT= 3 minutes) and set up times were approximately 30 minutes. Approximately 2 MBq were injected into each mouse. A 4-head small animal NanoSPECT/CT (Bioscan Inc., Washington DC) imaging camera with 1.4mm pinhole apertures was used to image the thyroid and other organs of the mice. The mice were anaesthetised using isoflurane (Induction – 4% Isoflurane, 0.5-1L/min O2; Maintenance – 2% Isoflurane, 0.5-1L/min O2) and placed on a heated animal bed.

After 48 hours, mice used for imaging were removed from the SPECT/CT camera and culled with CO_2 anaesthesia.

For biodistribution studies, the pancreas intestine, spleen, stomach, kidney, liver, heart, lungs, blood, muscle, tail and the thyroid were excised from the mice and processed and counted as previously described in section 2.2.12.

A CT scan was acquired with the following parameters:

No of projections = 180 projections

Frame resolution = Standard

Exposure time = 1000ms

Tube Voltage = 45kVp

Duration = 3 minutes.

Scan range = approx 20mm.

SPECT scans were acquired with following parameters:

No of projections = 16 projections

Time per projection = ranged from 300-400ms

Duration of thyroid 20mins/scan (4hours), 26mins/scan (24hours) and 23 mins/scan (48 hour)

Scan range = same as CT.

Images were reconstructed in a 256 x 256 matrix using HiSPECT (Scivis GmbH), a reconstruction software package, and images were fused using proprietary Bioscan InVivoScope (IVS) software.

2.2.14.2.1 Blood/Plasma stability study of ^{111}In-mAb9

Three mice were injected *i.v*. with 5 MBq ^{111}In-mAb9. One mouse was used for *ex vivo* blood studies and two mice were used for *in vivo* blood studies.

In the *ex vivo* study, the mouse was terminally anaesthesised and intracardially bled *in situ* 6 hours post-injection of ^{111}In-mAb9. Around 700 µl of blood was collected and 200 µl of ^{111}In-mAb9 (5MBq) was added to the blood sample and the sample was incubated for 6 hours at 37ºC.

In the *in vivo* study, 5 mice were culled 6 hours post ^{111}In-mAB9 *i.v* injection and the blood was collected using the same method as abovementioned.

1 µl of blood from the *in vivo* and *ex vivo* studies were then analysed by PHAST page SDS-PAGE electrophoresis together with a control ^{111}In-mAb9 sample that was incubated for 6 hours at 37ºC in PBS. See section 2.2.9.3 for a description of the methodology for phast page gel electrophoresis.

2.3 Methodology 2 (this methodology relates to the results section in chapter 4)

2.3.1 Radioiodination of rhTSH using enzymatic substitution

The lactoperoxidase enzymatic substitutiuon labelling method was adapted from Corsetti *et al.* [181]. The reaction was carried out at both pH 5.4 and pH 7 and the following concentrations and reagents were used (**table 2.6**).

Reagent	**Quantity**
rhTSH	1 µg
0.5 M sodium phosphate pH 5.4 or pH 7	2.5 µl
glucose oxidase	0.5 µl (0.01 mg/ml)
lactoperoxidase	0.5 µl (1mg/ml)
D-glucose	1 µl (10mg/ml)
^{125}I	3.7 MBq

Table 2. 6: concentrations used for the lactoperoxidase radioiodination method.

The reaction was scaled down or up depending on the quantity of ^{125}I-rhTSH needed. The reaction was stopped using sodium metabisulfate.

2.3.1.2 ITLC and SDS-PAGE to check purity of radiolabelled rhTSH

ITLC and SDS-PAGE electrophoresis were carried out to confirm the purity of ^{125}I radiolabelled rhTSH. The procedures were carried out as detailed in sections 2.2.9.1 and 2.2.9.3, respectively.

2.3.2 Effect of glucose oxidase and lactoperoxidase on ^{125}I-rhTSH labeling efficiency.

0.5, 0.05, 0.005 and 0.0005 µg of lactoperoxidase and 0.005, 0.0005, 0.00005 and 0.000005 µg of glucose oxidase were added to constant amounts of the other labeling components separately as in table 2.5 (exept ^{125}I). An ITLC was then carried out as detailed in section 2.2.9.1 to calculate the labeling efficiency.

2.3.3 SE-HPLC with rhTSH and ^{125}I-rhTSH

10 µg of rhTSH and ^{125}I-rhTSH were run on a size exclusion HPLC with 0.5 M phosphate buffer pH 7.0 with 20 mM EDTA used as a mobile phase. A YMC Pack™ Pro™column was used (Waters) 10 µl of a full length biosep molecular weight standard was also analysed in SE-HPLC in order to estimate the molecular weight of rhTSH.

10 µl of 1 mg/ml Carbonic anhydrase and 10 µl of 1mg/ml lysosyme were analysed in SE-HPLC using the same methodology as above. Carbonic anydrase and lysosyme have known molecular weights of approximately 29 kDa and 14.7 kDa respectively. Carbonic anydrase molecular weight corresponds to the approximate molecular weight of intact rhTSH (29-30 kDa) and lysosyme corresponds to the approximate molecular weight of TSH α subunit (14 kDa).

2.3.4 Reverse phasse HPLC

rhTSH was analysed in RP-HPLC using C_{18}ODS reverse phase column, and a gradient of aqueous 0.1% (v/v) trifluoroacetic acid (TFA) (Solvent A) and acetonitrile (ACN)/TFA (pH 2.5). UV detection was performed at 160-280 nm and radioactivity was detected using an in-line gamma-detector. The flow rate was 1 mL/min. Solvent A was passed through the column for ten minutes between injections to allow re-equilibration. The radiolabelled peptide was diluted 1:1 in PBS before injecting 20 - 30 µl samples. The initial gradient system used for analysis was as follows: 5% A : 50% B for 35 minutes, then B was increased linearly to 100% over the next 10 minutes to elute lipophilic impurities, and reduced to 5% (i.e. A was increased to 100%) linearly thereafter over 5 minutes. rhTSH and ^{125}I-rhTSH were then analysed with the following gradient: 5% A : 20% B for 30 minutes, then B was increased from 20% to 35% over 30 minutes followed by a linear increase of B from 35% to 100% over the next 10 minutes to elute lipophilic impurities, and reduced to 5% (i.e. A was increased to 100%) linearly thereafter over 5 minutes.

2.3.4.1 SDS-PAGE electrophoresis with ^{125}I-rhTSH treated with either pH 2.5 or pH 7

rhTSH was treated with both pH 7 and pH 2.5 by incubating in 0.1M TEAA (pH 7) and 0.1%TFA/water (pH 2.5) for a period of an hour and after analysed in a phast-page SDS-PAGE gel as described in section 2.2.9.3

2.3.5 Ion pairing RP-HPLC

rhTSH and ^{125}I-rhTSH were analysed in RP-HPLC using a C_{18}ODS reverse phase column, using a gradient of aqueous 0.01 M Triethylammonium acetate (TEAA) pH 5.5 and 0.1M TEAA pH7 (Solvent A) and acetonitrile(ACN) as a mobile phase. UV

detection was performed at 160-280 nm and radioactivity was detected using an in-line gamma-detector. The flow rate was 1 ml/min. Solvent A was passed through the column for ten minutes between injections to allow re-equilibration. The radiolabelled peptide was diluted 1:1 in PBS before injecting 20 - 30 µl samples and analysed with 0.1M TEAA pH7 (Solvent A) and acetonitrile(ACN)

The initial gradient system used for analysis was as follows: 25% A : 60% B for 20 minutes, then B was increased linearly to 100% over the next 10 minutes to elute lipophilic impurities, and reduced to 25% (i.e. A was increased to 100%) linearly thereafter over 5 minutes.

2.3.5.1 Ion pairing HPLC with oxidised TSH and cold labelled TSH at pH7

Glucose oxidase and lactoperoxidase were added to rhTSH- 'oxidised'- to stimulate an oxidation step. A 'cold labelled' rhTSH was created by adding NaI to rhTSH (**table 2.6**). Both 'oxidised' and 'cold labelled' rhTSH were analysed in RP-HPLC on a reverse-phase column, C_{18}ODS (Phenomenex), using a gradient of aqueous 0.1M TEAA pH7 (Solvent A) and acetonitrile(ACN). Radioactivity was detected using an in-line gamma-detector. The flow rate was 1 ml/min. The gradient used was the same as the previously used with rhTSH and ^{125}I-rhTSH in section 2.3.3.

'oxidised rhTSH' reaction mixture

Reagent	Quantity
rhTSH	10 ug
0.5 M sodium phosphate buffer pH 5.4	25 ul
Glucose oxidase	5 ul (0.01 mg/ml)
Lactoperoxidase	5 ul (1mg/ml)
D-glucose	10 ul (10 mg/ml)

'cold labelled rhTSH' reaction mixture

Reagent	Quantity
rhTSH	10 ug
0.5 M sodium phosphate buffer pH 5.4	25 ul
Glucose oxidase	5 ul (0.01 mg/ml)
Lactoperoxidase	5 ul (1mg/ml)
D-glucose	10 ul (10 mg/ml)
Sodium iodide (NaI)	20 ul (6 ug/ml)

Table 2.7: Preparation of 'oxidised rhTSH' and 'cold labelled rhTSH' reaction mixtures.

2.3.6 ^{125}I-rhTSH binding assays

Constant amounts of ^{125}I-rhTSH made up in different binding buffers – HAMS-F12, HBSS, Krebs and PBS/0.1BSA (all with 10% FBS and 0.04% sodium azide and pH 7),were added to GPI cells plated in 6 well plates and incubated for 2 hours at room temperature. Thereafter, the cells were lysed with 1 M NaOH and the radioactive signal read in the gamma counter.

2.3.6.1 Coated tube assay with ^{125}I-rhTSH cold rhTSH

In this assay a constant amount of ^{125}I-rhTSH was added to increasing concentrations of cold rhTSH. This assay was performed as described previously in section 2.2.10.1.

2.3.6.2 Saturation assay of ^{125}I-rhTSH in GPI cells

Saturation binding assays were performed with ^{125}I-rhTSH in GPI, TPC-1 and FTC-133 cells as previously described in section 2.2.11.4.

2.3.6.3 Competition assay with ^{125}I-rhTSH and cold rhTSH in GPI cells.

GPI cells were seeded at a density of $1x10^6$ cells per well in six-well plates and grown at 37°C for 48 hours. Dilutions of unlabelled rhTSH (competitor) corresponding to 0.01, 0.1, 0.3, 1, 3, 10, 100, 1000, 10000 nM in final (1.5ml) plate volume were made up in 1% PBS/BSA. After 48 hours incubation time, the cells were washed by adding 1 ml 1% FCS Media to each well and then 1.2 ml of HAMSF12 media with 1% FBS was added to each well. 150 µl of each concentration of competitor was then added in triplicate to the cells. ^{125}I-rhTSH diluted in 0.1% PBS/BSA was then added to the cells. The plates were then mixed gently and incubated for 2 hours at room temperature. Thereafter, the media was removed and the plates were washed 2 x with 1 ml PBS per well. 1 ml of 1M NaOH was then added to each well in order to lyse the cells during 15

minutes. The radioactivity was then counted in a gamma counter and results plotted on graphPrism software and IC_{50} values calculated.

2.3.7 ^{125}I-rhTSH internalisation and externalisation assays

2.3.7.1 Internalisation assays

For internalisation experiments, GPI cells were seeded at a density of $1x10^6$ cells per well in six-well plates (Corning,USA) and grown at 37°C for 48 hours. On the day of the experiment, cells were washed twice with ice cold internalisation medium (HAMS-F12 supplemented with 1 % (v/v) FBS), followed by incubation for 2 hours at 37°C in fresh medium (1.2 ml per well). Approximately 3 pmol of ^{125}I-rhTSH in 150 µl PBS/1%BSA was added to each well, along with either 150 µl PBS/1%BSA (for determining total binding) or 1.5 nmol unlabelled rhTSH in 150 µl PBS/1%BSA (for determining non-specific binding). The cells were incubated at 37°C for 10, 30, 60, 90 and 120 minutes. At each time point the medium was removed and the internalisation halted by rinsing the cells twice with ice cold internalisation medium. Thereafter, the cells were washed twice for 5 min in ice cold 50 mM glycine, pH 2.8, 0.1 MNaCl (glycine/NaCl), followed by a rapid rinse in the same buffer. The two resulting acid wash supernatants in each case were pooled and retained as the surface-associated fraction. The cells were lysed with 1 M NaOH and collected as the internalised radioligand fraction. Each fraction was prepared in triplicate and all fractions were counted in a gamma-counter (LKB-1282 Compugamma system). The protein concentrations in the lysates were determined using the DC protein assay (BioRad). The internalised radioligand fraction was expressed either as a percentage of the total activity added per mg cell protein, or as a percentage of the total cell associated activity (i.e.surface associated plus internalised activity).

2.3.7.2 Externalisation assay

GPI cells were seeded at a density of $1x10^6$ cells per well in six-well plates 48h prior to the experiment. Cells were incubated at 37°C for 120 minutes with approximately 3 pmol ^{125}I-rhTSH in a total volume of 1.5 ml, in the presence or absence of excess competitor (1.5 nmol cold peptide). Incubation was terminated by washing each well with 2 x 1 ml ice cold PBS/1%BSA. Membrane bound ligand was removed by incubating the cells twice for 5 minutes in 1 ml ice cold glycine buffer (pH2.8) per well at room temperature, followed by a rapid rinse in the same buffer. The supernatant was discarded, and 1.5 ml assay medium (HAMS-F12 1640/1%FBSpre- warmed to 37°C) with or without excess competitor (1.5nmol cold peptide) was added, followed by incubation at 37°C for 10, 30, 60, 90 and 120 min. Following incubation, the medium was removed and retained for analysis (externalised fraction).The cells were lysed with 1ml of 1MNaOH and collected (cell associated fraction). The externalised and cell associated fractions were counted in a gamma counter and expressed as a percentage of the total activity added per milligram of cell protein (as determined using a BioRadDC protein assay). Externalisation experiments were performed in triplicate.

TCA precipitation of the supernatant was performed to ensure that the majority of the radioiodine remained in a protein-bound form with minimal free iodide. The supernatants were collected and 20% trichloacetic acid (TCA) was added to each sample fraction to form a final solution of 10% TCA as to precipitate the protein in solution. After centrifuging the protein into a pellet, the supernatant was removed and both fractions were counted using the gamma counter. Both the supernatant and the pellet were analysed.

2.3.8 ^{125}I-rhTSH *in vivo* studies

2.3.8.1 ^{125}I-rhTSH SPECT/CT imaging and biodistribution studies

Biodistribution and imaging studies were carried out to investigate the binding of ^{125}I-rhTSH to the thyroid and FRTL5 grafted subcutaneously in mice. 4 weeks prior to the experiment, 10 male SCID beige mice (Charles River research animal diagnostic services, London) were injected subcutaneously with 5 million FRTL5 cells in the left shoulder and left to grow until tumours became visible under the skin. In the SPECT/CT imaging, a blocking control using excess rhTSH was used together with ^{125}I-rhTSH. All mice were given water with potassium iodide 3 days prior to imaging/biodistribution in order to saturate NIS and block the uptake of ^{125}I via this transporter. Sodium perchlorate was also injected (*i.p*) half an hour previous to imaging/biodistribution experiments. Sodium perchlorate acts by blocking the uptake of ^{125}I via NIS. For imaging studies, radiolabelled rhTSH and the blocking control were administered by intravenous tail injections and for biodistribution studies ^{125}I-rhTSH and ^{125}I-TI were also administered by intravenous tail injections.

Trypsin inhibitor was radiolabelled with ^{125}I-iodide and ^{125}I-TI was selected for to be used as a control for the initial biodistribution due to its similar molecular weight to the rhTSH- 23 kDa.

The biodistributed animals were culled 2 hours after ^{125}I-rhTH and ^{125}I-TI injections and their tumour, pancreas, intestines, spleen, stomach, kidney, liver, heart, lungs, blood, muscle, tail and the thyroid, removed and biodistributed. Biodistribution studies were carried out as described previously in section 2.2.12.

The imaging animals were scanned using SPECT/CT (Bioscan, UK) at several times post *i.v* injection: 1h, 2h, 2.5h, 3h, 4h, 5h, 6h. These times were chosen to allow monitoring of the distribution and both specific and non-specific uptake of the radioligand. The injections were staggered by 30 minutes since the total imaging

(SPECT scan = 48 minutes, CT= 3 minutes) and set up times were approximately 30 minutes. Approximately 5 MBq were injected into each mouse. A 4-head small animal NanoSPECT/CT (Bioscan Inc., Washington DC) imaging camera with 1.4 mm pinhole apertures was used to image the thyroid of the mice. The mice were anaesthetised using isoflurane (Induction – 4% Isoflurane, 0.5-1L/min O2; Maintenance – 2% Isoflurane, 0.5-1L/min O2) and placed on a heated animal bed.

A CT scan was acquired with the following parameters:
No of projections = 180 projections
Frame resolution = Standard
Exposure time = 500 ms
Tube Voltage = 45kVp
Duration = 3.45 minutes.
Scan range = approx 60 mm.

SPECT scans were acquired with following parameters:
No of projections = 16 projections
Time per projection = ranged from 300-400ms
Duration of 48 mins/scan (1hour), 48 mins/scan (3hours) and 48 mins/scan (6 hours)
Scan range = same as CT.
Images were obtained as described in section 2.2.12

2.3.8.1.1 Quantification

The tumour region of mice was quantified using IVS software. Elliptical regions of interest (ROIs) were manually drawn around target tumour from imaged mice. The ROI was manually drawn around the tumour, although all views were used to locate the tissue of interest. Data obtained from the ROIs drawn was expressed in terms of MBq/mm3, and the percentage of the injected dose in the total ROI was calculated by dividing this by the total radioactivity of ^{125}I injected.

2.3.8.1.2 Blood stability studies

Blood was collected from biodistributed mice 2 hours post ^{125}I-rhTSH and ^{125}I-TI injections. A TCA precipitation was carried out by adding 20%TCA to the same volume of ^{125}I-rhTSH/blood and ^{125}I-TI/blood to form a final solution of 10% TCA as to precipitate the protein in solution. After centrifuging the protein into a pellet, the supernatant was removed and both fractions were counted using the gamma counter. Both the supernatant and the pellet were analysed

SDS-PAGE electrophoresis using PHASTgel was also carried out to confirm the stability of ^{125}I-rhTSH and ^{125}I-TI conjugate in the blood. 1 µl of blood was collected from biodistributed animals at 2 hours post injection of ^{125}I-rhTSH and ^{125}I-TI. The collected 1 µl was loaded into a Phastgel SDS-GEL electrophoresis and a reduced and non-reduced gel was run together with a control radiolabelled ^{125}I-rhTSH and ^{125}I-TI incubated at 37°C in PBS for the same amount of time.

A detailed description of phastpage gel electrophoresis is pointed in section 2.2.9.3.

2.3.8.2 Final biodistribution studies with ^{125}I-rhTSH and ^{125}I-CA

Four weeks prior to the experiment, 10 male SCID beige mice were injected subcutaneously with 5 million FRTL5 cells in the left shoulder and the cells left to grow until tumours became visible under the skin. All mice were given water with potassium iodide 3 days prior to imaging/biodistribution in order to saturate NIS and block the uptake of ^{125}I via this transporter. Sodium perchlorate was also injected (*i.p*) half an hour previous to imaging/biodistribution results.

4 mice were injected with ^{125}I-rhTSH, 3 mice were injected with control ^{125}I radiolabelled carbonic anydrase and 3 mice were injected with excess rhTSH together with ^{125}I-rhTSH for the blocking control.

Carbonic anydrase (CA) was selected due to its non specific binding to TSHR as well as identical size to rhTSH of approximately 29 kDa. Mice were biodistributed at 3 hour time point post ^{125}I-rhTSH and ^{125}I-CA injections. Biodistribution studies were carried out as previously described in section 2.2.12.

CHAPTER 3. MAB9 STUDY

In recent years, monoclonal antibodies have become useful tools in the management of cancer including its diagnosis, monitoring and treatment [182-186].

Antibodies have the capacity to recognise and bind with high specificity and affinity to cell surface receptors that are expressed in a wide variety of malignant tissues. This property can allow radiolabelled antibodies to offer more precise diagnostic imaging and can also increase the effectiveness and decrease the potential side effects of radiotherapy [121, 127, 183, 187, 188].

Most thyroid cancers are usually treated with radioactive iodine (RAI) which is taken up by the thyroid via NIS. However, some thyroid cancers can de-differentiate into an aggressive form that loses the expression of NIS and thus becomes resistant to radioiodine therapy [78-81, 86].

TSHR is a G protein coupled receptor expressed in at least some radioiodine resistant de-differentiated thyroid cancers [11, 27]. A monoclonal antibody (mAb9) against TSHR was investigated for its use in pre-clinical targeting of radioiodine resistant de-differentiated thyroid cancer.

Aims:

- Assess the integrity and purity of unlabelled mAb9 with HPLC and SDS-PAGE electrophoresis.
- Study the binding of unlabelled mAb9 to the TSHR in coated tubes and in a range of thyroid cancer cells using FACS and Western blot.
- Determine the expression of TSHR in a range of thyroid cancer cell lines with RT-PCR, FACS and Western blot.
- Label mAb9 with ^{125}I and ^{111}In radioisotopes.
- Test the ability of radiolabelled mAb9 to bind to TSHR in thyroid cancer cell lines, TSHR transfected cells and pre-coated tubes *in vitro*.
- Investigate the binding of radiolabelled mAb9 to the TSHR in the mouse thyroid *in vivo.*

3.1 mAb9 study results

3.1.1 Confirmation of the integrity and purity of unlabelled mAb9

3.1.1.1 Size Exclusion HPLC

The first step was to perform size exclusion HPLC in order to determine the integrity and purity of mAb9. The method for these studies is detailed in 2.2.1.

The Size exclusion HPLC chromatogram **(figure 3.1)** showed a single defined peak at a retention time of 13.4 minutes with a very small degree of shouldering at retention time 12.35 minutes which most likely represents antibody aggregates. The surface area percentage for the intact antibody is 97.5 while the surface area percentage for the shouldering peak is 2.52. The purity and integrity of mAb9 was shown to be relatively high due to the lack of major alternative peaks.

Bio-Rad gel filtration standards were also analysed in the SE-HPLC in order to calibrate the size exclusion column (**figure 3.2**).

A table with the Bio-Rad's gel filtration components respective molecular weights and the retention times obtained with Biosep 2000 column in size exclusion HPLC is shown **(Table 3.1).**

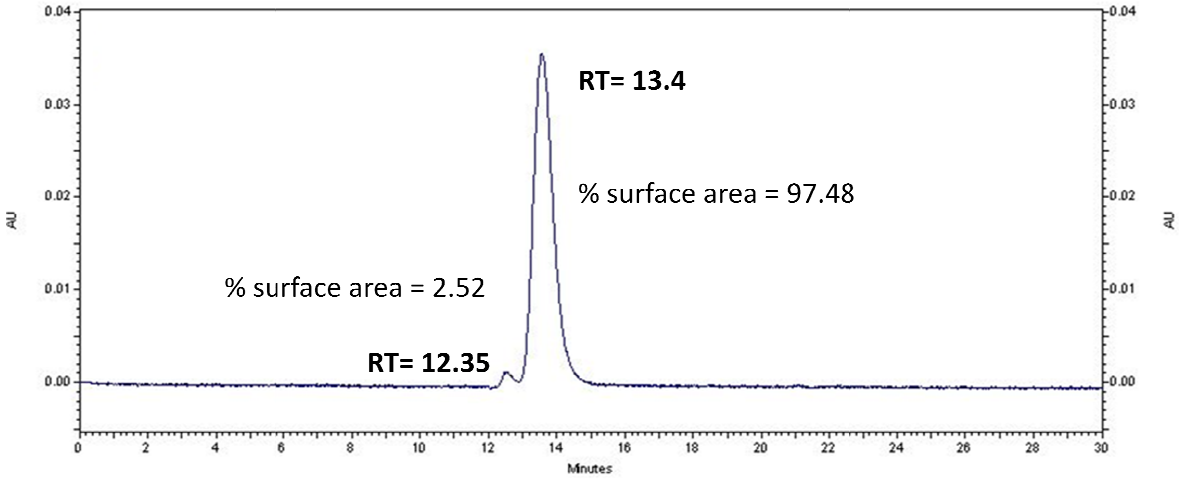

Figure 3.1: UV chromatogram (280nm) of mAb9 using size exclusion HPLC. The chromatogram shows a main peak at retention time 13.4 that corresponds to mAb9.

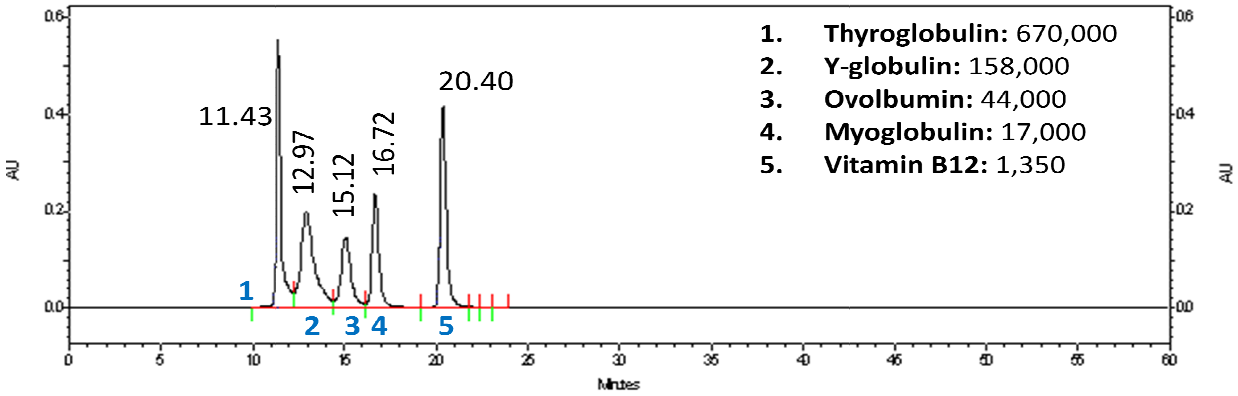

Figure 3.2: UV chromatogram of Biorad gel filtration standards (280nm). Thyroglobulin (Mwt 670,000Da) at retention time (RT) 11.43, γ-globulin (Mwt 158,000) at RT 12.97, Ovalbumin (44,000 Da) at RT 15.12, Myoglobin (17,000 Da) at RT 16.72 and Vitamin B12 (Mwt 1,350 Da) at RT 20.40 are shown.

The approximate size of proteins/antibodies can be determined by extrapolating their retention times from a graph of known Log molecular weight gel **(figure 3.4).**

Component	Molecular Weight (Da)	Retention Time
Thyroglobulin (bovine)	670,000	11.43
γ-globulin (bovine)	158,000	12.97
Ovalbumin (chicken)	44,000	15.12
Myoglobin (horse)	17,000	16.72
Vitamin B12	1,350	20.40

Table 3.1: Biorad gel filtration molecular weight standards. The table shows the molecular weight corresponding to the retention time obtained with size exclusion HPLC.

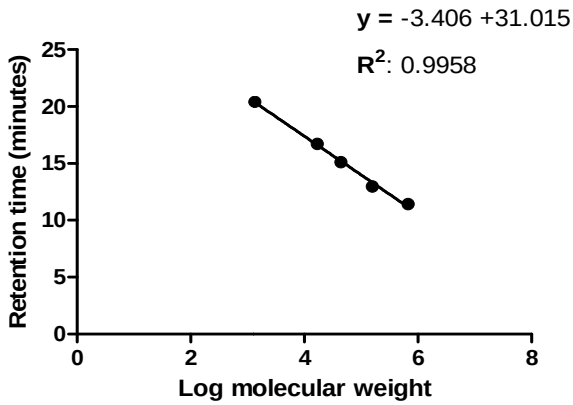

Figure 3.4: Linear regression of retention time obtained in SE-HPLC with BioRad standards against Log standard molecular weight of Biorad's components.

The approximate molecular weight of mAb9 was calculated by using the formula, Log (molecular weight) = RT-B/A. taken from the equation of the graph: Y = A*x + B. A retention time of 13.4 minutes corresponds to 148,970 Da. This correlates with the generally accepted molecular weight of IgG antibodies and mAb9 antibody of 150,000 Da.

3.1.1.2 SDS-PAGE electrophoresis of unlabelled mAb9

SDS-PAGE electrophoresis was performed as an additional means of confirming the integrity and purity of mAb9. See section 2.2.2 for a detailed methodology.

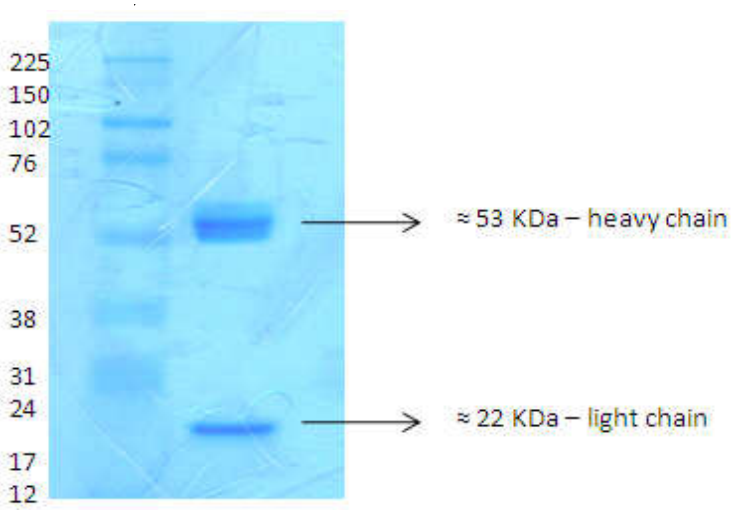

Figure 3.5: SDS page electrophoresis analysis of mAb9. Showing mAb9 heavy chain (53 kDa) and light chain (22 kDa).

Two main bands of approximately 53 kDa and 22 kDa were detected (**figure 3.5**). These molecular weights correspond to the antibody heavy and light chain respectively. The heavy chain band had two very close bands, one fainter than the other. The most likely explanation for the fainter band is the heterogeneity in the glycosylation of the heavy

chain of the IgG antibody. SDS electrophoresis thus confirmed the integrity and purity of mAb9.

3.1.2 Binding of mAb9 to the TSHR in pre-coated tubes and cells

3.1.2.1 Coated tube assay for the measurement of mAb9 binding to TSHR

The next step was to determine the binding of mAb9 to the TSHR, which was investigated by using TSHR pre-coated tubes. In this assay, the binding of mAb9 to TSHR was investigated by assessing the ability of increasing concentrations of cold/unlabelled mAb9 to inhibit the binding of ^{125}I-radiolabelled TSH (^{125}I-rhTSH) to TSHR coated in the tubes. See section 2.2.10.1 for a detailed prototcol.

The first experiment with this assay was to look at the competition of increasing concentrations of mAb9 and PR1A3 control antibody with ^{125}I-TSH . This was in order to determine if unlabelled mAB9 bound to the TSHR coated on the tubes (**figure 3.6**).

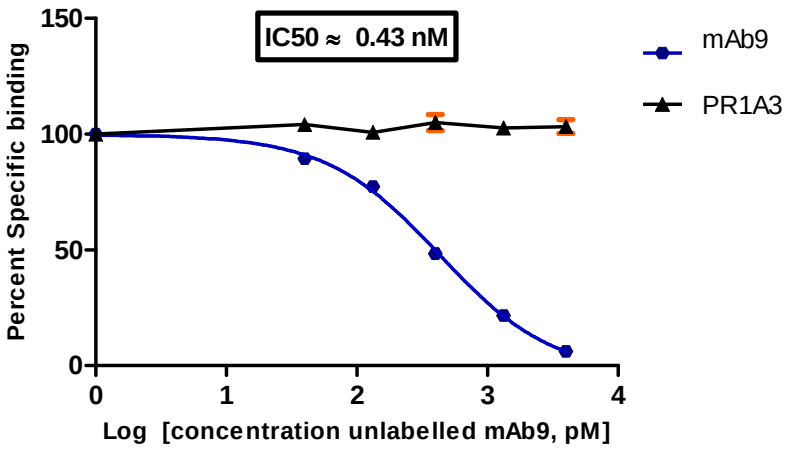

Figure 3.6 Competition assay of ^{125}I-TSH with unlabelled mAb9 in TSHR pre coated tubes. Increasing concentrations of cold mAb9 inhibited the binding of ^{125}I-TSH by about 97%. mAb9 bound to the TSHR in the tubes with an IC_{50} of 0.43 nM. Values are the mean of triplicate determinations +- SEM.

Increasing concentrations of unlabelled mAb9 competed with ^{125}I-TSH for the binding of TSHR coated in the tubes, as it inhibited the binding of ^{125}I-TSH in a concentration dependent manner with the highest concentration inhibiting 96% of the binding. (**figure**

3.6). These results also indicate that mAb9 bound to the TSHR with an apparent affinity of 0.43 nM. The control antibody PR1A3 showed no competition for ^{125}I-TSH binding.

3.1.2.2 Binding of unlabelled mAb9 to cells

3.1.2.2.1 Fluorescence activated cell sorting (FACS) to measure the binding of mAb9 to TSHR in TPC-1, FTC-133 and GPI cells.

After confirming the integrity and purity of the mAb9 preparation and confirming the ability of mAb9 to bind to TSHR pre-coated in tubes, the next step was to carry out FACS experiments in order to assess the binding of both mAb9 and 4C1 monoclonal antibodies to the TSHR in a range of cell lines. Cell lines used included FTC-133 and TPC-1, GPI and two control cell lines: CHO and MKN45. See section 2.2.4 for a detailed methodology.

FACS using GPI cells and 4C1 and mAb9 as primary antibodies

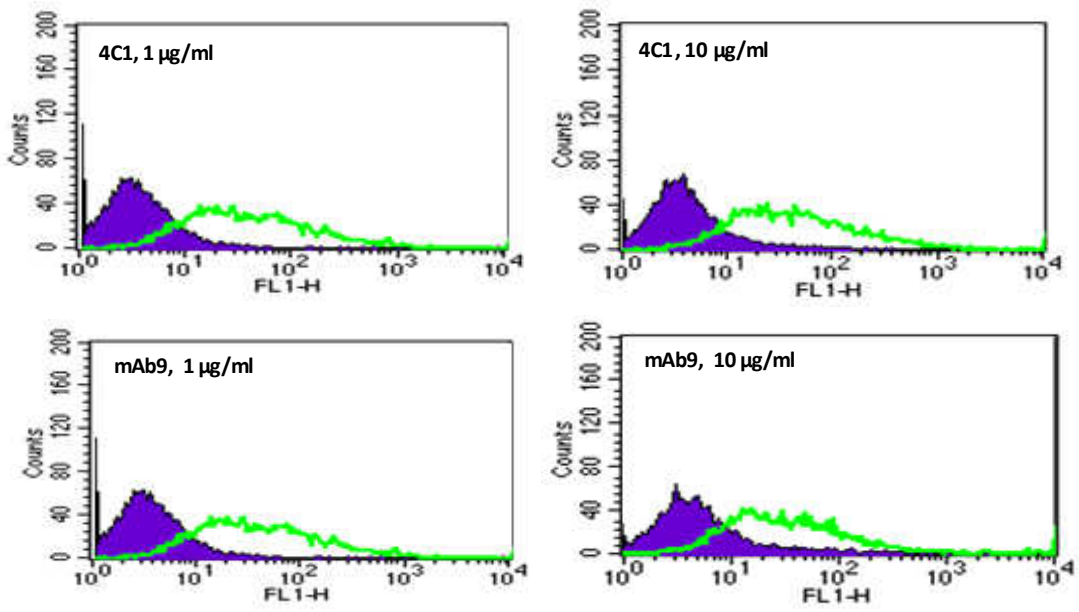

Figure 3.7: FACS analysis of TSHR expression in GPI (green) and CHO cells (dark blue). A significant shift is seen with 4C1 and mAb9 antibodies when compared with control cell lines. An isotype-matched control antibody was used as a negative control (data not shown).

Both 4C1 (commercial anti-TSHR monoclonal antibody) and mAb9 antibodies induced a substantial positive shift in GPI cells when compared with control cell lines (**figure 3.7**). FACS with GPI cells showed a very broad peak. This suggests that expression of TSHR in GPI cells is heterogeneous, with some cells expressing THSR in high quantities, and others in lower amounts.

FACS using TPC-1 cells and 4C1 and mAb9 as primary antibodies

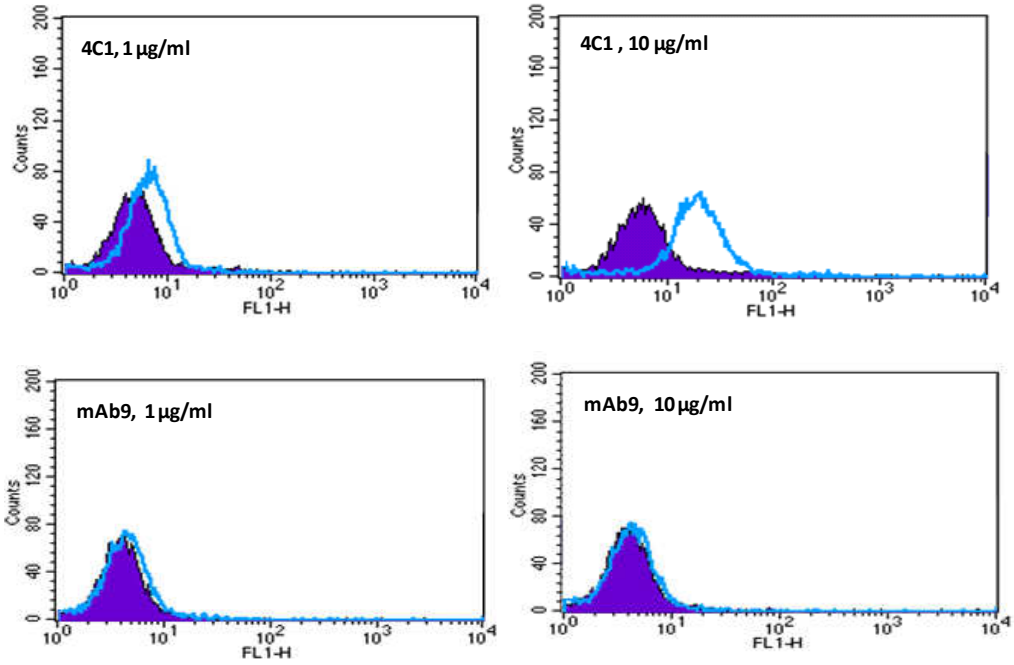

Figure 3.8: FACS analysis of TSHR expressed in TPC-1(light blue) and MKN45 (dark blue) cells. At 10 µg/ml of 4C1, a moderate positive shift is seen in TPC-1 cells. With mAb9 at both 1 µg/ml and 10 µg/ml no shift was seen. An isotype-matched control antibody was used as a negative control (data not shown).

4C1 (10 µg/ml) antibody induced a marginal positive in TPC-1 cells shift when compared to controls. (**figure 3.8**). This suggests that 4C1 is binding to low levels of TSHR in TPC-1 cells. mAb9 however did not induce a shift when compared to controls. This indicates that mAb9 is not binding to the low levels of TSHR in TPC-1 cells.

FACS with FTC-133 cells and 4C1 and mAb9 as primary antibodies

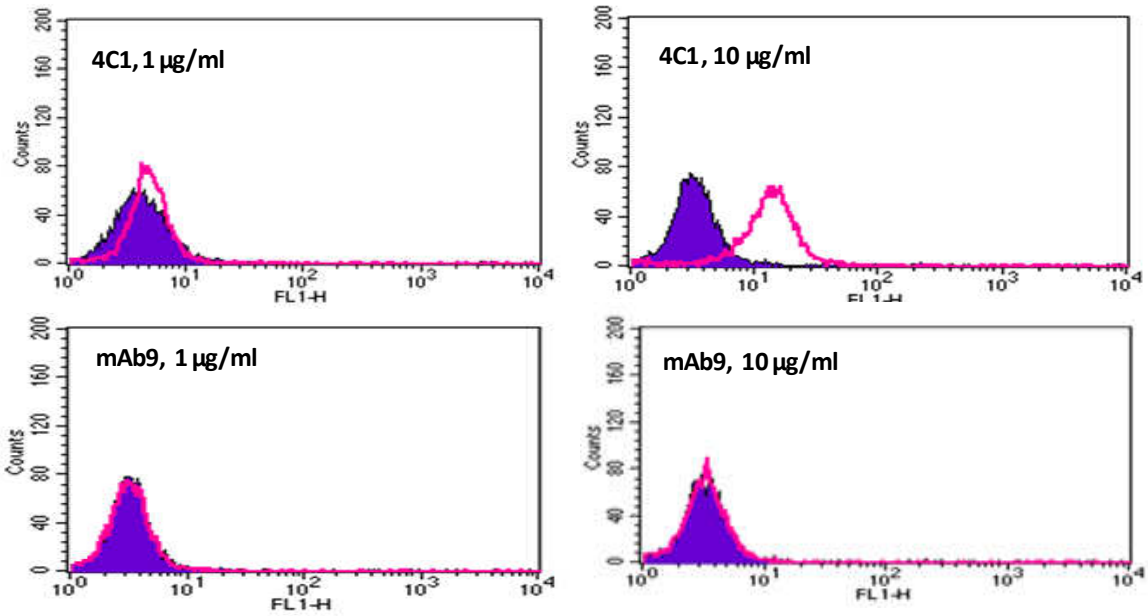

Figure 3.9: FACS analysis of TSHR expressed in FTC-133(pink) and MKN45 cells (dark blue). At 10 µg/ml of 4C1, a moderate positive shift was seen in FTC-133 cells, when compared with control cell lines. With mAb9 at both 1 µg/ml and 10 µg/ml no shift was seen. An isotype-matched control antibody was used as a negative control (data not shown).

A moderate positive shift was again observed with 10 µg/ml of 4C1 antibody in FTC-133 cells (**figure 3.9**). This suggests that 4C1 binds to the TSHR in FTC-133 cells. However mAb9 did not induce a positive shift in FTC-133 cells again indicating that mAb9 is not binding to the low levels of TSHR expressed in FTC-133 cells.

FACS using FRTL5 cells and 4C1 and mAb9 as primary antibodies

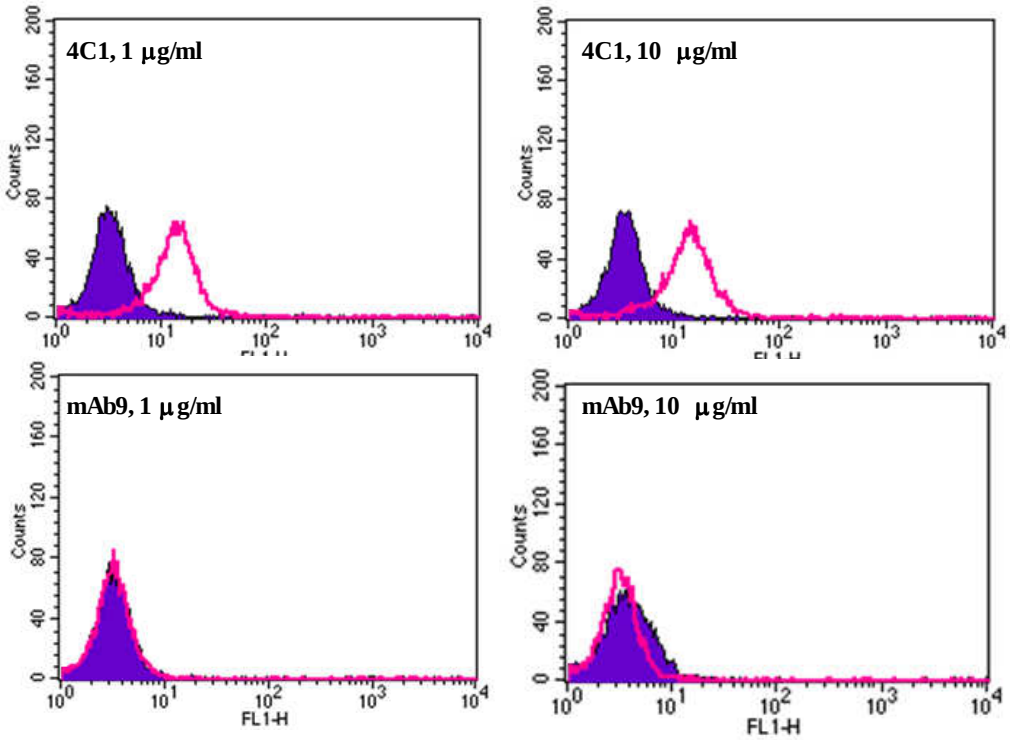

Figure 3.10: FACS analysis of TSHR expressed in FRTL5 (pink) and CHO cells (dark blue). At 1 µg/ml and 10 µg/ml of 4C1, a moderate positive shift was seen in FRTL5 cells, when compared with control cell lines. With mAb9 at both 1 µg/ml and 10 µg/ml no shift was seen. An isotype-matched control antibody was used as a negative control (data not shown).

A moderate positive shift was observed with 4C1 antibody (**figure 3.10**) suggesting that 4C1 binds to TSHR in FRTL5 cells. However, once again, mAb9 did not induce a positive shift in FRTL5 cells indicating that mAb9 did not bind to the TSHR expressed in FRTL5 cells.

A graph summarising and comparing MFU values obtained in FACS is shown in **figure 3.11**.

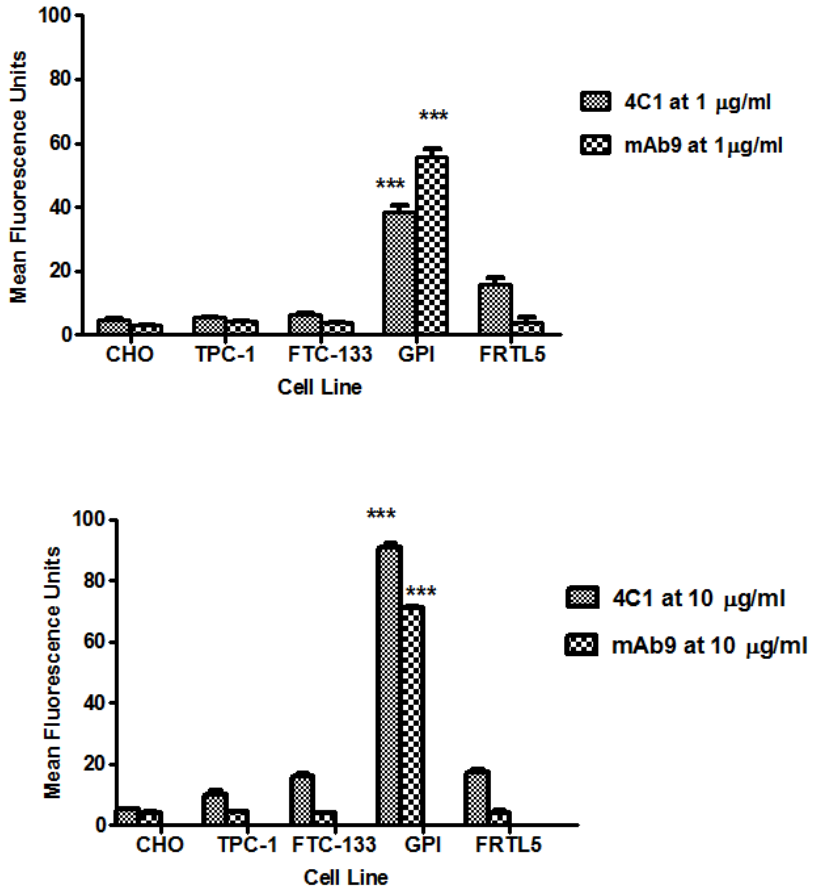

Figure 3.11: Comparison of mean fluorescent units (MFUs) of performed FACS with both 4C1 and mAb9 at 1 µg /ml and 10 µg /ml. Both mAb9 and 4C1 antibodies induced significant differences in the MFUs of GPI cells. ***** P < 0.001**. Values are the Mean+-SEM, n = 3. A One way ANOVA with Dunnetts post hoc test was used to compare all the cell lines used.

In summary, FACS experiments showed that 4C1 and mAb9 antibodies are able to bind significantly to the TSHR in GPI cells. mAb9 did not bind to any of the other cell lines studied. 4C1 bound moderately to FTC-133 and FRTL5 cells, however, the binding shown was however not statistically significant when compared with the control cell line.

3.1.2.2.2 Immunohistochemitry characterisation of TSHR expressed in FTC-133, TPC-1 and GPI cells

Immunohistochemical staining of FTC-133, TPC-1 and GPI cells was carried out with the purpose to further verify FACS results. Detailed methodology of immunohistochemistry can be found in section 2.2.5.

Images of representative sections of the immunofluorescent staining are shown in figures 3.12, 3.13, 3.14 and 3.15.

4C1 and mAb9, CHO cells

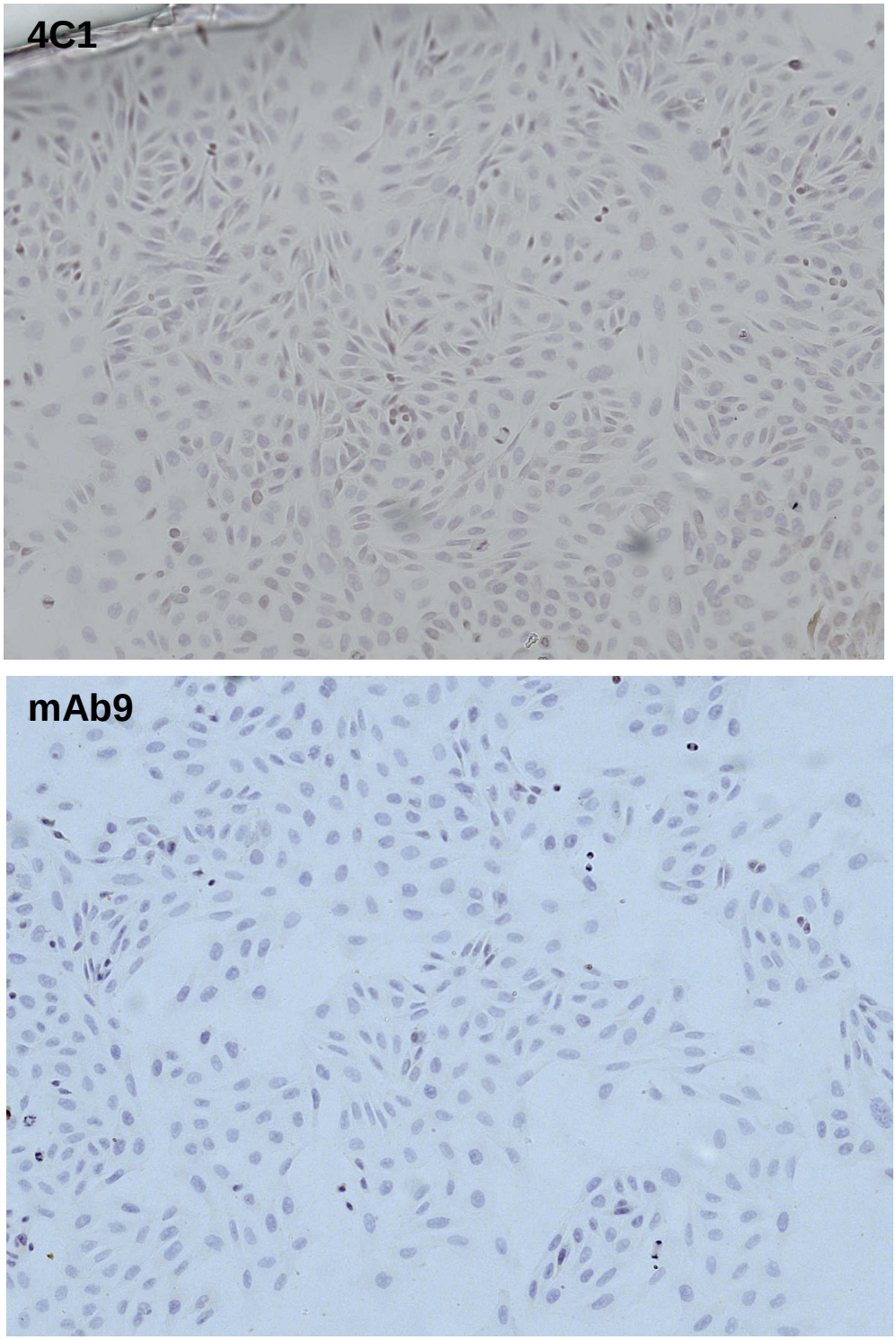

Figure 3.12: Immunohistochemistry performed on CHO cells to investigate TSHR expression Blue staining shows haematoxylin stained nuclei. TSHR staining is shown in brown. No specific binding was shown in CHO cells with both 4C1 and mAb9 antibodies. Images were taken at 20x magnification

4C1 and mAb9, FTC-133 cells

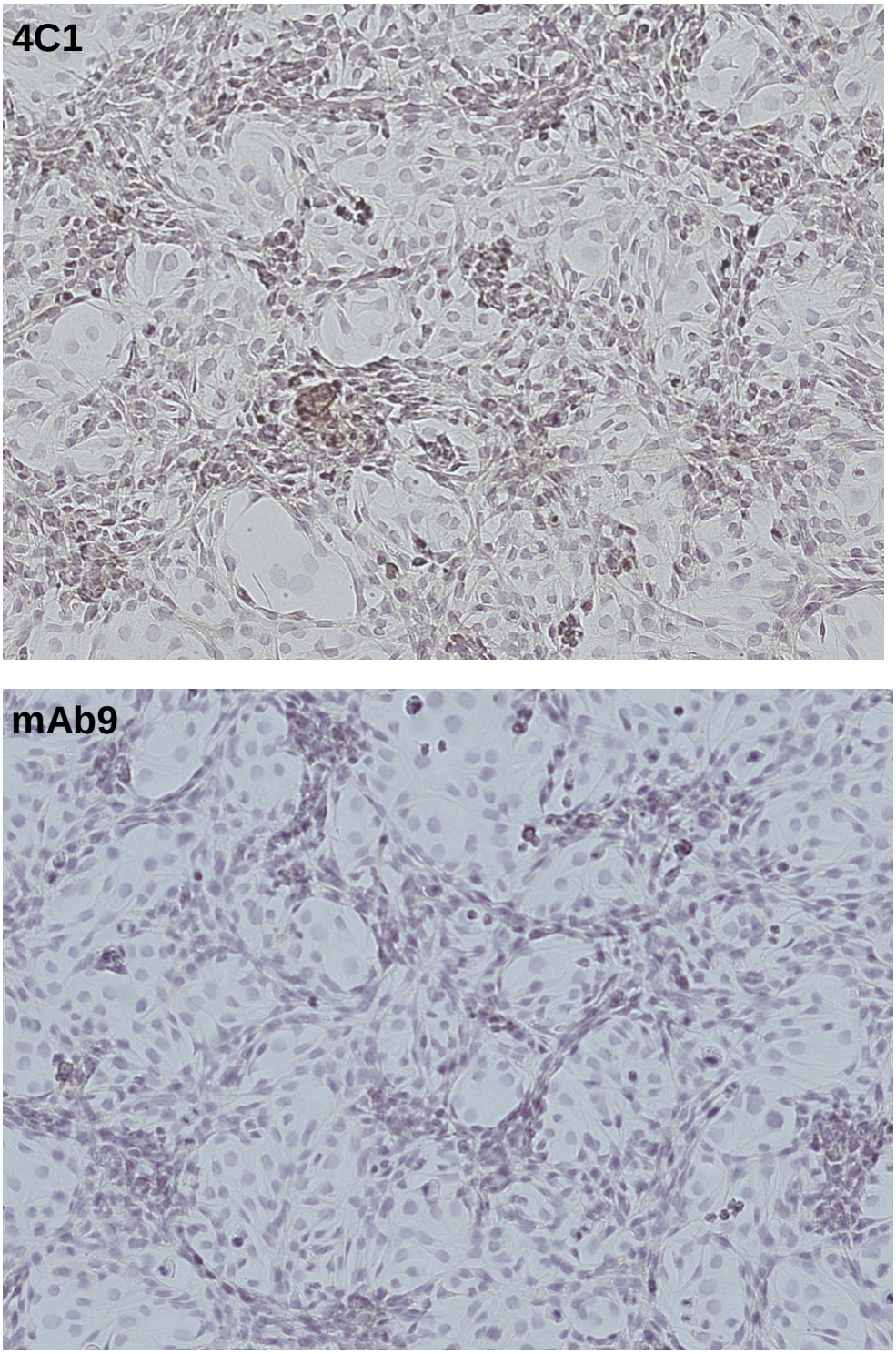

Figure 3.13 Immunohistochemistry performed on FTC-133 cells to investigate TSHR expression. TSHR staining is shown in brown. Blue staining shows haematoxylin stained nuclei. No specific binding was shown in FTC-133 with both 4C1 and mAb9 antibodies. Images were taken at 20 x magnification

4C1 and mAb9, TPC-1 cells

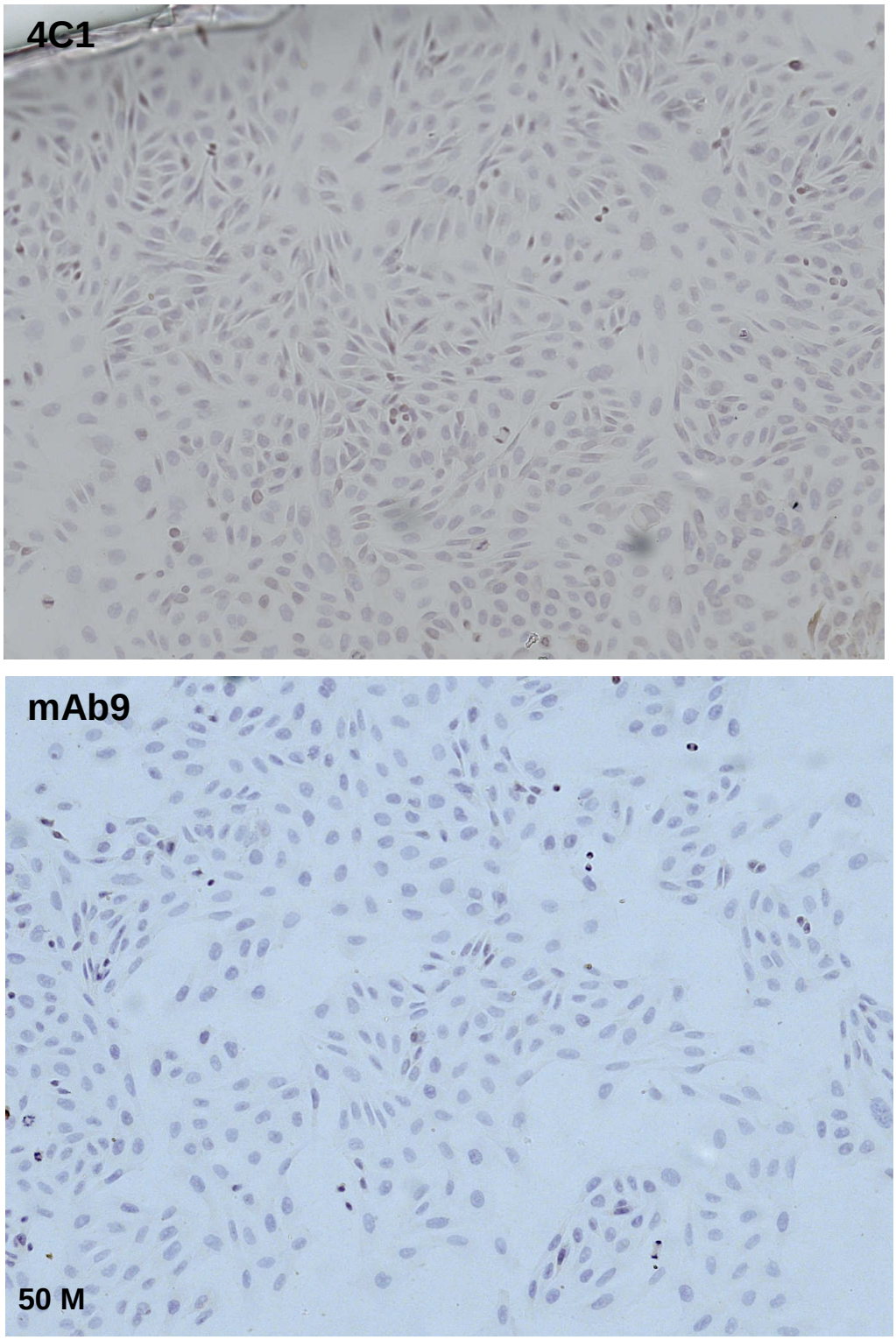

Figure 3.14: Immunohistochemistry performed on TPC-1 cells to investigate TSHR expression Blue staining shows haematoxylin stained nuclei. TSHR staining is shown in brown. No specific binding was shown in TPC-1 cells with both 4C1 and mAb9 antibodies. Images were taken 20 x magnification.

4C1 and mAb9, GPI cells

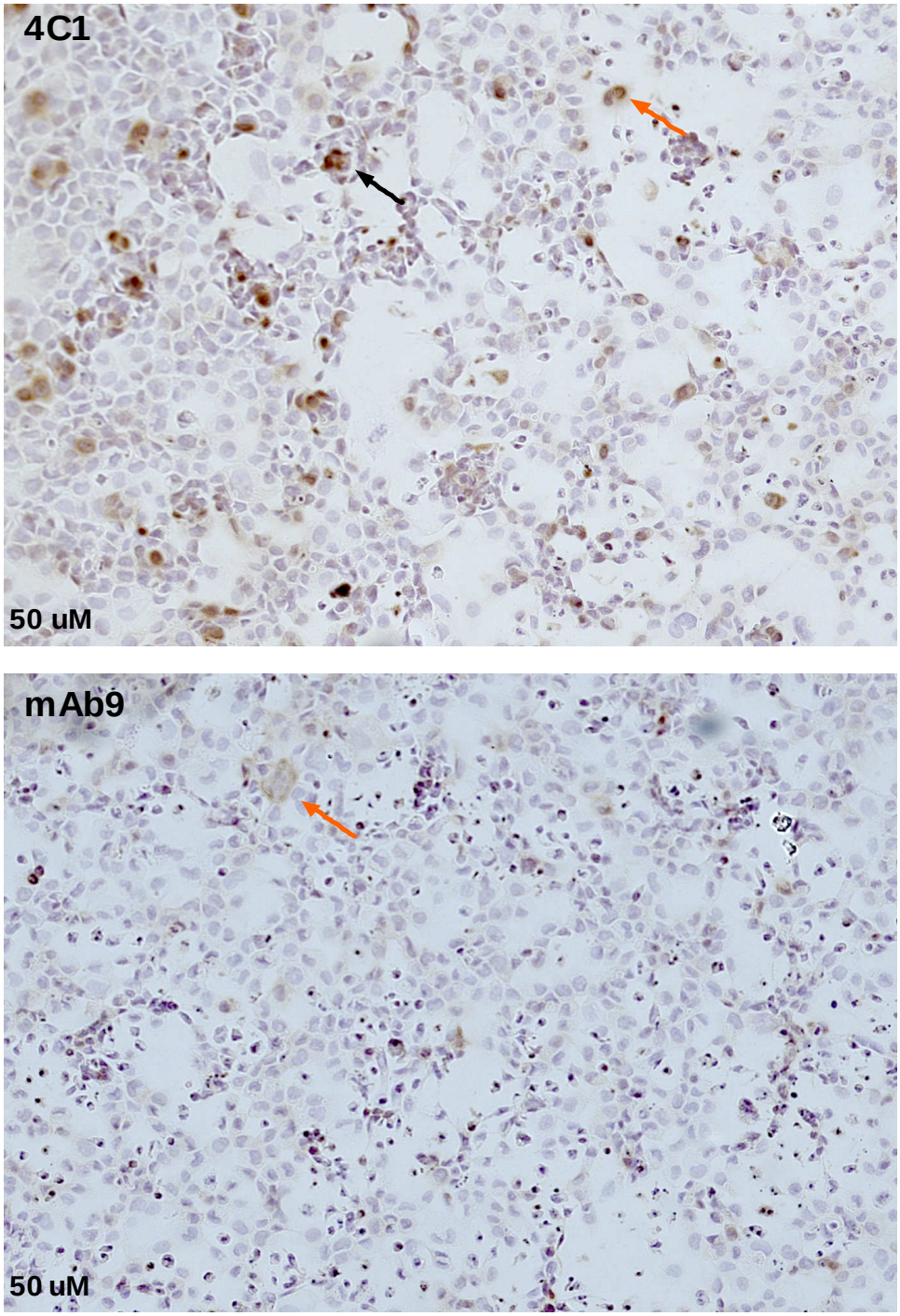

Figure 3.15: Immunohistochemistry performed on GPI cells to investigate TSHR expression. TSHR staining is shown in brown. Blue staining shows haematoxylin stained nuclei. TSHR positive staining was shown with mAb9 and 4C1 antibody. The black arrow is pointing at TSHR expressed in the nucleus and the red arrow is pointing at TSHR expressed in the cell membrane. Images were taken at 20 x magnification.

No staining was observed with 4C1 in the negative control cell line, CHO, as well as in FTC-133 and TPC-1 cells. 4C1 and mAb9 antibodies stained GPI cells in the nucleus as well as in the cell membrane.

Both FACS and immunohistochemistry results showed varying patterns of expression of TSHR in GPI cells. Some GPI cells expressed/stained high numbers of TSHR while other GPI cells expressed/stained lower levels of TSHR. Also, in immunohistochemistry studies, some GPI cells TSHR stained mainly in the nucleus while in other GPI cells mainly in the cell membrane.

No staining was observed with mAb9 in CHO, FTC-133 and TPC-1 cells however some degree of staining was observed with mAb9 in GPI cells. This could be due to these cells not expressing TSHR at high enough levels in order for it to be detected. To study this further, a Real-Time PCR study was performed.

3.1.3 Characterising TSHR in cell lines

3.1.3.1 RT-PCR relative quantification

In order to determine and compare the mRNA expression levels of TSHR in TPC-1, FTC-133 and GPI cells a quantitative RT-PCR assay was conducted.

Relative quantification can be achieved by analysing the Ct value obtained. The Ct value is the number of cycles required for the fluorescent signal to cross a threshold.

To quantify the RT-PCR results the comparative Ct method was used. In this method, the Ct values of the samples are compared with the Ct values of a negative control i.e. the calibrator. The Ct values of both calibrator and samples are normalised against a suitable endogenous housekeeping gene, in this case GAPDH. See section 2.2.6 for a detailed methodology.

Relative quantification was performed in FTC-133, TPC-1 and GPI cell lines and TSHR expression was compared with that from the calibrator, the non TSHR expressing cell line, CHO (**figure 3.16**).

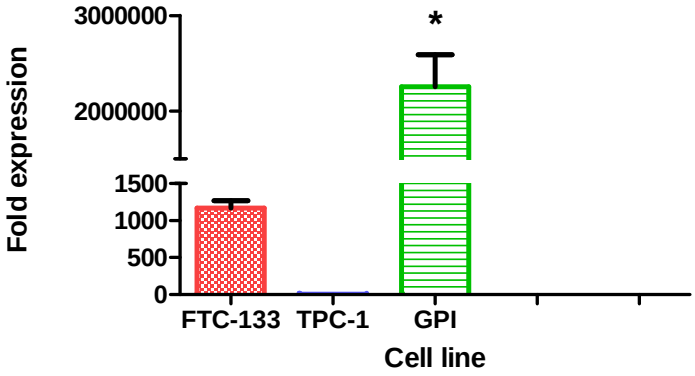

Figure 3.16: Quantitative RT-PCR to determine TSHR expression over CHO (calibrator) in all thyroid cell lines. GPI cells are shown to have high expression of TSHR when compared with the calibrator cell line. FTC-133 and TPC-1 did not show significant expression of TSHR. Values are mean ± SEM (n=3). ANOVA, *** P <0.05** with a Dunnett post-hoc test.

TSHR mRNA was expressed at significantly higher levels in GPI cells when compared to the calibrator cell line, CHO (**figure 3.16**). FTC-133 cells showed some expression of TSHR mRNA when compared with the calibrator cell line, CHO, but this was not statistically significant. There was no apparent expression of TSHR mRNA in TPC-1 cells.

3.1.3.2 Western blot experiments

Western blot experiments were carried out to measure TSHR protein levels in FTC-133, GPI and TPC-1 cell lines. See chapter 2.2.7 for a detailed methodology.

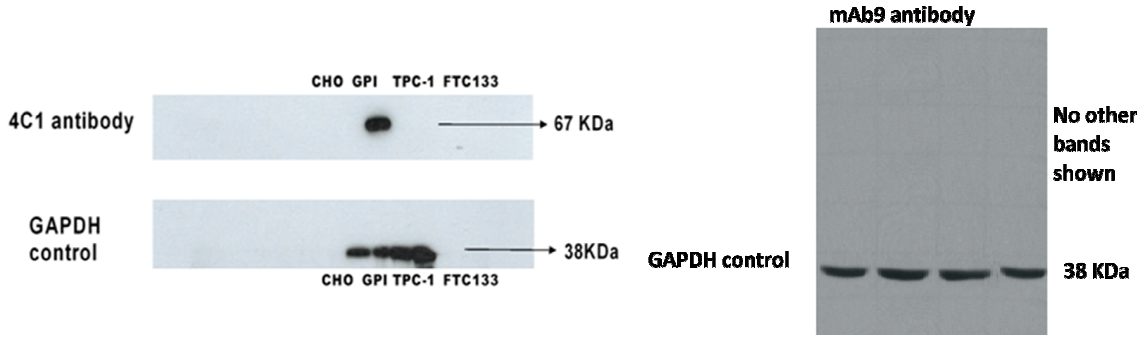

Figure 3.17 Western blot analysis of cell lysates with 4C1 and mAb9 antibodies in GPI cells. With 4C1 a band at 67 kDa was shown but mAb9 did not show any band. The 67 kDa band represents the TSHR in GPI cells.

Western blot analysis with 4C1 in GPI cells (**figure 3.17**) detected a single band of protein at a molecular weight of 67 kDa. This corresponds to the expected molecular weight of TSHR in GPI cells. No band was observed in CHO, TPC-1 and FTC-133 cells. These results support the RT-PCR results, where TSHR mRNA was shown not to be expressed in TPC-1 and FTC-133 cells.

The Western blot analysis with mAb9 in GPI cells detected no bands.

3.1.4 Radiolabelling of mAb9 with ^{125}I

mAb9 was radiolabelled with ^{125}I using the Iodogen method at low (10 MBq/20 µg) and high (10 MBq/5 µg) specific activity. See section 2.2.8 for a detailed methodology.

After the radiolabelling using the Iodogen method three experiments were conducted in order to confirm the labelling efficiency of ^{125}I-mAb9. First, instant thin layer chromatography (ITLC) was carried out in order to determine the labelling efficiency of the radiolabelled monoclonal antibody. Secondly, Radio-High performance liquid chromatography (Radio-HPLC) was carried out to confirm the results obtained by ITLC and also to test the integrity of the radiolabelled mAb9. Lastly, SDS-PAGE electrophoresis was also carried out to determine the size of the radiolabelled antibody and also to test for the presence of any degradation or aggregates.

3.1.4.1 Determination of the purity and radiolabelling efficiency of radiolabelled mAb9

3.1.4.1.1 Instant Thin Layer Chromatography (ITLC)

ITLC was performed in order to determine the radiolabelling efficiency of ^{125}I-mAb9. See section 2.2.9.1 for a detailed methodology. ITLC results showed most of the activity in the origin of the strip, indicating that ^{125}I-mAb9 had high labelling efficiency ranging from 94% to close to 100% (**figure 3.18** and **table 3.2**).

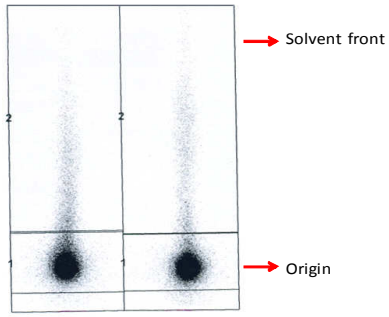

Figure 3.18: Analysis of the radiolabelled product using ITLC-SG strips run in 85% methanol. The origin represents the labelled compound whereas the solvent front represents free ^{125}I.

Labelling experiment	CPM Origin	CPM Solvent	%labelling
1	1577646	36046	98
2	2822337	17414	99.8
3	393839	28041	94.4
4	574026	36716	93.9
5	555450	29883	94.9
6	326520	18365	94.7

Table 3.2: Representative examples of results of ITLC quality control of ^{125}I-mAb9 radiolabelling efficiency. All radiolabellings were above 94% labelling efficiency.

3.1.4.1.2 Radio Size-exclusion HPLC

To further validate results, size exclusion Radio-HPLC was also performed. This was in order to determine the radiolabelling efficiency of ^{125}I-mAb9, as well as to determine the radiochemical and chemical purity of ^{125}I-mAb9. ITLC separates antibody-bound radioactivity from free ^{125}I but is not able to detect the presence of undesired antibody impurities. Therefore size-exclusion Radio-HPLC was carried out to provide additional

information on the integrity of the radiolabelled antibody. See section 2.2.9.2 for a detailed methodology.

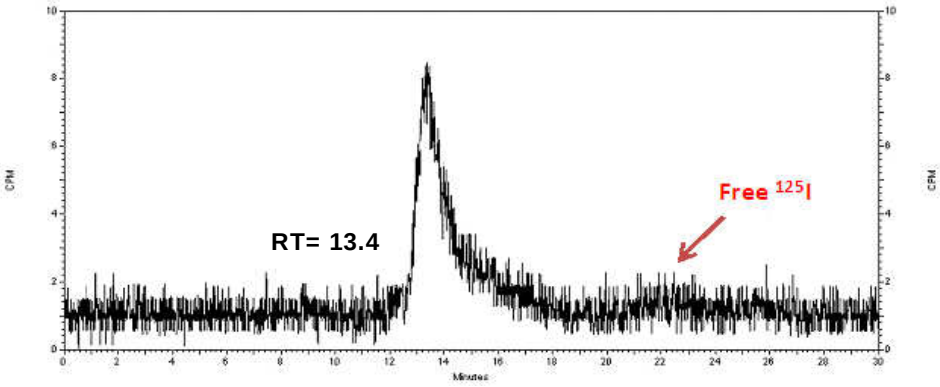

Figure 3.20: Radio-HPLC analysis of ^{125}I radiolabelled mAb9. A single major peak at retention time 13.4 minutes is shown. This peak represents a radiolabelling efficiency close to 100%.

Radio-HPLC results showed a main peak at retention time 13.4 minutes (**figure 3.20**), similar to that seen in the analysis with the unlabelled antibody (section 3.1.2). HPLC results thus confirm that ^{125}I-mAb9 was of a high labelling efficiency. The radioactive trace shows a high degree of 'noise' due to the high background of the radioactive detector (Raytest) as a result of the relatively low levels of activity being analysed. The highlighted arrow in the figure represents the retention time where free ^{125}I would be expected to elute. These results are similar to those obtained with control ^{125}I radiolabelled 4C1 anti-TSHR antibody, which also showed a major intact peak at a similar retention time (results not shown).

3.1.4.1.3 SDS-PAGE gel electrophoresis and phosphor imaging system to determine molecular weight and purity of ^{125}I-mAb9.

The resolution of size exclusion HPLC is not particularly high and therefore usually it does not separate molecules with fewer than thousands of Da difference. For this reason, SDS page gel electrophoresis SDS-PAGE gel electrophoresis was carried out in

order to determine the molecular weight and purity of ^{125}I-mAb9. See section 2.2.9.3 of methodology for a detailed protocol.

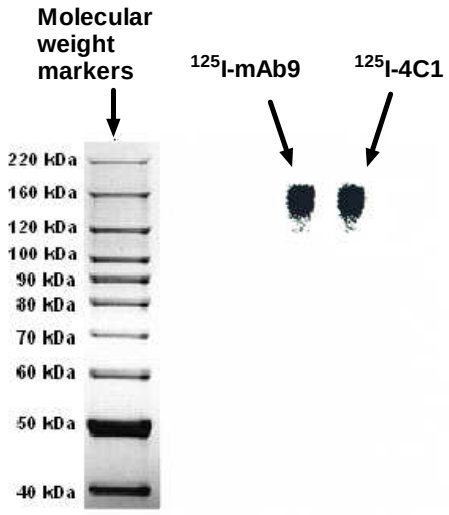

Figure 3.21: SDS page gel autoradiography. ^{125}I-mAb9 is shown at a molecular weight of 150 kDa.

A single band was detected at approximately 150 kDa in SDS-PAGE electrophoresis (**figure 3.21**). It can therefore be concluded that ^{125}I-mAb9 was of high purity.

These quality control experiments showed that ^{125}I-mAb9 was labelled to a high efficiency and without degradation or aggregation of the protein. The next step was therefore to study the binding proprieties of ^{125}I-mAb9 to TSHR, both in pre-coated tubes and in thyroid cancer and TSHR transfected cells, GPI cells.

3.1.5 ^{125}I-mAb9 binding Assays

3.1.5.1 TSHR Pre-coated tube assays

Coated tube assay for the measurement of ^{125}I-mAb9 binding to TSHR

The TSHR coated tube assay assessed the ability of unlabelled mAb9 to compete with radiolabelled ^{125}I-mAb9 for the binding to TSHR coated in the tubes. See section 2.2.10.1 for a detailed protocol.

A high and a low specific activity of ^{125}I-mAb9 were tested in this assay in order to find out the effects of specific activity on receptor binding (**figure 3.22).**

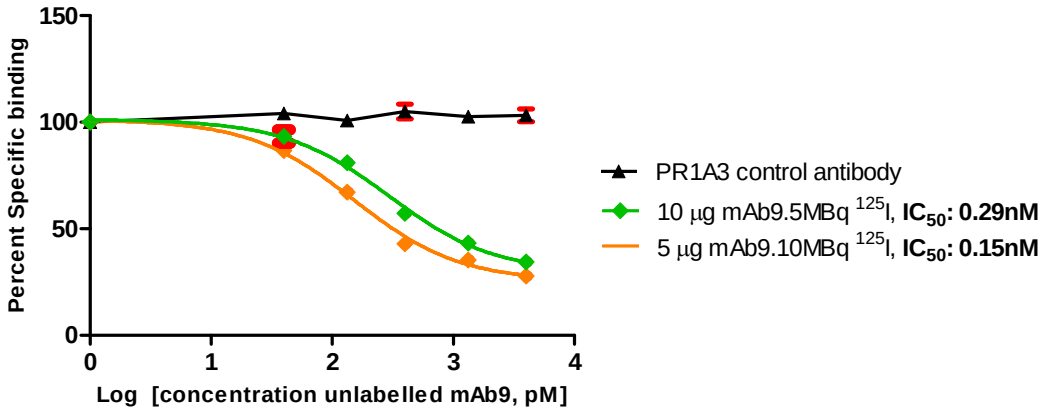

Figure 3.22: Competition assay of of ^{125}I-mAb9 with unlabelled mAb9 to the TSHR in pre coated tubes. Increasing concentrations of mAb9 competed with 5 µg mAb9 labelled with 10 MBq of ^{125}I (higher specific activity) and 20 µg mAb9 labelled with 10 MBq ^{125}I (lower specific activity). Values are the mean of duplicate determinations.

When using ^{125}I radiolabelled mAb9 at a low or high specific activity, only incomplete inhibition of binding was seen compared with the complete inhibition seen in **figure 3.6** (**figure 3.23**). This may be due to a higher non-specific binding of the ^{125}I-mAb9 as compared to ^{125}I-TSH. The radiolabelling of antibodies with ^{125}I can potentially damage the antigen-binding activity of the antibody through oxidative damage caused by binding/attachment of the isotope to the tyrosine rich antigen site. To further explore if the mAb9 binding ability was damaged, additional TSHR pre-coated tube assays and FACS assays were performed (figure 3.2.3, 3.2.4 and 3.2.5). See sections 2.2.4 and 2.2.10.1 for a detailed protocol.

Three preparations were compared:

- mAb9 incubated alone in an Iodogen tube- ***'oxidised mAb9'.***
- mAb9 co-incubated with cold iodine (potassium [^{127}I] iodide) in an Iodogen tube – ***'cold labelled' mAb9.***
- mAb9 mixed with potassium iodide (KI) – ***'mixed mAb9'.***

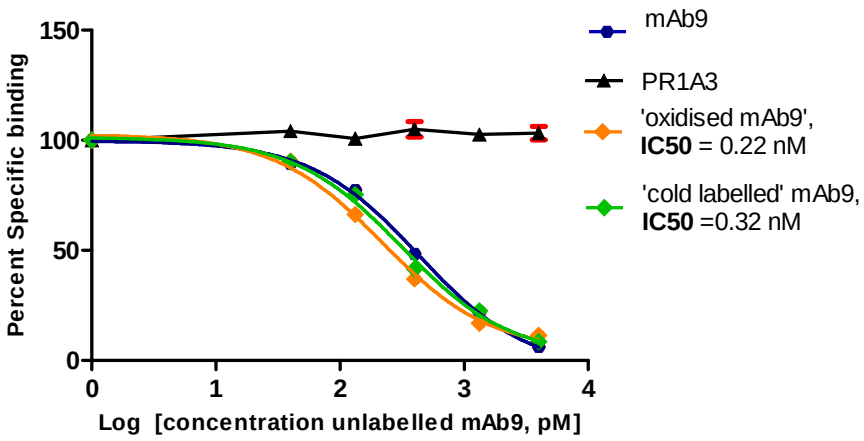

Figure 3.23: Competition assay of ^{125}I-mAb9 with 'oxidised mAb9' and 'cold labeled mAb9' in TSHR pre coated tubes. Indicated concentrations of 'cold labelled mAb9' as well as oxidised mAb9 competed with ^{125}I-mAb9 in a concentration dependent manner. PRA1A3 was used as a control antibody. Values are the mean of duplicate determinations.

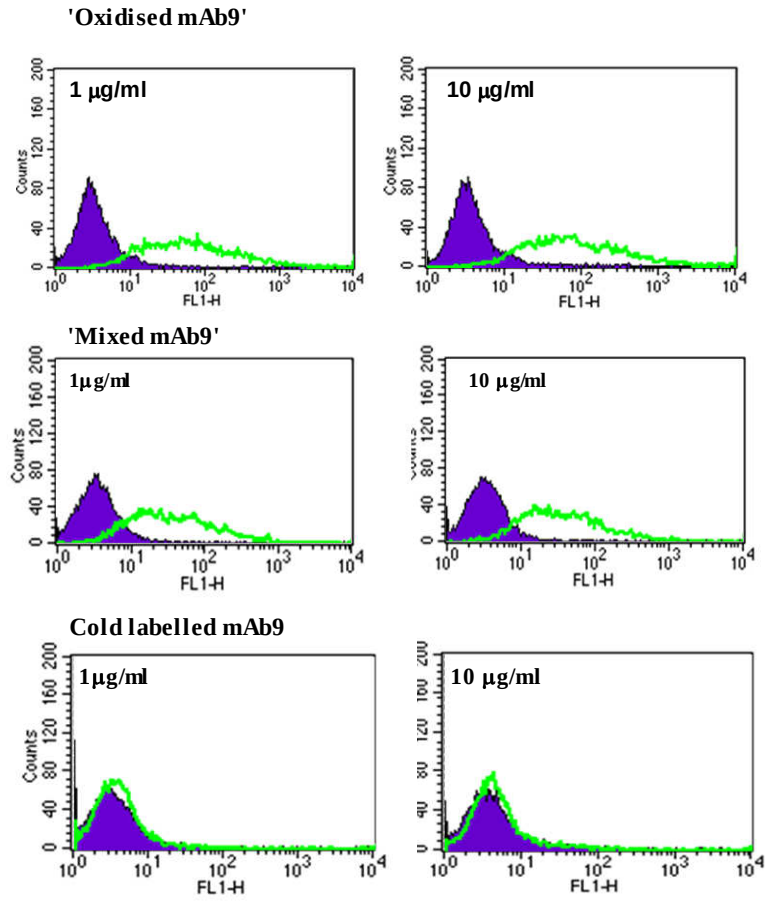

Figure 3.24: FACS analysis on GPI cells using different mAb9 preparations. 'Mixed mAB9' and 'oxidised mAb9' showed a positive shift. No shift was detected with 'cold labelled mAb9. CHO control cells are shown in dark blue and GPI cells are shown in green.

Similar experiments were also carried out with 4C1antibody (**figure 3.25**).

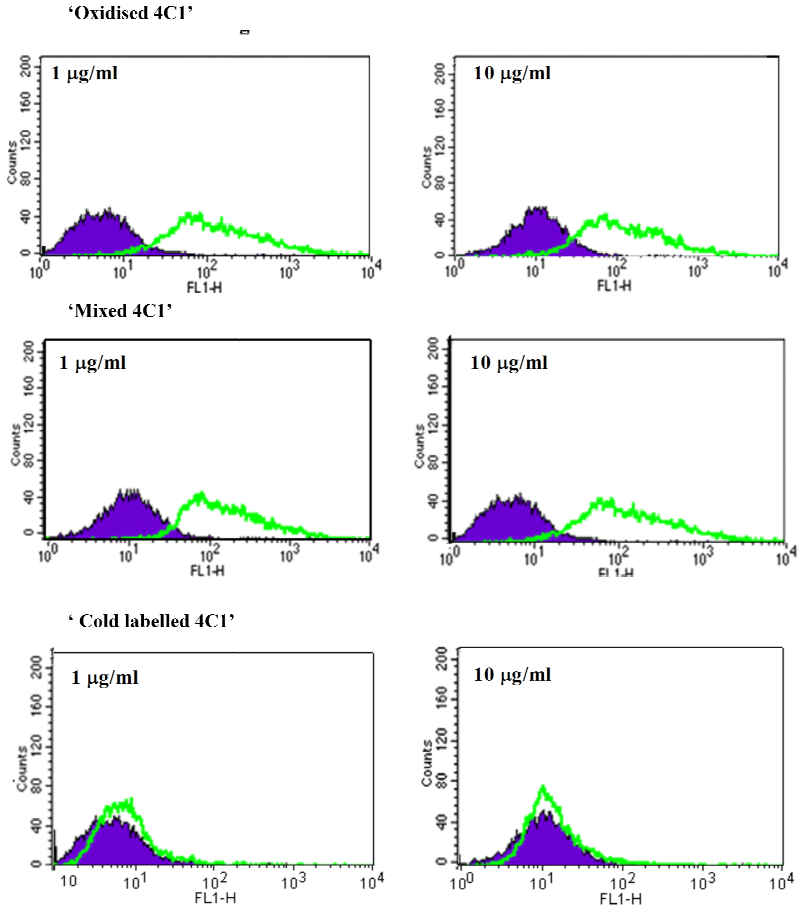

Figure 3.25: FACS analysis of 4C1 preparations. 'Oxidised 4C1' and 'Mixed 4C1' show a positive shift. No shift was seen with 'cold-labelled 4C1'. CHO cells are shown in dark blue and GPI cells are shown in green.

'Cold labelled mAb9' and 'oxidised' mAb9 were able to compete with ^{125}I-TSH for the binding of TSHR coated in the tubes (**figure 3.23**). From these results it can be concluded that the oxidation inflicted by the Iodogen labelling method was not damaging the antibody's ability to bind to the TSHR coated in the tubes. In FACS, however, 'cold labelled mAb9' and 'cold labelled 4C1' did not bind to TSHR in GPI cells (**figure 3.24** and **3.25**).

3.1.5.2 ^{125}I-mAb9 cell binding assays

In section 3.1.2, unlabelled mAb9 was shown to bind to the TSHR in GPI cells and pre-coated tubes. Once the mAb9 was successfully radiolabelled, it was important to determine whether it had retained its receptor binding affinity. ^{125}I radiolabelled mAb9 also bound to TSHR in pre-coated tubes, therefore the next step was to assess the binding of ^{125}I-mAb9 to the TSHR in cells.

3.1.5.2.1 Assay development and optimisation

Effect of temperature and time in TSHR cell binding assays

The first condition to be considered was the effect that temperature and incubation time have on the binding of ^{125}I-mAb9 to the TSHR in FTC-133, TPC-1 and GPI cells. See sections 2.2.11.1 and 2.11.2 for a detailed protocol.

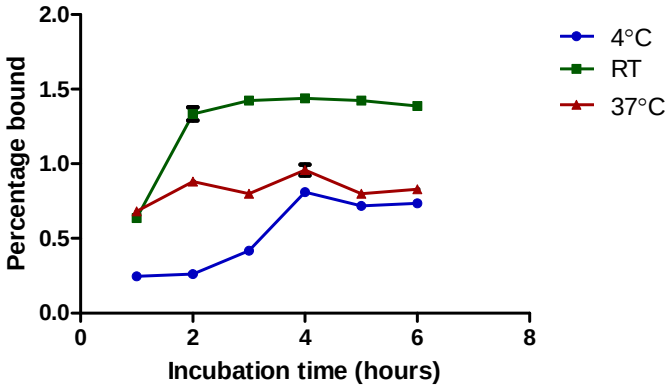

Figure 3.26: Effect of temperature and time in the binding of ^{125}I-mAb9 to GPI cells. Cells were incubated for up to 6 hours at 4°C, room temperature (RT) and 37°C. Cells incubated at RT showed the highest percentage of bound antibody. This assay was carried out with triplicate samples and repeated twice.

Incubation at room temperature for around 2 to 3 hours appeared to be the most favourable conditions to be used in the GPI cell binding assay, as it gave the highest percentage of bound mAb9 (**figure 3.26**), and the later conditions were thus used in future experiments.

A TCA precipitation assay was performed over a 6 hour period to find out if the ^{125}I remained antibody-bound and did not dissociate during the assay. See section 2.2.11.1 of methodology for a detailed protocol.

TCA precipitation assay

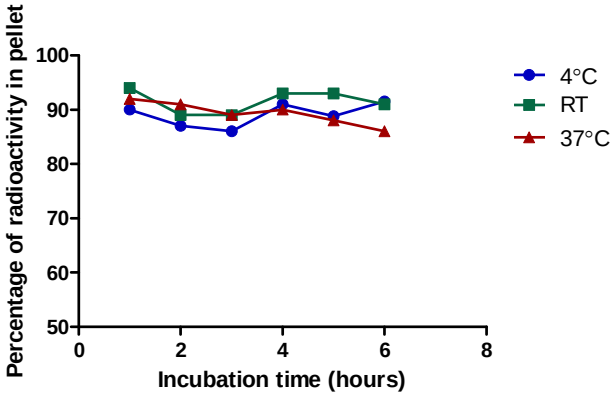

Figure 3.27: TCA precipitation assay of ^{125}I-mAb9 over a period of 6 hours. Most of the ^{125}I remained bound to the mAb9 antibody over a period of 6 hours.

This assay showed that at most times and at different temperatures the protein remained bound to ^{125}I (**figure 3.27**) and therefore results were not being confounded by the presence of ^{125}I metabolites.

Effect of media in TSHR cell binding assays

In order to identify the most effective buffer to use in the cell binding experiments, a number of different buffers were tested in TSHR transfected GPI cells.

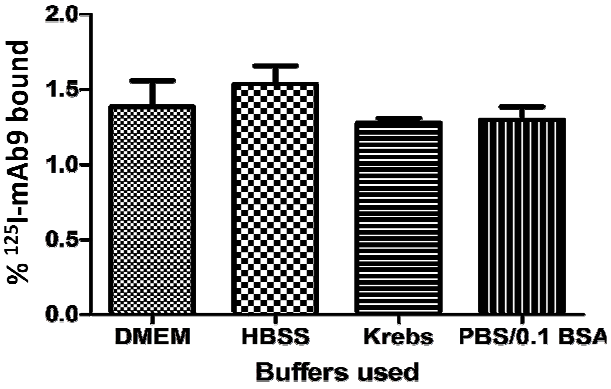

Figure 3.28: Graph showing binding of ^{125}I-mAb9 to GPI cells in different buffers. No significant difference in binding was observed.

The different buffers used were found not to have a significant effect on the binding as there was no significant difference in the proportion of ^{125}I-mAb9 bound to GPI cells in DMEM, HBSS, Krebs and PBS/0.1%BSA buffers (**figure 3.28**). Therefore in future binding experiments any of the buffers could potentially be used. DMEM binding buffer was selected to be used in future binding studies.

3.1.5.2.2 Immunoreactive fraction asssay

The first step in the assay development was to perform a direct radioimmunoassay in order to measure the immunoreactivity of the radiolabelled mAb9, i.e. the proportion of radioactive antibody having the ability to bind the TSHR. See section 2.2.11.3 for a detailed methodology. Immunoreactive fraction assays were performed on GPI, FTC-133 and TPC-1 cells, however, FTC-133 and TPC-1 cells failed to show any antibody binding therefore it was not possible to determine an (immunoreactive fraction) IRF value for these cells. The immunoreactivity was calculated to be 5.1 %, which suggests that about 5% of the radioactive antibody is able to bind to the TSHR (**figure 3.29**).

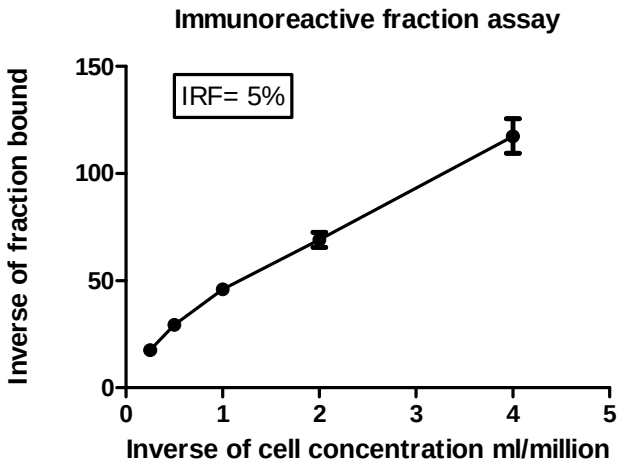

Figure 3.29: Immunoreactive fraction assay with ^{125}I-mAb9 in GPI cells. Graph of reciprocal of fraction bound against the reciprocal of cell concentrations.

3.1.5.2.3 Saturation assay using ^{125}I-mAb9 in GPI cells

Saturation assays were then performed with ^{125}I-mAb9 in order to measure the specific radioligand binding to cells at equilibrium to determine both the receptor numbers (Bmax) and binding affinity (Kd) of ^{125}I-mAb9. See section 2.2.11.4 of methodology for a detailed protocol. mAb9 bound to TSHR in GPI cells (**figure 3.30**) with a binding affinity of 3.6 nM and Bmax of 2816 fmol/mg protein.

^{125}I-mAB9 GPI binding assay

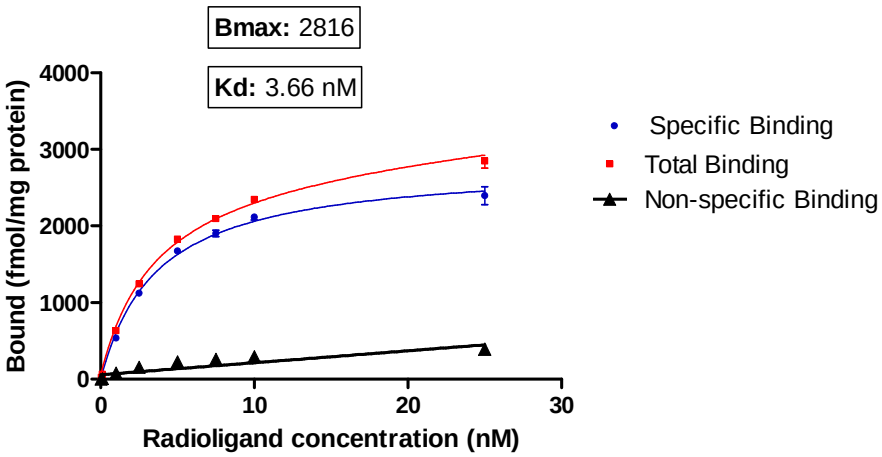

Figure 3.30: Equilibrium saturation binding of ^{125}I-mAb9 to GPI cells. ^{125}I-mAb9 bound to GPI cells with a kD of 3.66 nM and Bmax 2816 fmol/mg Results represent specific binding (total minus nonspecific binding) of triplicate determinations. Mean (±SEM)

^{125}I-4C1 GPI binding assay

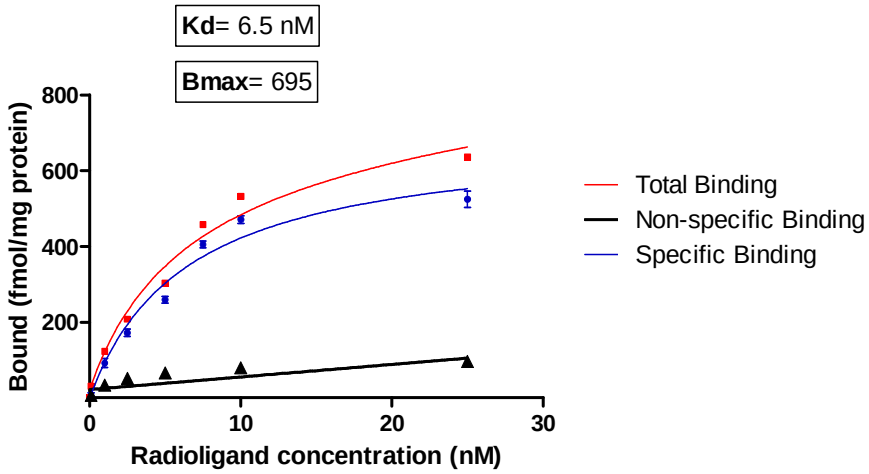

Figure 3.31: Equilibrium saturation binding of ^{125}I-4C1 to GPI cells. Results represent specific binding (total minus nonspecific binding) of triplicate determinations. Mean (±SEM)

^{125}I-4C1 bound to GPI cells with a kD of 6.5 nM and Bmax of 695 fmol/mg (**figure 3.31**). The binding affinity with ^{125}I-4C1 does not differ greatly from the value obtained with ^{125}I-mAb9 (**figure 3.30**).

3.1.5.2.4 Saturation assay with ^{125}I-mAb9 in FRTL5 cells

Saturation binding assays were also performed in FRTL5 cells. Although ^{125}I-mAb9 appeared to bind to FRTL5 cells, the majority of the binding was non-specific binding (**figure 3.32**).

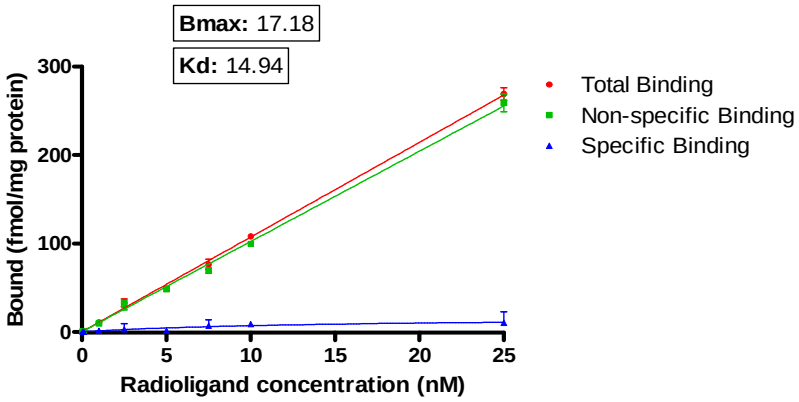

Figure 3.32: Equilibrium saturation binding of ^{125}I-mAb9 to FRTL5 cells. Results represent specific binding (total minus nonspecific binding) of triplicate determinations

From the cell binding assay result, it can be concluded that ^{125}I-mAb9 binds specifically to GPI cells with a binding affinity of 3.6 nM. ^{125}I-mAb9 does not, however, bind specifically to FRTL-5 cells.

3.5.2.5 Saturation assay with ^{125}I-mAb9 and ^{125}I-4C1 in FTC-133 and TPC-1 cells

Saturation assays were also performed in FTC-133 and TPC-1 cells using the same conditions as previously in the conducted saturation assays. Saturation assays were repeated 3 times however no binding was detected. This was possibly due to the very low amount of TSHR expression in these cells hence resulting in very negligible binding.

3.1.6 Imaging

3.1.6.1 Imaging of mice injected with radiolabelled mAb9 and ^{125}I-iodide using SPECT/CT

SPECT/CT imaging experiments were performed in mice, in order to assess the binding of ^{125}I-mAb9 to the TSHR expressed in the normal thyroid of the mouse. See section 2.2.12 for a detailed methodology.

Representative images are shown below and the results are summarised in **figure 3.33**.

Group A (^{125}I radiolabelled mAb9)

4 hours - High uptake in both thyroid and salivary glands seen

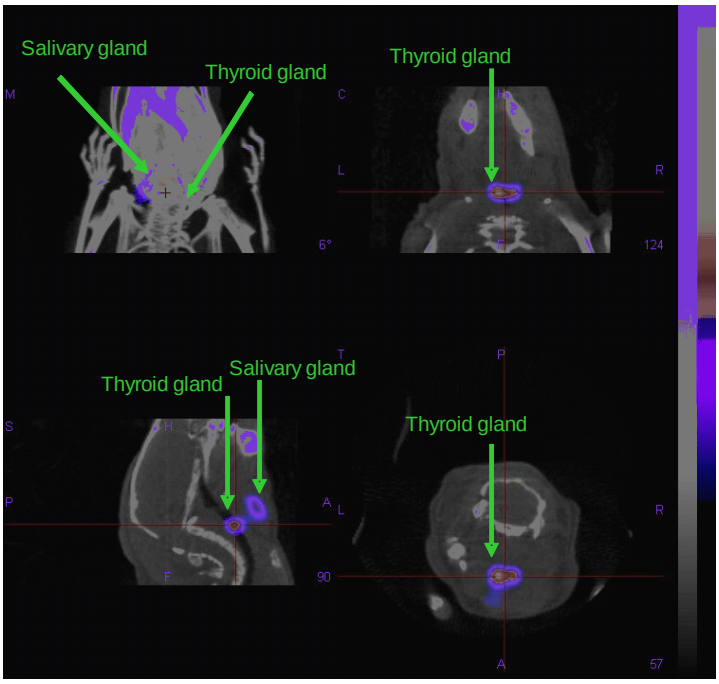

Group A (^{125}I radiolabelled mAb9)

24 hours – High uptake in the thyroid only

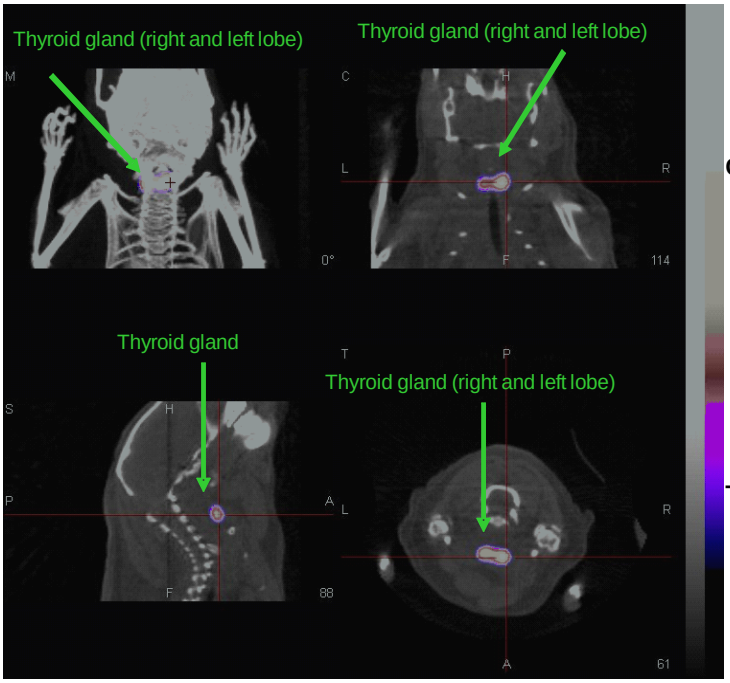

Group B (sodium perchlorate followed by ^{125}I radiolabelled mAb9)

4 Hours - Some uptake seen in the thyroid only

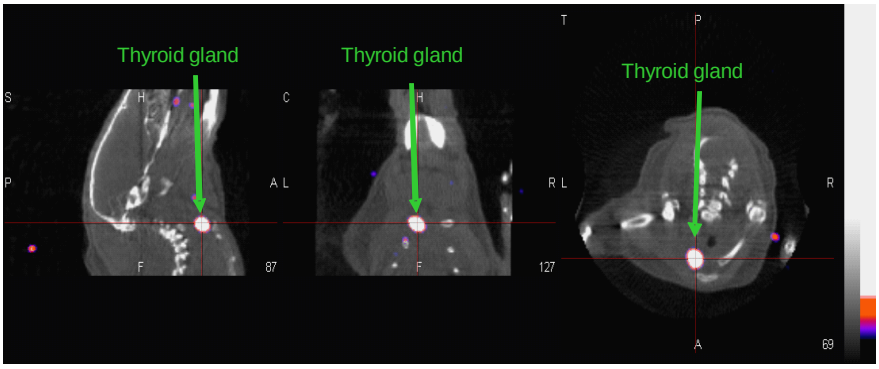

Saggital Coronal Transverse

Group B (sodium perchlorate followed by ^{125}I radiolabelled mAb9

24 hours – No uptake seen

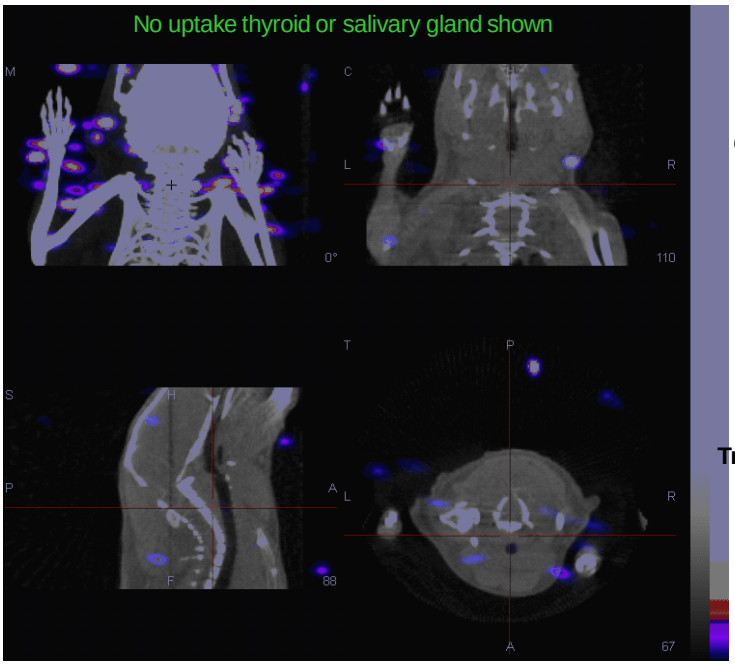

MIP **Coronal**

Sagittal **Transverse**

Group C (^{125}I-iodide at the same activity as group A)

4 hours – Uptake seen in both thyroid and salivary gland. Much higher in latter.

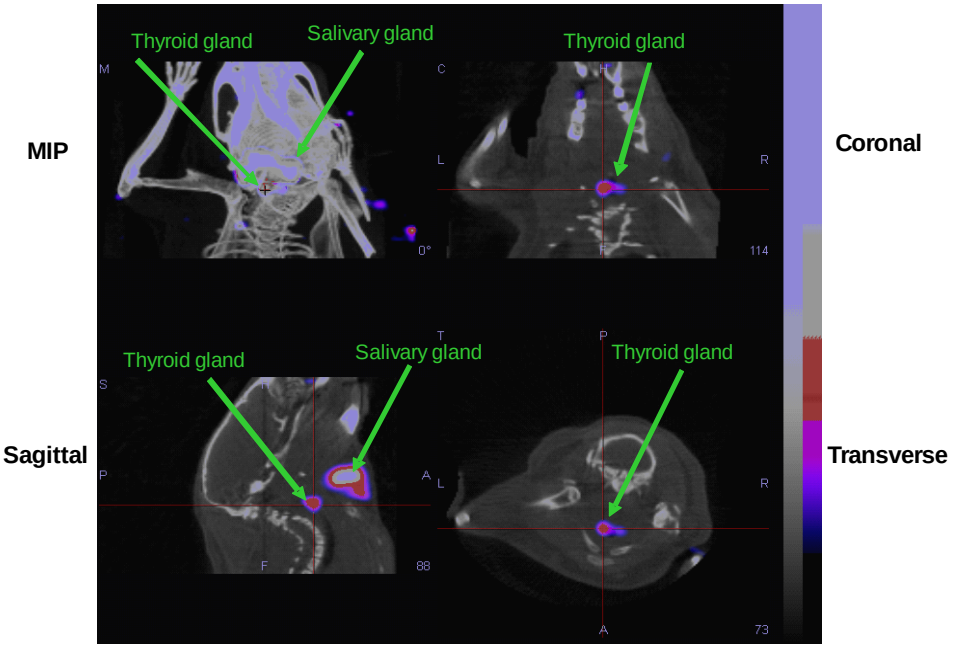

Group C (^{125}I-iodide at the same activity as group A)

24 hours – Uptake in thyroid only

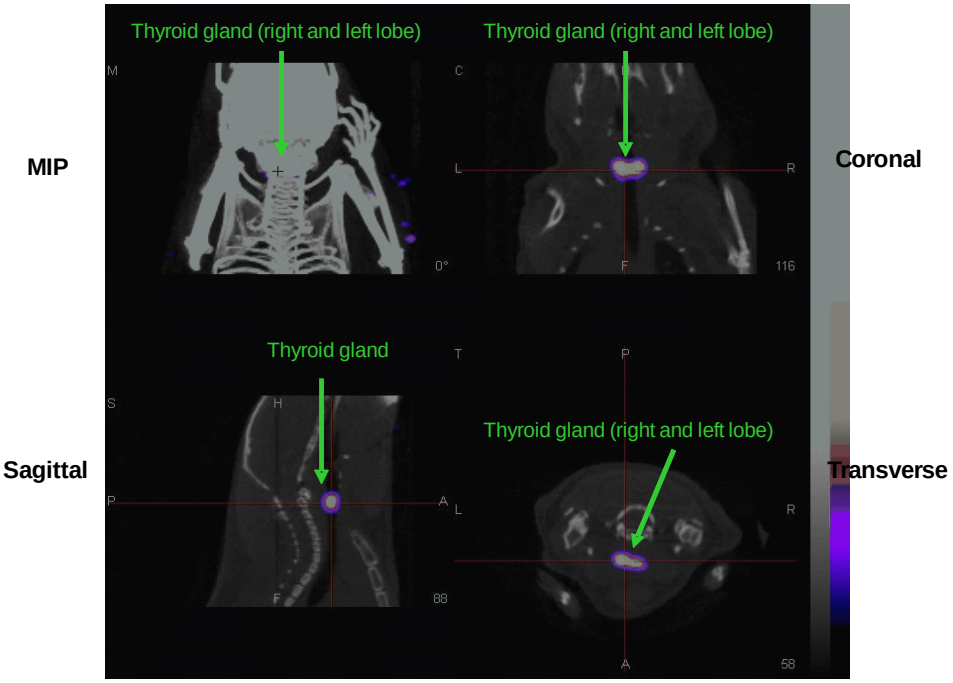

Group D (sodium perchlorate followed by ^{125}I-iodide)

4 hours – No uptake seen

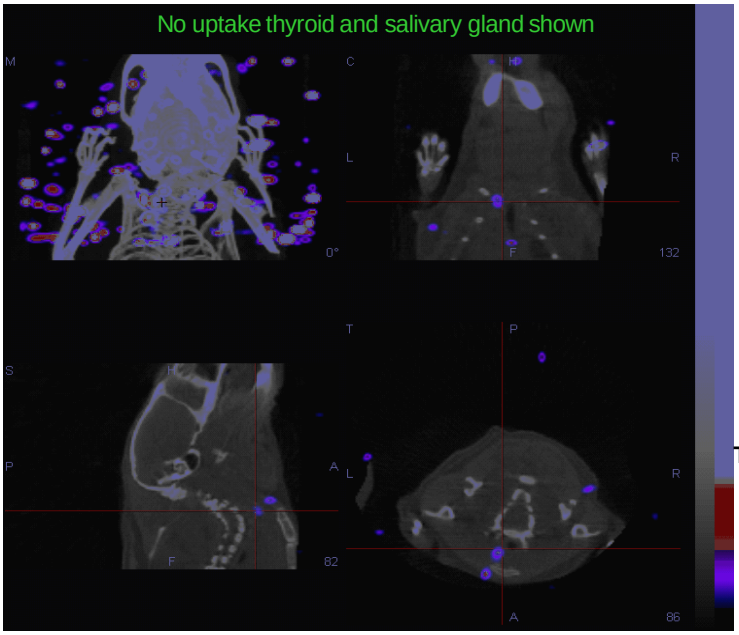

Group D (sodium perchlorate followed by ^{125}I-iodide)

24 hours – No uptake seen

		EXPRESSED AS % OF INJECTED DOSE					
	GROUP	Mouse	Time (hours)	Thyroid	Salivary gld	Salivary gld	Salivary gld
	A	1	4	2.4	0.6	0.9	6.8
^{125}I-mAb9			24	2.5	0.0	0.0	0.0
	A	2	4	2.0	3.1	4.8	4.6
			24	2.4	0.0	0.0	0.0
^{125}I-mAb9	B	3	4	0.2	0.0	0.0	0.0
+			24	0.0	0.0	0.0	0.0
perchlorate	B	4	4	0.1	0.0	0.0	0.0
			24	0.0	0.0	0.0	0.0
^{125}I-iodide	C	5	4	1.2	14.3	13.8	0.0
			24	0.7	0.0	0.0	0.0
	C	6	4	0.7	7.1	0.0	0.0
			24	0.5	0.0	0.0	0.0
^{125}I-iodide	D	7	4	0.0	0.0	0.0	0.0
+			24	0.0	0.0	0.0	0.0
perchlorate	D	8	4	0.0	0.0	0.0	0.0
			24	0.0	0.0	0.0	0.0

Table 3.3: % of injected dose of radioactivity in the thyroid gland and salivary gland. 4 and 24 hour time points were used.

Group A (mice injected with ^{125}I-radiolabelled mAb9) showed similar activity in the thyroid at both 4 and 24 hour time points. It also showed activity in the salivary gland at the 4 hour time point, however it did not show any activity in the salivary gland after 24 hours. Because ^{125}I is taken up into salivary glands via NIS, it is clear that *in vivo* metabolism of the ^{125}I-mAb9 is occurring *in vivo* resulting in the release of ^{125}I. The thyroid uptake in group A may therefore be due either ^{125}I-mAb9 binding to the TSHR or to ^{125}I being taken up by to NIS. In order to understand if this uptake was due to the actual binding of mAb9 to the TSHR, in group B sodium perchlorate was used to block the uptake of iodine by NIS.

Group B (where perchlorate was added prior to the injection of ^{125}I-mAb9) showed no uptake in the salivary glands but some activity in the thyroid in both mice at the 4 hours time point, however this is less than that seen in Group A and there is no uptake

after 24 hours. The lack of uptake in the salivary glands indicates that the perchlorate effectively blocked NIS and suggests that the thyroid uptake is due to binding to the TSHR *in vivo*.

In **group C** (**^{125}I at the same activity as group A**) there was activity in the thyroid at both 4 hours and 24 hour time points, however the activity was lower than group A, which again may suggest the higher uptake in Group A is due to mAb9 binding to TSHR. As expected, the salivary gland had activity at the 4 hour time point, this correlates with studies that have shown ^{125}I to be taken up by this gland [16, 79]. At the 24 hour time point, activity was seen in the thyroid however not in the salivary glands, since iodide is not organified in these tissues.

Although all mice were given potassium iodide in order to block the thyroid, this did not block the uptake of iodine in those groups which were not also treated with perchlorate.

Group D (perchlorate prior to the injection of ^{125}I) showed no activity in the thyroid on all time points as well as no activity in the salivary glands. These results confirm that the sodium perchlorate is efficiently blocking the uptake of iodine by the thyroid.

Although ^{125}I-mAb9 showed binding to the TSHR in the thyroid of mice in group B, the percentage of injected dose was extremely low, and thus, results are unable to categorically indicate whether the radioactivity seen in the images is due to the specific binding of ^{125}I-mAb9 to the TSHR or due to free ^{125}I being taken up by the thyroid via NIS.

3.1.7 Radiolabelling of mAb9 with ^{111}In

As previously discussed, radiolabelling mAb9 with ^{125}I might be damaging its structure, and by doing so, hindering its ability to bind to the TSHR. Moreover, most importantly, there is a chance that free ^{125}I can be taken up into the thyroid via NIS and interfere with

in vivo imaging and biodistribution studies. This problem can potentially be solved by radiolabelling mAb9 with a different radioisotope. In this section, mAb9 was radiolabelled with ^{111}In. ^{111}In was used due to its beneficial imaging properties and also due to its easy availability in the lab but most importantly because it is not taken up by the thyroid.

3.1.7.1 Conjugation of mAb9 with SCN-Bz-DOTA

The first step was to conjugate the chelating agent to the antibody via lysine side chain amino groups. See section 2.2.13.1 for a detailed methodology.

3.1.7.2 Assessing the purity and integrity of the Benzyl-DOTA-mAB9 conjugate.

3.1.7.2.1 Size Exclusion- HPLC

Benzyl-DOTA-mAb9 was analysed by size-exclusion HPLC to determine the integrity and purity of the newly conjugated mAb9. See section 2.2.13.2 for a detailed methodology. A single peak at retention time 13.4 minutes was observed in size exclusion HPLC, indicating that Benzyl-DOTA-mAb9 was of high purity and integrity (**figure 3.34**). The molecular size of Benzyl-DOTA-mAb9 was estimated to be around 150,000 Da according to the gel filtration standards previously analysed by SE-HPLC (**section 3.1.2**, **figure 3.2**).

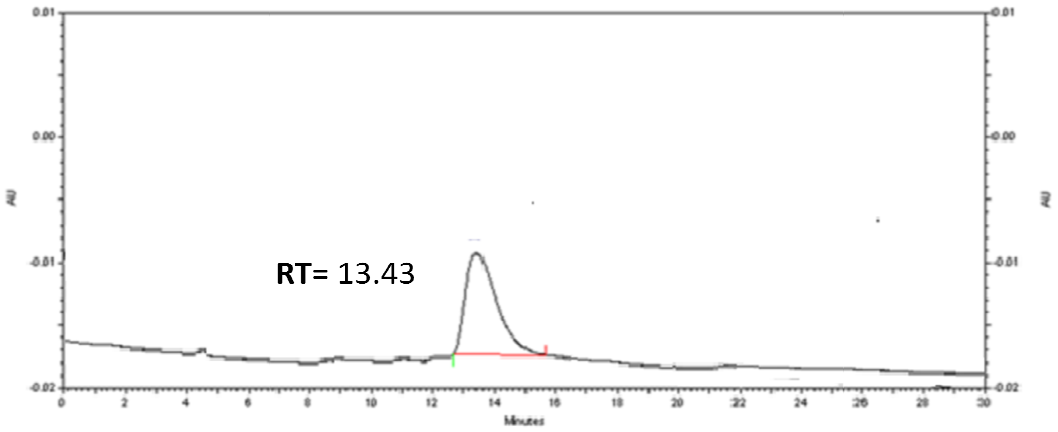

Figure 3.34: Size-exclusion HPLC with ScnBzDOTA-mAb9. A single peak eluted at retention time 13.43 minutes.

3.1.7.2.2 Assessing the binding ability of Benzyl-DOTA-mAb9 to TSHR.

Once mAb9 had been conjugated to DOTA, it was important to determine whether the conjugated antibody had retained its receptor binding affinity and that this had not been compromised in any way. In order to do that a FACS with GPI cells and the TSHR coated tube assay were performed with the newly conjugated Benzyl-DOTA-mAb9. See sections 2.2.13.3 and 2.2.13.4 for a detailed methodology.

3.1.7.2.3 Benzyl-DOTA-mAb9 FACS

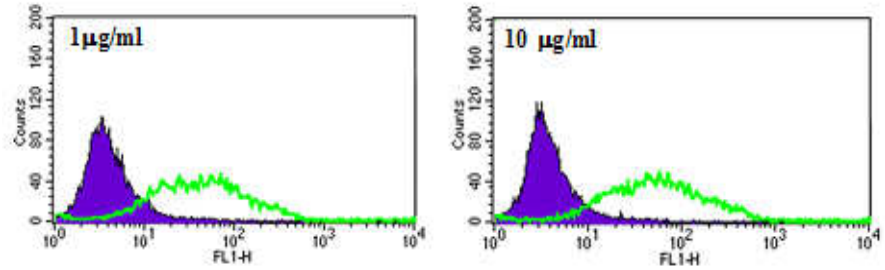

Figure 3.35: FACS analysis with Bz-DOTA-mAb9 in GPI (green) and CHO (dark blue) cells. A significant positive shift was seen at both 1 µg /ml and 10 µg /ml Benzyl-DOTA-mAb9.

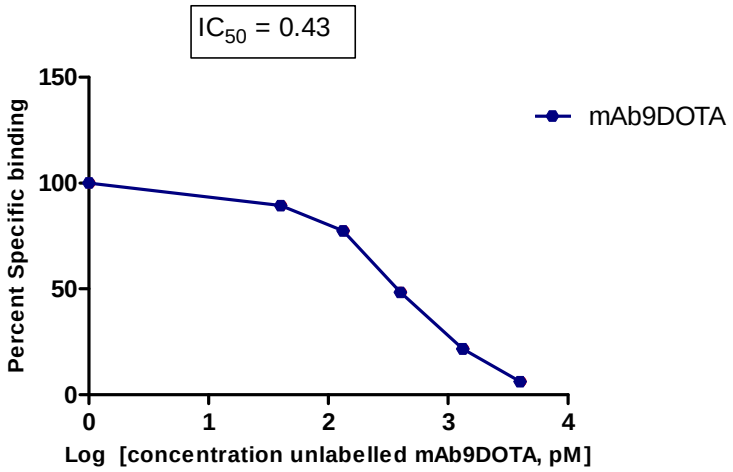

Figure 3.36: Competition assay of ^{125}I-TSH with Bz-DOTA-mAb9 to the TSHR in pre coated tubes. indicated concentrations of Bz-DOTA-mAb9 competed with ^{125}I-TSH in a concentration dependent manner. Values = Mean (±SEM).

Benzyl-DOTA-mAb9 bound to TSHR in GPI cells (**figure 3.35**). The shift and MFU obtained with Benzyl-DOTA-mAb9 were similar to the shift and MFU obtained with unconjugated mAb9. Benzyl-DOTA-mAb9 also inhibited the binding of TSHR in the coated tube assays by up to 97%, as increased concentrations of antibody conjugate competed with ^{125}I-TSH for the binding to the TSHR (**figure 3.36**). FACS and coated tube assay experiments thus indicate that the conjugation of mAb9 does not appear to harm its ability to bind to TSHR in GPI cells and in pre-coated tubes.

3.1.7.3 ^{111}In labelling to Benzyl-DOTA mAb9

Once Bz-DOTA-mAb9 was generated, it could then be labelled with ^{111}In. See section 2.2.14 of methodology for a detailed protocol.

3.1.7.3.1 Assessing labelling efficiency of ^{111}In-mAb9

Benzyl-DOTA-mAb9^{111}In (^{111}In-mAb9) labelling efficacy was confirmed by SE-HPLC and ITLC. See section 2.2.14.1 for a detailed methodology. Representative results of HPLC and ITLC are shown in **figures 3.37** and **3.38** below.

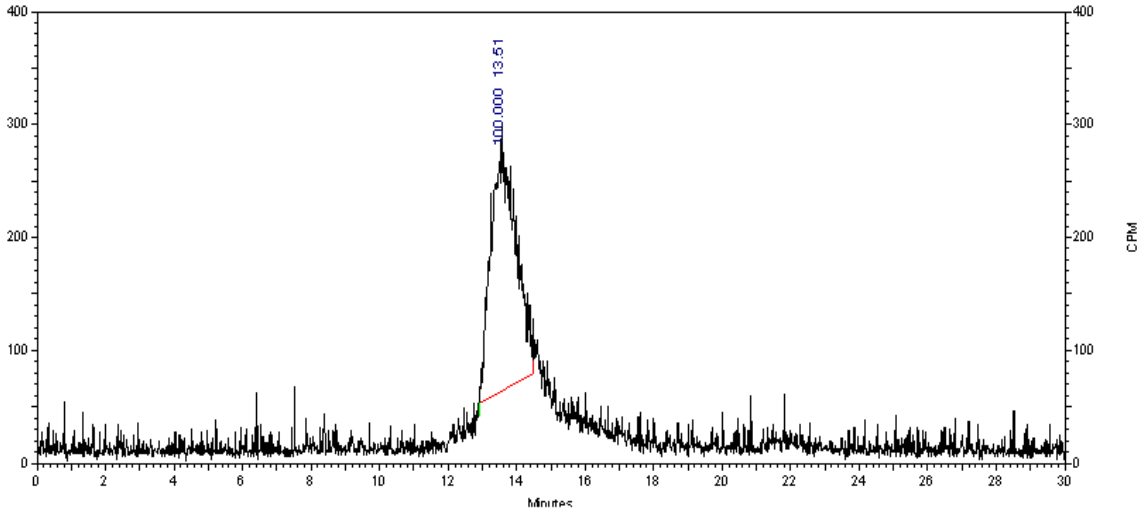

Figure 3.37: Radio size-exclusion HPLC with ^{111}In-mAb9. A single intact peak eluted at retention time 13.51 minutes. This peak represents a radiolabelling efficiency close to 100%.

ITLC analysis

A representative example of ITLC analysis read in a phosphor imager is shown in **figure 3.38**.

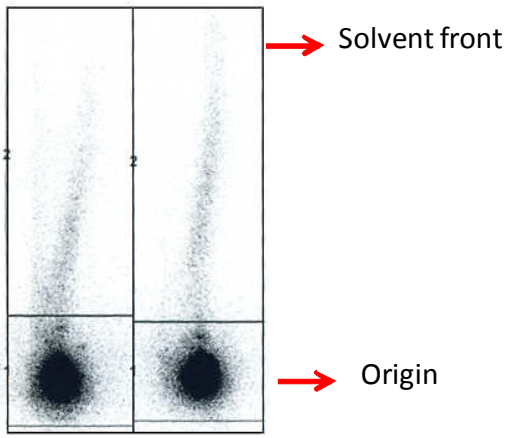

Figure 3.38: Analysis of the radiolabelled product using ITLC-SG strips run in 0.1M ammonium acetate/EDTA pH 5.5. The origin represents the labelled compound whereas the solvent front represents unbound ^{111}In.

Radio HPLC showed a main peak of ^{111}In-mAb9 eluted at retention time 13.5 minutes and ITLC showed around 98% of the activity remained in the origin of the ITLC strip

(**figure 3.37** and **figure 3.38**). It thus can be concluded that a high purity and high labelling efficiency ^{111}In-mAb9 was produced.

3.1.8 ^{111}In-mAb9 binding assays

3.1.8.1 TSHR Pre-coated tube assay with ^{111}In-mAb9

In order to investigate whether ^{111}In-mAb9 retained its TSHR binding ability, a TSHR pre-coated tube assay was carried out. This assay determined if cold mAb9 competed with ^{111}In-mAb9 for the binding of TSHR coated in the tubes. See section 2.2.14.1.1 of methodology for a detailed protocol.

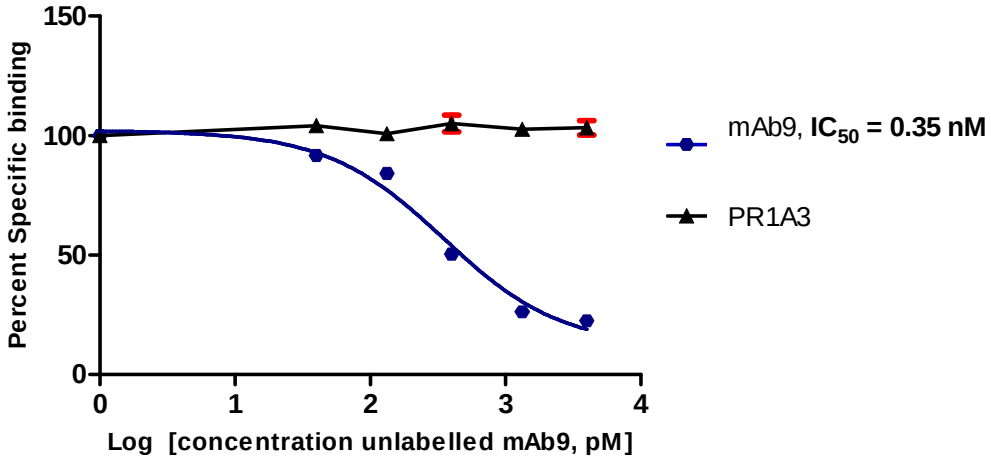

Figure 3.39: Competition assay of ^{111}In-mAb9 with unlabelled mAb9 in TSHR pre coated tubes. Indicated concentrations of cold mAb9 competed with ^{111}In-mAb9 in a concentration dependent manner. The IC_{50} of mAb9 was 0.35 nM. Values are the mean of triplicate determinations.

Cold mAb9 competed with ^{111}In-mAb9 for the TSHR coated in the tubes in a concentration dependent manner. This indicated that ^{111}In-mAb9 bound to the TSHR in the tubes (**figure 3.39**). As expected, no competition was seen with control antibody PR1A3.

3.1.8.2 ^{111}In-mAb9 saturation cell binding assays

Saturation binding assays were performed to measure the specific radioligand binding to cells at equilibrium in order to determine the number of receptors and binding affinity of ^{111}In-mAb9 to GPI, FRTL5, TPC-1 and FTC-133 cell lines. See section 2.2.14.1.2 of methodology for a detailed protocol.

3.1.8.2.1 Saturation binding assay in GPI cells

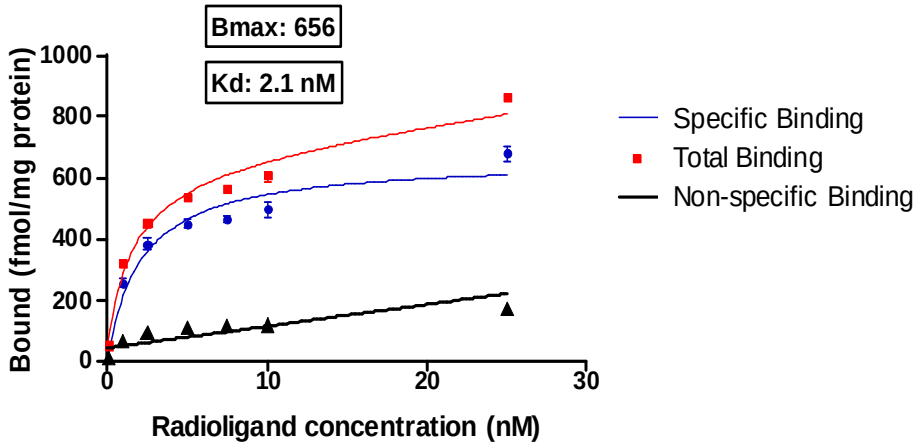

Figure 3.40: Equilibrium saturation binding of ^{111}In-mAb9 to GPI cells. ^{111}In-mAb9 bound to GPI cells with a kD of 2.1 nM and Bmax 656 fmol/mg. Results represent specific binding (total minus nonspecific binding) of triplicate determinations

^{111}In-mAb9 bound to TSHR in GPI cells with a binding affinity of 2.1 nM (**figure 3.40**) and a Bmax of 656 fmol/mg. This is a high affinity binding, however, not as high as the binding affinity of ^{111}In-mAb9 to the TSHR coated in the tubes (section 3.1.8.1).

3.1.8.2.2 Saturation Binding assays with ^{111}In-mAb9 in FTC-133 and TPC-1 cells

Saturation binding assays with ^{111}In-mAb9 were also performed in FTC-133 and TPC-1 cells. After a number of repetitions, no binding was shown in the abovementioned cells.

This may be due to the very low amount of TSHR in these cells resulting in negligible binding.

3.1.8.2.3 ^{111}In-mAb9 binding to FRTL5 cells.

Although ^{111}In-mAb9 bound to FRTL5 cells, the majority of the binding was due to non specific binding (**figure 3.41)**.

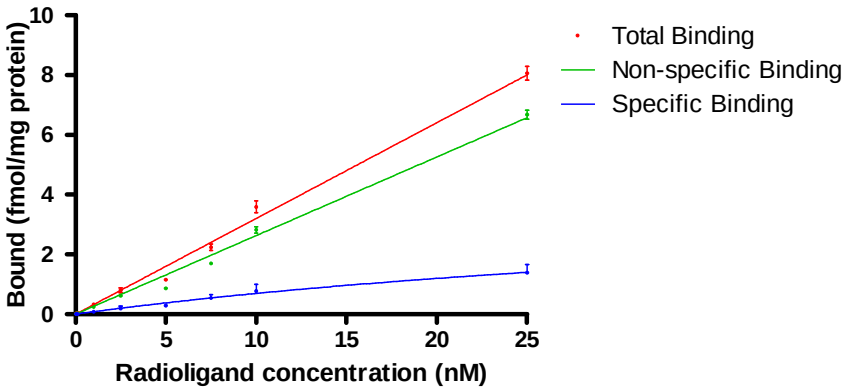

Figure 3.41: Equilibrium saturation binding of ^{111}In-mAb9 to FRTL-5 cells. Results represent specific binding (total minus nonspecific binding) of triplicate determinations

^{111}In-mAb9 binds to TSHR in coated tubes and THSR in GPI cells. It did not, however, bind specifically to FRTL5 cells. Since ^{111}In-mAb9 appeared to bind to TSHR with a high affinity, the next step was to perform an imaging experiment *in vivo* to determine if ^{111}In-mAb9 bound to the TSHR in the normal thyroid of mice.

3.1.9 SPECT/CT imaging of ^{111}In-mAb9 in mice

As previously discussed, imaging of mice with ^{125}I-mAb9 may be complicated by the fact that free ^{125}I can be taken up to the thyroid via NIS and thus complicates interpretation of the imaging and biodistribution results. Please refer to section 2.2.14.2 of methodology for detailed protocol. Representative images of the mice at different time points are shown below.

SPECT/CT scan of M1, 4 hours after ^{111}In-mAb9 *i.v* injection. No uptake seen in the thyroid.

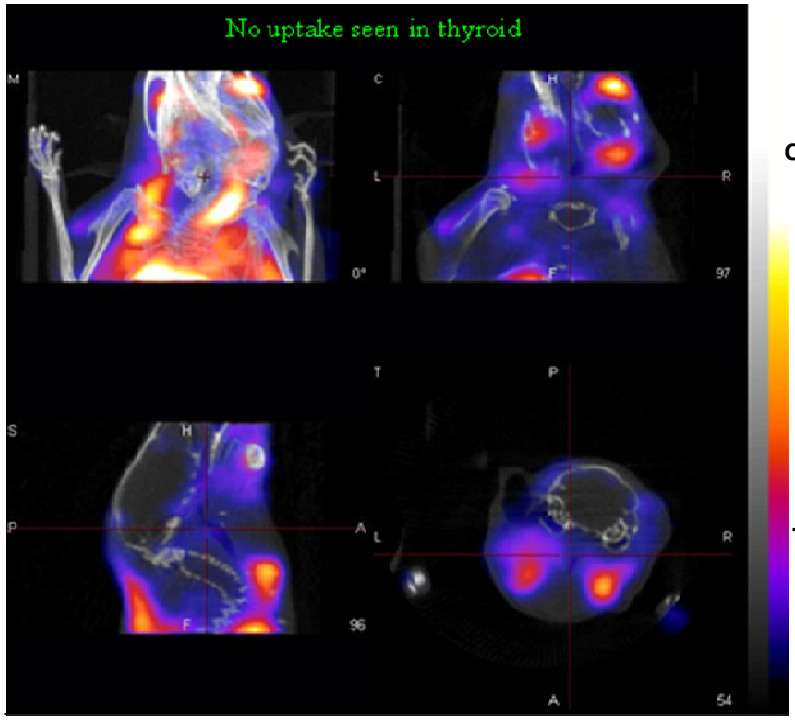

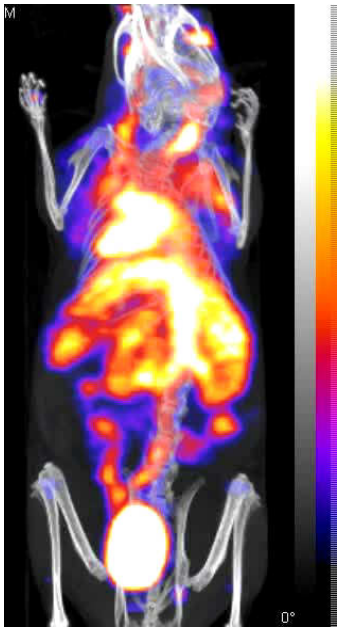

Whole body SPECT/CT scan

SPECT/CT scan of M1, 24 hours after ^{111}In-mAb9 *i.v* injection. No uptake seen in the thyroid.

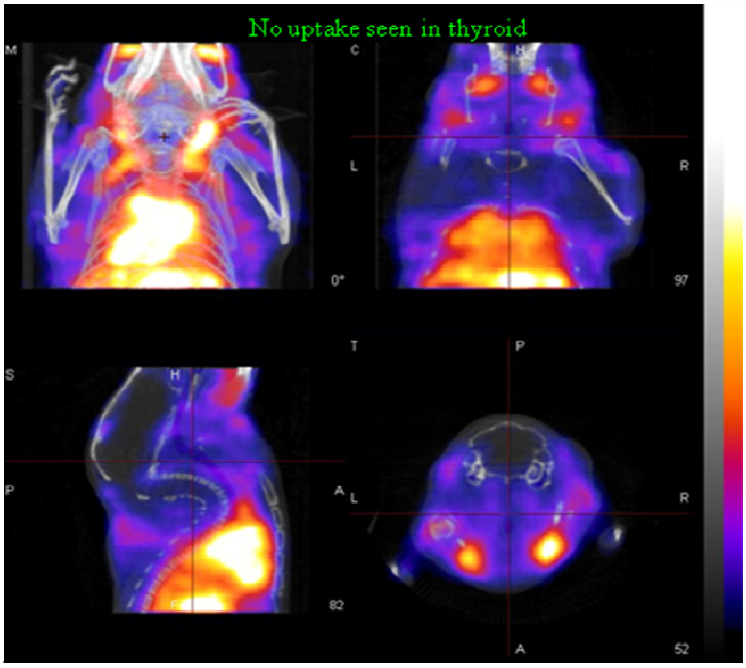

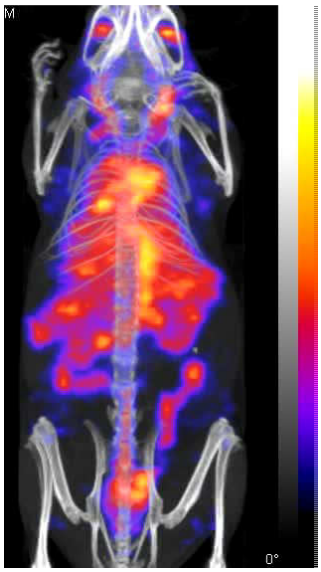
whole body SPECT/CT scan

SPECT/CT scan of M1, 48 hours after ^{111}In-mAb9 *i.v* injection. No uptake seen in the thyroid.

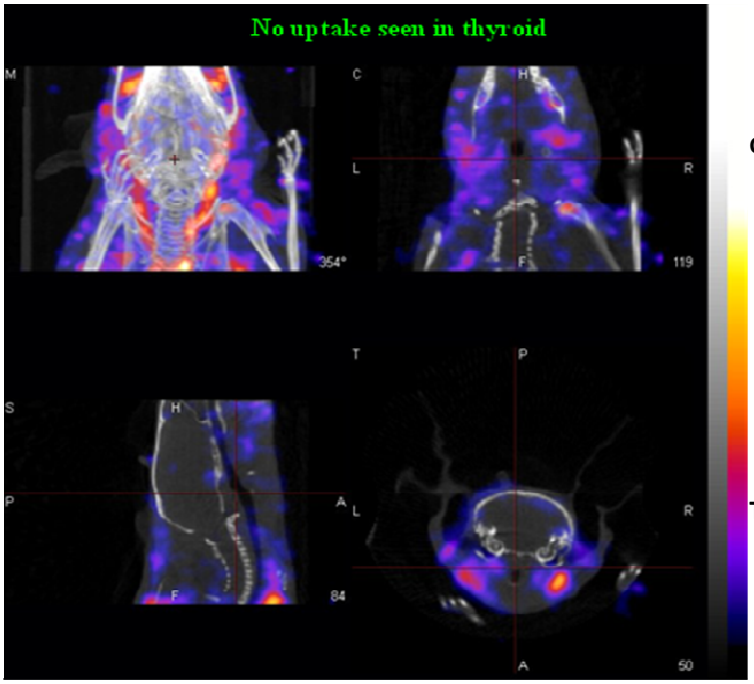

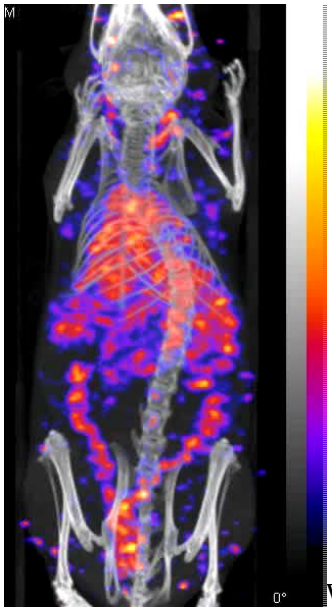
Whole body SPECT/CT scan

SPECT/CT imaging showed no specific uptake of ^{111}In-mAb9 into the thyroid of either Mouse 1 or Mouse 2. Four hours post injection, the majority of the injected ^{111}In-mAb9 was located in the bladder, heart, liver, lungs and also in the eyes. 24 and 78 hours after injection, a similar pattern was observed to the 4 hour post injection time point, however, with less overall activity. This distribution pattern corresponds to that normally seen with ^{111}In labelled antibodies in mice [189].

A biodistribution study was performed at 48 hours with both mice. Tables showing the biodistribution in different tissues of the mouse are shown in **figure 3.43**.

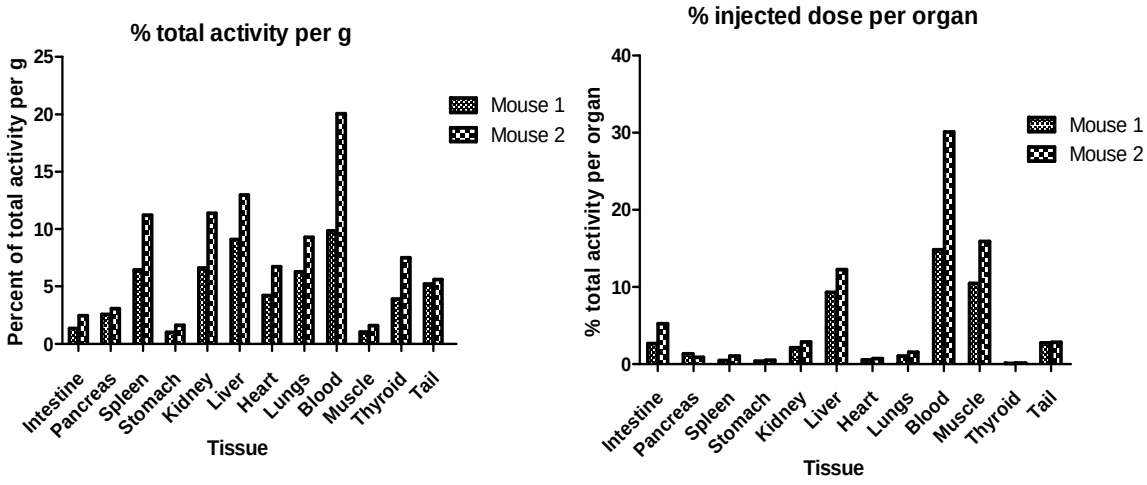

Figure 3.43: Biodistribution results for ^{111}In-mAb9. The mean amount of radiotracer measured in 2 mice is shown. Y axis represents the percent of total activity per g and uptake of injected dose per organ . Results show that most activity ended up in the blood.

Results of both the imaging and biodistribution studies suggest that there is no specific binding of ^{111}In-mAb9 to the thyroid of mice. The blood and liver showed the highest uptake of all the organs, with an uptake of 13-15% injected dose per organ. No further animal studies using ^{111}In-mAb9 were performed.

3.1.9.1 Blood/Plasma stability study of ^{111}In-mAb9

^{111}In-mAb9 bound to TSHR *in vitro* but not *in vivo*. One explanation for this is that ^{111}In-mAb9 might be broken down in the blood and hence ^{111}In-mAb9 loses its antigen binding ability. Please refer to section 2.3.8.1.2 of methodology for a detailed methodology. Results of SDS-PAGE electrophoresis can be seen in (**figure 3.44**).

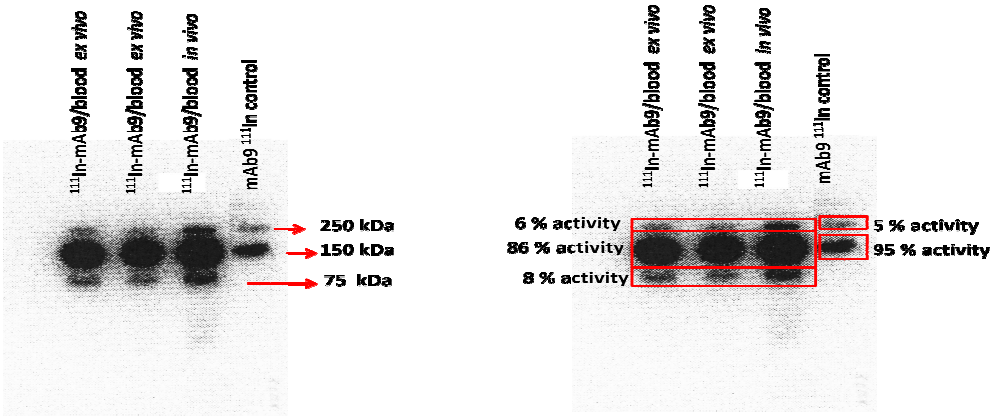

Figure 3.44: Phosphorimager image of non reduced SDS-PAGE electrophoresis of ^{111}In-mAb9/blood. ^{111}In-mAb9/blood *ex vivo* and *in vivo* contain three bands corresponding to molecular weights of 250 kDa, 150 kDa and 75 kDa and control ^{111}In-mAb9 contains two bands corresponding to molecular weights of 250 kDa and 150 kDa.

SDS-PAGE electrophoresis of the control antibody showed two radiolabelled bands comprising 6% of the activity at 250 kDA and the remainder at 150 kDa. In the ^{111}In-mAb9 incubated in the blood either *ex-vivo* or *in-vivo* a similar pattern was seen except that there was an additional band at 75 kDa comprising around 8% of the activity.

These results indicate that it is unlikely that the instability of ^{111}In-mAb9 in the blood is the cause of the lack of receptor targeting since the majority of the labelled antibody appeared to be still circulating intact in the blood.

3.2 Discussion of mAb9 studies

Monoclonal antibodies have developed into important tools to be used in the diagnosis and treatment of cancer. Antibodies and antibody fragments can be constructed so that they recognise and bind with high specificity and affinity to cell surface receptors that are expressed in a wide variety of malignant tissues [122, 182, 185, 190-194]. This property potentially allows radiolabelled antibodies to offer more precise diagnostic imaging and also can greatly increase the effectiveness and decrease the potential side effects of radiotherapy [183, 187, 190, 195-199]. The first radiolabelled monoclonal antibody to be approved by the FDA for the diagnostic imaging of cancer was an ^{111}In labelled monoclonal antibody, CYT-103 (OncoScint OV/CR) [200-209]. CYT-103 is a murine monoclonal antibody (mAb) that binds to TAG-72, a cell surface antigen expressed at high levels on the majority of colorectal and ovarian adenocarcinomas. ^{111}In CYT-103-mAb imaging in patients with suspected recurrent colorectal carcinomas prevents many patients from undergoing unnecessary surgery [200-210]. Two radiolabelled antibodies have been approved by FDA for the treatment of non-Hodgkins lymphoma . ^{131}I-tositumomab (Bexxar) from Corixa Corporation and ^{90}Y- Ibritumomab tiuxetan- (Zevalin®) from Schering corporation [128, 129, 211, 212]. Both are murine monoclonal antibodies and target the CD20 antigen expressed on the surface of normal and malignant B lymphocytes. These radiolabelled antibodies have proved very successful in comparison with chemotherapy, untargeted radiotherapy and unlabelled mAbs [128-131].

In this project, mAb9, a monoclonal antibody that targets the TSHR in the thyroid, and, more specifically, thyroid tumour cells, was studied for its suitability as a diagnostic imaging and radiotherapy agent to be used in radioiodine resistant thyroid cancer. As the TSHR is almost exclusively expressed in thyroid tissue and its expression is maintained in some thyroid tumours, the TSHR is an promising target for directing

monoclonal antibodies to the thyroid or thyroid tumour cells As thyroid cancers progress, thyroid-associated proteins, such as NIS, may gradually be lost [88, 115, 213]. Loss of NIS greatly impairs conventional RAI therapy, as the ability to accumulate iodine is dependent on NIS expression [115, 213]. The TSHR may prove to be an alternative target in these tumours as TSHR expression is sometimes maintained for longer in de-differentiated tumours [115].

3.2.1 Confirming the purity and immunological integrity of mAb9

The first step was to confirm the purity and immunological integrity of the mAb9 monoclonal antibody. In order to demonstrate this, mAb9 was analysed by SE-HPLC and SDS page electrophoresis. In SE-HPLC, the approximate molecular weight of a protein/antibody can be determined by comparing it with known molecular weight gel filtration standards analysed in the SE-HPLC with the same column and under the same conditions. This approached showed that the mAb9 peak corresponded to a molecular weight of approximately 150 kDa, which corresponded to the reported molecular weight of whole IgG antibodies [214-216]. SDS-PAGE gel electrophoresis also confirmed the purity of mAb9 by showing two main bands of approximately 53 KDa and 22 KDa, that correspond approximately to the antibody heavy and light chain respectively [214, 217]. In the SDS-PAGE electrophoresis gel, the band corresponding to the antibody heavy chain contained two very close bands, one fainter than the other. The most likely explanation for the fainter band is the heterogeneity in the glycosylation of the heavy chain of the IgG antibody [218, 219]. IgG contains two identical light chains and two identical heavy chains linked through disulfide bonds and are composed of four distinct domains; three constant domains, CH1, CH2 and CH3 and a variable domain [219-221]. The CH2 and CH3 domains constitute the constant (Fc) portion of the IgG, whereas the variable and CH1 domains together constitute the antibody binding

fragment (Fab) portion of the IgG molecule [219-221]. IgG molecules have an N-linked glycosylation site located at Asn297 in the CH2 domain of the Fc portion of IgG [219, 222]. Variation in glycosylation can occur between IgG molecules because of differences in terminal sialic acid, galactose, N-acetylglucosamine, and fucosylation of the core [219, 223]. These differences can lead to as many as 32 possible glycosylation patterns [219, 223, 224]. Glycosylation of IgG can be influenced by the cell clone in which it is produced, as well as the cell culture conditions such as pH, temperature, and medium [219, 222].

There is no glycosylation occurring in the antibody Fab portion [219, 225], which explains why glycosylation exerts little effect on the antigen binding property of the antibodies and also why the light chain in SDS-PAGE does not show any extra bands.

The glycosylation of CH2 domains is essential for the effector functions of IgG antibodies such as antibody dependent cellular cytoxicity (ADCC), complement dependent cytoxicity (CDC) and rapid elimination of antigen-antibody complexes from circulation [219, 222].

No other bands were detected by the SDS page analysis, indicating that the mAb9 samples were free of aggregates and impurities. Therefore, the mAb9 antibody was considered to be of a sufficiently high purity and integrity.

3.2.2 Binding of unlabelled mAb9 to TSHR pre-coated in tubes

Once mAb9 integrity and purity was confirmed, the next step was to assess whether unlabelled mAb9 bound to the TSHR as expected. This was first investigated by performing a ‘coated tube assay’, in which tubes pre-coated with TSHR were used. This assay was originally developed for Graves autoimmune thyroid patients with the intent to measure the ability of anti-TSHR antibodies, contained in patients serum, to compete with ^{125}I-TSH for the binding of TSHR coated in the tubes [226]. In these coated tubes,

an engineered chimeric TSHR (chimera A), composed of the N-terminal part of the human TSHR cDNA substituted with amino acids 1–165 of the rat LH-CG receptor, is immobilized to the polystyrene tubes [226]. Specific binding of ^{125}I-labeled bovine TSH to this TSHR chimera A has been shown to be preserved and indistinguishable from the wild type TSHR [226]. Coated tube assay studies carried out with mAb9 showed that mAb9 competed with ^{125}I-TSH for the binding of TSHR. Binding of ^{125}I-TSH was inhibited by more than 90% and the binding affinity was 0.43 nM. Therefore these results concluded that mAb9 bound to the receptor coated in the tube with high affinity.

Jacqueline A. Gilbert *et al.* [227] tested mAb9 using the same coated tube assay system and also concluded that mAb9 was inhibiting the binding of ^{125}I-TSH to the TSHR coated in the tubes, with an apparent binding affinity of 0.022 nM. The binding affinity in Gilbert's study was around 10 fold higher than the binding affinity obtained in this experiment. This discrepancy occurred perhaps due to a different batch of mAb9 antibody being used in these experiments resulting in a different binding affinity or alternatively it might be due to differences in the experimental design.

3.2.3 Binding of unlabelled mAb9 to cells.

The binding characteristics of mAb9 to the TSHR in thyroid cancer and TSHR transfected cell lines were studied by performing FACS and immunohistochemistry assays using FTC-133, TPC-1, FRTL5 and GPI cells.

3.2.4 FACS with unlabelled mAb9

To investigate whether the selected cell lines expressed TSHR, as well as to study the binding of mAb9 to the TSHR in different cell lines, FACS experiments were carried out with TPC-1, FTC-133, GPI and FRLT5 cells. Both 4C1 and mAb9 antibodies were used. 4C1 anti-TSHR antibody was obtained commercially and recognises an epitope

located in the region of amino acid residues 381 to 384 of TSH Receptor [228]. An isotype-matched control antibody was also used as a control as a means to distinguish non-specific staining from specific antibody staining. Non-specific antibody staining can occur due to the binding to Fc receptors on target cells; non-specific protein interactions with cellular proteins, lipids, or carbohydrates, and cell auto-fluorescence [184, 229]. These factors can vary depending on the cell type and the isotype of the primary antibody [184, 229]. For this reason it is essential that isotype controls are matched to the species and isotype of the specific primary antibodies. [184, 229].

4C1 antibody was shown to bind moderately to the TSHR in FTC-133 and FRTL5 cells, however statistical analysis showed no significant difference in the MFU compared with the control cells. mAb9 did not show any binding to FTC-133 and FRTL5 cells. Both 4C1 and mAb9 bound substantially to GPI cells but showed no binding to TPC-1 cells.

These results suggest that TSHR is expressed to some extent in FTC-133, FRTL5 and GPI cells, however, while 4C1 antibody was able to bind to all cell lines except TPC-1 cells, mAb9 solely bound to GPI cell lines. One possible explanation for the discrepancy between the binding of mAb9 and 4C1 to FTC-133 and FRTL5 cells is that mAb9 recognises a TSHR binding epitope that is not present in these cells but is present in GPI TSHR transfected cell lines. Shepherd *et al.* [34] compared the epitope specificity and variable region sequences of novel monoclonal antibodies which recognise native hTSHR [230]. This study found that 4C1 recognised antibodies in the native hTSHR in position 381-384 of the receptor [230]. Other studies also confirmed this recognition of this binding epitope on the TSHR by 4C1 [228].

Antibodies to different epitopes of the receptor can influence thyroid function [227, 230]. The epitopes of TSHR to which mAb9 binds are not known and further studies are needed to characterise them [231]. From these results it can be assumed that 381-384 residues are present in FTC-133, GPI, FRTL5 cells since 4C1 antibody bound to all

these cell lines but the epitope to which mAb9 binds in the transfected GPI cells is not present in the non-transfected FTC-133 and FRTL5 cell lines. GPI FACS shift patterns showed that some cell populations expressed TSHR in higher quantities than others. This may be due to the transfection methods used in the production of this particular cell line that resulted in some cells having high expression of the TSHR while others have low expression of TSHR. Transfected cell lines often show different levels of expression depending on particular gene/plasmid combinations introduced and the methodology used.

In a similar FACS study where 4C1 antibody, amongst others, was used in GPI cells, a similar shift was obtained to the one observed in this study [230]. Another study used the same GPI cell line with different anti-TSHR antibodies and also reported a similar pattern [232].

3.2.5 Immunohistochemistry to characterise TSHR in cells

Immunohistochemistry with 4C1 and mAb9 antibodies failed to show specific binding to the TSHR in the thyroid cancer cell lines TPC-1 and FTC-133 with both antibodies. GPI was the only cell line that stained positively for the TSHR with both 4C1 and mAb9 antibodies.

In GPI cells, different staining patterns of TSHR were seen, with some groups of cells showing more positive staining for TSHR than others, indicating that some cells expressed high numbers of receptors while others expressed lower levels of TSHR. This coincides with the profile obtained in FACS where different levels of TSHR expression were also reported.

GPI cells showed TSHR staining in the cytoplasm as well as in the nucleus. There is convincing evidence showing that some GCPRs are localised in the nucleus. This suggested mode of genomic regulation by GPCRs implies the endocytosis and nuclear

translocation of peripheral-liganded GPCR and (or) the activation of nuclearly located GPCR by endogenously produced, non-secreted ligands.

Although there are no specific studies conducted with TSHR to date, it may be that TSHR, like other GCPRs, is translocated and localised in the nucleus [233].

Although 4C1 antibody showed some binding to the TSHR in FTC-133 cells in the FACS analysis, in the immunohistochemistry studies no TSHR positivity was observed with 4C1. It is possible therefore that this antibody was not suitable for this purpose and that the levels of expression in these cells were lower than the sensitivity of this assay.

3.2.6 Characterising TSHR in cell lines

3.2.6.1 RT-PCR to evaluate the expression of TSHR in cells.

To further evaluate the expression of TSHR in the selected cell lines, TSHR mRNA expression was determined in the cells using relative quantitative PCR. Relative expression of TSHR in the different cells was compared to CHO, the non-expressing cell line. FTC-133 and GPI cells revealed some expression of TSHR mRNA; in GPI cells considerably more was detected than in FTC-133 cells. TPC-1 revealed negligible relative fold expression of TSHR. The results obtained were thus comparable in some respects to those from the FACS and immunohistochemistry assays, in which GPI cells showed the highest level of TSHR expression and staining with the mAb9 and 4C1 antibodies while no or moderate staining was observed in FTC-133 cells. TPC-1 cells showed negligible staining for TSHR. It is important to note that RT-PCR only gives an account of the mRNA levels of the receptor and hence the fact that these cells express TSHR mRNA does not necessarily prove that there will be TSHR protein in these cells. While one study by Schmutzler C [234] reported mRNA expression in FTC-133 cell lines, another study did not show TSHR mRNA expression as well as expression of most thyroid specific genes in both TPC-1 and FTC-133 cells [235]. This discrepancy

seen in the TSHR expression in FTC-133 cells observed in different studies may be due to different TSHR primer sequences being used, or also due to the FTC-133 cell lines used in different labs being slightly different from one another due to different media and growing/passaging conditions being used.

3.2.6.2 Western blot analysis to detect TSHR protein in cells

The next step was to perform Western blot experiments to detect TSHR protein in TPC-1, FTC-133 and GPI cell lines. TSHR, a member of the GPCR family, is composed of a large extracellular domain or ECD, of a molecular weight of 45 kDa, a seven transmembrane region and a c-terminal cytoplasmic tail [11, 27, 236, 237]. The ECD region is thought to be solely responsible for ligand interaction, while the transmembrane and cytoplasmic regions are involved in signal transduction [11, 27, 236, 237]. TSHR expressing GPI cells were constructed in Da Costa *et al.* laboratory [238] by using an ECD region anchored via glycosylphosphatidylinositol **(**GPI) to CHO cells. In the latter paper, immunoblotting studies, using both Graves disease patient serum and anti-TSHR antibodies detected a TSHR band of around 70 kDa [152]. In the present study 4C1 antibody detected a single band of around 68 kDa, which therefore corresponds to the TSHR in GPI cells. 4C1 antibody however failed to detect TSHR protein in the western experiments in FTC-133 and TPC-1 cell lines, suggesting that there is low expression of TSHR in these cell lines. In the Western blots, mAb9 did not detect TSHRs in FTC-133, TPC-1 and GPI cell lines.

The reason for the lack of detection of TSHR in GPI cells with the mAb9 antibody is that Western blot is carried out under denaturing conditions. It might be that the denaturation of the cell line lysate changes the conformation of the TSHR protein binding epitope in GPI cells therefore not permitting mAb9 to bind to the TSHR protein in its denatured form.

3.2.7 Radiolabelling of mAb9 with ^{125}I

After the purity and integrity of the mAb9 antibody had been confirmed, TSHR expression in the cell lines used characterised, and binding of unlabelled mAb9 to the cells studied, the next step was to label mAb9 antibody with ^{125}I. Labelling was performed using the Iodogen tube method. In this method, a water-insoluble oxidant [196-tetrachloro-3t~,6t~-diphenyl glycoluril, Iodogen] is dissolved in an organic solvent and it is coated on the walls of the glass reaction tube [179]. ^{125}I is incorporated into tyrosine amino acids of the antibody by chemical oxidation. By using this method, oxidation damage to the antibody can be diminished during the radiolabelling process.

After labelling mAb9 with ^{125}I, the labelling efficiency of ^{125}I-mAb9 was measured with Radio-HPLC and ITLC. Both radio-HPLC and ITLC results showed a high labelling efficiency ^{125}I-mAb9. However, resolution of size exclusion HPLC and ITLC is not particularly high and therefore usually it does not separate molecules with less than a few thousands of Da difference and it cannot always detect partial degradation of proteins/antibodies. For this reason, SDS page gel electrophoresis was also performed. SDS page electrophoresis analysis indicated that ^{125}I-mAb9 was of high purity, with a single band of around 150 kDa and no further impurities or aggregates were detected.

3.2.8 ^{125}I-mAb9-TSHR binding assays

3.2.8.1 Pre coated tube assays

The binding of the newly labelled ^{125}I-mAb9 to the TSHR was first investigated in TSHR pre-coated tubes [226]. When using ^{125}I radiolabelled mAb9 at a low specific activity, only incomplete inhibition of binding was seen. This indicated that the integrity of the radiolabelled complex integrity might have been disrupted. A loss of integrity could result from three possible reasons. First, oxidation by the Iodogen pre-coated tube method itself might have damaged the structure of the antibody. Second, radiolabelling

of mAb9 could have damaged the structure of the antibody. Lastly, the initially radiolabelled ^{125}I-mAb9 might not have been of a sufficiently high specific activity to allow sufficient competition with the unlabelled antibody. The immunointregrity of an antibody depends on the preservation of its antigen binding activity [239]. Previous studies have shown that modification in the amino acid sequence of the hypervariable region of an antibody can result in the binding strength of the antibody being reduced [240]. The antibody sites targeted during a radiolabelling procedure include tyrosine residues, oligosaccharide moieties, δ-amino groups of lysine, β- or γ-carboxyl and thiol groups, as well as glutamic acid and thiol groups generated by the reduction of cystine. Most antibodies have tyrosine residues in their hypervariable region [239]. The antibody sites targeted on mAb9 when radiolabelling with ^{125}I are thought to be the tyrosine residues on the mAb9, and it is thus possible that the labelling process might have disrupted the conformation of mAb9.

To investigate whether cold labelling, oxidation or the addition of iodine to mAb9 was damaging its structure, TSHR coated tube assay studies and FACS experiments were carried out.

In these assays, three preparations were compared. In the first preparation, the oxidation effects of Iodogen on mAb9 were studied and in order to do this mAb9 was incubated alone in an Iodogen tube to produce ‘oxidised mAb9’. In the second preparation, the effects of cold labelling iodination on mAb9 were studied, and in order to do this mAb9 was co-incubated with cold potassium iodide in an iodogen tube to produce ‘cold labelled mAb9’. In the final preparation, mAb9 was simply mixed with cold iodine, and this was called ‘mixed mAb9’.

In the TSHR coated tube assay, ‘oxidised mAb9’ was able to compete with ^{125}I-TSH for the binding of TSHR. This showed that oxidation of mAb9 by Iodogen was not damaging the structure of the antibody. ‘Cold labelled mAb9’ was also able to compete

with ^{125}I-TSH and therefore substitution of radioiodine into the antibody was not likely to be damaging the ability of the antibody to bind to the TSHR in coated tubes.

FACS analysis suggested that the oxidation step itself was not interfering with the binding of mAb9 and 4C1 to GPI cells, however the cold iodide labelling of both mAb9 and 4C1 impaired the ability of these antibodies to bind to the TSHR in all of the cells used. These results contradicted the coated tube assay results in which cold labelled mAb9 was able to bind to the TSHR coated in the tubes.

It is possible that the substitution ratio of cold labelled antibody was higher than the radiolabelled antibody and hence it had a harsher effect on mAb9 than the radiolabelled material. Also, the coated tubes are coated with a TSHR chimera produced in the lab which has a different conformation from the TSHR construct transfected into the GPI cells. Perhaps iodination of mAb9 changes the conformation of the antibody portion that binds to the TSHR in GPI cells but does not alter the antibody portion that binds to the TSHR construct coated in the tubes. Also, it might be possible that the secondary antibody used in FACS is not recognising the cold labelled mAb9 and 4C1 reaction and thus no positive shifts were shown.

It can be concluded that the oxidation inflicted by the Iodogen labelling method and the cold labelling of mAb9 were not damaging the antibody's ability to bind to the TSHR coated in the tubes. Howver, some doubt remains as to the effect of cold iodine labelling on the ability of mAb9 and 4C1 to bind to the TSHR in GPI cells.

3.2.8.2 Cell binding assays

The binding of ^{125}I-mAb9 to TSHR in cell lines was further studied in thyroid cancer (TPC-1 and FTC-133), TSHR transfected (GPI) and rat thyroid cancer cells (FRTL5) by performing direct radioligand cell binding assays. The efficiency of the binding of radiolabelled compounds to cells may be affected by several conditions which include

the incubation time and temperature of incubation at as well as the characteristics of the binding buffer. For this reason the effect of the temperature and time on the binding efficiency of mAb9 to TSHR in the cells as well as the effect of different binding buffers were tested before saturation cell binding assays were conducted. The temperature that gave the highest binding efficiency was room temperature and the optimal incubation time was between 2 and 3 hours. A study using different buffers at room temperature incubated for approximately two hours determined that most buffers used produced a similar outcome in the cell binding assays. Therefore room temperature and 2 to 3 hours incubation time were used in further binding assays.

After determining the best incubation conditions, a direct radioimmunoassay was performed to measure the immunoreactivity of the labelled fragments, i.e. the proportion of radioactive antibody fragments that have the ability to bind to the antigen. The immunoreactivity was calculated to be 5.1 %, which indicates that only about 5% of the radioactive antibody was able to bind to the TSHR. The immunoreactivity of mAb9 is, thus, very low compared to most antibodies studied and thus raises doubts about the quality of the antibody.

3.2.8.2.1 Saturation assay

Radioligand binding assays were performed on all the thyroid cancer cell lines in order to measure the specific radioligand binding to cells at equilibrium, and to determine both the receptor numbers (Bmax) and the binding affinity (Kd) of mAb9 by analysis of non specific binding and total binding. Non-specific binding occurs in many types of binding assays and it is therefore crucial to account for this.

Unlabelled mAb9 was used as the competitor to measure non-specific binding to ensure that all the target receptors were occupied, under which conditions any binding

observed would be to other receptors, or due to interactions with the cell membrane. The concentration used (1000 μM) was adequate to block all the receptors.

GPI cell lines showed a high level of TSHR expression as well as a relatively high binding affinity. FRTL5 bound to TSHR, however the majority of binding was due to non specific binding. A study by van der Kallen *et al.* [241] also detected a binding site in FRTL5 cells with extremely low affinity and high capacity which represented a non-specific binding site: Kd= 56±24 nM and BMax (binding capacity) 134±20. [242] ^{125}I-mAb9 did not show any binding to FTC-133 and TPC-1 cells, as expected since these cells had been shown to express very low or negligible amounts of TSHR.

Radiolabelled antibodies must retain their receptor binding capacity if they are to function as effective radiopharmaceuticals and although the immunoreactive fraction was found to be low the saturation binding study with GPI cells did show high levels of specific binding indicating that ^{125}I-mAb9 most likely kept its receptor binding capacity to the TSHR in GPI cells.

3.2.9 SPECT/CT imaging experiments

Imaging experiments were performed in order to assess the binding of ^{125}I-mAb9 to the TSHR present in the thyroid of normal mice. In order to perform this study, mAb9 was labelled with ^{125}I, a radioactive nuclide used for SPECT/CT imaging of small animals.

Metabolism of the ^{125}I-mAb9 conjugate after its systemic injection into mice can lead to the formation of radiolabelled metabolites including free ^{125}I, which can be taken up into the thyroid by the NIS. This would confound the imaging results as a radioactive signal detected in the thyroid could be caused wholly or partly by the accumulation of free ^{125}I rather than being caused by the binding of ^{125}I-mAb9 to TSHRs on the thyroid of the mice. To ensure that ^{125}I-mAb9 binding rather than that of free ^{125}I was measured, binding of mAb9 to the thyroid was imaged in the presence and absence of the NIS

inhibitor sodium perchlorate. In the absence of perchlorate, approx 2.4% binding was observed in the thyroid, whereas ~0.2% binding was observed in the thyroid in the presence of perchlorate. The substantial reduction in ^{125}I-mAb9 binding to the thyroid after the pre-treament with perchlorate indicates that a large proportion of the administered ^{125}I-mAb9 underwent metabolism and was released as free ^{125}I, which accumulated in the thyroid.

The 0.2% binding observed after perchlorate treatment suggests that mAb9 may be binding to TSHRs. In a further control group mice were administered with free ^{125}I in the presence and absence of perchlorate. When ^{125}I was administered it produced an uptake of 1.7% in the thyroid, but this uptake was completely blocked by perchlorate treatment. This suggests that the relatively low signal of 0.2% achieved in the mAb9 + perchlorate group is not the result of a sub maximally effective dose of perchlorate being used.

Previous studies have shown that radioiodine is taken up by the salivary gland, stomach, lactating breast and nasal mucosa via NIS [91, 243]. This explains why activity in the salivary gland is also seen at the 4 hour time point in mice injected with either ^{125}I-mAb9 or free ^{125}I in the absence of perchlorate. Lack of uptake of ^{125}I into the salivary gland in perchlorate treated mice indicate that perchlorate is effectively blocking NIS and thus thyroid uptake may be due to ^{125}I-mAb9 binding to TSHR *in vivo*.

Although ^{125}I-mAb9 showed some binding to the TSHR in the thyroid of mice, the percentage of injected dose was extremely low, and thus, results are unable to categorically indicate whether the radioactivity seen in the images is due to the specific binding of ^{125}I-mAb9 to the TSHR or due to free ^{125}I being taken up by the thyroid via NIS.

3.2.10 ^{111}In-labelled mAb9

When using ^{125}I radiolabelled compounds, there is always a chance that free ^{125}I can be taken up into the thyroid via NIS and interfere with *in vivo* imaging and biodistribution studies. Although in the imaging and biodistribution studies ^{125}I-mAb9 was radiolabelled to an efficiency close to 100% and sodium perchlorate was used to block the uptake of ^{125}I into the thyroid, it is still possible that free ^{125}I will, to some extent, interfered with the interpretation of the results. This problem can potentially be solved by radiolabelling mAb9 with a radioisotope that does not get taken up into the thyroid. For this reason in this project, ^{111}In was used because it is not taken up by the thyroid but also due to its useful imaging properties ready availability.

^{111}In does not form strong interactions directly with antibodies/proteins but can form highly stable complexes with a number of bifunctional chelating agents, chelating agents which have a chemically active group that can bind covalently to the antibody. The Macrocyclics chelating compound p-SCN-Benzyl-DOTA was selected to be conjugated to mAb9.

3.2.11.1 Conjugation of mAb9 with p-SCN-Bz-DOTA

SCN-Bz-DOTA conjugates to the antibodies via lysine side chain amino groups. After conjugation, the antibody was purified in order to remove any free chelate before the ^{111}In was added. In order to assess the purity and integrity of Bz-DOTA-mAB9, prior to radiolabelling, a size exclusion HPLC (SE-HPLC) was performed.

The SE-HPLC indicated that the integrity and purity of mAb9 was not altered by the addition of Bz-DOTA. FACS analysis with Bz-DOTA mAb9 revealed that the chelated compound was still able to bind to TSHR in GPI cells. Bz-DOTA mAB9 was also still able to compete with ^{125}I-TSH for the binding of TSHR in the pre-coated tubes. This

again confirmed that the conjugated chelator was not influencing the ability of mAb9 to bind to the TSHR.

3.2.10.2 ^{111}In labelling of BzScnDOTA mAb9

Bz-DOTA mAb9 was radiolabelled with ^{111}In. A range of concentrations of mAb9 and ^{111}In were evaluated and different incubation times were employed until an optimal radiolabelled compound of around 99% labelling efficiency was produced. After the radiolabelling of the mAB9 with ^{111}In, ITLC and size exclusion HPLC indicated that the radiolabelled compound was of high purity.

3.2.10.3 ^{111}In-mAb9 binding assays

Once stable ^{111}In-mAb9 was produced successfully, the next step was to investigate whether the radiolabelled complex retained its binding capacity. A TSHR pre-coated tube assay showed that ^{111}In-mAb9 still kept its ability to bind to the TSHR. and its binding was inhibited by 80% with cold mAb9.

^{111}In-mAb9 binding to TSHR in GPI cells was demonstrated in a saturation binding assay. The number of receptors- Bmax- was estimated to be 656 fmol/mg and binding affinity, Kd, 2.1 nM. The binding affinity of ^{125}I-mAb9 in GPI cells was 3.66 nM, similar to binding affinity of ^{111}In-mAb9 to the same cells. This suggests that ^{111}In-mAb9 binds the TSHR in GPI cells with a similar affinity to ^{125}I-mAb9. There appears to be a big difference between the number of receptors observed in GPI cells in ^{125}I-mAb9 and ^{111}In-mAb9 saturation assays. This variability may be due to different passages of GPI cells being used when the saturation assays were performed. ^{111}In-mAb9 bound to the TSHR in FRTL5 cells, however most binding was due to non-specific binding. A study by van der Kallen *et al.* [241] also reported non specific

binding to FRTL5 cells [242]. ^{111}In-mAb9 did not bind to FTC-133 and TPC-1 cells, presumably due to the very low or negligible expression of TSHR in these cells.

3.2.11 SPECT/CT imaging of ^{111}In-mAb9 in mice

As explained previously, ^{125}I-mAb9 can be metabolised into free ^{125}I, which can be taken up by the thyroid and interfere with imaging and biodistribution results. For this reason mAb9 was radiolabelled with ^{111}In and after *in vitro* studies confirmed its binding to TSHR, the next step was to perform preliminary animal studies in order to assess the binding of ^{111}In-mAb9 to the TSHR expressed in the normal thyroid of the mouse. SPECT/CT animal studies did not show specific binding of ^{111}In-mAb9 to the TSHR and radioactivity was widely distributed in the body of the mice after ^{111}In-mAb9 injection. This radioactive distribution pattern corresponds to that previously seen n mice [244]. Results of both the imaging and biodistribution studies suggest that there is no specific binding of ^{111}In-mAb9 to the thyroid of mice, and for that reason no further animal studies were conducted with ^{111}In-mAb9.

3.2.11.1 Blood/Plasma stability study with ^{111}In-mAb9

^{111}In-mAb9 bound to TSHR in coated tubes and in GPI cells *in vitro*, however, it failed to show specific binding to the TSHR of normal mice *in vitro*. One explanation for this is that ^{111}In-mAb9 might be broken down in the blood as a result lose its antigen binding ability. In order to investigate this possibility, *in vivo* and *ex vivo* stability studies were performed in the blood of mice.

The control ^{111}In-mAb9 showed two bands on SDS-PAGE, one at molecular weight 250 kDa and the other at 150 kDa. The 250 kDa band (presumably an antibody dimer) contained 5% of the total radioactivity whereas the 150k Da band contained 95% of the total activity.

^{111}In-mAb9 incubated in the blood either ex vivo and *in vivo* gave similar results. In both studies, bands were also detected at 250 kDa: comprising 6% of total activity and 150 kDA (86% total activity) and also showed a band at 75 kDa containing 8% total activity). This indicates that it is not extravascular metabolism in mice causing the third band to appear, but that there may be some break down of ^{111}In-mAb9 in the blood. Although this suggests that the antibody may be break down in the blood of mice to a small extent, there is still a considerable amount of intact radiolabelled ^{111}In-mAb9 (86%) circulating in the blood at 6 hours, and hence it is unlikely that the small degree of breaking down of the antibody in the blood is causing radiolabelled antibody not to bind *in vivo*.

3.2.12 Conclusion for mAb9 studies

mAb9, a purified IgG2b monoclonal antibody developed from an experimental murine model of hyperthyroid Graves' disease, has been shown in previous studies to exhibit potent thyroid stimulating activity [227]. In the latter studiy, mAb9 induced full stimulation of TSHR and acted as a full agonist for the receptor. It also demonstrated high affinity *in vitro* for binding of the TSHR coated in tubes and CHO cells stably transfected with the TSHR receptor [227]. In this study, mAb9 was investigated both *in vitro* and *in vivo* for its potential to act as a imaging and treatment tool for radioiodine resistant thyroid cancer. *In vitro* studies showed that ^{125}I and ^{111}In radiolabelled mAb9 were able to bind specifically to TSHR pre-coated in tubes and in GPI cells (CHO cells stably transfected with the TSHR). *In vivo*, though, the outcome was different. Both ^{111}In-mAb9 and ^{125}I-mAb9 failed to show specific binding to the TSHR in the normal mice. Possible reasons for this are discussed in chapter 5. Radiolabelled mAb9 is therefore unlikely to be of use the diagnosis and treatment of radioiodine resistant de-differentiated thyroid cancer.

mAb9 bound to the TSHR *in vitro* however it did not bind to the TSHR *in vivo*. For this reason, mAb9 is unlikely to be of use in the diagnosis and treatment of radioiodine resistant thyroid cancer. A new approach was therefore needed to target the TSHR.

In this study human recombinant thyroid stimulating receptor (rhTSH) was used to target the TSHR. rhTSH binds to the TSHR and is commercially available. It was approved for clinical use by the FDA(1998) [245, 246] and in Europe (2001) [247]. It has a combined molecular weight of 30,000 Da, which makes it advantageous for a tumour targeting compound due to its relatively small size.

Due to these features, radiolabelled rhTSH was evaluated as a potential candidate to stage radioiodine resistant thyroid cancer. The overall objective of this study was to radiolabel rhTSH and study its binding to the TSHR both in *in vitro* and *in vivo*.

Aims of rhTSH studies:

- Radioiodinate rhTSH with ^{125}I and produce a radiolabelled compound with high purity.
- Study the structure and chemical properties of rhTSH and ^{125}I-rhTSH using SDS page electrophoresis, size exclusion HPLC and reverse phase HPLC.
- Assess the binding of ^{125}I-rhTSH to TSHR pre-coated tubes and in thyroid cancer cells.
- Investigate the binding of ^{125}I-rhTSH to the thyroid and grafted thyroid tumours in mice *in vivo* with SPECT/CT imaging to establish if radiolabelled rhTSH can be used as a potential imaging and treatment agent for radioiodine resistant metastatic thyroid cancer.

4.1 rhTSH study results

4.1.1 Radioiodination of rhTSH using enzymatic substitution

rhTSH was first radioiodinated with ^{125}I using the lactoperoxidase enzymatic substitution method. Please refer to section 2.3.1 for a detailed protocol. ITLC analysis showed that most of the radioactivity remained in the bottom of the ITLC strip, which indicates a high purity labelled ^{125}I-rhTSH with approximately 95% labelling efficiency (**figure 4.1-A**). SDS-PAGE gel electrophoresis analysis showed two main intact bands which correspond to the α subunit (17 kDa) and β subunit (21 kDa) but no extra bands (**figure 4.1-B**). These results indicate that a high purity and high integrity ^{125}I radiolabelled rhTSH was obtained.

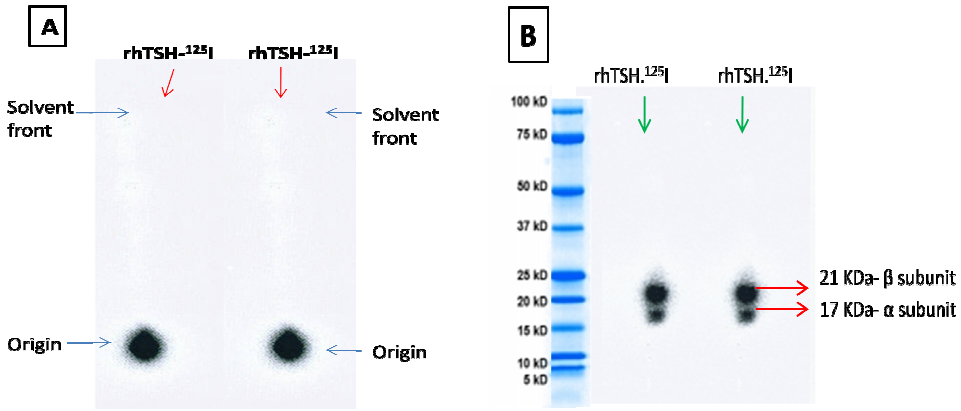

Figure 4.1: Phosphorimager images of ITLC and SDS PAGE electrophoresis analysis of ^{125}I-rhTSH. A: ITLC strips showing 95% labelling efficiency (calculated by the phosphorimager software). B: SDS gel electrophoresis of $1^{125}I$-rhTSH showing two main bands of approximately 21 kDa and 17 kDa, which correspond to the rhTSH β-subunit and α-subunit respectively.

The effect of increasing concentrations of lactoperoxidase and glucose oxidase in the ^{125}I-rhTSH labelling efficiency was determined using ITLC. Please refer to section 2.3.2 for a detailed protocol. The results demonstrated that increasing concentrations of lactoperoxidase and glucose oxidase independently increase the labelling efficiency (**figure 4.2**). Both the 0.005 and 0.5 µg quantities of glucose oxidase and lactoperoxidase resulted in labelling efficiencies of close to 100%.

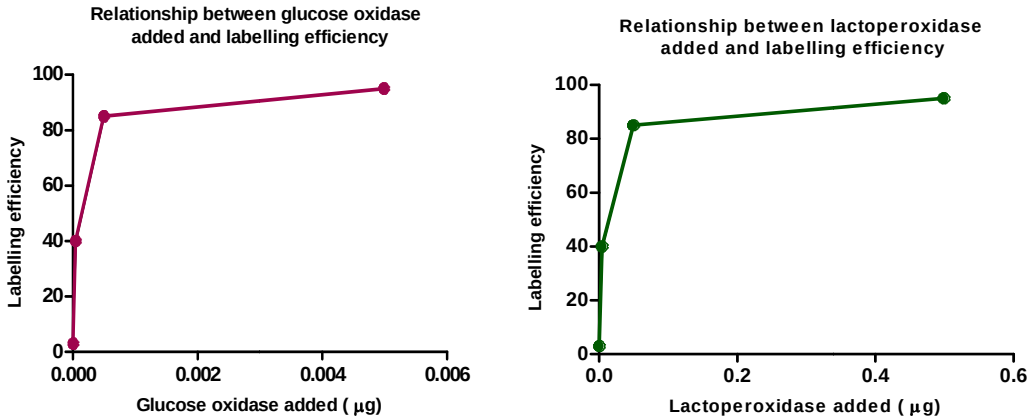

Figure 4.2: Relationship between glucose oxidase and lactoperoxidase in the ^{125}I-rhTSH radioiodination reaction against the labelling efficiency. The labelling efficiency increases sharply after an addition of 0.001 µg glucose oxidase and 0.1 µg lactoperoxidase.

4.1.2 HPLC Studies with rhTSH and ^{125}I-rhTSH

4.1.2.1 Size exclusion HPLC (SE-HPLC)

To further confirm the efficiency and structural integrity of ^{125}I-rhTSH, SE-HPLC was carried out. First, unlabelled rhTSH was analysed with UV absorption detection SE-HPLC. See section 2.3.3 for a detailed protocol. A single sharp peak of rhTSH eluted at 12.33 minutes (**figure 4.3**).

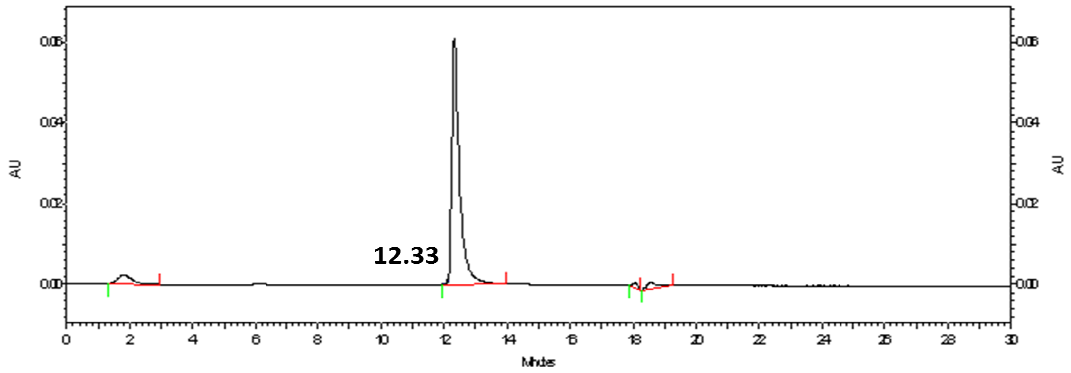

Figure 4.3: UV size exclusion HPLC chromatogram (280 nm) for rhTSH. An intact peak at retention time 12.33 is shown.

A series of Bio-Rad gel filtration standards were also analysed in order to estimate the molecular weight of rhTSH however only 3 peaks were detected from the 5 distinct peaks expected (**figure 4.4**). The SE-HPLC column employed for this analysis was therefore not able to achieve good separation with these molecular weight standards.

For this reason, carbonic anhydrase and lysosyme were also analysed and used as additional molecular weight standards. Carbonic anydrase and lysosyme have theoretical molecular weights of approximately 29 kDa and 14.7 kDa, respectively, which are similar to the molecular weight of rhTSH (~30 kDa) and the rhTSH α subunit (~14 kDa). The retention time obtained in the SE-HPLC chromatogram with carbonic anydrase, 12.52 minutes (**figure 4.5**), was very similar to the retention time obtained with rhTSH, 12.33 minutes (**figure 4.3**). This indicates that the rhTSH analysed has the predicted molecular weight of approximately 30 kDa.

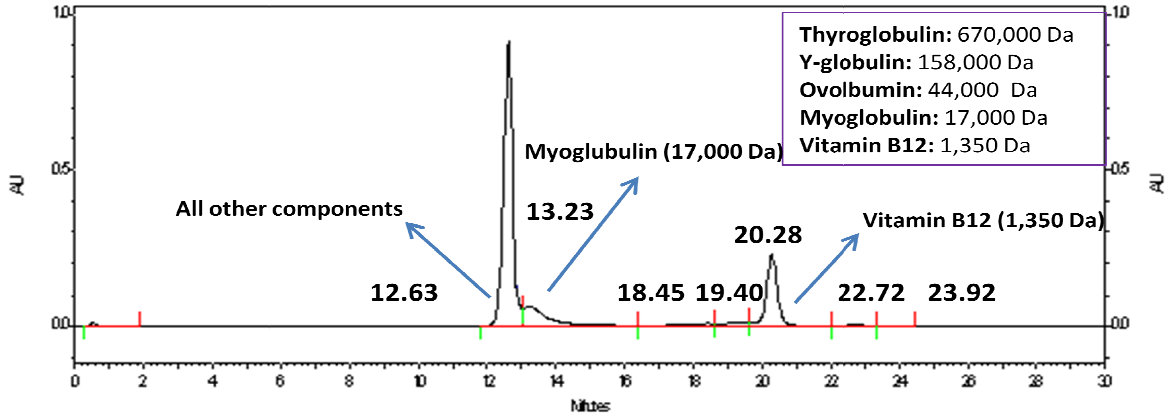

Figure 4.4: UV size exclusion chromatogram (280 nm) of BioSep molecular weight standards. 3 peaks were detected at retention time 12.63, 13.23 and 19.4 minutes.

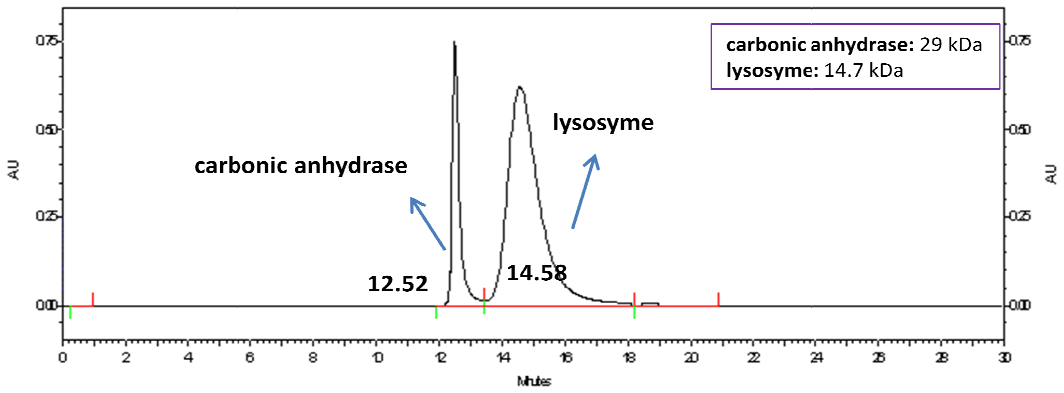

Figure 4.5: UV size exclusion HPLC chromatogram of carbonic anydrase and lysosyme. Two peaks were obtained at retention times 12.52 and 14.58 minutes corresponding to carbonic anhydrase and lysosyme respectively.

In order to investigate the effects of the radioiodination of rhTSH with ^{125}I, ^{125}I-rhTSH was analysed by radio-SE-HPLC. Please refer to section 2.3.1.2 in methodology for a detailed protocol.

In the radio-SE-HPLC a main peak at retention time 13.30 minutes was detected followed by smaller peaks at retention times 19.27, 20.85, 24.19 and 26.22 minutes (**figure 4.6**). The 13.30 minutes retention time peak most likely shows the radiolabelled rhTSH whereas the peak at 20.85 minutes most likely corresponds to the free ^{125}I. The other extra peaks seen are probably a result of radiolabelling impurities being present in the mixture. There is a shift of approximately 1 minute in the retention time of ^{125}I-rhTSH in comparison with rhTSH, which might indicate that the radiolabelling method has altered the structure of rhTSH.

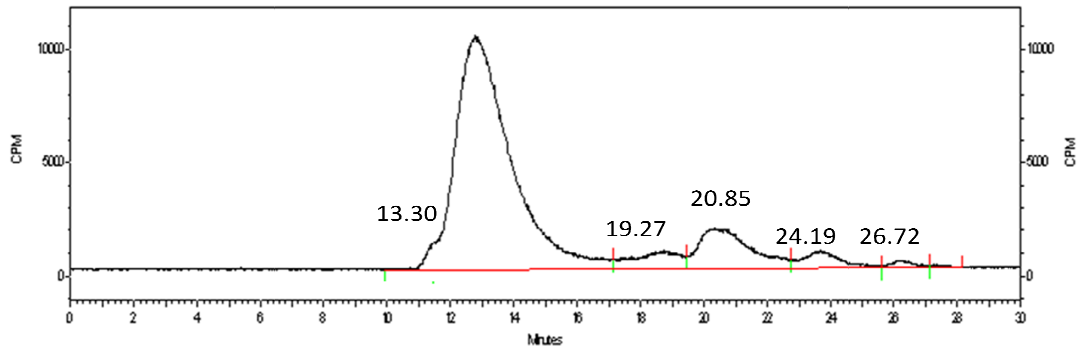

Figure 4.6: Size exclusion radio-HPLC analysis of ^{125}I radiolabelled rhTSH. A major intact peak eluted at retention time 13.30 followed by minor peaks at retention times of 19.27, 20.85, 24.19, 26.72.

4.1.2.2 Reverse phase HPLC

RP-HPLC studies were carried out in order to further study the purity of rhTSH and determine whether rhTSH retains its structure/integrity after being radiolabelled.

Unlabelled rhTSH was analysed by RP-HPLC using 0.1% TFA/water and acetonitrile(ACN)/TFA (pH 2.5) as a mobile phase in a C18 column. rhTSH was run in a 5 to 50% ACN gradient for 35 minutes, and then 50 to 100% ACN for 10 minutes (**figure 4.7**). Please refer to section 2.3.4 for a detailed protocol.

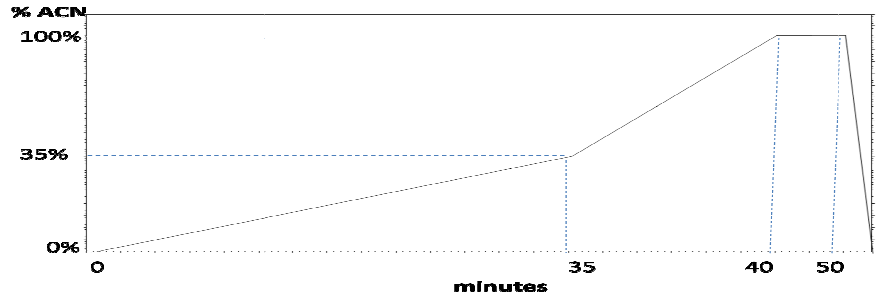

Figure 4.7: Gradient elution pattern of rhTSH in RP-HPLC. A gradient of 5 to 50% in 35 minutes followed by 50 to 100% in 10 minutes was used as indicated.

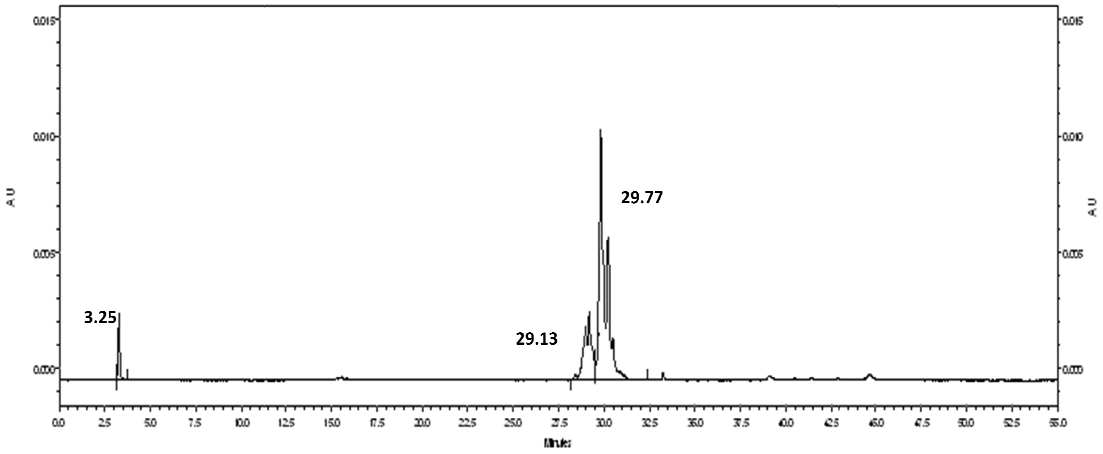

Figure 4.8: UV chromatogram of the elution of rhTSH from RP-HPLC using a C18 column and mobile phase 0.1%TFA/water and ACN/TFA (pH 2.5). A number of sharp peaks eluted from the column with two main separated peaks at retention times 29.13 and 29.77 minutes.

rhTSH eluted as a number of sharp peaks (**figure 4.8**). In order to try to achieve a better separation of the sharp peaks, a number of gradients were tested (not shown). The gradient that achieved the best separation was 5 to 20% ACN for 30 minutes, 20 to 35% for 30 minutes, 35 to 100% ACN for 5 minutes (**figure 4.9**). With this gradient, rhTSH was separated into 3 main groups of peaks with retention times of approximately 20, 21 and 22 minutes (**figure 4.10**). It was not however possible to further separate these peaks.

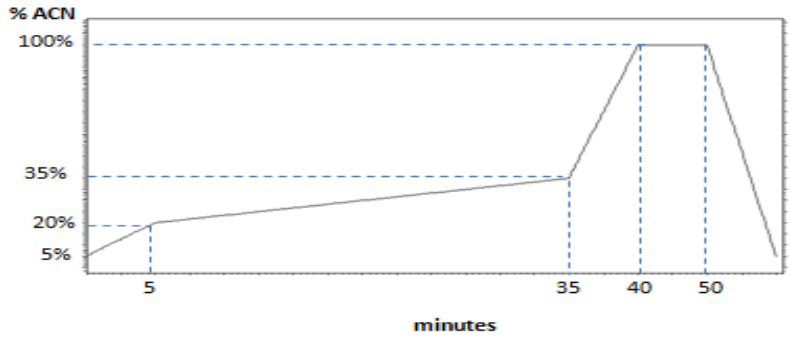

Figure 4.9: Organic solvent gradient used to elute rhTSH RP-HPLC. A gradient of 5 to 20% ACN for 30 minutes, 20 to 35% for 30 minutes, 35 to 100% ACN for 5 minutes was used as indicated.

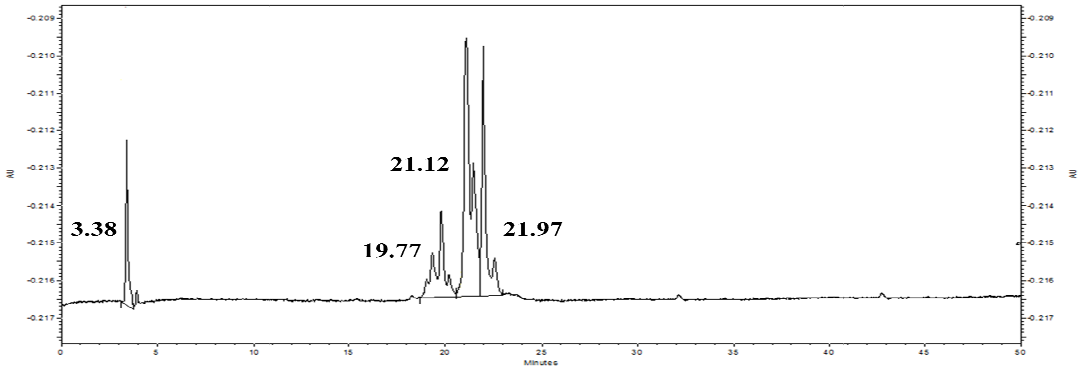

Figure 4.10: UV chromatogram and radiochromatogram of the elution of unlabelled rhTSH from a RP-HPLC using a C18 column and 0.1%TFA/water and ACN/TFA (pH 2.5) as a mobile phase. Each run was repeated at least 3 times.

^{125}I-rhTSH was then analysed using the same conditions with RP-HPLC in order to understand if the radiolabelling changed the structure of rhTSH (**figure 4.11**).

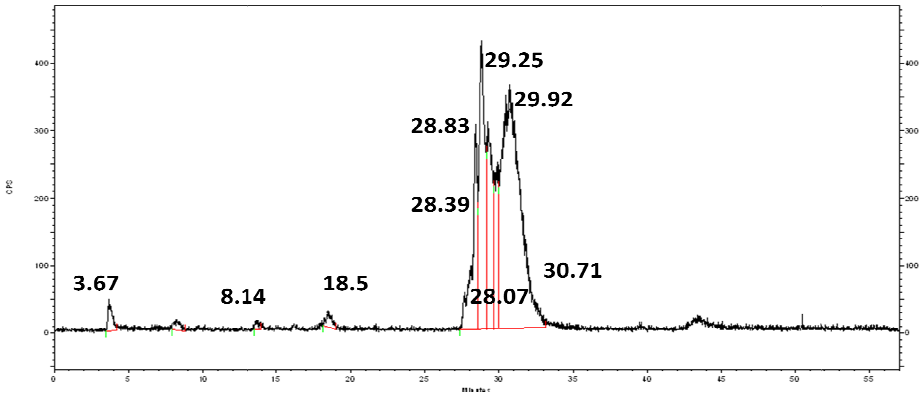

Figure 4.11: Radiochromatogram of the elution of ^{125}I-rhTSH from a RP-HPLC with a C18 column and 0.1%TFA/water and ACN/TFA (pH 2.5) as a mobile phase. A number of different peaks were obtained. 55% of rhTSH was recovered from the column. Each run was repeated at least 3 times.

As with unlabelled rhTSH, several peaks were obtained rather than a single peak (**figure 4.11**) but with retention times considerably bigger than the unlabelled compound.

The different peaks obtained in SE-HPLC analysis with rhTSH and ^{125}I-rhTSH could possibly be due to damage caused to rhTSH by the pH of the mobile phase which is pH 2.5. In order to explore this possibility, a SDS-PAGE electrophoresis with ^{125}I-rhTSH treated with either pH 2.5 or pH 7 was carried out. Please refer to section 2.3.4.1 for a detailed protocol.

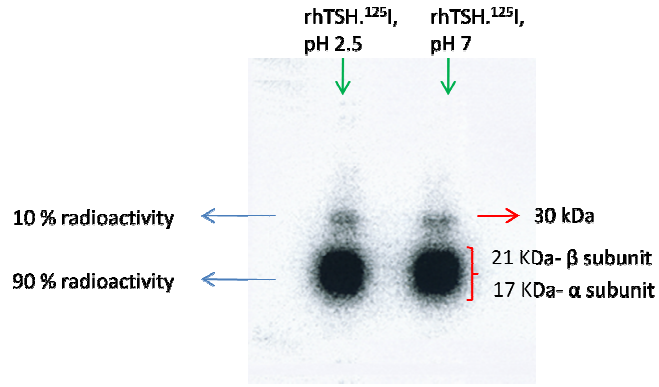

Figure 4.12: SDS gel electrophoresis of ^{125}I-rhTSH treated with pH 2.5 and pH 7. Both pH 2.5 and pH7 treated rhTSH showed a main band ranging from 17 to 21 kDa containing 90% of the total radioactivity. A band at 30 kDA which represented 10% of the total radioactivity was also detected.

rhTSH treated with pH7 and pH 2.5 showed identical bands that range from 21 to 17 kDa, which most likely represent the α and β subunit of rhTSH merged together as the resolution was not high enough to separate them onto two distinct bands (**figure 4.12**). A band at around 30 kDa is also shown at both pH7 and pH 2.5, which represents around 10% of total activity. This band most likely corresponds to the rhTSH dimer. This similarity between results at pH 2.5 and pH 7 suggests that pH 2.5 does not affect/damage the structure of rhTSH and ^{125}I-rhTSH.

4.1.2.2.1 Ion pairing RP-HPLC

In order to try to optimise the separation of rhTSH in the RP-HPLC, rhTSH was analysed using ion pairing RP-HPLC. Two different ion pairing RP-HPLC conditions

were studied: 0.01 M Triethylammonium acetate (TEAA) at pH 5.5 and 0.1 M TEAA at pH 7. See section 2.3.5 for a detailed protocol.

rhTSH in 0.1M TEAA/water pH 7 and 0.01M TEAA/water pH 5.5 eluted as a single peak at early retention times of 8.77 and 8.68 respectively (**figure 4.13**). In 0.1MM TEAA/water pH 5.5, a broader peak and a certain degree of tailing was seen, when compared with TEAA at pH 7. The TEAA/pH7 mobile phase was therefore selected as the preferred mobile phase to analyse rhTSH with.

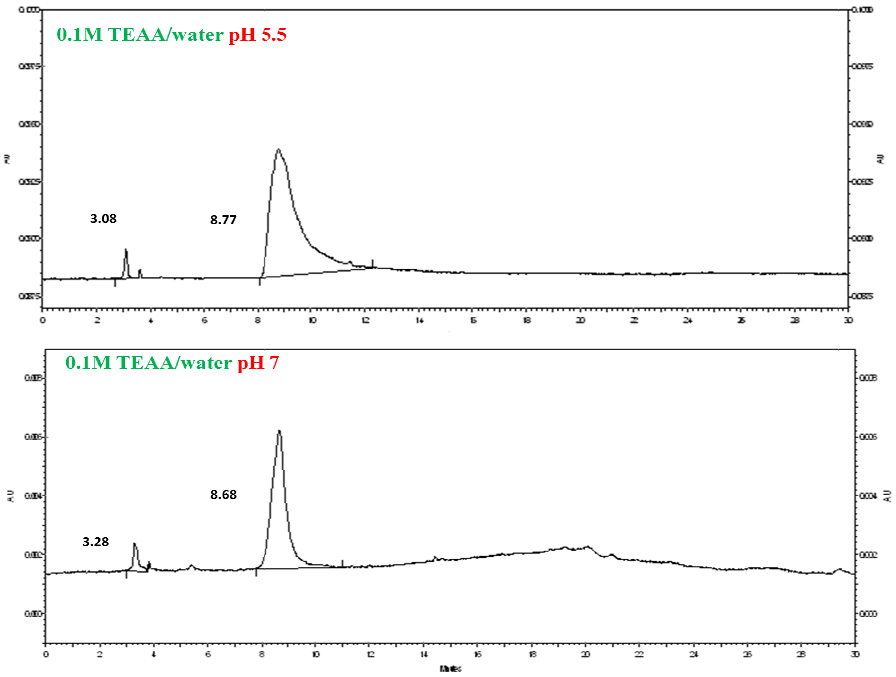

Figure 4.13: RP-HPLC of rhTSH with 0.01M TEAA/water pH 5.5 and 0.01MTEAA/water pH 7. rhTSH eluted at 8.77 and 8.68 minutes respectively.

In order to assess the effects of the radioiodination with rhTSH with ^{125}I, ^{125}I-rhTSH was analysed by RP-HPLC at the selected conditions of 0.1M TEAA/water pH7.

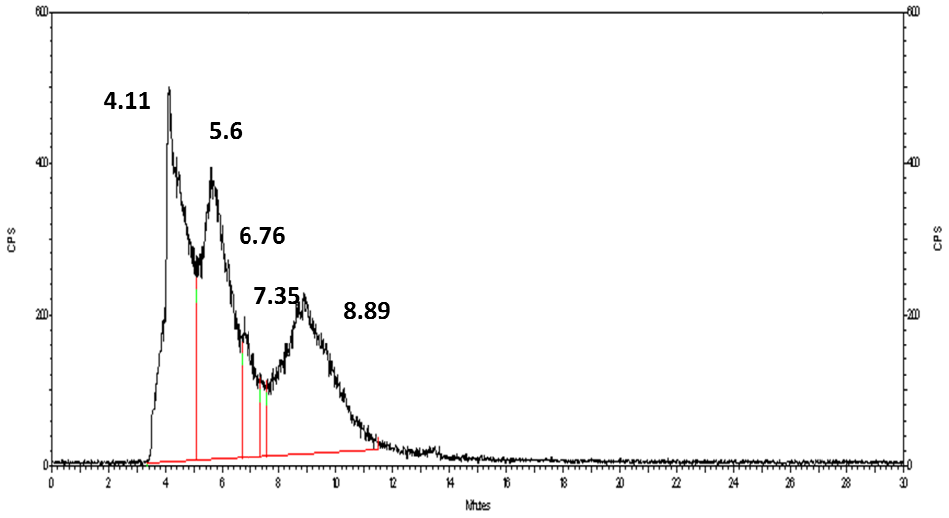

Figure 4.14: Radio RP-HPLC chromatograms of ^{125}I-rhTSH with 0.01M TEAA/water, pH 5.5 and 0.1M TEAA/water pH 7. Three main peaks are shown at retention times 4.11 minutes, 5.6 minutes and 8.89 minutes.

In contrast to unlabelled rhTSH, in which a single peak was obtained, 3 main peaks eluted with ^{125}I-rhTSH (**figure 4.14**). These extra peaks possibly indicate that the radioiodination or oxidation of rhTSH with ^{125}I is significantly altering the structure of rhTSH.

In order to investigate if the oxidation process was damaging the structure of rhTSH, rhTSH was incubated with lactoperoxidase and glucose oxidase to produce 'oxidised rhTSH' and in order to investigate if the labelling process was damaging the structure of rhTSH, rhTSH was incubated with glucose oxidase, lactoperoxidase and sodium [^{127}I] iodide: 'cold labelled rhTSH'. 'Oxidised rhTSH' and 'cold labelled' rhTSH were analysed in ion pairing RP-HPLC with 0.1M TEAA/water pH7. 'Oxidised rhTSH' analysis showed a single sharp peak at retention time 8.33 minutes (**figure 4.15**), identical to the peak obtained with unlabelled rhTSH (**figure 4.13**). This indicates that the oxidation of rhTSH is not altering the structure of rhTSH.

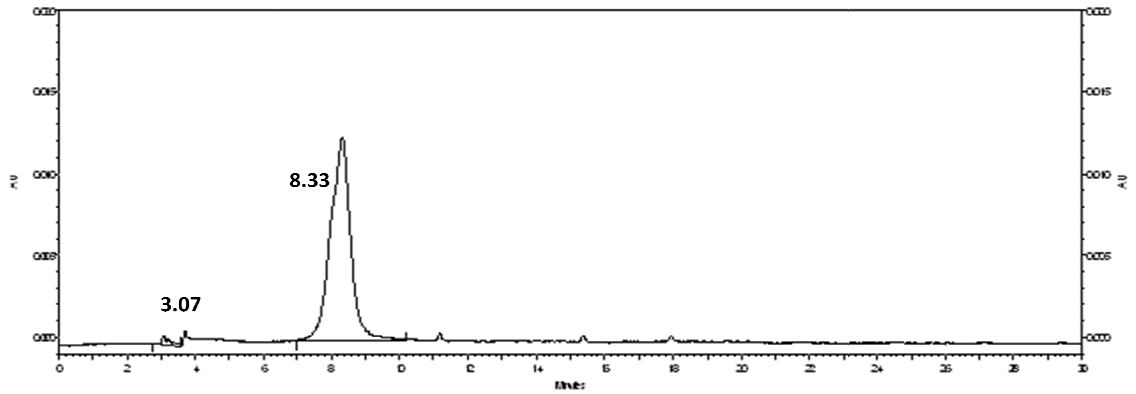

Figure 4.15: 'Oxidised rhTSH' analysis in RP-HPLC with 0.1M TEAA/water pH7. A main peak at retention time 8.33 minutes is detected.

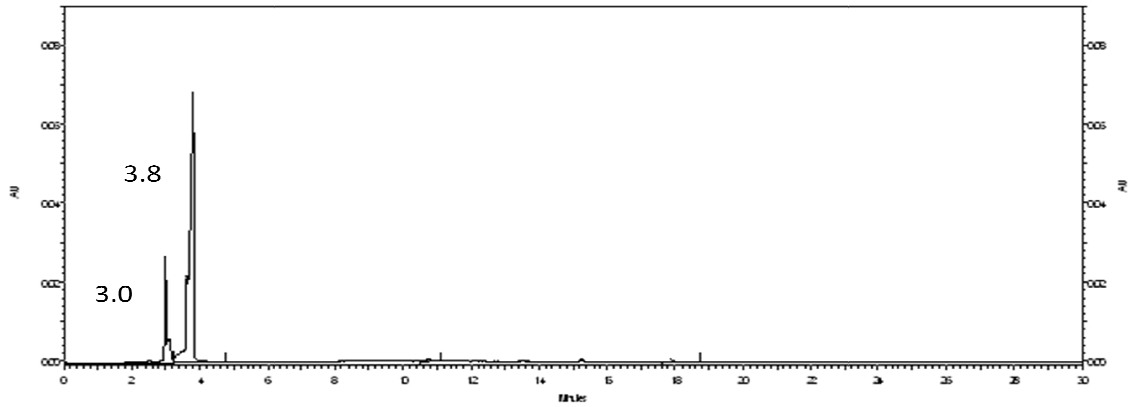

Figure 4.16: 'cold labelled' rhTSH analysis in RP-HPLC with 0.1M TEAA/water pH7. A peak at retention time 3.0 and 3.8 minutes was detected.

Analysis of the 'cold labelled' rhTSH (**figure 4.16**) showed two peaks at low retention times of 3.0 and 3.8 minutes, however, no peak is shown at a retention time of 8 minutes, as was obtained with unlabelled rhTSH and oxidised rhTSH. This indicates that the iodination process is most likely affecting the structure of rhTSH.

4.1.3 ^{125}I-rhTSH binding assays

The next step was to investigate whether ^{125}I-rhTSH bound to the TSHR both in TSHR pre-coated tubes and cells expressing the receptor.

In order to identify the most effective binding buffer to be used in the cell binding experiments, a number of different buffers were tested in order to determine which buffer gave rise to the highest binding to THSR expressing GPI cells. Please refer to section 2.3.6 in methodology for a detailed protocol. The percentage of rhTSH that

bound to the TSHR in GPI cells was significantly higher with HAMS-F12 binding buffer in comparison with the other binding buffers tested (**figure 4.17**). Thereby, in further experiments, HAMS-F12 buffer was employed in cell binding experiments.

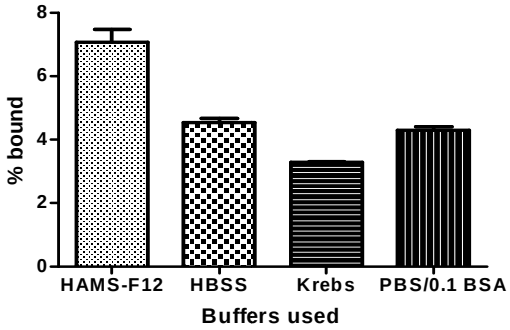

Figure 4.17: Effect of buffers used on binding to cells in cell binding assays. HAMS-F12 buffer gave the highest percentage of binding. ANOVA with Dunnett post-hoc was performed using HAMS-F12 as the control cell line. P<0.0001.

4.1.3.1 Coated tube assay with ^{125}I-rhTSH and cold labelled rhTSH

In order to determine if ^{125}I-rhTSH bound to TSHR, a competition binding assay using TSHR pre-coated tubes was carried out. (Please refer to section 2.3.6 in methodology for a detailed protocol). Increasing concentrations of rhTSH inhibited the binding of ^{125}I-rhTSH to the TSHR in the coated tubes in a concentration dependent manner, with maximal inhibition of around 90% being achieved. (**figure 4.18**). rhTSH bound to TSHR coated in the tubes with an IC_{50} of 360 nM. Coated tube assay studies indicated that ^{125}I-rhTSH retained its receptor binding ability.

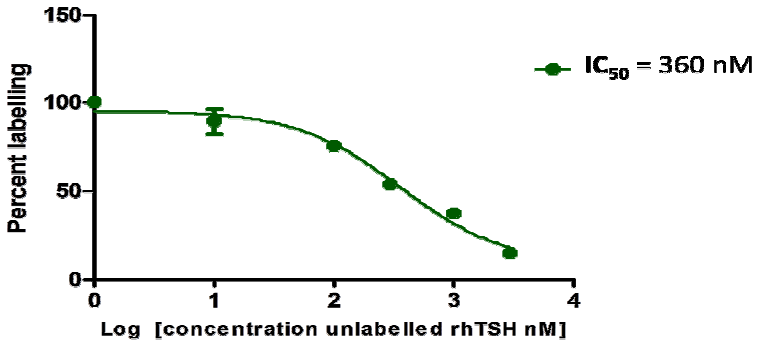

Figure 4.18: Competition assay of ^{125}I-rhTSH with unlabelled rhTSH to the TSHR in pre coated tubes. ^{125}I-rhTSH competed with rhTSH for the binding of TSHR in the tubes.

4.1.3.2 Cell binding assays with ^{125}I-rhTSH

The next step was to assess the binding of ^{125}I-rhTSH to the TSHR in TSHR expressing cells. In order to do this, competition assays and saturation binding assays were performed. Cell binding assays were performed in GPI, TPC-1 and FTC-133 cells. Please refer to section 2.3.6 for a detailed protocol.

4.1.3.2.1 Saturation assay with ^{125}I-rhTSH in GPI cells

A saturation binding assay was carried out in GPI cells in order to determine the kD and Bmax of ^{125}I-rhTSH. Results with GPI cells showed that ^{125}I-rhTSH bound specifically to these cells with a binding affinity of 2.8 nM and a Bmax of 1292 fmol/protein (**figure 4.19**).

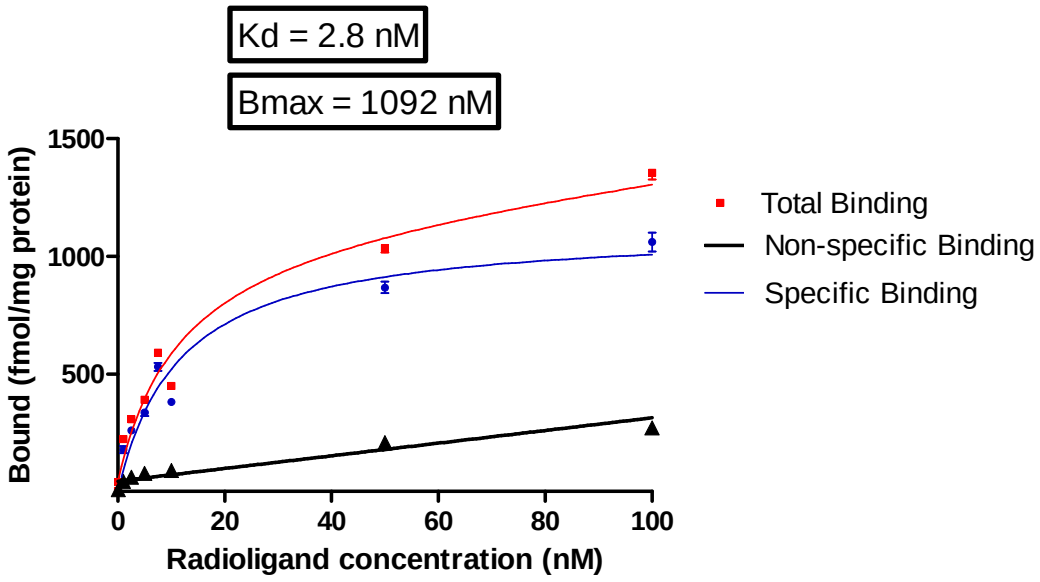

Figure 4.19: Equilibrium saturation binding of ^{125}I-rhTSH to GPI cells. ^{125}I-rhTSH bound specifically to GPI cells with a kD of 2.8 nM and a Bmax of 1092 fmol/mg. Results represent specific binding (total minus nonspecific binding) of triplicate determinations. Mean (±SEM)

4.1.3.2.2 Saturation assay with ^{125}I-rhTSH in TPC-1 and FTC-133 cells

Saturation assay results with ^{125}I-rhTSH in TPC-1 and FTC-133 cells demonstrated no binding (results not shown).

4.1.3.3 Competition assay with ^{125}I-rhTSH and cold rhTSH in GPI cells

Results from the competition assays with ^{125}I-rhTSH in GPI cells demonstrated that rhTSH inhibited the binding of ^{125}I-rhTSH by around 98%, in a concentration dependent manner (**figure 4.20**). rhTSH bound to the TSHR with an IC_{50} of 980 nM.

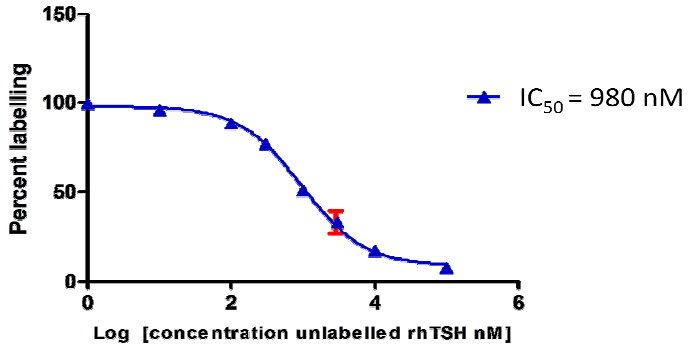

Figure 4.20: competition assay of ^{125}I-rhTSH with unalabelled rhTSH in GPI cells. rhTSH inhibited the binding of ^{125}I-rhTSH in a concentration dependent manner with the highest concentration of rhTSH achieving an inhibition of 98%. rhTSH bound to the TSHR with a IC_{50} of 980 nM.

4.1.4 ^{125}I-rhTSH internalisation and externalisation assays

4.1.4.1 Internalisation assay

The receptor-mediated internalisation of ^{125}I-rhTSH was studied in GPI cells in order to find out if ^{125}I-rhTSH /TSHR complexes were being internalised into cells. Please refer to section 2.3.7 for a detailed procedure.

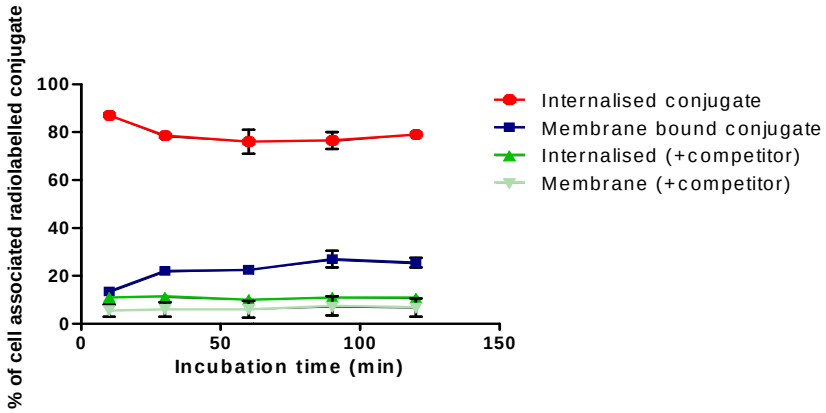

Figure 4.21: Internalisation assay to determine the amount of conjugate that is internalised over a period of 120 minutes. The bound excess competitive inhibitor was also used to determine the degree of non specific binding. Around 80% of conjugate was internalised and 20% was membrane bound after 120 minutes incubation.

Internalisation was very rapid with approx 80% of the cell associated radiolabelled conjugate being internalised after 15 minutes, whereas the membrane-bound fraction accounted for the other 20% of the total conjugate at this time point (**figure 4.21**). The non specific binding of rhTSH was on average less than 5% of the total activity.

From these results it is apparent that the degree of internalisation is greater than the remaining rhTSH found on the outer-membrane of the GPI cells. Externalisation assays provide more information about the degree of recycling of the radiolabelled ligand.

Because of the possibility of metabolism of internalised ^{125}I-labelled proteins the internalisation/externalisation assay may be misinterpreted by assuming that the supernatant radioactivity is immunoprotein bound when in fact the activity may be due to low molecular weight metabolites in solution.

In order to discriminate between these two possibilities, the supernatants were collected and a TCA precipitation assay was performed so that protein was precipitated out of the solution. Please refer to section 2.3.8 in methodology for a detailed procedure. Results show that more than 90% of the radioiodine remains protein bound and that metabolism does not confound interpretation of the results (**figure 4.22**).

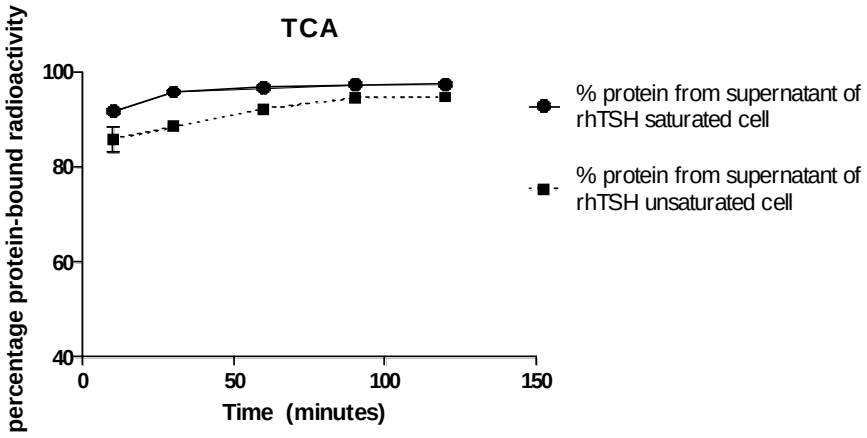

Figure 4.22: TCA precipitation assay to determine the amount of protein bound radioactivity over a period of 120 minutes. The percentage of the total counts of supernatant and pellet sample are shown.

4.1.4.2 Externalisation assay

An externalisation assay was carried out in order to determine the rate of rhTSH externalisation and the integrity of externalised rhTSH. Please refer to section 2.3.7 for detailed protocol. 60 % of the internalised activity had become externalised after 120 minutes (**Figure 4.23**). There was no major difference between externalisation in the presence and absence of competitor, suggesting that most of the externalised rhTSH was degraded.

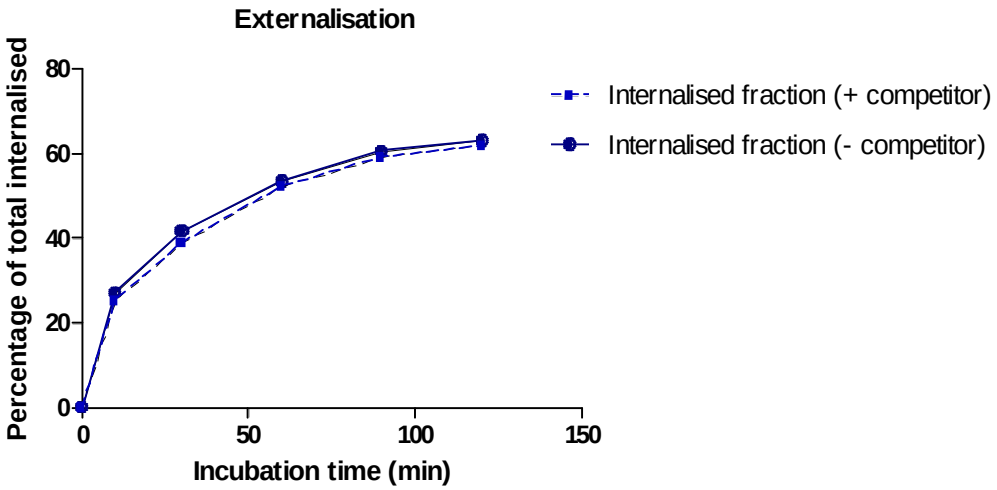

Figure 4.23: Time dependant externalisation of pre-internalised ^{125}I-rhTSH in GPI cells, in the presence and absence of competitor. 60% of internalised activity became externalised and there was no major difference in the presence and absence of competitor.

As with the internalisation assay, a control experiment was also carried out to ensure that the immunoconjugate remained bound to ^{125}I. Please refer to section 2.3.8 for a detailed protocol. Results show that more than 85% of the radioiodine remained protein bound and that, as above, the metabolism of ^{125}I-rhTSH does not confound interpretation of the results (**figure 4.24**).

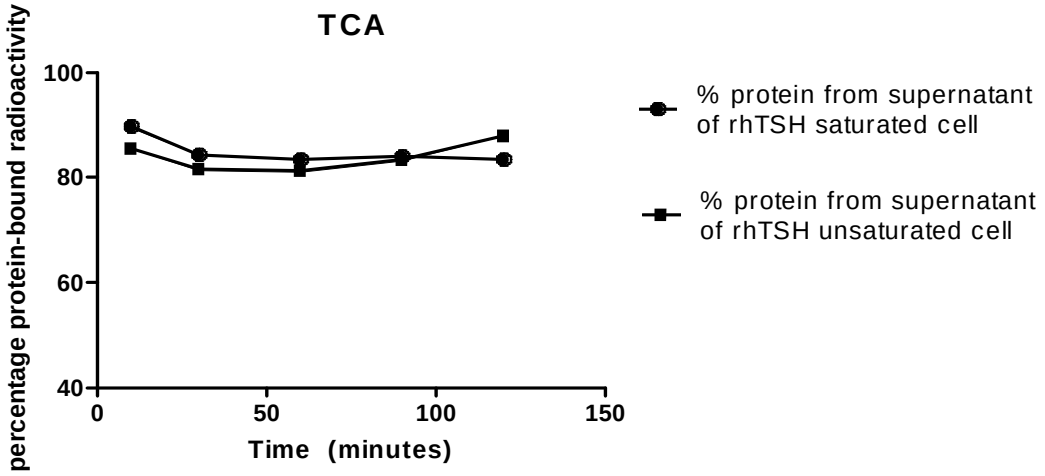

Figure 4.24: TCA precipitation assay to determine the amount of protein bound radioactivity over a period of 120 minutes. This graph is displayed as a percentage of the total counts of supernatant and pellet sample.

4.1.5 *In vivo* binding

^{125}I-rhTSH selectively bound to the TSHR both in TSHR pre coated tubes as well as TSHR expressing GPI cells. For this reason it was considered worthwhile to assess the binding of ^{125}I-rhTSH *in vivo*.

Biodistribution and imaging studies were carried out to investigate the binding of ^{125}I-rhTSH to the thyroid and subcutaneously grafted FRTL5 tumours in mice. Animals were injected intravenously with either ^{125}I-rhTSH alone or ^{125}I-rhTSH together with an excess of unlabelled rhTSH (blocking control) and scanned using SPECT/CT at several time points post injection. Please refer to section 2.3.8 in methodology for detailed protocol. A representative image at the 2.5 hour time point is shown in **Figure 4.25**.

For the bioodistribution study, mice were injected with either ^{125}I-rhTSH or ^{125}I-trypsin inhibitor as a negative control tracer due to its similar molecular weight to the rhTSH (23 kDa). Mice were killed and tissues dissected and counted 2 hours after injection.

4.1.5.1 ^{125}I-rhTSH SPECT/CT imaging studies

In the SPECT imaging studies, accumulation of ^{125}I-rhTSH in the kidney and the bladder was clearly visible after 1 hour (**figure 4.25).** However, no thyroid uptake was observed. There was uptake in the tumour in both the blocking control and ^{125}I-rhTSH, at all time points. Invivo-scope software analysis was used to quantify the signal in the tumour. (**figure 4.26**). Please refer to methodology for detailed protocol.

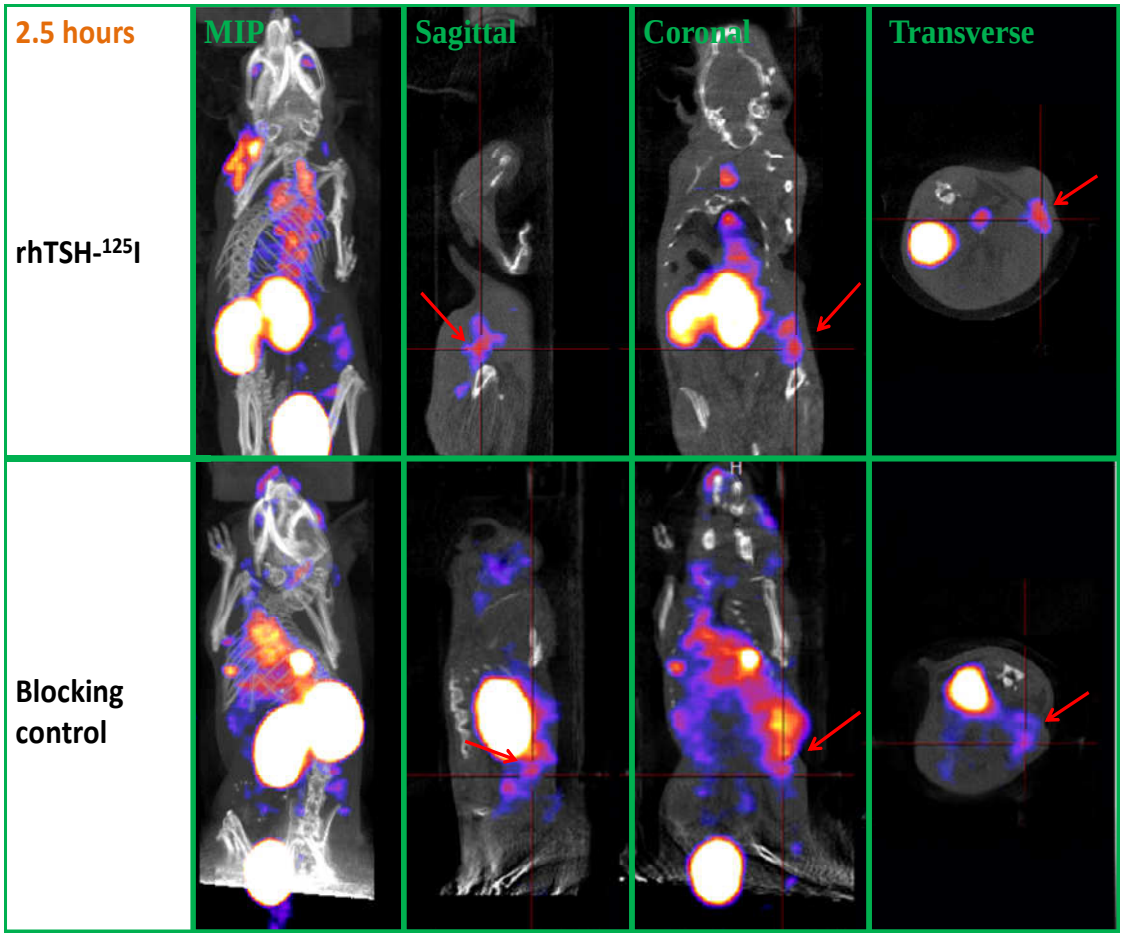

Figure 4.25: SPECT/CT imaging of mice at 2.5 hour time point after ^{125}I-rhTSH injection. Upper half: ^{125}I-rhTSH MIP, Sagittal, Coronal and Transverse region of mice and lower half: Blocking control: Sagittal, Coronal and Transverse region of mice and lower half. The red arrow points to the grafted FRTL5 tumour.

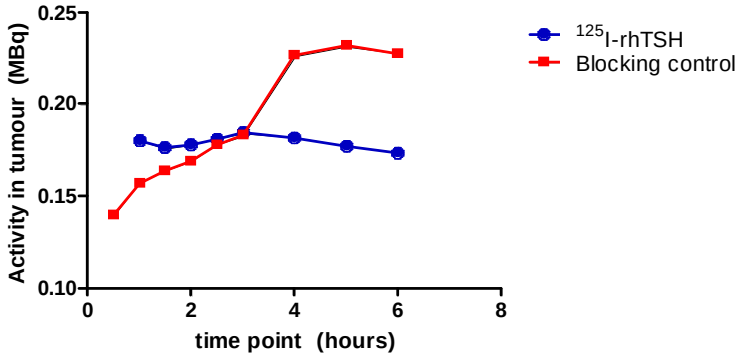

Figure 4.26: Invivoscope ROI quantification analysis of ^{125}I-rhTSH and blocking control. 3 mice were analysed at 0.5, 1,2,3,4,5,6 hours post ^{125}I-rhTSH injection.

Quantitative analysis of the ROI's demonstrated a constant activity in tumour with ^{125}I-rhTSH at all time points up to 6 hours (around 0.17 MBq) (**figure 4.26**). With the blocking control, an increase in the activity in the tumour is observed ranging from 0.13 MBq at 30 minutes to 0.23 MBq at 6 hours (**figure 4.26**). This suggests that most uptake is in fact occurring due to non specific mechanisms.

4.1.5..2 Biodistribution

Biodistribution studies were conducted in order to confirm the imaging results and to explore whether ^{125}I-rhTSH bound to the thyroid and FRTL5 grafts in mice. Please refer to section 2.3.8.1 for a detailed protocol.

^{125}I-rhTSH uptake measured in the tumour and thyroid was higher than that obtained with the ^{125}I Trypsin Inhibitor (TI) -control (**figure 4.27**). However the levels measured in the blood were much higher with ^{125}I-rhTSH indicating that ^{125}I-rhTSH is circulating for longer in the blood than ^{125}I-TI. The uptake of ^{125}I-rhTSH was also higher than that of ^{125}I-TI in the intestine, pancreas, spleen, stomach, liver, heart, lung, muscle and tail. Since the uptake of ^{125}I-rhTSH was not only higher in the tumour and the thyroid but also in receptor negative organs, it cannot be concluded that the uptake observed with ^{125}I-rhTSH in the thyroid and tumour is due specific receptor binding.

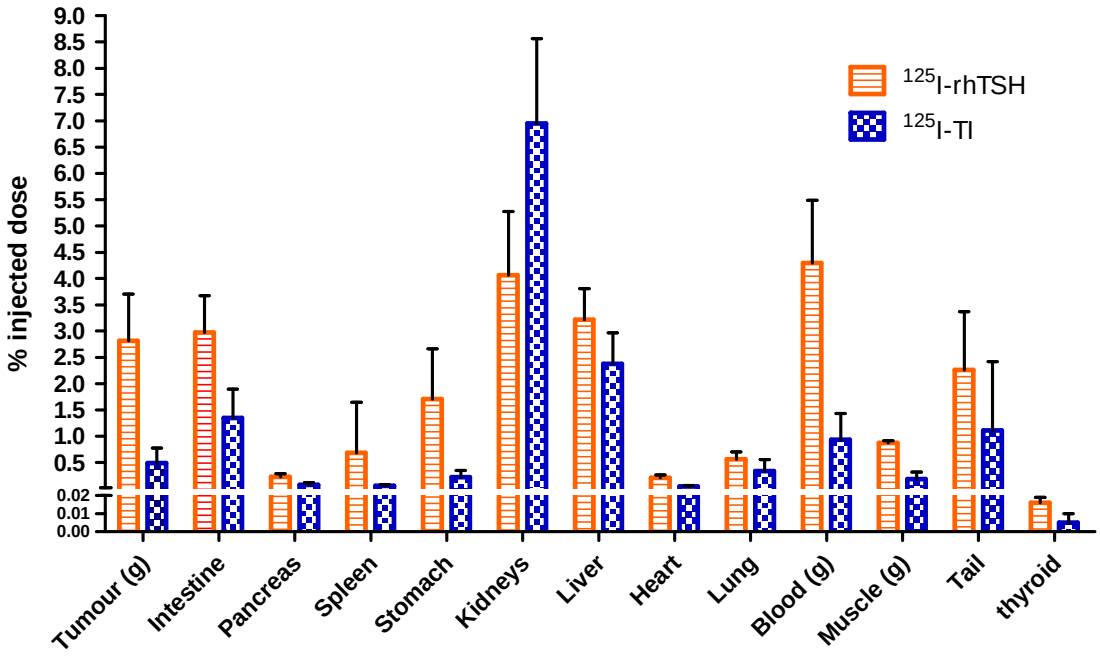

Figure 4.27: Biodistribution of ^{125}I-rhTSH in mice. The average amount of radiotracer measured in mice, is shown. Y axis represents the percent of total activity per g and uptake of injected dose per organ.

4.1.5.3 Blood stability studies

Blood stability studies were performed to see whether the radiolabelled rhTSH remained intact *in vivo* during the imaging study. TCA precipitation assays and SDS-PAGE electrophoresis were carried out on blood samples after injection of ^{125}I-rhTSH into mice. Please refer to section 2.3.8.1.2 for a detailed protocol.

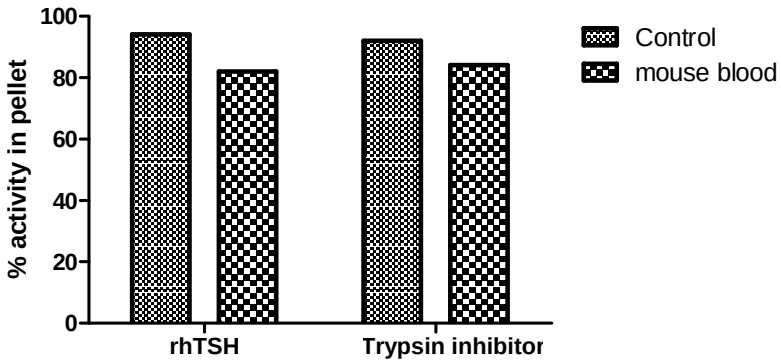

Figure 4.28: TCA precipitation assay on blood removed from mice 2 hour post injection of ^{125}I-rhTSH and ^{125}I-TI. The percentage in the pellet in ^{125}I-rhTSH and ^{125}I-TI is shown.

Results from the TCA precipitation assay showed that the majority of the activity remained in the pellet with both ^{125}I-rhTSH and ^{125}I-TI (**figure 4.28**). This confirms that both ^{125}I-rhTSH and ^{125}I-TI remained intact in the blood during the *in vivo* studies.

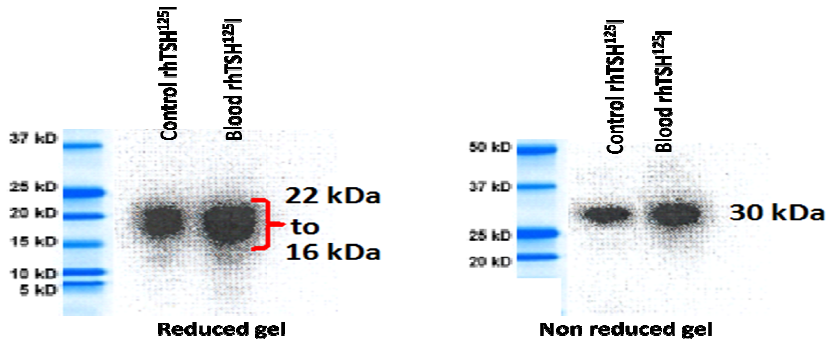

Figure 4.29: Phosphorimager image of reduced and non reduced SDS-PAGE electrophoresis of ^{125}I-rhTSH incubated in the blood of mice. Two animals were injected i.v. with ^{125}I-rhTSH and after 6 hours their blood removed.

Results from SDS-PAGE electrophoresis of ^{125}I-rhTSH in blood samples analysed under reducing conditions showed a band ranging from 16 to 22 kDa, which most likely represents the α and β subunit of rhTSH (**figure 4.29**). The non reduced gel showed a band at approximately 30 kDa which represents the rhTSH dimer. These studies therefore show that the stability of ^{125}I-rhTSH was most likely not compromised *in vivo*.

4.1.5.4 Second biodistribution study of ^{125}I-rhTSH in tumour grafted mice

One possible explanation for the lack of blocking of receptor uptake observed in the SPECT/CT imaging study might be that an insufficient dose of cold rhTSH was used which may have been insufficient to saturate the receptors. A second biodistribution study was therefore performed using a higher dose of cold rhTSH. This study also used an alternative non-specific control tracer, ^{125}I-labelled Carbonic anydrase (Mwt: 29kDa) in the hope that its kinetics would match those of ^{125}I-rhTSH more closely. Please refer to section 2.3.8.2 for a detailed protocol.

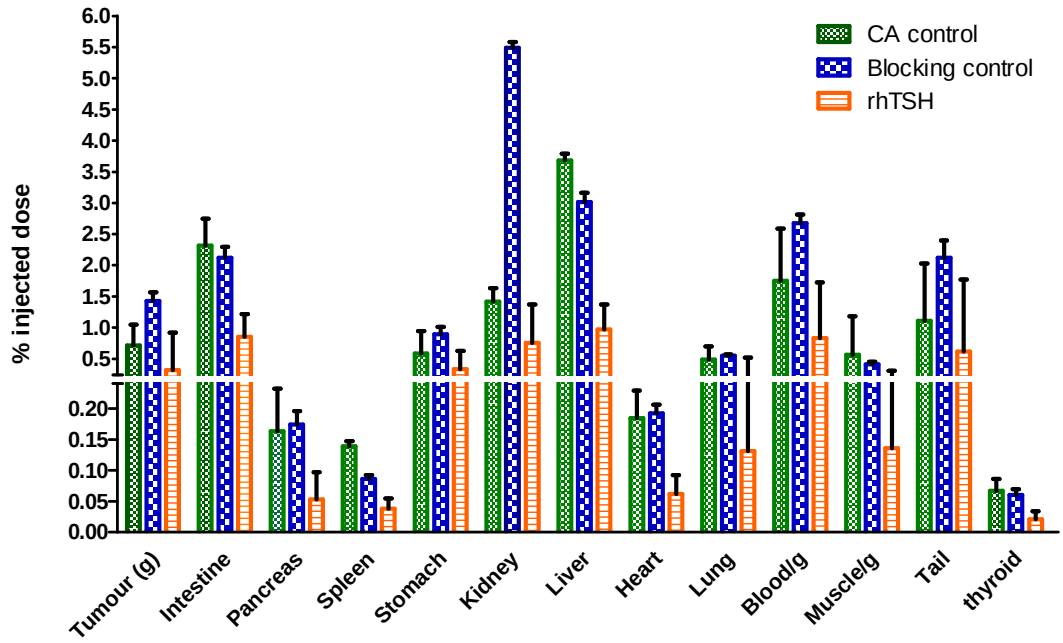

Figure 4.30: Biodistribution of ^{125}I-rhTSH, ^{125}I-CA and blocking control in mice. The average amount of radiotracer measured in 2 mice, is shown. Y axis represents the percent of total activity per g and uptake of injected dose per organ . Results show uptake of the blocking control and CA control in the tumour and thyroid was much higher than with ^{125}I-rhTSH.

The results of this biodistribution study (**figure 4.30**) unexpectedly showed that the radioactive uptake in the thyroid and tumour with the blocking control and ^{125}I radiolabelled carbonic anydrase control was higher compared to that of ^{125}I-rhTSH. This was also the case for all other tissues sampled. These results suggest that the uptake observed for ^{125}I-rhTSH in the tumour and thyroid was primarily due to non specific mechanisms.

4.2 Discussion of rhTSH studies

Radiolabelled proteins and peptides have emerged as useful agents in the diagnosis and treatment of cancer [155, 156]. Radiolabelled peptides offer the advantages of being small, low in antigenicity, fast in clearance and rapid in tissue and tumour penetration [248, 249]. Furthermore, with the advance in peptide and protein synthesis techniques it is easy and relatively cheap to produce new peptides/proteins to be tested as potential radiopharmaceuticals [248, 249].

As previously discussed, some differentiated thyroid cancers de-differentiate and lose the expression of NIS, and thereby the ability to readily take up radioiodine into the thyroid [109, 250, 251]. This impairs the staging of recurrent disease with radioactive iodine. There have been reports, however, that showed that some radioiodine resistant thyroid cancers still express the TSHR [247]. Therefore, TSHR could potential be used as a marker for radioiodine resistant de-differentiated thyroid cancer.

In chapter 3, mAb9 anti-TSHR antibody was investigated for its potential to target radioiodine resistant thyroid cancer. mAb9 monoclonal antibody bound specifically to the TSHR *in vitro*, however it did not bind specifically the TSHR in the thyroid of mice *in vivo*. For this reason, an alternative approach for targeting radioiodine resistant thyroid cancer was evaluated in which radiolabelled rhTSH (Genzyme) was used instead of mAb9 to target radioiodine resistant thyroid cancer. TSH is an endogenous ligand for the TSHR and it was considered appropriate to use because of its relatively small size of approximately 30 kDa. Also, Corsetti *et al.* [181] previously radioiodinated rhTSH with ^{125}I and performed binding assays that showed ^{125}I-rhTSH to bind to TSHR expressing cells (PTC-1) [181]. In these studies, ^{125}I-rhTSH also appeared to bind to PTC-1 tumour xenografts in mice [181]. However, these experiments were just preliminary and further experiments are required in order to

conclusively show that this is the case. In this chapter experiments were carried out to try and confirm these findings.

4.2.1 Radioiodination of rhTSH with ^{125}I

The first step was to radiolabel rhTSH with ^{125}I. Several different methods can be employed in the radioiodination of proteins, antibodies and peptides and they usually differ mostly in the nature of the oxidising agent for converting I- into the reactive species of I^2 and I^+ [169]. These reactive species most often substitute into tyrosine residues of proteins, however substitution can also occur in histidine, cysteine and tryptophan residues [169]. These methods include the two oxidation methods chloroamine-T [252] and the Iodogen [253] method, and enzymatic substitution method which uses lactoperoxidase enzyme [172].

The first step in this study was to attempt to produce a high purity ^{125}I radiolabelled rhTSH. The direct hydrogen peroxide enzymatic radioiodination method was used for this purpose. This radioiodination method was first introduced by Marchalonis *et al.* [172] and employs lactoperoxidase in the presence of a trace of hydrogen peroxide to oxidise the radioactive iodide [172]. The hydrogen peroxide used in this reaction can either be used directly or produced in solution by glucose oxidase. This technique may result in less denaturation to susceptible proteins than Chloramine-T and Iodogen [172]. In this study the lactoperoxide method in which glucose oxidase generates hydrogen peroxide *in situ* was used.

The most effective concentrations of glucose oxidase and lactoperoxidase for the lactoperoxidase/glucose oxidase labelling method were experimentally determined and they coincided with the amounts used by Corsetti *et al.* [181]. In order to estimate the radiolabelling purity, ITLC was used. ITLC results showed a labelling efficiency close to 100%. ITLC is a good indicator of the approximate labelling efficiency of a

radiolabelled compound, however, alone it does not provide information on the presence of small aggregates and impurities in the radiolabelled compound and for this reason a SDS-PAGE gel electrophoresis was also conducted. SDS-PAGE results showed two bands of 21 kDa and 17 kDa, which most likely represent the α and β subunit of the rhTSH respectively . The predicted molecular weights of the α and β subunit of rhTSH are 13,829 and 15,840 Da respectively, and the theoretical molecular weight for the rhTSH dimer is 29,660 Da [96]. Cole *et al*. ran rhTSH in a SDS-PAGE electrophoresis and detected bands of 20,940 Da and 16,630 Da corresponding to α and β subunit respectively [96]. Both ITLC and SDS-PAGE results clearly indicated that a high purity ^{125}I radiolabelled rhTSH was therefore prepared.

4.2.2 HPLC studies with rhTSH

HPLC studies were conducted to study in more detail the purity of rhTSH and ^{125}I-rhTSH. Due to its intermediate size of 30,000 Da, it is not certain whether the most suitable method to analyse it would be size exclusion HPLC or reverse phase-HPLC (RP-HPLC). Usually size exclusion HPLC is used to separate and analyse proteins/compounds of higher molecular weight, whereas RP-HPLC is most efficient for the analysis of smaller molecular weight peptides. Therefore experiments were carried out with each of these systems to identify the optimal conditions for the analysis of rhTSH. Ion pairing RP-HPLC can further improve separation and therefore was also used to analyse rhTSH.

4.2.2.1 Size exclusion-HPLC (SE-HPLC)

The first HPLC system to be evaluated was size exclusion HPLC (SE-HPLC) and results showed a single peak corresponding to the approximate molecular weight of rhTSH. The size of a compound analysed in SE-HPLC can be determined by measuring

their retention times from a column calibrated against known standards. In this particular case, the SE-HPLC did not manage to separate the different components of the molecular weight markers into distinct peaks. This is probably because the type of SE-HPLC column used, YMC, has very small pores and, thus does not separate the larger molecules, just smallest ones. Small proteins in this column usually elute relatively quickly from the column and there is poorer resolution between bigger and smaller proteins but better resolution of small proteins from lower molecular weight contaminants. In order to overcome this problem, a compound with a similar molecular weight to the α subunit, lysosyme, and one with similar molecular weight to the rhTSH dimer, carbonic anydrase, were analysed in the SE-HPLC. Carbonic anydrase and lysosyme have a theoretical molecular weight of 29 kDa and 14.7 kDa respectively, which are similar to the theoretical molecular weight of the rhTSH dimer of 29,660 and α subunit, 13.820 Da. The retention time obtained with carbonic anydrase was very close to the retention time obtained with rhTSH, which indicates that the rhTSH analysed by the SE-HPLC eluted as a rhTSH dimer of an approximate molecular weight of 30,000 Da. Radiolabelled ^{125}I-rhTSH eluted approximately 1 minute later than unlabelled rhTSH in this SE-HPLC column. This could be caused by the radioiodination process altering the structure of rhTSH.

4.2.2.2 Reverse phase HPLC (RP-HPLC)

The resolution of SE-HPLC is not very high and therefore there usually needs to be differences of around thousands of Da in order to achieve separation [254]. For this reason smaller proteins and peptides of hydrophobic nature are usually better analysed using reverse phase-HPLC (RP-HPLC) rather than size-exclusion HPLC. Moreover, separation in RP-HPLC offers the advantages of the resolution being improved by the use of buffered mobile phases and ion-pairing agents [254].

The separation in RP-HPLC depends on the hydrophobic binding of the solute molecule from the mobile phase to the immobilised hydrophobic ligands attached to the stationary phase [254]. The solute mixture is initially applied to the stationary phase in the presence of aqueous buffers, and the solutes are eluted by the addition of organic solvent to the mobile phase (usually acetonitrile). Elution is usually achieved by gradient elution where the amount of organic solvent is increased over a period of time. The solutes are, therefore, eluted in order of increasing molecular hydrophobicity, rather than size [254].

RP-HPLC is a very useful technique for the analysis of peptides and proteins due to a number of factors. First, it is possible to achieve excellent resolution using a range of chromatographic conditions for very closely related molecules as well as structurally very distinct molecules. Second, the mobile phase characteristics can be changed in order to manipulate chromatographic selectivity and lastly, excellent reproducibility of repetitive separations carried out over a long period of time can be achieved, due to the stability of the stationary phase materials under a varied range of mobile phase conditions [254]. A number of factors should be taken into account when considering RP-HPLC separation analysis. These factors include column components and specifications, the solvents used, elution gradient, flow rate and sample preparation [254].

Trifluoroacetic acid (TFA) at pH 2.5 is normally used as a starting condition mobile phase in RP-HPLC as the low pH can suppress the ionisation of the acidic groups in the solute molecules and generate sharper peaks [254]. Most peptides elute from a C_{18} reverse phased column in 30%ACN, and in order to improve separation a shallower gradient can be used.

rhTSH was analysed initially in a 0.1%TFA/pH 2.5 mobile phase solution. If the solute was homeogenous, rhTSH should elute as a single peak, however rhTSH analysis

showed several peaks indicating heterogeneity in the sample. In order to try and optimise the elution of rhTSH, different gradients were tested in an attempt to further separate the different peaks. Of the different gradients tested, just one (5 to 20% ACN for 30 minutes, 20 to 35% for 30 minutes, 35 to 100% ACN for 5 minutes) achieved a better peak separation, as it managed to clearly separate the peaks into 3 main groups.

^{125}I-rhTSH was also analysed in RP-HPLC using the same conditions as that used with unlabelled rhTSH and as with rhTSH, several peaks were seen but with longer retention times suggesting that the components had become more hydrophobic.

One reason why rhTSH and ^{125}I-rhTSH analysed in 0.1%TFA/water at pH 2.5 were showing a number of different peaks in the RP-HPLC could be due to the low pH 2.5 damaging the structure of rhTSH. In order to investigate this possibility, an SDS-PAGE gel electrophoresis was carried out with rhTSH treated at pH 2.5 and pH 7. There was no indication that the low pH was in fact damaging the rhTSH, and for that reason it is unlikely that the extra peaks obtained with rhTSH and ^{125}I-rhTSH analysed in RP-HPLC were the result of degradation caused by the low pH.

4.2.2.3 Ion pairing RP-HPLC

The retention times of solutes such as proteins and peptides can be modified by adding ion pairing agents to the mobile phase. Ion pairing agents bind to the solute through ionic interactions, which can result in an increase in the solute hydrophobicity and by doing so change its selectivity. Ion pairing RP-HPLC has the advantage of improving the chance of achieving complete resolution of the sample components.

In order to try and improve separation on the RP-HPL, ion pairing RP-HPLC was tested with triethylammonium acetate buffer (TEAA) at both pH 5.5 and pH 7. TFA and TEAA are both weak hydrophobic ion pairing agents hence any change in retention times found with the TEAA system relative to the TFA system are mainly due to a

change in the pH and the resulting differences in the ionization of the carboxyl side chains of glutamic acid and aspartic acid and the terminal carboxyl group [254]. Peptides exhibit increased hydrophilic character in the TEAA system and for that reason retention times are reduced dramatically.

When unlabelled rhTSH was analysed, a single sharp rhTSH peak was obtained with pH 7. At pH 5.5 a broader single peak with a degree of tailing was obtained. After these analyses it was concluded that the optimal method to analyse rhTSH was ion pairing RP-HPLC with TEAA/water pH7.

The next step was therefore to determine if the radioiodination of rhTSH was damaging/altering the structure of rhTSH. In order to do this, ^{125}I-rhTSH was analysed under the previously determined optimal conditions: TEAA/water at pH 7. Two extra peaks were shown with ^{125}I-rhTSH in comparison with rhTSH. This indicated that the radioiodination process was possibly damaging the structure of rhTSH. Also, the recovery of ^{125}I-rhTSH from the column was measured and showed that around 40% of ^{125}I-rhTSH was being retained in the column.

The radioiodination process can potentially interfere with the receptor binding site of a ligand and damage the binding ability of the protein through oxidative damage caused by the labelling reagents. Damage may also occur as a result of substitution of the isotope into the receptor-binding site if the latter is tyrosine-rich. These possibilities were explored by RP-HPLC using the previously optimised conditions. To investigate whether oxidation was damaging rhTSH, rhTSH was incubated with glucose oxidase and lactoperoxidase: to produce ‘oxidised rhTSH’ and to investigate whether the iodine substitution process was damaging the rhTSH, rhTSH was incubated with glucose oxidase, lactoperoxidase and cold iodine (Na[^{127}I]I) to produce ‘cold labelled rhTSH. Results showed that oxidation of rhTSH did not appear to affect rhTSH, however cold

labelling of rhTSH did appear to inflict some degree of damage to rhTSH. It is however unknown if this would interfere with the binding of rhTSH to the TSHR.

4.2.3 Binding of radiolabelled rhTSH to the TSHR in vitro

Radiolabelled peptides must retain their receptor-binding capacity if they are to function as effective radiopharmaceuticals. In order to investigate ^{125}I-rhTSH's receptor-binding ability, studies were conducted in tubes pre-coated with TSHR and in cells expressing the TSHR.

4.2.3.1 Coated tube assay

A competition assay was carried out in which tubes coated with TSHR were used to assess the ability of rhTSH to inhibit the binding of ^{125}I-rhTSH.

rhTSH inhibited the binding of ^{125}I-rhTSH in a concentration dependent manner, with the maximal concentration of rhTSH achieving 90% inhibition. The IC_{50} value of rhTSH was 360 nM. This indicated that ^{125}I-rhTSH bound to the TSHR coated in the tubes.

4.2.3.2 Cell binding assays:

The next step was to study the ability of ^{125}I-rhTSH to bind to the TSHR in cells. Saturation and competition radioligand binding assays were carried on the thyroid cancer cell lines: FTC-133, and TPC-1 cells and a TSHR transfected cell line, GPI cells, in order to determine both the receptor number (Bmax) and the binding affinity (Kd) of ^{125}I-rhTSH in the different cells. In addition to specific binding to target receptors, radioligands may also bind non-specifically to other sites, notably the cell membrane. These non-specific interactions may be occurring due to the charge and hydrophobicity of the ligand, more so than because of the sequence-specific structure [255].

Unlabelled rhTSH was used as the competitor to measure non-specific binding to ensure that all the target receptors were occupied, so that any binding observed would be to other receptors, or be due to interactions with the cell membrane. There are many characteristics that can influence the outcome of binding assays, one of them is the binding assay buffer used. In order to identify which binding assay buffer yielded the most favourable results, the percentage of binding was studied with different binding buffers in TSHR expressing GPI cells. HAMS-F12 was found to be the most efficient buffer, and therefore this buffer was used in subsequent binding assays.

Measurable Bmax and Kd values were obtained for GPI cells only. FTC-133 and TPC-1 cells showed no binding, most probably due to the very low or negligible expression of TSHR in these cells, as demonstrated by RT-PCR, FACS and Western blot experiments carried out in chapter 2.

Studies in GPI cells showed rhTSH to bind to TSHR with a a Kd of 2.8 nM and Bmax of 1092 fmol/mg. Cornelis *et al.* used ^{125}I radiolabelled bovine TSH (^{125}I-bTSH) in TSHR transfected GPI cells and reported a Kd of 1.56 nM [256]. The reported binding affinity of 1.56 nM was thus similar to the Kd obtained in this study. In another study, the binding of ^{125}I-rhTSH was used in TSHR transfected cell lines and a Kd of 56 nM was reported, which is slightly lower than the Kd obtained in this study [257]. The differences between the kD in the paper and this study, could be due to the use of two different batches of rhTSH. Different batches of rhTSH have different degrees of sialylation and sulphation and it has been shown that this can affect biological activity. The differences reported in these studies could also be a result of differences in experimental setting such as incubation times, binding buffers, binding buffers, pH and other conditions that can influence the results of a binding assay.

Competition binding assays carried out in TSHR expressing GPI cells showed that rhTSH inhibited the binding of ^{125}I-rhTSH to the TSHR in a concentration dependent

manner with the highest concentration of rhTSH inhibiting the binding to the TSHR by around 98%. This assay reported an IC_{50} of 980 nM, which is considerably higher than the Kd obtained in the saturation assay studies.

4.2.4 Internalisation and externalisation assays

In the thyroid, TSH binds and activates the TSHR, a G protein coupled receptor, and consequently triggers G-protein-regulated effectors including adenyl cyclase, phospholipase C, calcium channels) [258]. Most activated GPCRs are rapidly desensitised at the cell surface in a process that involves phosphorylation and B-arrestin binding. GPCRs are internalised via clathrin-coated pits or other less understood pathways, and they can be either dephosphorylated and efficiently recycled back to the cell surface or sorted from endosomes to lysosomes and degraded [258]. The rate of GPCR internalisation, recycling and lysosomal sorting differ widely among receptors [258]. Previous studies suggest that the TSHR is recycled back to the cell surface [69]. However, additional studies need to be conducted in order to conclusively determine how exactly the TSHR is internalised and show conclusively whether it is recycled back to the cell surface or degraded in lysosomal vesicles.

Internalisation and externalisation assays are commonly used tools for *in vitro* characterisation of novel radiopharmaceuticals [250, 259-261]. An optimal receptor–ligand would, in addition to having high tumour specificity, also provide lysosomal targeting and trapping of the radioisotope, coupled with rapid recycling of the receptor to the surface [262, 263]. In this way the radioisotope could accumulate and be retained in target cells for some time and consequently a high imaging contrast or strong therapeutic effect could be achieved.

Results from internalisation assays showed 80% of cell associated radiolabelled conjugate was internalised at two hours, whereas around 20% of the total conjugate

accounted for the membrane-bound fraction at this time point. These results indicate that most of the radiolabelled rhTSH is internalised. These results are in accordance with previously reported studies that concluded that the majority of TSH is internalised. Due to the possibility of ^{125}I being metabolised into free ^{125}I, internalisation assays may be confounded by assuming that the supernatant radioactivity is bound to the protein when in fact the activity may be due to free iodide in solution. A TCA protein precipitation assay confirmed that most of the ^{125}I was still bound to the rhTSH, as there was just a small amount of metabolised free ^{125}I detected. It was therefore unlikely that the small degree of free ^{125}I was interfering with the accurate interpretation of the internalisation assay.

The presence and integrity of externalised ligand can be detected in externalisation assays performed in the presence and absence of competitor. Externalisation assays are undertaken by performing internalisation into the cells and then incubating them further for 2 hours . After the incubation time the externalised fraction can be determined. After 2 hours incubation at 37°C approximately 60% of internalised activity had become externalised. There was however no significant difference between externalisation in the presence and absence of competitor, suggesting that most or all of the externalised peptide was degraded. A study by Baratti-Elbaz *et al.* [264] reported the majority of internalised receptor molecules (90%) were recycled to the cell surface. The study used stably transfected L cells that express the TSH receptor, ^{125}I-labeled bTSH, and anti-TSHR antibodies. These results have reported substantially higher recycling of rhTSH, however some other studies also reported a lower amount of TSH being recycled back onto the membrane, with most of it being degraded in the lysosomes.

4.2.5 *In vivo* binding

In vitro experiments performed previously confirmed that ^{125}I-rhTSH bound specifically to the TSHR both in the TSHR coated tubes and in TSHR expressing GPI cells. For this reason, it was considered worthwhile to investigate the binding of ^{125}I-rhTSH *in vivo*. FRTL5 cells are a fast growing rat thyroid cell-line, which maintains functional characteristics of iodide uptake and thyroglobulin synthesis over prolonged periods of culturing. FRTL5 cells derive from primary cultures of Fischer rat thyroid glands. FRTL5 cells are employed in a series of assays which measure thyroid stimulatory or inhibitory factors [265].

In chapter 3.1.2.2.1, FRTL5 cells were demonstrated to express the TSHR, and ^{125}I-rhTSH was also shown to bind specifically to FRTL5 in previous studies. Due to these features, these cells were injected subcutaneously in mice with the intention of studying the binding of ^{125}I-rhTSH to a the TSHR *in vivo*.

4.2.5.1 SPECT/CT imaging studies in mice with ^{125}I-rhTSH

SPECT/CT imaging studies were first carried out with mice. Three mice bearing FRTL5 grafted tumours were selected for imaging. These mice were injected *i.v* with ^{125}I-rhTSH and were scanned at intervals of 1 to 6 hours post injection.

As explained previously, interpretation of results from this experiment is complicated by the fact that radioiodine released in-vivo by metabolism of the labelled peptide may also be taken up by the thyroid via the sodium iodine symporter (NIS). In order to control for this possibility, mice were given potassium iodide in their water 3 days prior to experiments as well as sodium perchlorate administered intraperitoneally immediately before injection of the ^{125}I-rhTSH. Sodium perchlorate is a potent inhibitor of the NIS function and thus an effective inhibitor of active iodide transport [4, 266-268].

A blocking study using co-injection of unlabelled rhTSH was also carried out in order to determine whether any uptake observed was due to specific or non-specific binding. Some degree of non-specific binding is expected due to hydrophobic and ionic interactions with other sites on the cell surface, however, this percentage must be relatively low enough to allow specific binding to be observed [269]. The tumour region of mice was quantified using invivo-scope software. The quantification analysis indicated that no substantial differences in the activity in the tumour was observed between ^{125}I-rhTSH and the blocking control. It would be thus expected that the blocking control study should have shown reduced activity in the tumour and the thyroid, and this therefore raises questions about the specificity of the ^{125}I-rhTSH uptake in the tumour. These results suggest that most of the binding of ^{125}I-rhTSH to the FRTL5 grafted tumours is in fact due non-specific binding although one alternative possible explanation is that the dose of cold rhTSH was not enough to saturate TSHR receptors and effectively block the binding of ^{125}I-rhTSH

.

4.2.5.2 Biodistribution with ^{125}I-rhTSH

Biodistribution studies were performed in order to assess the binding of ^{125}I-rhTSH to TSHR in both the thyroid and the FRTL5 grafted tumours in mice. Trypsin inhibitor (TI) was initially used as a control in the biodistribution studies as it has a similar molecular weight to rhTSH, 23 kDa. In order to block the uptake of free ^{125}I into the thyroid and tumour via NIS, mice were given water with potassium iodide as well as injected with sodium perchlorate prior to the ^{125}I-rhTSH, as detailed in 2.3.8.1.

In this biodistribution study the uptake of ^{125}I-rhTSH in the tumour and the thyroid was much higher than the ^{125}I-TI control and this could be interpreted to be specific binding to the receptor. However, the activity seen in the blood was also higher than the control so it can be assumed that ^{125}I-rhTSH is circulating for longer in the blood than the ^{125}I-

TI. Possibly as a result of this longer half-life in the blood, the uptake of ^{125}I-rhTSH was not only higher in the thyroid and the tumour but also higher in non specific organs such as muscle, heart, liver, spleen and pancreas compared to ^{125}I-TI. Since there is no significant expression of THSR in these organs, this suggests that the increase in activity seen in the tumour with ^{125}I-rhTSH in comparison to control ^{125}I-TI is due to non specific mechanisms. It also suggests that the control used, ^{125}I-TI, is not an appropriate control to be used with rhTSH because of its more rapid clearance.

4.2.5.3 Second biodistribution study with ^{125}I-rhTSH

A second biodistribution study was conducted to address the question of whether the amount of cold rhTSH added in the blocking control was not enough to saturate the receptors and therefore not enough to completely block the binding of ^{125}I-rhTSH to the thyroid and tumour. A different ^{125}I radiolabelled control peptide with a similar molecular weight to rhTSH, carbonic anydrase (CA) was also used in these experiments.

In this study, the blocking control and the ^{125}I-CA control showed higher uptake than the ^{125}I-rhTSH group in the tumour as well as in the thyroid. This clearly suggests that most uptake of radioactivity occurring in the tumour and thyroid was due to non specific binding and not due to the specific binding of ^{125}I-rhTSH to the TSHR in the thyroid and grafted tumour.

Corsetti *et al.* [181] in a similar study showed that ^{125}I radioiodinated rhTSH bound to TSHR in PTC-1 TSHR positive cell lines. In this study rhTSH was successfully radioiodinated with ^{125}I and binding assays were performed to assess its binding to TSHR expressed in PTC-1 cells. This study showed that ^{125}I-rhTSH bound to the TSHR in these cells with a high affinity. The authors of this study then carried out biodistribution studies to assess the binding of ^{125}I-rhTSH to PTC-1 tumours grafted

into mice. ^{125}I-rhTSH appeared to bind to PTC-1 xenografts in mice compared with non TSHR expressing cell xenografts. However, there were some potential flaws in this study that may have misguided the author to this conclusion.

Only two animals of each cell line (two did not express TSHR, ARO and two expressed TSHR, PTC-1) were used for the biodistribution studies, and no statistical analysis was employed. Perhaps the slightly higher uptake reported in TSHR positive grafted tumours was therefore due to the variability of data. Also, there was no blocking control included so perhaps most of the binding that reported in the study was due to non specific binding.

4.2.5.4 Stability of ^{125}I-rhTSH blood *in vivo* and *ex vivo* studies

One possible reason why ^{125}I-rhTSH showed binding to the TSHR *in vitro* but not *in vivo* may be due to the ^{125}I-rhTSH breaking down in the blood. In order to investigate this possibility ^{125}I-rhTSH was incubated in blood both *in vivo* and *ex vivo* and after 2 hours the blood was analysed using TCA precipitation assays and SDS-PAGE electrophoresis. The results showed that most of the ^{125}I-rhTSH structure remained intact, and for that reason it could be concluded that ^{125}I-rhTSH was not breaking down in blood and instability of the tracer was not the cause of the imaging and biodistribution results obtained.

4.2.6 Conclusion of rhTSH studies

rhTSH presented as a promising potential radioligand to target the TSHR in radioiodine resistant thyroid cancer, and robust *in vitro* binding to TSHR expressing cells was encouraging. However, *in vivo* studies showed that rhTSH does not bind *in vivo*, and for that reason rhTSH cannot therefore be considered a suitable candidate to target the TSHR in radioiodine resistant thyroid cancer.

CHAPTER 5. GENERAL SUMMARY AND CONCLUSIONS

Differentiated thyroid cancer (DTC) is usually treated with total thyroidectomy, followed by ^{131}I radioiodine ablation in order to eliminate any thyroid remnants. To diagnose and stage recurrent thyroid cancer, radioactive iodine (RAI) whole body scanning (WBS) is used [76, 77, 80]. Some thyroid cancers de-differentiate and lose the expression of the sodium iodide symporter (NIS), which is responsible for the uptake of radioactive iodine into the thyroid and thyroid tumours [108, 210, 243]. Without this transporter, the disease cannot be staged and treated with radioactive iodine WBS, therefore a new approach is needed.

There have been some reports that showed that radioiodine resistant thyroid cancers still express the thyroid stimulating hormone receptor (TSHR) [114, 118]. These studies indicated that TSHR might be a valuable target to stage and treat radioactive resistant de-differentiated thyroid cancer, and therefore experiments were carried out to investigate this.

Monoclonal antibodies have emerged as useful tools to target specific receptors in a number of cancers and therefore the aim of the first part of this study was to use radiolabelled mAb9, a whole IgG anti TSHR monoclonal antibody, to target TSHR in radioiodine resistant thyroid cancer *in vitro* and *in vivo.* FTC-133, TPC-1 and GPI cell lines were used in this study and the expression of TSHR in these cells was evaluated using FACS, RT-PCR and Western blot studies to ensure that these cell lines expressed the TSHR. Results from these studies showed that GPI cells expressed TSHR at high levels but that the non- transfected human cell lines FTC-133, TPC-1 as well as the rat FTRL5 cell line had much lower or undetectable levels of TSHR expression.

Thereafter, mAb9 was radiolabelled with ^{125}I and ^{111}In, and *in vitro* binding studies in the above mentioned TSHR expressing cells showed that ^{125}I-mAb9 and ^{111}In-mAb9

bound to the THSR in GPI cells with a high binding affinity but showed no or negligible binding to the other cell lines. This showed that the antibody retained its binding ability after radiolabelling and showed specific interactions with receptor expressing cells, but not receptor negative cells *in vitro*. *In vivo* studies in mice were then carried out to evaluate the specific binding of ^{125}I-mAb9 and ^{111}In-mAb9 to the TSHR in the thyroid of mice, a tissue known to express TSHR, however no significant binding *in vivo* was seen. Thus, these studies concluded that although radiolabelled mAb9 bound to TSHR with a high affinity *in vitro*, it failed to bind to the TSHR in the thyroid of mice. For this reason, mAb9 was considered not suitable to be used as a potential aid in the diagnosis and treatment of radioiodine resistant thyroid cancer and hence no further studies were carried out with radiolabelled mAb9.

In the second part of this study, rhTSH was explored for the targeting of the TSHR. This approach appeared promising due to a previous preliminary study that showed radiolabelled rhTSH bound to TSHR expressing cells and grafted thyroid tumours in mice [181]. Studies were carried out to evaluate the robustness of this strategy by testing whether radiolabelled rhTSH bound to TSHR in a number of different experimental contexts as those used in the preliminary paper. In *in vitro* binding studies, the ability of ^{125}I-rhTSH to bind to TSHR was tested in a number of cell lines that were not previously used in the preliminary study. Furthermore, different radiolabelling methods were employed and extensive optimisation steps were undertaken until the best radiolabelled product was achieved.

Additionally, because an n number of only two animals was used in the preliminary study, it was not possible to show if the binding observed was statistically significant. In the studies carried out in this thesis, a higher n number of animals were tested, which allowed to determine if any binding observed was actually statistically significant.

In the first stage of this study, rhTSH was radiolabelled with ^{125}I and cell binding assays were carried out to assess its binding *in vitro*. ^{125}I-rhTSH was shown to bind to the TSHR expressing cells and therefore the next step was to evaluate the binding of ^{125}I-rhTSH *in vivo* to grafted thyroid tumours and to the thyroid of mice. SPECT/CT imaging studies and biodistribution studies failed to show specific binding of ^{125}I-rhTSH to the thyroid and thyroid cancer grafted tumours. The conclusion of these rhTSH studies was therefore that although radiolabelled rhTSH bound to the TSHR *in vitro*, it did not bind to either grafted tumour or the thyroid in mice *in vivo*. These studies concluded that, like radiolabelled mAb9, ^{125}I-rhTSH was not a suitable diagnosis/treatment tool to be used in radioiodine de-differentiated thyroid cancer. However, the animal model used in these *in vivo* studies was not ideal, as it was shown *in vitro* that most binding of ^{125}I-rhTSH to these tumour cells was due to non specific binding.

The reasons for the lack of uptake of mAb9 and rhTSH *in vivo* are not clear. It may be that the levels of TSHR expression in the thyroid of mice are not high enough for effective targeting despite being sufficient to maintain normal thyroid function in these animals. Future studies should therefore include a measurement of these expression levels using a suitable *ex vivo* technique. Another possible reason for lack of uptake could be due to endogenous TSH competing for radiolabelled rhTSH in mice. This issue could be addressed in future studies by performing experiments where mice were given thyroxine to block their levels of endogenous TSH before carrying out experiments with radiolabelled rhTSH and mAb9. A dose response curve could also be performed to determine if higher concentrations of ^{125}I-rhTSH could overcome any competition from mice endogenous TSH *in vivo.* The *in vitro* binding studies of radiolabelled mAb9 and rhTSH were performed in cells expressing the human TSHR and although published studies have reported that both compounds also bind to the mouse receptor it would be

appropriate to perform studies to confirm that radiolabelled mAb9 and rhTSH do bind to the mouse receptor *in vitro*.

Although the hypothesis behind this project is that de-differentiated thyroid cancer cells continue to express TSHR, the cell lines studied were found to express only very low levels of TSHR. The published literature is divided on this issue. Gerard *et al.* [116] used immunohistochemistry to analyse the expression of TSHR in human follicular and papillary thyroid cancer samples and concluded that TSHR expression persisted virtually in all cases of thyroid cancer. Matsumoto H. *et al.* [118] used immunohistochemistry and detected decreased expression of TSHR in poorly differentiated human thyroid cancer samples. Park HJ *et al.* [117] and Ohta *et al.* [119] found TSHR mRNA to be expressed in thyroid cancer, however at lower levels than in the thyroid controls. Elisei *et al.* [120] did not detect expression of TSHR mRNA in human samples of primary anaplastic thyroid cancer.

It is therefore important that the levels of TSHR expression in a series of clinical examples be confirmed before extensive targeting studies aimed at this receptor are undertaken. An important component of any further studies should be robust non-transfected cell lines that have been confirmed to express higher levels of TSHR (if indeed such lines exist). These cell lines could then be used to create more robust mice models to further test the binding of ^{125}I-rhTSH *in vivo*.

Whole antibodies might not be ideal to use *in vivo* due to their large sizes. In a future project, antibody fragments with better pharmacokinetic properties could be tested. The ideal tumor-targeting antibodies are intermediate-sized multivalent molecules, which provide rapid tissue penetration, high target retention and rapid blood clearance. Recent biodistribution studies [266] indicate that bivalent antibodies such as diabodies (60 kDa), and minibodies (80 kDa) may be best suited for tumor imaging and therapy due to a higher total tumor uptake and better tumor-to-blood ratios than intact IgG molecules.

Also, some small molecules TSHR agonists have been developed and these could be radiolabelled and tested for their potential use in the diagnosis and treatment of radioiodine resistant thyroid cancer [267, 268].

Another plausible future option would be to find a different approach to target radioiodine resistant thyroid cancer, however so far no new biomarker has been found to be uniquely associated with de-differentiated thyroid cancer.

6. REFERENCES

1. Silverthorn, D.U., *Human Physiology: An Integrated Approach with IP-10 (International Edition) [Paperback]* 5ed2009: Pearson Education. 992 pages
2. Gillian Pocock, C.D.R., *Human physiology: the basis of medicine*. 3, illustrated ed, ed. O.m. publications2006, Oxford: Oxford University Press. 638 pages.
3. Brian Saunders, M.a.P.G., MD *Evaluation of the Thyroid Nodule, Thyroid Cancer and Benign Disease* Division of Endocrine Surgery, Department of Surgery University of Michigan Medical Center.
4. Eskandari, S., et al., *Thyroid Na+/I- symporter. Mechanism, stoichiometry, and specificity.* The Journal of biological chemistry, 1997. **272**(43): p. 27230-8.
5. Dai, G., O. Levy, and N. Carrasco, *Cloning and characterization of the thyroid iodide transporter.* Nature, 1996. **379**(6564): p. 458-60.
6. Smanik, P.A., et al., *Cloning of the human sodium lodide symporter.* Biochemical and biophysical research communications, 1996. **226**(2): p. 339-45.
7. De La Vieja, A., et al., *Molecular analysis of the sodium/iodide symporter: impact on thyroid and extrathyroid pathophysiology.* Physiological reviews, 2000. **80**(3): p. 1083-105.
8. Hill, R.N., et al., *Thyroid follicular cell carcinogenesis.* Fundamental and applied toxicology : official journal of the Society of Toxicology, 1989. **12**(4): p. 629-97.
9. Greer, M.A., A.K. Stott, and K.A. Milne, *Effects of thiocyanate, perchlorate and other anions on thyroidal iodine metabolism.* Endocrinology, 1966. **79**(2): p. 237-47.
10. Kuehn, F.S. and M.P. Lozada, *Thyroid hormones : functions, related diseases and uses*. Endocrinology research and clinical developments series2009, New York: Nova Biomedical Books. xiii, 220 p.
11. Rapoport, B., et al., *The thyrotropin (TSH) receptor: interaction with TSH and autoantibodies.* Endocr Rev, 1998. **19**(6): p. 673-716.
12. Dumont, J.E., J.C. Jauniaux, and P.P. Roger, *The cyclic AMP-mediated stimulation of cell proliferation.* Trends in biochemical sciences, 1989. **14**(2): p. 67-71.
13. Vassart, G. and J.E. Dumont, *The thyrotropin receptor and the regulation of thyrocyte function and growth.* Endocrine reviews, 1992. **13**(3): p. 596-611.
14. Szkudlinski, M.W., et al., *Thyroid-stimulating hormone and thyroid-stimulating hormone receptor structure-function relationships.* Physiological reviews, 2002. **82**(2): p. 473-502.
15. Green, E.D. and J.U. Baenziger, *Asparagine-linked oligosaccharides on lutropin, follitropin, and thyrotropin. I. Structural elucidation of the sulfated and sialylated oligosaccharides on bovine, ovine, and human pituitary glycoprotein hormones.* The Journal of biological chemistry, 1988. **263**(1): p. 25-35.
16. Thotakura, N.R. and D.L. Blithe, *Glycoprotein hormones: glycobiology of gonadotrophins, thyrotrophin and free alpha subunit.* Glycobiology, 1995. **5**(1): p. 3-10.
17. Thotakura, N.R., et al., *The role of the oligosaccharide chains of thyrotropin alpha- and beta-subunits in hormone action.* Endocrinology, 1992. **131**(1): p. 82-8.
18. Takata, K., et al., *The role of the carboxyl-terminal 6 amino acid extension of human TSH beta subunit.* Biochemical and biophysical research communications, 1989. **165**(3): p. 1035-42.

19. Weintraub, B.D. and M.W. Szkudlinski, *Development and in vitro characterization of human recombinant thyrotropin.* Thyroid : official journal of the American Thyroid Association, 1999. **9**(5): p. 447-50.
20. Silversides, D.W., et al., *Bovine thyrotropin receptor cDNA is characterized by full-length and truncated transcripts.* Journal of molecular endocrinology, 1997. **18**(2): p. 101-12.
21. Vanderhaeghen, P., et al., *Molecular cloning and chromosomal mapping of olfactory receptor genes expressed in the male germ line: evidence for their wide distribution in the human genome.* Biochemical and biophysical research communications, 1997. **237**(2): p. 283-7.
22. Nagayama, Y., et al., *Molecular cloning, sequence and functional expression of the cDNA for the human thyrotropin receptor.* Biochemical and biophysical research communications, 1989. **165**(3): p. 1184-90.
23. Stein, S.A., et al., *Identification of a point mutation in the thyrotropin receptor of the hyt/hyt hypothyroid mouse.* Molecular endocrinology, 1994. **8**(2): p. 129-38.
24. Akamizu, T., et al., *Cloning, chromosomal assignment, and regulation of the rat thyrotropin receptor: expression of the gene is regulated by thyrotropin, agents that increase cAMP levels, and thyroid autoantibodies.* Proceedings of the National Academy of Sciences of the United States of America, 1990. **87**(15): p. 5677-81.
25. Szkudlinski, M.W., et al., *Thyroid-stimulating hormone and thyroid-stimulating hormone receptor structure-function relationships.* Physiol Rev, 2002. **82**(2): p. 473-502.
26. Szkudlinski, M.W., et al., *Human thyroid-stimulating hormone: structure-function analysis.* Methods, 2000. **21**(1): p. 67-81.
27. Sanders, J., et al., *Understanding the thyrotropin receptor function-structure relationship.* Baillieres Clin Endocrinol Metab, 1997. **11**(3): p. 451-79.
28. Chazenbalk, G.D., et al., *Functional analysis of the cytoplasmic domains of the human thyrotropin receptor by site-directed mutagenesis.* The Journal of biological chemistry, 1990. **265**(34): p. 20970-5.
29. Vlaeminck-Guillem, V., et al., *Activation of the cAMP pathway by the TSH receptor involves switching of the ectodomain from a tethered inverse agonist to an agonist.* Molecular endocrinology, 2002. **16**(4): p. 736-46.
30. Harfst, E., A.P. Johnstone, and S.S. Nussey, *Interaction of thyrotropin and thyroid-stimulating antibodies with recombinant extracellular region of human TSH receptor.* Lancet, 1992. **339**(8786): p. 193-4.
31. Vlase, H., et al., *Folding-dependent binding of thyrotropin (TSH) and TSH receptor autoantibodies to the murine TSH receptor ectodomain.* Endocrinology, 1997. **138**(4): p. 1658-66.
32. Osuga, Y., et al., *Soluble ecto-domain mutant of thyrotropin (TSH) receptor incapable of binding TSH neutralizes the action of thyroid-stimulating antibodies from Graves' patients.* Endocrinology, 1998. **139**(2): p. 671-6.
33. Costagliola, S., D. Khoo, and G. Vassart, *Production of bioactive amino-terminal domain of the thyrotropin receptor via insertion in the plasma membrane by a glycosylphosphatidylinositol anchor.* FEBS letters, 1998. **436**(3): p. 427-33.
34. Shepherd, P.S., et al., *Identification of an important thyrotrophin binding site on the human thyrotrophin receptor using monoclonal antibodies.* Molecular and cellular endocrinology, 1999. **149**(1-2): p. 197-206.

35. de Roux, N., et al., *Microsatellites and PCR primers for genetic studies and genomic sequencing of the human TSH receptor gene.* Molecular and cellular endocrinology, 1996. **117**(2): p. 253-6.
36. Jordan, B.A., et al., *Oligomerization of opioid receptors with beta 2-adrenergic receptors: a role in trafficking and mitogen-activated protein kinase activation.* Proceedings of the National Academy of Sciences of the United States of America, 2001. **98**(1): p. 343-8.
37. Devi, L.A. and L.S. Brady, *Dimerization of G-protein coupled receptors.* Neuropsychopharmacology : official publication of the American College of Neuropsychopharmacology, 2000. **23**(4 Suppl): p. S3-4.
38. Trapaidze, N., et al., *Opioid receptor endocytosis and activation of MAP kinase pathway.* Brain research. Molecular brain research, 2000. **76**(2): p. 220-8.
39. Overton, M.C. and K.J. Blumer, *G-protein-coupled receptors function as oligomers in vivo.* Current biology : CB, 2000. **10**(6): p. 341-4.
40. Latif, R., P. Graves, and T.F. Davies, *Oligomerization of the human thyrotropin receptor: fluorescent protein-tagged hTSHR reveals post-translational complexes.* The Journal of biological chemistry, 2001. **276**(48): p. 45217-24.
41. Latif, R., P. Graves, and T.F. Davies, *Ligand-dependent inhibition of oligomerization at the human thyrotropin receptor.* The Journal of biological chemistry, 2002. **277**(47): p. 45059-67.
42. Furmaniak, J. and B.R. Smith, *Immunity to the thyroid-stimulating hormone receptor.* Springer Semin Immunopathol, 1993. **14**(3): p. 309-21.
43. Chazenbalk, G.D., et al., *The functional expression of recombinant human thyrotropin receptors in nonthyroidal eukaryotic cells provides evidence that homologous desensitization to thyrotropin stimulation requires a cell-specific factor.* Endocrinology, 1990. **127**(3): p. 1240-4.
44. Harfst, E. and A.P. Johnstone, *Characterization of the glutamine synthetase amplifiable eukaryotic expression system applied to an integral membrane protein--the human thyrotropin receptor.* Anal Biochem, 1992. **207**(1): p. 80-4.
45. Matsuba, T., et al., *Expression of recombinant human thyrotropin receptor in myeloma cells.* J Biochem, 1995. **118**(2): p. 265-70.
46. Elisei, R., et al., *Expression of thyrotropin receptor (TSH-R), thyroglobulin, thyroperoxidase, and calcitonin messenger ribonucleic acids in thyroid carcinomas: evidence of TSH-R gene transcript in medullary histotype.* J Clin Endocrinol Metab, 1994. **78**(4): p. 867-71.
47. Gerard, A.C., et al., *Correlation between the loss of thyroglobulin iodination and the expression of thyroid-specific proteins involved in iodine metabolism in thyroid carcinomas.* J Clin Endocrinol Metab, 2003. **88**(10): p. 4977-83.
48. Libert, F., et al., *Cloning, sequencing and expression of the human thyrotropin (TSH) receptor: evidence for binding of autoantibodies.* Biochem Biophys Res Commun, 1989. **165**(3): p. 1250-5.
49. Misrahi, M., et al., *Cloning, sequencing and expression of human TSH receptor.* Biochem Biophys Res Commun, 1990. **166**(1): p. 394-403.
50. Rees Smith, B., S.M. McLachlan, and J. Furmaniak, *Autoantibodies to the thyrotropin receptor.* Endocr Rev, 1988. **9**(1): p. 106-21.
51. Endo, T. and T. Kobayashi, *Thyroid-stimulating hormone receptor in brown adipose tissue is involved in the regulation of thermogenesis.* Am J Physiol Endocrinol Metab, 2008. **295**(2): p. E514-8.
52. Dutton, C.M., et al., *Thyrotropin receptor expression in adrenal, kidney, and thymus.* Thyroid, 1997. **7**(6): p. 879-84.

53. Clerget-Froidevaux, M.S., I. Seugnet, and B.A. Demeneix, *Thyroid status co-regulates thyroid hormone receptor and co-modulator genes specifically in the hypothalamus.* FEBS Lett, 2004. **569**(1-3): p. 341-5.
54. Bockmann, J., et al., *Cloning and expression of a brain-derived TSH receptor.* Biochem Biophys Res Commun, 1997. **238**(1): p. 173-8.
55. Sun, F.Y., et al., *[Gene and protein expression of thyrotropin-receptor in retro-bulbar tissue from thyroid-associated ophthalmopathy]*. Zhonghua Yan Ke Za Zhi, 2006. **42**(2): p. 155-8.
56. Drvota, V., et al., *Evidence for the presence of functional thyrotropin receptor in cardiac muscle.* Biochem Biophys Res Commun, 1995. **211**(2): p. 426-31.
57. Ellerhorst, J.A., et al., *Human melanoma cells express functional receptors for thyroid-stimulating hormone.* Endocr Relat Cancer, 2006. **13**(4): p. 1269-77.
58. Wang, J., M. Whetsell, and J.R. Klein, *Local hormone networks and intestinal T cell homeostasis.* Science, 1997. **275**(5308): p. 1937-9.
59. Novack, D.V., *TSH, the bone suppressing hormone.* Cell, 2003. **115**(2): p. 129-30.
60. Marians, R.C., et al., *Defining thyrotropin-dependent and -independent steps of thyroid hormone synthesis by using thyrotropin receptor-null mice.* Proceedings of the National Academy of Sciences of the United States of America, 2002. **99**(24): p. 15776-81.
61. Pierce, K.L., R.T. Premont, and R.J. Lefkowitz, *Seven-transmembrane receptors.* Nature reviews. Molecular cell biology, 2002. **3**(9): p. 639-50.
62. Hanyaloglu, A.C. and M. von Zastrow, *Regulation of GPCRs by endocytic membrane trafficking and its potential implications.* Annual review of pharmacology and toxicology, 2008. **48**: p. 537-68.
63. Sorkin, A. and M. von Zastrow, *Endocytosis and signalling: intertwining molecular networks.* Nature reviews. Molecular cell biology, 2009. **10**(9): p. 609-22.
64. Pippig, S., S. Andexinger, and M.J. Lohse, *Sequestration and recycling of beta 2-adrenergic receptors permit receptor resensitization.* Molecular pharmacology, 1995. **47**(4): p. 666-76.
65. Yu, S.S., R.J. Lefkowitz, and W.P. Hausdorff, *Beta-adrenergic receptor sequestration. A potential mechanism of receptor resensitization.* The Journal of biological chemistry, 1993. **268**(1): p. 337-41.
66. Krueger, K.M., et al., *The role of sequestration in G protein-coupled receptor resensitization. Regulation of beta2-adrenergic receptor dephosphorylation by vesicular acidification.* The Journal of biological chemistry, 1997. **272**(1): p. 5-8.
67. Mathew, D., et al., *Wingless signaling at synapses is through cleavage and nuclear import of receptor DFrizzled2.* Science, 2005. **310**(5752): p. 1344-7.
68. Lahuna, O., et al., *Thyrotropin receptor trafficking relies on the hScrib-betaPIX-GIT1-ARF6 pathway.* The EMBO journal, 2005. **24**(7): p. 1364-74.
69. Frenzel, R., C. Voigt, and R. Paschke, *The human thyrotropin receptor is predominantly internalized by beta-arrestin 2.* Endocrinology, 2006. **147**(6): p. 3114-22.
70. Levy, O., et al., *N-linked glycosylation of the thyroid Na+/I- symporter (NIS). Implications for its secondary structure model.* The Journal of biological chemistry, 1998. **273**(35): p. 22657-63.
71. Dohan, O., et al., *The sodium/iodide Symporter (NIS): characterization, regulation, and medical significance.* Endocrine reviews, 2003. **24**(1): p. 48-77.

72. Spitzweg, C., et al., *Analysis of human sodium iodide symporter gene expression in extrathyroidal tissues and cloning of its complementary deoxyribonucleic acids from salivary gland, mammary gland, and gastric mucosa.* The Journal of clinical endocrinology and metabolism, 1998. **83**(5): p. 1746-51.
73. Ajjan, R.A., et al., *Regulation and tissue distribution of the human sodium iodide symporter gene.* Clinical endocrinology, 1998. **49**(4): p. 517-23.
74. Smanik, P.A., et al., *Expression, exon-intron organization, and chromosome mapping of the human sodium iodide symporter.* Endocrinology, 1997. **138**(8): p. 3555-8.
75. Venkatesh, Y.S., et al., *Anaplastic carcinoma of the thyroid. A clinicopathologic study of 121 cases.* Cancer, 1990. **66**(2): p. 321-30.
76. Schlumberger, M.J., *Papillary and follicular thyroid carcinoma.* N Engl J Med, 1998. **338**(5): p. 297-306.
77. Sherman, S.I., *Thyroid carcinoma.* Lancet, 2003. **361**(9356): p. 501-11.
78. Tan, R.K., et al., *Anaplastic carcinoma of the thyroid: a 24-year experience.* Head Neck, 1995. **17**(1): p. 41-7; discussion 47-8.
79. Demeter, J.G., et al., *Anaplastic thyroid carcinoma: risk factors and outcome.* Surgery, 1991. **110**(6): p. 956-61; discussion 961-3.
80. Ain, K.B., *Anaplastic thyroid carcinoma: a therapeutic challenge.* Semin Surg Oncol, 1999. **16**(1): p. 64-9.
81. Ain, K.B., *Anaplastic thyroid carcinoma: behavior, biology, and therapeutic approaches.* Thyroid, 1998. **8**(8): p. 715-26.
82. Hodgson, N.C., J. Button, and C.C. Solorzano, *Thyroid cancer: is the incidence still increasing?* Ann Surg Oncol, 2004. **11**(12): p. 1093-7.
83. Moore, J.H., Jr., B. Bacharach, and H.Y. Choi, *Anaplastic transformation of metastatic follicular carcinoma of the thyroid.* J Surg Oncol, 1985. **29**(4): p. 216-21.
84. Pacini, F., et al., *Radioiodine ablation of thyroid remnants after preparation with recombinant human thyrotropin in differentiated thyroid carcinoma: results of an international, randomized, controlled study.* J Clin Endocrinol Metab, 2006. **91**(3): p. 926-32.
85. Torlontano, M., et al., *Follow-up of low risk patients with papillary thyroid cancer: role of neck ultrasonography in detecting lymph node metastases.* J Clin Endocrinol Metab, 2004. **89**(7): p. 3402-7.
86. Are, C. and A.R. Shaha, *Anaplastic thyroid carcinoma: biology, pathogenesis, prognostic factors, and treatment approaches.* Ann Surg Oncol, 2006. **13**(4): p. 453-64.
87. Tosiek, M., et al., *[Estimation of sodium/iodide symporter gene expression (NIS) in thyroid cancer by RT-PCR technique (preliminary study)]*. Endokrynol Pol, 2005. **56**(1): p. 25-9.
88. Carvalho, D.P. and A.C. Ferreira, *The importance of sodium/iodide symporter (NIS) for thyroid cancer management.* Arq Bras Endocrinol Metabol, 2007. **51**(5): p. 672-82.
89. Wolny, M. and A. Syrenicz, *[Sodium iodide symporter in physiology and diseases -- the current state of knowledge]*. Endokrynol Pol, 2007. **58**(6): p. 512-21.
90. Spencer, C.A., M. Takeuchi, and M. Kazarosyan, *Current status and performance goals for serum thyrotropin (TSH) assays.* Clinical chemistry, 1996. **42**(1): p. 140-5.
91. Shen, D.H., et al., *Sodium iodide symporter in health and disease.* Thyroid, 2001. **11**(5): p. 415-25.

92. Mazzaferri, E.L. and S.M. Jhiang, *Long-term impact of initial surgical and medical therapy on papillary and follicular thyroid cancer.* Am J Med, 1994. **97**(5): p. 418-28.
93. Shimura, H., et al., *Iodide uptake and experimental 131I therapy in transplanted undifferentiated thyroid cancer cells expressing the Na+/I- symporter gene.* Endocrinology, 1997. **138**(10): p. 4493-6.
94. Mitchell, G., R. Huddart, and C. Harmer, *Phase II evaluation of high dose accelerated radiotherapy for anaplastic thyroid carcinoma.* Radiother Oncol, 1999. **50**(1): p. 33-8.
95. Wong, C.S., J. Van Dyk, and W.J. Simpson, *Myelopathy following hyperfractionated accelerated radiotherapy for anaplastic thyroid carcinoma.* Radiother Oncol, 1991. **20**(1): p. 3-9.
96. Cole, E.S., et al., *Recombinant human thyroid stimulating hormone: development of a biotechnology product for detection of metastatic lesions of thyroid carcinoma.* Bio/technology, 1993. **11**(9): p. 1014-24.
97. Wondisford, F.E., et al., *Isolation and characterization of the human thyrotropin beta-subunit gene. Differences in gene structure and promoter function from murine species.* The Journal of biological chemistry, 1988. **263**(25): p. 12538-42.
98. Thotakura, N.R., et al., *Biological activity and metabolic clearance of a recombinant human thyrotropin produced in Chinese hamster ovary cells.* Endocrinology, 1991. **128**(1): p. 341-8.
99. Huber, G.K., et al., *Recombinant human thyroid-stimulating hormone: initial bioactivity assessment using human fetal thyroid cells.* The Journal of clinical endocrinology and metabolism, 1991. **72**(6): p. 1328-31.
100. Colzani, R.M., et al., *The effect of recombinant human thyrotropin (rhTSH) on thyroid function in mice and rats.* Thyroid : official journal of the American Thyroid Association, 1998. **8**(9): p. 797-801.
101. Ramirez, L., et al., *Recombinant human thyrotropin is a potent stimulator of thyroid function in normal subjects.* The Journal of clinical endocrinology and metabolism, 1997. **82**(9): p. 2836-9.
102. Torres, M.S., et al., *Effect of various doses of recombinant human thyrotropin on the thyroid radioactive iodine uptake and serum levels of thyroid hormones and thyroglobulin in normal subjects.* The Journal of clinical endocrinology and metabolism, 2001. **86**(4): p. 1660-4.
103. Barbaro, D., et al., *Radioiodine treatment with 30 mCi after recombinant human thyrotropin stimulation in thyroid cancer: effectiveness for postsurgical remnants ablation and possible role of iodine content in L-thyroxine in the outcome of ablation.* The Journal of clinical endocrinology and metabolism, 2003. **88**(9): p. 4110-5.
104. Pacini, F., et al., *Ablation of thyroid residues with 30 mCi (131)I: a comparison in thyroid cancer patients prepared with recombinant human TSH or thyroid hormone withdrawal.* The Journal of clinical endocrinology and metabolism, 2002. **87**(9): p. 4063-8.
105. Ringel, M.D. and P.W. Ladenson, *Diagnostic accuracy of 131I scanning with recombinant human thyrotropin versus thyroid hormone withdrawal in a patient with metastatic thyroid carcinoma and hypopituitarism.* The Journal of clinical endocrinology and metabolism, 1996. **81**(5): p. 1724-5.
106. Russo, D., et al., *Absence of sodium/iodide symporter gene mutations in differentiated human thyroid carcinomas.* Thyroid : official journal of the American Thyroid Association, 2001. **11**(1): p. 37-9.

107. Arturi, F., et al., *Iodide symporter gene expression in human thyroid tumors.* The Journal of clinical endocrinology and metabolism, 1998. **83**(7): p. 2493-6.
108. Neumann, S., et al., *Lack of correlation for sodium iodide symporter mRNA and protein expression and analysis of sodium iodide symporter promoter methylation in benign cold thyroid nodules.* Thyroid : official journal of the American Thyroid Association, 2004. **14**(2): p. 99-111.
109. Ringel, M.D., et al., *Expression of the sodium iodide symporter and thyroglobulin genes are reduced in papillary thyroid cancer.* Modern pathology : an official journal of the United States and Canadian Academy of Pathology, Inc, 2001. **14**(4): p. 289-96.
110. Dohan, O. and N. Carrasco, *Advances in Na(+)/I(-) symporter (NIS) research in the thyroid and beyond.* Molecular and cellular endocrinology, 2003. **213**(1): p. 59-70.
111. Caillou, B., et al., *Na+/I- symporter distribution in human thyroid tissues: an immunohistochemical study.* The Journal of clinical endocrinology and metabolism, 1998. **83**(11): p. 4102-6.
112. Jhiang, S.M., et al., *An immunohistochemical study of Na+/I- symporter in human thyroid tissues and salivary gland tissues.* Endocrinology, 1998. **139**(10): p. 4416-9.
113. Castro, M.R., et al., *Development of monoclonal antibodies against the human sodium iodide symporter: immunohistochemical characterization of this protein in thyroid cells.* The Journal of clinical endocrinology and metabolism, 1999. **84**(8): p. 2957-62.
114. Castro, M.R., et al., *Monoclonal antibodies against the human sodium iodide symporter: utility for immunocytochemistry of thyroid cancer.* The Journal of endocrinology, 1999. **163**(3): p. 495-504.
115. Gerard, A.C., et al., *Correlation between the loss of thyroglobulin iodination and the expression of thyroid-specific proteins involved in iodine metabolism in thyroid carcinomas.* The Journal of clinical endocrinology and metabolism, 2003. **88**(10): p. 4977-83.
116. Park, H.J., et al., *Expressions of human sodium iodide symporter mRNA in primary and metastatic papillary thyroid carcinomas.* Thyroid : official journal of the American Thyroid Association, 2000. **10**(3): p. 211-7.
117. Matsumoto, H., et al., *Decreased expression of the thyroid-stimulating hormone receptor in poorly-differentiated carcinoma of the thyroid.* Oncology reports, 2008. **19**(6): p. 1405-11.
118. Ohta, K., T. Endo, and T. Onaya, *The mRNA levels of thyrotropin receptor, thyroglobulin and thyroid peroxidase in neoplastic human thyroid tissues.* Biochemical and biophysical research communications, 1991. **174**(3): p. 1148-53.
119. Elisei, R., et al., *Expression of thyrotropin receptor (TSH-R), thyroglobulin, thyroperoxidase, and calcitonin messenger ribonucleic acids in thyroid carcinomas: evidence of TSH-R gene transcript in medullary histotype.* The Journal of clinical endocrinology and metabolism, 1994. **78**(4): p. 867-71.
120. Richard A. Goldsby, T.J.K., Barbara A. Osborne, and Janis Kuby, *Immunology* Vol. 978. 2003,W.H.Freeman & Co Ltd; 5th Revised edition edition.
121. Hale, G., E. Berrie, and P. Bird, *Design and manufacture of monoclonal antibodies for radioimmunotherapy.* Q J Nucl Med Mol Imaging, 2004. **48**(4): p. 258-66.
122. Adams, G.P. and L.M. Weiner, *Monoclonal antibody therapy of cancer.* Nat Biotechnol, 2005. **23**(9): p. 1147-57.

123. Britton, K.E., M. Granowska, and S.J. Mather, *Radiolabelled monoclonal antibodies in oncology. I. Technical aspects.* Nucl Med Commun, 1991. **12**(1): p. 65-76.
124. Juweid, M.E., *Radioimmunotherapy of B-cell non-Hodgkin's lymphoma: from clinical trials to clinical practice.* Journal of nuclear medicine : official publication, Society of Nuclear Medicine, 2002. **43**(11): p. 1507-29.
125. Illidge, T.M. and S. Brock, *Radioimmunotherapy of cancer: using monoclonal antibodies to target radiotherapy.* Current pharmaceutical design, 2000. **6**(14): p. 1399-418.
126. Harding, K. and S.J. Mather, *Investigative clinical studies with radiopharmaceuticals.* Nucl Med Commun, 2007. **28**(1): p. 1-2.
127. Britton, K.E., S.J. Mather, and M. Granowska, *Radiolabelled monoclonal antibodies in oncology. III. Radioimmunotherapy.* Nucl Med Commun, 1991. **12**(4): p. 333-47.
128. Cheson, B., *Bexxar (Corixa/GlaxoSmithKline).* Curr Opin Investig Drugs, 2002. **3**(1): p. 165-70.
129. Grillo-Lopez, A.J., *Zevalin: the first radioimmunotherapy approved for the treatment of lymphoma.* Expert Rev Anticancer Ther, 2002. **2**(5): p. 485-93.
130. Wiseman, G.A., et al., *Radioimmunotherapy of relapsed non-Hodgkin's lymphoma with zevalin, a 90Y-labeled anti-CD20 monoclonal antibody.* Clin Cancer Res, 1999. **5**(10 Suppl): p. 3281s-3286s.
131. Goldenberg, D.M., *Targeted therapy of cancer with radiolabeled antibodies.* Journal of nuclear medicine : official publication, Society of Nuclear Medicine, 2002. **43**(5): p. 693-713.
132. Bross, P.F., et al., *Approval summary: gemtuzumab ozogamicin in relapsed acute myeloid leukemia.* Clin Cancer Res, 2001. **7**(6): p. 1490-6.
133. Migkou, M., et al., *Applications of monoclonal antibodies for the treatment of hematological malignancies.* Expert Opin Biol Ther, 2009. **9**(2): p. 207-20.
134. El Kinge, A.R., et al., *Gemtuzumab Ozogamicin is a promising post-remission therapy for acute myeloid leukemia.* Leuk Res, 2009. **33**(4): p. 565-6.
135. Ravandi, F., et al., *Effective treatment of acute promyelocytic leukemia with all-trans-retinoic acid, arsenic trioxide, and gemtuzumab ozogamicin.* J Clin Oncol, 2009. **27**(4): p. 504-10.
136. Sharkey, R.M. and D.M. Goldenberg, *Targeted therapy of cancer: new prospects for antibodies and immunoconjugates.* CA Cancer J Clin, 2006. **56**(4): p. 226-43.
137. Goldenberg, D.M., *Targeted therapy of cancer with radiolabeled antibodies.* J Nucl Med, 2002. **43**(5): p. 693-713.
138. Stockwin, L.H. and S. Holmes, *The role of therapeutic antibodies in drug discovery.* Biochem Soc Trans, 2003. **31**(2): p. 433-6.
139. Gilbert, J.A., et al., *Monoclonal pathogenic antibodies to the thyroid-stimulating hormone receptor in Graves' disease with potent thyroid-stimulating activity but differential blocking activity activate multiple signaling pathways.* Journal of immunology, 2006. **176**(8): p. 5084-92.
140. Burman, K.D. and J.R. Baker, Jr., *Immune mechanisms in Graves' disease.* Endocrine reviews, 1985. **6**(2): p. 183-232.
141. Bottazzo, G.F. and D. Doniach, *Autoimmune thyroid disease.* Annual review of medicine, 1986. **37**: p. 353-9.
142. Hughes, P., et al., *The costs of using unauthenticated, over-passaged cell lines: how much more data do we need?* BioTechniques, 2007. **43**(5): p. 575, 577-8, 581-2 passim.

143. MacLeod, R.A., et al., *Widespread intraspecies cross-contamination of human tumor cell lines arising at source.* International journal of cancer. Journal international du cancer, 1999. **83**(4): p. 555-63.
144. Chatterjee, R., *Cell biology. When 60 lines don't add up.* Science, 2007. **315**(5814): p. 929.
145. Masters, J.R., et al., *Short tandem repeat profiling provides an international reference standard for human cell lines.* Proceedings of the National Academy of Sciences of the United States of America, 2001. **98**(14): p. 8012-7.
146. Goretzki, P.E., et al., *Growth regulation of normal thyroids and thyroid tumors in man.* Recent results in cancer research. Fortschritte der Krebsforschung. Progres dans les recherches sur le cancer, 1990. **118**: p. 48-63.
147. Schweppe, R.E., et al., *Deoxyribonucleic acid profiling analysis of 40 human thyroid cancer cell lines reveals cross-contamination resulting in cell line redundancy and misidentification.* The Journal of clinical endocrinology and metabolism, 2008. **93**(11): p. 4331-41.
148. van Staveren, W.C., et al., *Human thyroid tumor cell lines derived from different tumor types present a common dedifferentiated phenotype.* Cancer research, 2007. **67**(17): p. 8113-20.
149. Vitti, P et a.l, *Clinical determination and/or quantification of thyrotropin and a variety of thyroid stimulatory or inhibitory factors performed in vitro with an improved thyroid cell line, FRTL-5*, in *U.S. Pat. 4,609,622.* 1986, Interthyr Research Foundation Inc.: US.
150. Vitti, P., et al., *Graves' IgG stimulation of continuously cultured rat thyroid cells: a sensitive and potentially useful clinical assay.* Journal of endocrinological investigation, 1982. **5**(3): p. 179-82.
151. Valente, W.A., et al., *The relationship of growth and adenylate cyclase activity in cultured thyroid cells: separate bioeffects of thyrotropin.* Endocrinology, 1983. **112**(1): p. 71-9.
152. Da Costa, C.R. and A.P. Johnstone, *Production of the thyrotrophin receptor extracellular domain as a glycosylphosphatidylinositol-anchored membrane protein and its interaction with thyrotrophin and autoantibodies.* J Biol Chem, 1998. **273**(19): p. 11874-80.
153. Rapoport, B., et al., *The thyrotropin (TSH) receptor: interaction with TSH and autoantibodies.* Endocrine reviews, 1998. **19**(6): p. 673-716.
154. Chazenbalk, G.D., et al., *Thyroid-stimulating autoantibodies in Graves disease preferentially recognize the free A subunit, not the thyrotropin holoreceptor.* The Journal of clinical investigation, 2002. **110**(2): p. 209-17.
155. Britton, K.E., *Towards the goal of cancer-specific imaging and therapy.* Nuclear medicine communications, 1997. **18**(11): p. 992-1007.
156. Hosseinimehr, S.J., *Potential utility of radioprotective agents in the practice of nuclear medicine.* Cancer biotherapy & radiopharmaceuticals, 2009. **24**(6): p. 723-31.
158. Hustinx, R. and G. Lucignani, *PET/CT in head and neck cancer: an update.* European journal of nuclear medicine and molecular imaging, 2010. **37**(3): p. 645-51.
159. Almuhaideb, A., N. Papathanasiou, and J. Bomanji, *18F-FDG PET/CT imaging in oncology.* Annals of Saudi medicine, 2011. **31**(1): p. 3-13.
160. Mariani, G., et al., *A review on the clinical uses of SPECT/CT.* European journal of nuclear medicine and molecular imaging, 2010. **37**(10): p. 1959-85.
161. Grewal, R.K., et al., *The effect of posttherapy 131I SPECT/CT on risk classification and management of patients with differentiated thyroid cancer.*

Journal of nuclear medicine : official publication, Society of Nuclear Medicine, 2010. **51**(9): p. 1361-7.
162. Spanu, A., et al., *131I SPECT/CT in the follow-up of differentiated thyroid carcinoma: incremental value versus planar imaging.* Journal of nuclear medicine : official publication, Society of Nuclear Medicine, 2009. **50**(2): p. 184-90.
163. Schmidt, D., et al., *Five months' follow-up of patients with and without iodine-positive lymph node metastases of thyroid carcinoma as disclosed by (131)I-SPECT/CT at the first radioablation.* European journal of nuclear medicine and molecular imaging, 2010. **37**(4): p. 699-705.
164. Tharp, K., et al., *Impact of 131I-SPECT/CT images obtained with an integrated system in the follow-up of patients with thyroid carcinoma.* European journal of nuclear medicine and molecular imaging, 2004. **31**(10): p. 1435-42.
165. Franc, B.L., et al., *Small-animal SPECT and SPECT/CT: important tools for preclinical investigation.* Journal of nuclear medicine : official publication, Society of Nuclear Medicine, 2008. **49**(10): p. 1651-63.
166. Mather, S., Sosabowski, J., Finucane, C., Foster, J., King, R., Vassaux, G., and Garrood, T.,, *High resolution, small animal SPECT-CT imaging as a tool in preclinical development.* www.spect-ct.com, 2009.
167. Domokos Mathe, I.F., Lajos Balogh, *Quantitative imaging of mouse thyroids wiwth 99mTc 123,131I using NanoSPECT/CT.* Www.spect-ct.com.
168. Mather, S., Sosabowski, J., Finucane, C., Foster, J., King, R., Vassaux, G., and Garrood, T.,, *High resolution, small animal SPECT-CT imaging as a tool in preclinical development, www.spect-ct.com.* 2009.
169. Wilbur, D.S., *Radiohalogenation of proteins: an overview of radionuclides, labeling methods, and reagents for conjugate labeling.* Bioconjugate chemistry, 1992. **3**(6): p. 433-70.
170. McConahey, P.J. and F.J. Dixon, *Radioiodination of proteins by the use of the chloramine-T method.* Methods in enzymology, 1980. **70**(A): p. 210-3.
171. Salacinski, P.R., et al., *Iodination of proteins, glycoproteins, and peptides using a solid-phase oxidizing agent, 1,3,4,6-tetrachloro-3 alpha,6 alpha-diphenyl glycoluril (Iodogen).* Analytical biochemistry, 1981. **117**(1): p. 136-46.
172. Marchalonis, J.J., *An enzymic method for the trace iodination of immunoglobulins and other proteins.* The Biochemical journal, 1969. **113**(2): p. 299-305.
173. Weiner, R.E., et al., *The relative stabilities of 67 Ga complexes of lactoferrin and transferrin at various pH's.* International journal of nuclear medicine and biology, 1981. **8**(4): p. 371-8.
174. Sundberg, M.W., et al., *Chelating agents for the binding of metal ions to macromolecules.* Nature, 1974. **250**(467): p. 587-8.
175. Hnatowich, D.J., F. Virzi, and P.W. Doherty, *DTPA-coupled antibodies labeled with yttrium-90.* Journal of nuclear medicine : official publication, Society of Nuclear Medicine, 1985. **26**(5): p. 503-9.
176. Brown, D.H., et al., *A quantitative study of the subcellular localization of 67Ga.* Cancer research, 1976. **36**(3): p. 956-63.
177. Martell, E., et al., *Stabilities of trivalent metal ion complexes of the tetraacetate derivatives of 12-, 13- and 14-membered tetraazamacrocycles* Inorganica Chimica Acta, 1991. **Volume 190**(1): p. 37-46.
178. Froidevaux, S., et al., *Preclinical comparison in AR4-2J tumor-bearing mice of four radiolabeled 1,4,7,10-tetraazacyclododecane-1,4,7,10-tetraacetic acid-*

somatostatin analogs for tumor diagnosis and internal radiotherapy. Endocrinology, 2000. **141**(9): p. 3304-12.
179. Fraker, P.J. and J.C. Speck, Jr., *Protein and cell membrane iodinations with a sparingly soluble chloroamide, 1,3,4,6-tetrachloro-3a,6a-diphrenylglycoluril.* Biochem Biophys Res Commun, 1978. **80**(4): p. 849-57.
180. Lindmo, T., et al., *Determination of the immunoreactive fraction of radiolabeled monoclonal antibodies by linear extrapolation to binding at infinite antigen excess.* J Immunol Methods, 1984. **72**(1): p. 77-89.
181. Corsetti, F., et al., *Radioiodinated recombinant human TSH: a novel radiopharmaceutical for thyroid cancer metastases detection.* Cancer biotherapy & radiopharmaceuticals, 2004. **19**(1): p. 57-63.
182. Boyiadzis, M. and K.A. Foon, *Approved monoclonal antibodies for cancer therapy.* Expert opinion on biological therapy, 2008. **8**(8): p. 1151-8.
183. Britton, K.E., *Radiolabeled monoclonal antibodies in diagnosis and therapy of cancer. Summary and perspectives.* Acta oncologica, 1996. **35**(3): p. 385-90.
184. Goding, J.W., *Monoclonal antibodies: principles and practice : production and application of monoclonal antibodies in cell biology, biochemistry and immunology*. 3 ed, ed. J.W. Goding1996: Academic Press.
185. Goldenberg, D.M., *Monoclonal antibodies in cancer detection and therapy.* The American journal of medicine, 1993. **94**(3): p. 297-312.
186. Gruber, R., E. Holz, and G. Riethmuller, *Monoclonal antibodies in cancer therapy.* Springer seminars in immunopathology, 1996. **18**(2): p. 243-51.
187. Bethge, W.A. and B.M. Sandmaier, *Targeted cancer therapy using radiolabeled monoclonal antibodies.* Technology in cancer research & treatment, 2005. **4**(4): p. 393-405.
188. Goldenberg, D.M. and R.M. Sharkey, *Advances in cancer therapy with radiolabeled monoclonal antibodies.* Q J Nucl Med Mol Imaging, 2006. **50**(4): p. 248-64.
189. Sabbah, E.N., et al., *In vitro and in vivo comparison of DTPA- and DOTA-conjugated antiferritin monoclonal antibody for imaging and therapy of pancreatic cancer.* Nuclear medicine and biology, 2007. **34**(3): p. 293-304.
190. Sharkey, R.M. and D.M. Goldenberg, *Targeted therapy of cancer: new prospects for antibodies and immunoconjugates.* CA: a cancer journal for clinicians, 2006. **56**(4): p. 226-43.
191. Goldenberg, D.M., *New developments in monoclonal antibodies for cancer detection and therapy.* CA: a cancer journal for clinicians, 1994. **44**(1): p. 43-64.
192. Gatto, B., *Monoclonal antibodies in cancer therapy.* Current medicinal chemistry. Anti-cancer agents, 2004. **4**(5): p. 411-4.
193. Gutheil, J., *The promise of monoclonal antibodies for the therapy of cancer.* Critical reviews in oncology/hematology, 2001. **38**(1): p. 1-2.
194. Oldham, R.K. and R.O. Dillman, *Monoclonal antibodies in cancer therapy: 25 years of progress.* Journal of clinical oncology : official journal of the American Society of Clinical Oncology, 2008. **26**(11): p. 1774-7.
195. Goldenberg, D.M., *Advancing role of radiolabeled antibodies in the therapy of cancer.* Cancer immunology, immunotherapy : CII, 2003. **52**(5): p. 281-96.
196. Trail, P.A., H.D. King, and G.M. Dubowchik, *Monoclonal antibody drug immunoconjugates for targeted treatment of cancer.* Cancer immunology, immunotherapy : CII, 2003. **52**(5): p. 328-37.
197. Bethge, W.A. and B.M. Sandmaier, *Targeted cancer therapy and immunosuppression using radiolabeled monoclonal antibodies.* Seminars in oncology, 2004. **31**(1): p. 68-82.

198. Divgi, C.R., *Status of radiolabeled monoclonal antibodies for diagnosis and therapy of cancer.* Oncology, 1996. **10**(6): p. 939-53; discussion 954, 957-8.
199. Goldenberg, D.M., *Imaging and therapy of cancer with radiolabeled monoclonal antibodies.* Progress in clinical and biological research, 1989. **288**: p. 413-27.
200. Markowitz, A., K. Saleemi, and L.M. Freeman, *Role of In-111 labeled CYT-103 immunoscintigraphy in the evaluation of patients with recurrent colorectal carcinoma.* Clinical nuclear medicine, 1993. **18**(8): p. 685-700.
201. Doerr, R.J., L. Herrera, and H. Abdel-Nabi, *In-111 CYT-103 monoclonal antibody imaging in patients with suspected recurrent colorectal cancer.* Cancer, 1993. **71**(12 Suppl): p. 4241-7.
202. Neal, C.E., et al., *In-111 CYT-103 immunoscintigraphy in the imaging of ovarian carcinoma.* Clinical nuclear medicine, 1993. **18**(6): p. 472-6.
203. Surwit, E.A., et al., *Clinical assessment of 111In-CYT-103 immunoscintigraphy in ovarian cancer.* Gynecologic oncology, 1993. **48**(3): p. 285-92.
204. Petersen, B.M., Jr., et al., *Use of the radiolabeled murine monoclonal antibody, 111In-CYT-103, in the management of colon cancer.* American journal of surgery, 1993. **165**(1): p. 137-42; discussion 142-3.
205. Abdel-Nabi, H.H. and R.J. Doerr, *Multicenter clinical trials of monoclonal antibody B72.3-GYK-DTPA 111In (111In-CYT-103; OncoScint CR103) in patients with colorectal carcinoma.* Targeted diagnosis and therapy, 1992. **6**: p. 73-88.
206. Jusko, W.J., L.P. Kung, and R.F. Schmelter, *Immunopharmacokinetics of 111In-CYT-103 in ovarian cancer patients.* Targeted diagnosis and therapy, 1992. **6**: p. 177-90.
207. Surwit, E.A., *Impact of 111In-CYT-103 on the surgical management of patients with ovarian cancer.* Targeted diagnosis and therapy, 1992. **6**: p. 125-40.
208. Gallup, D.G., *Multicenter clinical trial of 111In-CYT-103 in patients with ovarian cancer.* Targeted diagnosis and therapy, 1992. **6**: p. 111-24.
209. Neal, C.E., et al., *Immunoscintigraphy of colorectal carcinoma utilizing 111In-labeled monoclonal antibody conjugate CYT-103.* Gastrointestinal radiology, 1991. **16**(3): p. 251-5.
210. Collier, B.D., et al., *A practical approach to planar and SPECT imaging of 111In-CYT-103.* Targeted diagnosis and therapy, 1992. **6**: p. 191-210.
211. Cheson, B., *Bexxar (Corixa/GlaxoSmithKline).* Current opinion in investigational drugs, 2002. **3**(1): p. 165-70.
212. Goldsmith, S.J., *Radioimmunotherapy of lymphoma: Bexxar and Zevalin.* Seminars in nuclear medicine, 2010. **40**(2): p. 122-35.
213. Shen, D.H., et al., *Sodium iodide symporter in health and disease.* Thyroid : official journal of the American Thyroid Association, 2001. **11**(5): p. 415-25.
214. Schroeder, H.W., Jr. and L. Cavacini, *Structure and function of immunoglobulins.* The Journal of allergy and clinical immunology, 2010. **125**(2 Suppl 2): p. S41-52.
215. Schmitt, C. and J.P. Fermand, *[Immunoglobulins. Structure, monoclonal or polyclonal characteristics, genetic bases and function]*. La Revue du praticien, 1994. **44**(3): p. 395-402.
216. Bene, M.C., *[Immunoglobulins. Structure, function, monoclonal or polyclonal character]*. La Revue du praticien, 1991. **41**(11): p. 1010-2.
217. Jefferis, R., *Structure-function relationships in human immunoglobulins.* The Netherlands journal of medicine, 1991. **39**(3-4): p. 188-98.

218. Leibiger, H., et al., *Glycosylation analysis of a polyreactive human monoclonal IgG antibody derived from a human-mouse heterohybridoma.* Mol Immunol, 1995. **32**(8): p. 595-602.
219. Schroeder, H.W., Jr. and L. Cavacini, *Structure and function of immunoglobulins.* J Allergy Clin Immunol. **125**(2 Suppl 2): p. S41-52.
220. Edelman, G.M. and W.E. Gall, *The antibody problem.* Annu Rev Biochem, 1969. **38**: p. 415-66.
221. Jefferis, R., *Structure-function relationships in human immunoglobulins.* Neth J Med, 1991. **39**(3-4): p. 188-98.
222. Wright, A. and S.L. Morrison, *Effect of glycosylation on antibody function: implications for genetic engineering.* Trends Biotechnol, 1997. **15**(1): p. 26-32.
223. Liu, H., G.G. Bulseco, and J. Sun, *Effect of posttranslational modifications on the thermal stability of a recombinant monoclonal antibody.* Immunol Lett, 2006. **106**(2): p. 144-53.
224. Siberil, S., et al., *Selection of a human anti-RhD monoclonal antibody for therapeutic use: impact of IgG glycosylation on activating and inhibitory Fc gamma R functions.* Clin Immunol, 2006. **118**(2-3): p. 170-9.
225. Mizuochi, T., et al., *Structural and numerical variations of the carbohydrate moiety of immunoglobulin G.* J Immunol, 1982. **129**(5): p. 2016-20.
226. Minich, W.B., et al., *A coated tube assay for the detection of blocking thyrotropin receptor autoantibodies.* J Clin Endocrinol Metab, 2004. **89**(1): p. 352-6.
227. Gilbert, J.A., et al., *Monoclonal pathogenic antibodies to the thyroid-stimulating hormone receptor in Graves' disease with potent thyroid-stimulating activity but differential blocking activity activate multiple signaling pathways.* J Immunol, 2006. **176**(8): p. 5084-92.
228. Johnstone, A.P., et al., *A functional site on the human TSH receptor: a potential therapeutic target in Graves' disease.* Clin Endocrinol (Oxf), 2003. **59**(4): p. 437-41.
229. Givan, A.L., *Flow cytometry: first principles.* 2, illustrated ed2001: John Wiley and Sons. 273 pages.
230. Shepherd, P.S., et al., *Identification of an important thyrotrophin binding site on the human thyrotrophin receptor using monoclonal antibodies.* Mol Cell Endocrinol, 1999. **149**(1-2): p. 197-206.
231. Dromey, J.A., et al., *Mapping of epitopes for autoantibodies to the type 1 diabetes autoantigen IA-2 by peptide phage display and molecular modeling: overlap of antibody and T cell determinants.* J Immunol, 2004. **172**(7): p. 4084-90.
232. Rao, P.V., et al., *Contrasting activities of thyrotropin receptor antibodies in experimental models of Graves' disease induced by injection of transfected fibroblasts or deoxyribonucleic acid vaccination.* Endocrinology, 2003. **144**(1): p. 260-6.
233. Gobeil, F., et al., *G-protein-coupled receptors signalling at the cell nucleus: an emerging paradigm.* Can J Physiol Pharmacol, 2006. **84**(3-4): p. 287-97.
234. Schmutzler, C., et al., *Human thyroid carcinoma cell lines show different retinoic acid receptor repertoires and retinoid responses.* Eur J Endocrinol, 2004. **150**(4): p. 547-56.
235. van Staveren, W.C., et al., *Human thyroid tumor cell lines derived from different tumor types present a common dedifferentiated phenotype.* Cancer Res, 2007. **67**(17): p. 8113-20.

236. Oda, Y., et al., *Epitope analysis of the human thyrotropin (TSH) receptor using monoclonal antibodies.* Thyroid, 2000. **10**(12): p. 1051-9.
237. Nagayama, Y., et al., *Molecular cloning, sequence and functional expression of the cDNA for the human thyrotropin receptor.* Biochem Biophys Res Commun, 1989. **165**(3): p. 1184-90.
238. Da Costa, C.R. and A.P. Johnstone, *Production of the thyrotrophin receptor extracellular domain as a glycosylphosphatidylinositol-anchored membrane protein and its interaction with thyrotrophin and autoantibodies.* The Journal of biological chemistry, 1998. **273**(19): p. 11874-80.
239. Mian, I.S., A.R. Bradwell, and A.J. Olson, *Structure, function and properties of antibody binding sites.* J Mol Biol, 1991. **217**(1): p. 133-51.
240. Getzoff, E.D., et al., *The chemistry and mechanism of antibody binding to protein antigens.* Adv Immunol, 1988. **43**: p. 1-98.
241. van der Kallen, C.J., et al., *Dissociation of thyrotropin receptor function and thyrotropin dependency in rat thyroid tumour cell lines derived from FRTL-5.* British journal of cancer, 1996. **74**(4): p. 606-12.
242. van der Kallen, C.J., et al., *Dissociation of thyrotropin receptor function and thyrotropin dependency in rat thyroid tumour cell lines derived from FRTL-5.* Br J Cancer, 1996. **74**(4): p. 606-12.
243. Filetti, S., et al., *Sodium/iodide symporter: a key transport system in thyroid cancer cell metabolism.* Eur J Endocrinol, 1999. **141**(5): p. 443-57.
244. Sabbah, E.N., et al., *In vitro and in vivo comparison of DTPA- and DOTA-conjugated antiferritin monoclonal antibody for imaging and therapy of pancreatic cancer.* Nucl Med Biol, 2007. **34**(3): p. 293-304.
245. McDougall, I.R. and R.J. Weigel, *Recombinant human thyrotropin in the management of thyroid cancer.* Current opinion in oncology, 2001. **13**(1): p. 39-43.
246. Durski, J.M., R.J. Weigel, and I.R. McDougall, *Recombinant human thyrotropin (rhTSH) in the management of differentiated thyroid cancer.* Nuclear medicine communications, 2000. **21**(6): p. 521-8.
247. Barbaro, D. and G. Boni, *Radioiodine ablation of post-surgical thyroid remnants after preparation with recombinant human TSH: why, how and when.* European journal of surgical oncology : the journal of the European Society of Surgical Oncology and the British Association of Surgical Oncology, 2007. **33**(5): p. 535-40.
248. Heppeler, A., et al., *Receptor targeting for tumor localisation and therapy with radiopeptides.* Current medicinal chemistry, 2000. **7**(9): p. 971-94.
249. Warner, R.R. and M. O'Dorisio T, *Radiolabeled peptides in diagnosis and tumor imaging: clinical overview.* Seminars in nuclear medicine, 2002. **32**(2): p. 79-83.
250. Maina, T., et al., *[(99m)Tc]Demotate 2 in the detection of sst(2)-positive tumours: a preclinical comparison with [(111)In]DOTA-tate.* European journal of nuclear medicine and molecular imaging, 2006. **33**(7): p. 831-40.
251. Ma, C., et al., *Recombinant human thyrotropin (rhTSH) aided radioiodine treatment for residual or metastatic differentiated thyroid cancer.* Cochrane database of systematic reviews, 2010(11): p. CD008302.
252. Hunter, W.M. and F.C. Greenwood, *Preparation of iodine-131 labelled human growth hormone of high specific activity.* Nature, 1962. **194**: p. 495-6.
253. Fraker, P.J. and J.C. Speck, Jr., *Protein and cell membrane iodinations with a sparingly soluble chloroamide, 1,3,4,6-tetrachloro-3a,6a-diphrenylglycoluril.* Biochemical and biophysical research communications, 1978. **80**(4): p. 849-57.

254. Snyder, L.R., J.J. Kirkland, and J.W. Dolan, *Introduction to modern liquid chromatography*. 3rd ed2010, Hoboken, N.J.: Wiley. xli, 912 p.
255. Motulsky, H. and A. Christopoulos, *Fitting models to biological data using linear and nonlinear regression : a practical guide to curve fitting*2004, Oxford ; New York: Oxford University Press. 351 p.
256. Cornelis, S., et al., *Purification and characterization of a soluble bioactive amino-terminal extracellular domain of the human thyrotropin receptor.* Biochemistry, 2001. **40**(33): p. 9860-9.
257. Szkudlinski, M.W., et al., *Purification and characterization of recombinant human thyrotropin (TSH) isoforms produced by Chinese hamster ovary cells: the role of sialylation and sulfation in TSH bioactivity.* Endocrinology, 1993. **133**(4): p. 1490-503.
258. Rockman, H.A., W.J. Koch, and R.J. Lefkowitz, *Seven-transmembrane-spanning receptors and heart function.* Nature, 2002. **415**(6868): p. 206-12.
259. De Jong, M., et al., *Internalization of radiolabelled [DTPA0]octreotide and [DOTA0,Tyr3]octreotide: peptides for somatostatin receptor-targeted scintigraphy and radionuclide therapy.* Nuclear medicine communications, 1998. **19**(3): p. 283-8.
260. Gandomkar, M., et al., *Preclinical evaluation of [99mTc/EDDA/tricine/HYNIC0, 1-Nal3, Thr8]-octreotide as a new analogue in the detection of somatostatin-receptor-positive tumors.* Nuclear medicine and biology, 2007. **34**(6): p. 651-7.
261. Hofland, L.J., et al., *Internalization of the radioiodinated somatostatin analog [125I-Tyr3]octreotide by mouse and human pituitary tumor cells: increase by unlabeled octreotide.* Endocrinology, 1995. **136**(9): p. 3698-706.
262. Simaan, M., et al., *Dissociation of beta-arrestin from internalized bradykinin B2 receptor is necessary for receptor recycling and resensitization.* Cellular signalling, 2005. **17**(9): p. 1074-83.
263. Vines, C.M., et al., *N-formyl peptide receptors internalize but do not recycle in the absence of arrestins.* The Journal of biological chemistry, 2003. **278**(43): p. 41581-4.
264. Baratti-Elbaz, C., et al., *Internalization and recycling pathways of the thyrotropin receptor.* Molecular endocrinology, 1999. **13**(10): p. 1751-65.
265. Vitti, P.e.a., *Clinical determination and/or quantification of thyrotropin and a variety of thyroid stimulatory or inhibitory factors performed in vitro with an improved thyroid cell line*, 1983, Interthyr Research Foundation, Inc. (MD).
266. Van Sande, J., et al., *Anion selectivity by the sodium iodide symporter.* Endocrinology, 2003. **144**(1): p. 247-52.
267. Weiss, S.J., N.J. Philp, and E.F. Grollman, *Iodide transport in a continuous line of cultured cells from rat thyroid.* Endocrinology, 1984. **114**(4): p. 1090-8.
268. Yoshida, A., et al., *Differences in the electrophysiological response to I- and the inhibitory anions SCN- and ClO-4, studied in FRTL-5 cells.* Biochimica et biophysica acta, 1998. **1414**(1-2): p. 231-7.
269. Sampson, C.B., *Textbook of radiopharmacy : theory and practice*. 2nd ed. Nuclear medicine,1994, New York: Gordon and Breach Publishers. xvii, 360 p.